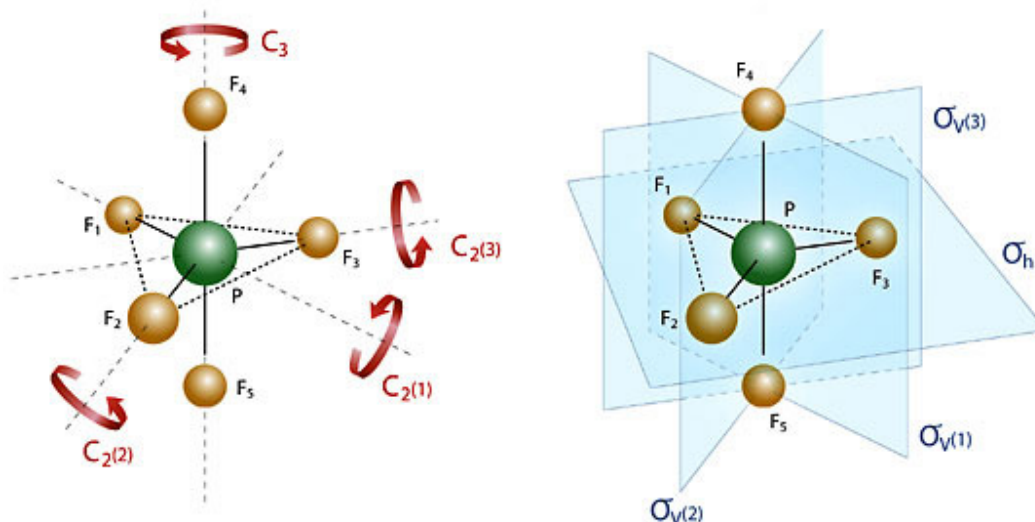




Mukthagangotri, Mysore – 570 006

## M.Sc. CHEMISTRY

(FOURTH SEMESTER)

name of  
the point  
group

symmetry elements for the group

$C_{2v}$	E	$C_2$	$\sigma_v(xy)$	$\sigma_v(yz)$		
$A_1$	1	1	1	1	z	$x^2, y^2, z^2$
$A_2$	1	1	-1	-1	$R_z$	xy
$B_1$	1	-1	1	-1	x, $R_y$	xz
$B_2$	1	-1	-1	1	y, $R_z$	yz

symmetry  
labels

Course: MCH T 4.1

Block 1,2,3 and 4

INORGANIC CHEMISTRY-IV

---

# **M.Sc. CHEMISTRY**

**FOURTH SEMESTER**

**COURSE: MCHT 4.1**

## **INORGANIC CHEMISTRY-IV**

---

---

## Course Design Committee

---

### Prof. Shivalingaiah. D

Vice-Chancellor & Chairperson  
Karnataka State Open University  
Mukthagangothri, Mysore - 570 006

### Prof. Devegowda .T. D

Dean (Academic) & Convenor  
Karnataka State Open University  
Mukthagangothri, Mysore - 570 006

---

## COURSE WRITER

---

### Dr. Prasannakumar. C. S

Senior scientist  
Dr. Reddy's laboratory  
Bangaluru

**Blocks 4.1.1, 4.1.2 and 4.1.3**

### Prof. Nagaraja Naik

Professor, Department of Studies in Chemistry  
University of Mysore, Manasagangothri,  
Mysuru

**Block 4.1.4**

---

## Course Coordinator

### Dr. M. Umashankara

Assistant Professor and Chairman  
Department of Studies in Chemistry  
Karnataka State Open University  
Mukthagangothri, Mysore - 570 006

## Course editor

### Dr. Prasannakumar. C. S

Senior scientist  
Dr.Reddy's laboratory  
Bengaluru

---

## PUBLISHER

---

### The Registrar

Karnataka State Open University  
Mukthagangothri, Mysore - 570 006

**Developed by Academic Section, KSOU, Mysore**

**Karnataka State Open University, 2013**

All rights reserved. No part of this work may be reproduced in any form, by mimeograph or any other means, without permission in writing from the Karnataka State Open University.

Further information on the Karnataka State Open University Programmes may be obtained from the University's office at Mukthagangothri, Mysore - 6

Printed and Published on behalf of Karnataka State Open University. Mysore – 6 by **Registrar (Administration)**

# TABLE OF CONTENTS

		Page No
<b>Block 4.1.1</b>	<b>GROUP THEORY AND ITS APPLICATIONS</b>	
Unit-1	Definition of groups, sub groups, cyclic groups, conjugates relationships.	1-21
Unit-2	Symmetry elements and symmetry operations, point groups (of molecules)	22-37
Unit-3	Reducible and irreducible representations, characters of representation.	38-47
Unit-4	Character tables and their uses (representations, of $C_n$ , $C_{nv}$ , $C_{nh}$ , $D_{nh}$ groups to be worked out)	48-62
<b>Block 4.1.2</b>	<b>SPECTROSCOPIC APPLICATIONS IN INORGANIC CHEMISTRY</b>	
Unit-5	Vibrational spectroscopy- vibrational spectra of diatomic, linear and bent triatomic, $AB_3$ , $AB_4$ , $AB_5$ and $AB_6$ molecules. Spectra of metal complexes, amines, amido, nitro, nitrito, latticewater, aquo and hydrido, carbonato, sulphato, cyanato, thiocyanato complexes, mono and multinuclear carbonyl complexes. Ethylene diamino and diketonate complexes	63-89
Unit-6	ESR-Spin polarization for atoms and transition metal ions, spin-orbit coupling and significance of g-tensors, zero/non zero field splitting, Kramer's degeneracy, applications to transition metal complexes (having one to five unpaired electrons) including biological molecules and free radicals such $PH_4$ , $F_2$ and $BH_3$ .	90-125
Unit-7	NMR- applications of $^{31}P$ , $^{19}F$ , $^{11}B$ NMR spectroscopy in the structural assessment of inorganic compounds, proton/ hydride interactions with Rh103, W 183, Pt 185 and Pb207 in metal complexes/organometallic compounds.	126-165
Unit-8	Mossbauer spectroscopy: principles, isomer shift, qudrupole splitting and magnetic hyperfine interactions. Applications to the study of bonding and structures $Fe^{2+}$ and $Fe^{3+}$ compounds, $Sn^{2+}$ and $Sn^{4+}$ compounds.	166-181

<b>Block 4.1.3</b>	<b>THERMAL METHODS OF ANALYSIS</b>	
Unit-9	Thermogravimetric analysis- principle, factors affecting TG curves, TG curve of calcium oxalate, instrumentation and applications of TG.	182-205
Unit-10	DTA and DSC: principles, instrumentations, and applications in the area of polymers.	206-223
Unit-11	Thermomechanical and dynamic mechanical analysis: Principle, instrumentation and applications.	224-237
Unit-12	Thermometric analysis: Principles, instrumentation and applications	238-244
<b>Block 4.1.4</b>	<b>HOMOGENEOUS AND HETEROGENEOUS CATALYSIS</b>	
Unit-13	Introduction, basic principle, industrial requirements, thermodynamic and kinetic aspects, classification of catalytic systems.	245-356
Unit-14	Principle, experimental techniques, acid-base catalysis, catalysis involving transition metal salts and metal complexes- hydrogenation, asymmetric hydrogenation, transfer hydrogenation, hydrosilation and hydrocyanation.	257-276
Unit-15	Fisher- tropesch process, Ziegler-Natta polymerization- Syndiotactic and isotactic polymers.	277-286
Unit-16	Zeolites as shape selective catalysts. Clays as catalyst, pillard clays- advantages, decomposition of isopropanol using oxide catalysts, catalytic converters.	287-299

---

## COURSE INTRODUCTION

---

Symmetry plays an central role in the analysis of the structure, bonding, and spectroscopy of molecules. In this course, you will explore the basic symmetry elements and operations and their use in determining the symmetry classification (point group) of different molecules. Spectroscopy is the study of the interaction of electromagnetic radiation with matter.

Spectroscopy has many applications in the modern world, ranging from nondestructive examination of materials to medical diagnostic imaging (e.g., MRIs, CAT scans). In a chemical context, spectroscopy is used to study energy transitions in atoms and molecules. The transitions are interpreted and can serve to identify the molecule or give clues about the molecular structure. In this course you will explore in detail application of spectroscopic methods like IR, ESR, Mössbauer etc to the inorganic compounds you will also study the NMR spectroscopy other than  $^1\text{H}$ , like  $^{13}\text{F}$ ,  $^{31}\text{P}$   $^{11}\text{B}$  etc....

Thermal analysis is the techniques in which a physical property of a substance is measured as a function of temperature whilst the substance is subjected to a controlled temperature programme. In this course you will going to explore different thermal analysis techniques like, Thermogravimetry (TG); Differential thermal analysis (DTA); Differential scanning calorimetry (DSC); etc.... and their applications.

Catalysis typically provides the technology to enable the efficient and cost-effective synthesis of pharmaceutical products. By definition, catalysis increases the reaction rate by lowering the activation energy of the reaction, therefore allowing the chemical transformation to take place under much milder conditions over the uncatalyzed process. Furthermore, the catalyst typically imparts chemo-, regio-, or stereoselectivities over the course of the reaction to enable highly efficient syntheses of target molecules. in this course you will explore on the homogenous and heterogeneous inorganic catalyst for various industrial applications.

**UNIT-1****Structure**

1.0 Objectives of the unit

1.1 Introduction

1.2 Symmetry operations and symmetry elements

1.3 Rotation about an n-fold axis of symmetry

1.4 Reflection through a plane of symmetry (mirror plane)

1.5 Reflection through a centre of symmetry (inversion centre)

1.6 Identity operator

1.7 Successive operations

1.8 Point groups

1.8.1  $C_1$  point group

1.8.2  $C_{\infty v}$  point group

1.8.3  $D_{\infty h}$  point group

1.8.4  $T_d$ ,  $O_h$  and  $I_h$  point groups

1.9 Determining the point group of a molecule or molecular ion

a) Determination of the point group for trans- $N_2F_2$  molecule

b) Determination of the point group for  $PF_5$

c) Determination of the point group for  $POCl_3$

1.10 Summary of the unit

1.11 Key words

1.12 References for further studies

1.13 Questions for self understanding

## 1.0 Objectives of the unit

After studying this unit you are able to

- Explain the symmetry operations and symmetry elements
- Explain the rotation about an n-fold axis of symmetry
- Explain the reflection through a plane of symmetry (mirror plane)
- Explain the reflection through a centre of symmetry (inversion centre)
- Explain the identity operator
- Explain the successive operations
- Explain the point groups

## 1.1 Introduction

For understanding the chemistry of the molecules, symmetry is very important. Also, understanding of symmetry is essential in discussions of molecular spectroscopy and calculations of molecular properties. For qualitative purposes, it is sufficient to refer to the shape of a molecule using terms such as tetrahedral, octahedral or square planar. However, the common use of these descriptors is not always precise, e.g. consider the structures of  $\text{BF}_3$ , and  $\text{BF}_2\text{H}$ , both of which are planar. A molecule of  $\text{BF}_3$  is correctly described as being trigonal planar, since its symmetry properties are fully consistent with this description. all the F-B-F bond angles are  $120^\circ$  and the B-F bond distances are all identical (131 pm). It is correct to say that the boron centre in  $\text{BF}_2\text{H}$ , is in a pseudo-trigonal planar environment but the molecular symmetry properties are not the same as those of  $\text{BF}_3$ . The F-B-F bond angle in  $\text{BF}_2\text{H}$  is smaller than the two H-B-F angles, and the B-H bond is shorter (119 pm) than the B-F bonds (131 pm).



The descriptor symmetrical implies that a species possesses a number of indistinguishable configurations. When  $\text{BF}_3$  molecule is rotated in the plane of the paper through  $120^\circ$ , the resulting structure is indistinguishable from the first; another  $120^\circ$  rotation results in a third indistinguishable molecular orientation. This is not true if we carry out the same rotational operations on  $\text{BF}_2\text{H}$ .

Group theory is the mathematical treatment of symmetry. In this unit we are going familiar to the fundamental language of group theory ie, symmetry operator, symmetry element, point group and character table. The unit does not set out to give a comprehensive survey of molecular symmetry, but rather introduce some common terminology and its meaning.



## 1.2 Symmetry operations and symmetry elements

If we applied  $120^\circ$  rotations to  $\text{BF}_3$ , each rotation generate a representation of the molecule that was indistinguishable from the first. Each rotation is an example of a symmetry operation.



**Figure 1:** Rotation of the trigonal planar  $\text{BF}_3$  molecule through  $120^\circ$  generates a representation of the structure that is indistinguishable from the first

The *Symmetry Operation* is defined as A transformation in three-dimensional space that preserves the size and shape of a molecule, and which brings it into an orientation in three dimensional space physically indistinguishable from the original one, or

*A symmetry operation is an operation performed on an object which leaves it in a configuration that is indistinguishable from, and superimposable on, the original configuration.*

The rotations described in the above figure 1 were performed about an axis perpendicular to the plane of the paper and passing through the boron atom. The axis is an example of a symmetry element.

Thus *Symmetry element* is defined as the geometrical plane, point, or axis associated with a particular symmetry operation or set of symmetry operations.

There are many types of symmetry operation are performed for study of symmetry of the molecule they are

- 1) Rotation about an n-fold axis
- 2) Reflection through a plane of symmetry
- 3) Reflection through a centre of symmetry
- 4) Identity operator

## 1.3 Rotation about an n-fold axis of symmetry

The symmetry operation of rotation about an n-fold axis (the symmetry element) is denoted by the symbol ' $C_n$ ', in which the angle of rotation is  $\frac{360^\circ}{n}$ , where n is an integer, e.g. 2, 3 or 4. Applying this notation to the  $\text{BF}_3$  molecule in Figure 1 gives a value of  $n = 3$  say that the  $\text{BF}_3$  molecule contains a  $C_3$  rotation axis. In this case, the axis lies perpendicular to the plane containing the molecule.

$$\text{Angle of rotation} = 120^\circ = \frac{360^\circ}{n} \text{ ----- (1)}$$

In addition,  $\text{BF}_3$  also contains three 2-fold ( $C_2$ ) rotation axes, each coincident with a B-F bond as shown in Figure 2.

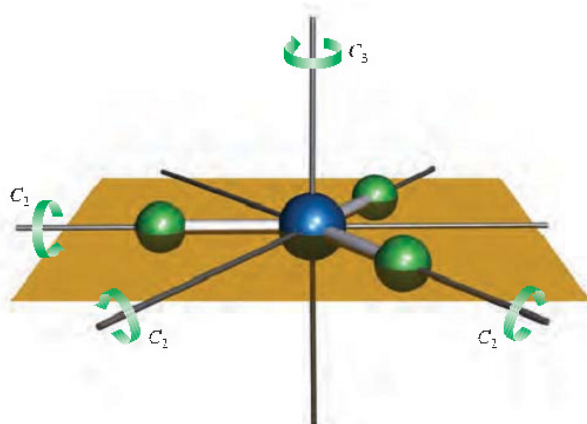


**Figure 2:** The 3-fold ( $C_3$ ) and three 2-fold ( $C_2$ ) axes of symmetry possessed by the trigonal planar  $\text{BF}_3$  molecule.

If a molecule possesses more than one type of  $n$ -axis, in such case *the axis of highest value of  $n$  is called the principal axis*. It is the axis of highest molecular symmetry. For example, in  $\text{BF}_3$ , the  $C_3$  axis is the principal axis.

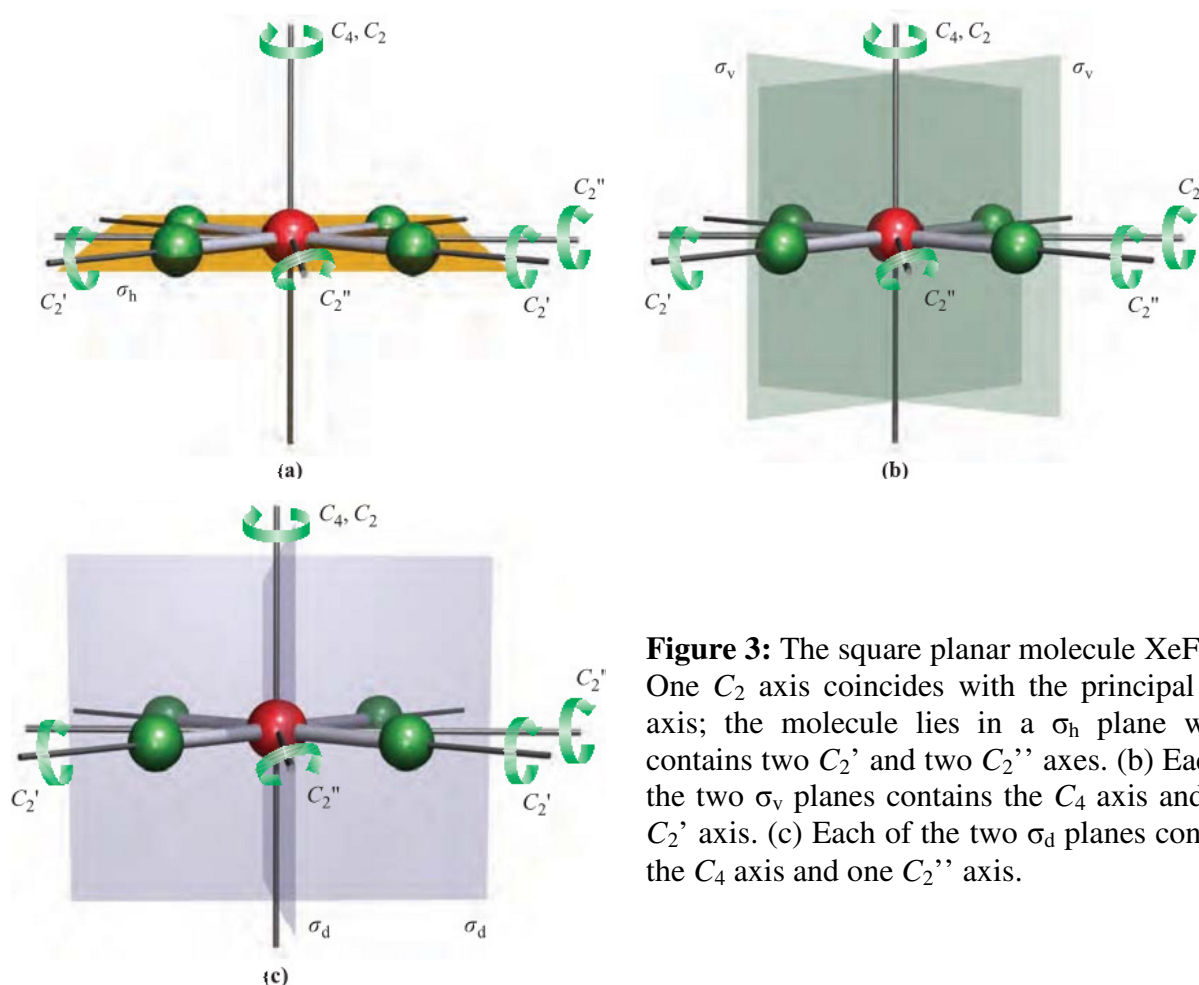


**Figure 3:** The square planar molecule  $\text{XeF}_4$ . (a) One  $C_2$  axis coincides with the principal ( $C_4$ ) axis; the molecule lies in a  $\sigma_h$  plane which contains two  $C_2'$  and two  $C_2''$  axes. (b) Each of the two  $\sigma_v$  planes contains the  $C_4$  axis and one  $C_2'$  axis. (c) Each of the two  $\sigma_d$  planes contains the  $C_4$  axis and one  $C_2''$  axis.

In some molecules, the principle axis also associated with lower order symmetry axis i.e, rotation axes of lower orders than the principal axis may be coincident with the principal axis. For example, in square planar  $\text{XeF}_4$ , the principal axis is a  $C_4$  axis but this also coincides with a  $C_2$  axis.

If a molecule contains more than one type of  $C_n$  axis, then they are distinguished by using prime marks, e.g.  $C_2$ ,  $C_2'$  and  $C_2''$ .

#### 1.4 Reflection through a plane of symmetry (mirror plane)

If reflection of all parts of a molecule through a plane produces an indistinguishable configuration, then the plane is called a plane of symmetry. The symmetry operation performed is a reflection and the symmetry element is a mirror plane and it is denoted by symbol ' $\sigma$ '. For  $\text{BF}_3$ , the plane containing the molecular framework is a mirror plane.

In such case, if the plane lies perpendicular to the vertical principal axis then it is denoted by the symbol ' $\sigma_h$ '.

The framework of atoms in a linear, bent or planar molecule can always be drawn in a plane, but this plane can be labelled as  $\sigma_h$  only if the molecule possesses a  $C_n$  axis perpendicular to the plane. If the plane contains the principal axis, it is labeled ' $\sigma_v$ '.

For example, consider the  $\text{H}_2\text{O}$  molecule. This possesses a  $C_2$  axis as shown in figure 4. But it also contains two mirror planes, one containing the  $\text{H}_2\text{O}$  framework, and one perpendicular to it. Each plane contains the principal axis of rotation and so may be denoted as  $\sigma_v$  but in order to distinguish between them, we use the notations  $\sigma_v$  and  $\sigma_v'$ . The  $\sigma_v$  label refers to the plane that bisects the H-O-H bond angle and the  $\sigma_v'$  label refers to the plane in which the molecule lies.

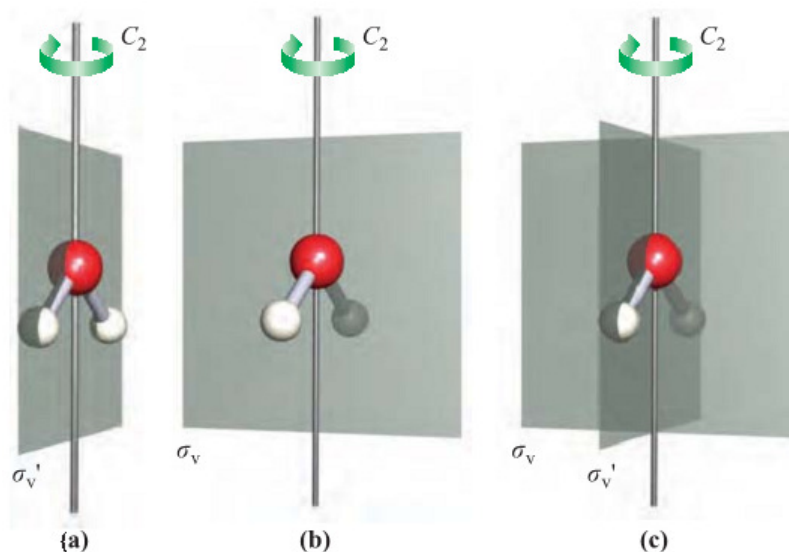


**Figure 4:** The  $\text{H}_2\text{O}$  molecule possesses one  $C_2$  axis and two mirror planes. (a) The  $C_2$  axis and the plane of symmetry that contains the  $\text{H}_2\text{O}$  molecule. (b) The  $C_2$  axis and the plane of symmetry that is perpendicular to the plane

A special type of plane which contains the principal rotation axis, but which bisects the angle between two adjacent 2-fold axes, is labelled  $\sigma_d$ . A square planar molecule such as  $\text{XeF}_4$  provides an example. Figure 3a shows that

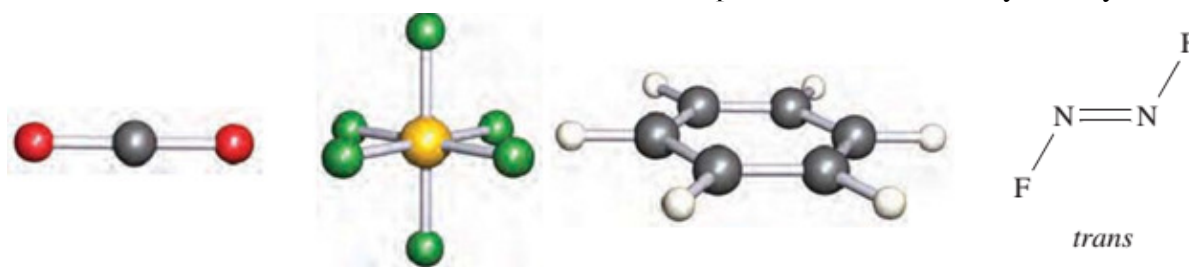
$\text{XeF}_4$  contains a  $C_4$  axis (the principal axis) and perpendicular to this is the  $h$  plane in which the molecule lies. Coincident with the  $C_4$  axis is a  $C_2$  axis. Within the plane of the molecule, there are two sets of  $C_2$  axes. One type (the  $C_2'$  axis) coincides with  $\text{F-Xe-F}$  bonds, while the second type (the  $C_2''$  axis) bisects the  $\text{F-Xe-F}$   $90^\circ$  angle. We can now define two sets of mirror planes. One type ( $\sigma_v$ ) contains the principal axis and a  $C_2'$  axis (Figure 3b), while the second type ( $\sigma_d$ ) contains the principal axis and a  $C_2''$  axis (Figure 3c). Each  $\sigma_d$  plane bisects the angle between two  $C_2'$  axes.

In the notation for planes of symmetry,  $\sigma$ , the subscripts  $h$ ,  $v$  and  $d$  stand for horizontal, vertical and dihedral respectively.

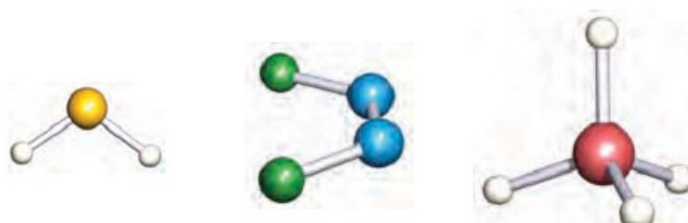
### 1.5 Reflection through a centre of symmetry (inversion centre)

If reflection of all parts of a molecule through the centre of the molecule produces an indistinguishable configuration, the centre is a centre of symmetry, also called a centre of inversion. It is designated by the symbol 'i' or 'I'.

Each of the molecules  $\text{CO}_2$ ,  $\text{trans-N}_2\text{F}_2$ ,  $\text{SF}_6$  and benzene possesses a centre of symmetry.



But  $\text{H}_2\text{S}$ ,  $\text{cis-N}_2\text{F}_2$  and  $\text{SiH}_4$  do not.



#### a) *Inversion Operation:*

One of the simplest symmetry operations encountered is the inversion operation, whose element is a single point in space. This operation puts a premium on the ability to recognize the origin of the coordinate system where all symmetry elements intersect. Several examples of molecules that contain inversion centers are shown in Figure 5

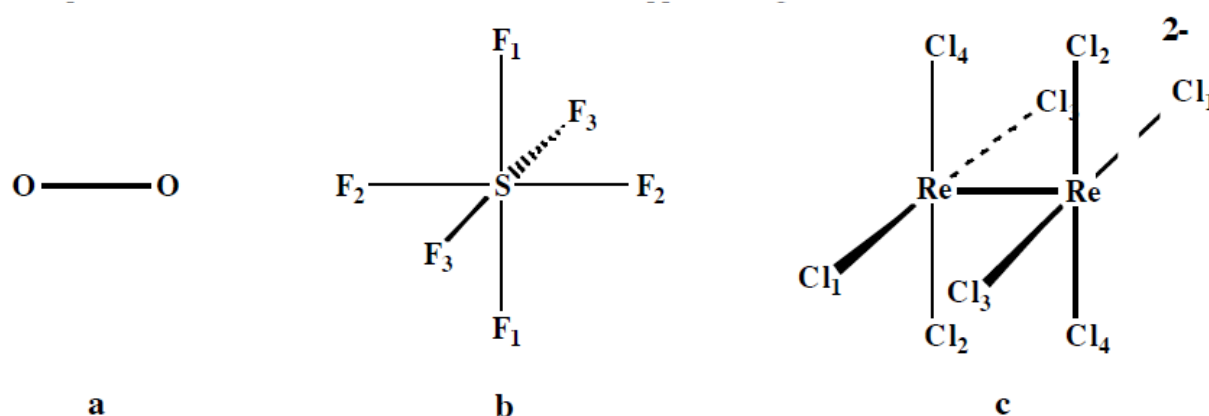


**Figure 5:** Examples of molecules that contain an inversion center a) dioxygen; b) sulfur hexafluoride; c) octachlorodirhenate (III) ion.

A center of inversion may be located at the center of an atom, such as on sulfur in  $\text{SF}_6$ , or between a pair of inversion related atoms, for example, midway between the O-O bond in  $\text{O}_2$  or the Re-Re bond in  $[\text{Re}_2\text{Cl}_8]^{2-}$ .

The inversion operation, denoted by symbol 'I' derives its name because it takes an atom with coordinates  $(x,y,z)$  and transforms them to the inverted position  $(-x,-y,-z)$ . The easiest way to perform this operation is to draw a line between an atom and the inversion center and then to continue this line an equal distance through the inversion center.

For example in figure 5, the three pairs of F atoms in  $\text{SF}_6$ , and the four pairs of Cl atoms related by the inversion operation have been denoted with subscripts 1,2, 3, and 4. The 6 F in  $\text{SF}_6$  and 8 Cl in  $[\text{Re}_2\text{Cl}_8]^{2-}$  are all equivalent. The inversion operation only relates pairs of atoms, or the unique sulfur atom to itself. Some molecules that look highly symmetrical, lack an inversion center, for example tetrahedral  $\text{TiCl}_4$  as shown in Figure 6.

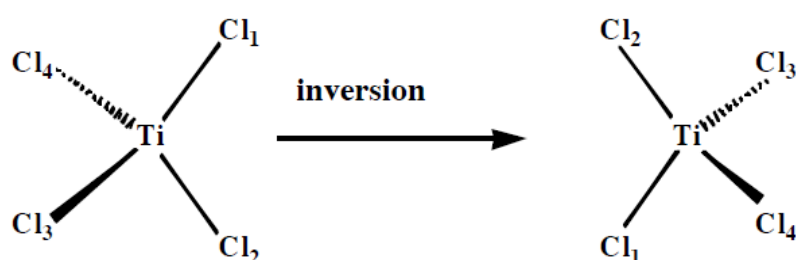


**Figure 6:** Illustration of the lack of an inversion center in a tetrahedral molecule, such as  $\text{TiCl}_4$

Application of the inversion operation centered at Ti produces an orientation distinguishable from the original one. The chlorine atoms in the drawing have been subscripted to illustrate

where the inversion operation moves them. Other examples of molecules that lack an inversion center are  $\text{BF}_3$ ,  $\text{HCl}$ , and trigonal bipyramidal  $\text{Fe}(\text{CO})_5$ .

b) *Rotation about an axis, followed by reflection through a plane perpendicular to this axis*

If rotation through  $\frac{360^\circ}{n}$  about an axis, followed by reflection through a plane perpendicular to that axis, yields an indistinguishable configuration, the axis is an  $n$ -fold rotation–reflection axis, also called an  $n$ -fold improper rotation axis. It is denoted by the symbol  $S_n$ . Tetrahedral species of the type  $\text{XY}_4$  (all Y groups must be equivalent) possess three  $S_4$  axes, and the operation of one  $S_4$  rotation–reflection in the  $\text{CH}_4$  molecule is illustrated in Figure 7.



**Figure 7:** An improper rotation (or rotation–reflection),  $S_n$ , involves rotation about  $\frac{360^\circ}{n}$  followed by reflection through a plane that is perpendicular to the rotation axis. The diagram illustrates the operation about one of the  $S_4$  axes in  $\text{CH}_4$ ; three  $S_4$  operations are possible for the  $\text{CH}_4$  molecule.

## 1.6 Identity operator

All objects can be operated upon by the identity operator  $E$ . This is the simplest operator and effectively identifies the molecular configuration. The operator  $E$  leaves the molecule unchanged.

## 1.7 Successive operations

As we know a particular symbol is used to denote a specific symmetry operation. For example, if say that  $\text{NH}_3$  possesses a  $C_3$  axis means that we can rotate the molecule through  $120^\circ$  results a molecular configuration that is indistinguishable from the first. And it takes three such operations to give a configuration of the  $\text{NH}_3$  molecule that exactly coincides with the first. The individual three  $120^\circ$  rotations are identified by using the notation in Figure 8. Actually it is difficult to distinguish between the three H atoms, but for clarity they are

labelled H(1), H(2) and H(3) in the figure. Since the third rotation,  $C_3$ , returns the  $\text{NH}_3$  molecule to its initial configuration, we can write equation 2, or, in general equation 3.

$$C_3^3 = E \text{ ----- } 2$$

$$C_n^n = E \text{ ----- } 3$$

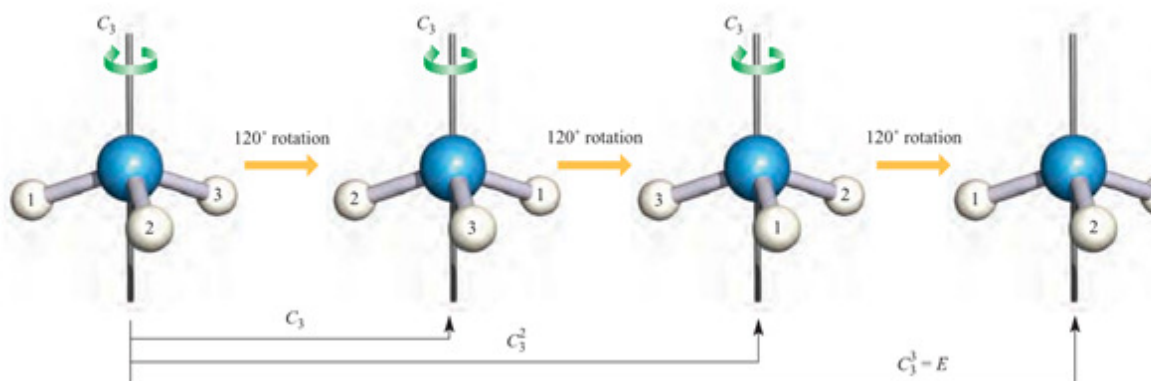


**Figure 8:** Successive  $C_3$  rotations in  $\text{NH}_3$  are distinguished using the notation  $C_3$ ,  $C_3^2$  and  $C_3^3$ . The effect of the last operation is the same as that of the identity operator acting on  $\text{NH}_3$  in the initial configuration.

Similar statements can be written to show the combined effects of successive operations. For example, in planar  $\text{BCl}_3$ , the  $S_3$  improper axis of rotation corresponds to rotation about the  $C_3$  axis followed by reflection through the  $\sigma_h$  plane. This can be written in the form of equation 4.

$$S_3 = C_3 X \sigma_h \text{ ----- } 4$$

### 1.8 Point groups

Point groups are a method of classifying the shapes of molecules according to their symmetry elements. Chemists classify molecules according to their symmetry. The collection of symmetry elements present in a molecule forms a “group”, typically called a point group. The question arising here is why is it called a “point group”? Because all the symmetry elements (points, lines, and planes) will intersect at a single point hence it is called point group.

Thus *each molecule has a set of symmetry operations that describes the molecule's overall symmetry. This set of operations defines the point group of the molecule.* The number and nature of the symmetry elements of a given molecule are conveniently denoted by its point group, and give rise to labels such as  $C_2$ ,  $C_{3v}$ ,  $D_{3h}$ ,  $D_{2d}$ ,  $T_d$ ,  $O_h$  or  $I_h$ . These point groups belong to the classes of  $C$  groups,  $D$  groups and Special groups, the latter containing groups that possess special symmetries, i.e. tetrahedral, octahedral and icosahedral.

It is important to note that the point groups to which a molecule belongs ultimately depends on its exact molecular geometry and its specific configuration and conformation. Without knowledge of the exact configuration or conformation, the determination of its point group is impossible. For example the staggered and eclipsed conformations of ethane, or the chair and boat conformations of cyclohexane have different symmetry properties. Similarly, the stereoisomers cis- and trans-1,2-dichlorocyclopropane have different configurations and therefore different symmetry properties belonging to different point groups.

The symmetry of a molecule in terms of one symmetry element (e.g. a rotation axis) provides information only about this property. For example, each of  $\text{BF}_3$  and  $\text{NH}_3$  possesses a 3-fold axis of symmetry, but their structures and overall symmetries are different.  $\text{BF}_3$  is trigonal planar and  $\text{NH}_3$  is trigonal pyramidal. On the other hand, description the symmetries of these molecules in terms of their respective point groups ( $D_{3h}$  and  $C_{3v}$ ), provides information about all their symmetry elements.

**Note:** It is not essential to memorize the symmetry elements of a particular point group. Which are widely available and are listed in character tables. Table 1 summarizes the most important classes of point group and gives their characteristic types of symmetry elements; E is, of course, common to every group.

**Table 1** Characteristic symmetry elements of some important classes of point groups. The characteristic symmetry elements of the  $T_d$ ,  $O_h$  and  $I_h$  are omitted because the point groups are readily identifiable. No distinction is made in this table between  $\sigma_v$  and  $\sigma_d$  planes of symmetry.

Point group	Characteristic symmetry elements	Comments
$C_s$	E, one $\sigma$ plane	
$C_i$	E, inversion centre	
$C_n$	E, one (principal) $n$ -fold axis	
$C_{nv}$	E, one (principal) $n$ -fold axis, $n$ $\sigma_v$ planes	
$C_{nh}$	E, one (principal) $n$ -fold axis, one $\sigma_h$ plane, one $S_n$ -fold axis which is coincident with the $C_n$ axis	The $S_n$ axis necessarily follows from the $C_n$ axis and $\sigma_h$ plane. For $n = 2, 4$ or $6$ , there is also an inversion centre.
$D_{nh}$	E, one (principal) $n$ -fold axis, $n$ $C_2$ axes, one $\sigma_h$ plane, $n$ $\sigma_v$ planes, one $S_n$ -fold axis	The $S_n$ axis necessarily follows from the $C_n$ axis and $\sigma_h$ plane. For $n = 2, 4$ or $6$ , there is also an inversion centre.
$D_{nd}$	E, one (principal) $n$ -fold axis, $n$ $C_2$ axes, $n$ $\sigma_v$ planes, one $S_{2n}$ -fold axis	For $n = 3$ or $5$ , there is also an inversion centre.
$T_d$		Tetrahedral
$O_h$		Octahedral
$I_h$		Icosahedral

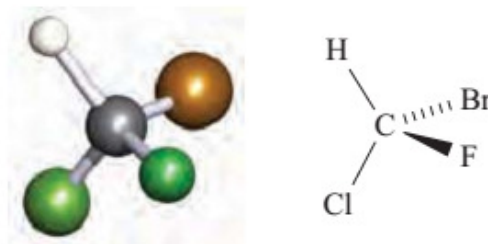
Some particular features of significance are given below.

### 1.8.1 $C_1$ point group

Molecules that appear to have no symmetry at all must possess the symmetry element E and effectively possess at least one  $C_1$  axis of rotation. Therefore they belong to the  $C_1$  point



group, although since  $C_1 = E$ , the rotational symmetry operation is ignored when we list the symmetry elements of this point group.



### 1.8.2 $C_{\infty v}$ point group

$C_{\infty}$  signifies the presence of an  $\infty$ -fold axis of rotation, i.e. that possessed by a linear molecule (Figure 9). For the molecular species to belong to the  $C_{\infty v}$  point group, it must also possess an infinite number of  $\sigma_v$  planes but no  $\sigma_h$  plane or inversion centre. These criteria are met by asymmetrical diatomics such as HF, CO and [CN], and linear polyatomic molecules that do not possess a centre of symmetry, e.g. OCS and HCN.

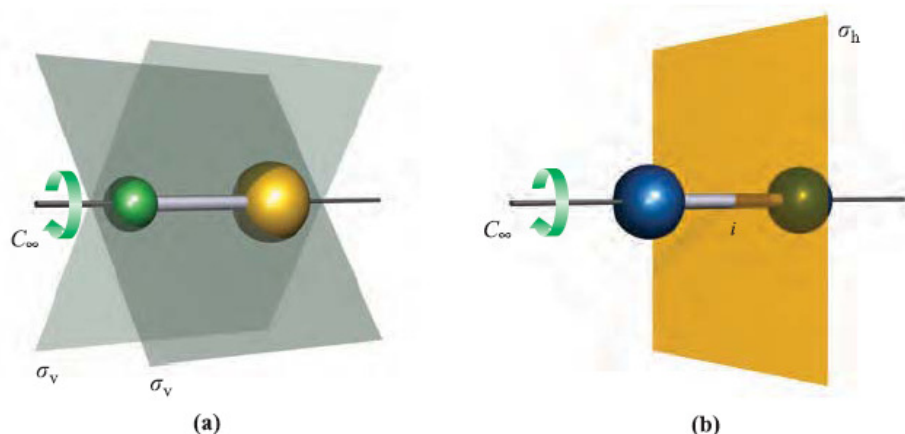


**Figure 9:** Linear molecular species can be classified according to whether they possess a centre of symmetry (inversion centre) or not. All linear species possess a  $C_{\infty}$  axis of rotation and an infinite number of  $\sigma_v$  planes. In (a) two such planes are shown and these planes are omitted from (b) for clarity. Diagram (a) shows an asymmetrical diatomic belonging to the point group  $C_{\infty v}$ , and (b) shows a symmetrical diatomic belonging to the point group  $D_{\infty h}$ .

### 1.8.3 $D_{\infty h}$ point group

Symmetrical diatomics (e.g.  $H_2$ ,  $[O_2]^{2-}$ ) and linear polyatomics that contain a centre of symmetry (e.g.  $[N_3]^-$ ,  $CO_2$ ,  $HC\equiv CH$ ) possess a  $\sigma_h$  plane in addition to a  $C_{\infty}$  axis and an infinite number of  $\sigma_v$  planes. These species belong to the  $D_{\infty h}$  point group.

### 1.8.4 $T_d$ , $O_h$ and $I_h$ point groups

Molecular species that belong to the  $T_d$ ,  $O_h$  or  $I_h$  point groups possess many symmetry elements (Figure 10), although it is seldom necessary to identify them all before the appropriate point group can be assigned. Species with tetrahedral symmetry include  $SiF_4$ ,

$[\text{ClO}_4]$  ,  $[\text{CoCl}_4]^{2-}$   $[\text{NH}_4]^+$  ,  $\text{P}_4$  and  $\text{B}_4\text{Cl}_4$ . Those with octahedral symmetry include  $\text{SF}_6$ ,  $[\text{PF}_6]^-$  ,  $\text{W}(\text{CO})_6$  and  $[\text{Fe}(\text{CN})_6]^{3-}$



**Figure 10:** The tetrahedron ( $T_d$  symmetry), octahedron ( $O_h$  symmetry) and icosahedron ( $I_h$  symmetry) possess four, six and twelve vertices respectively, and four, eight and twenty equilateral-triangular faces respectively.

There is no centre of symmetry in a tetrahedron but there is one in an octahedron, and this distinction has consequences with regard to the observed electronic spectra of tetrahedral and octahedral metal complexes. Members of the icosahedral point group are uncommon, e.g.  $[\text{B}_{12}\text{H}_{12}]^{2-}$  shown in figure 11.

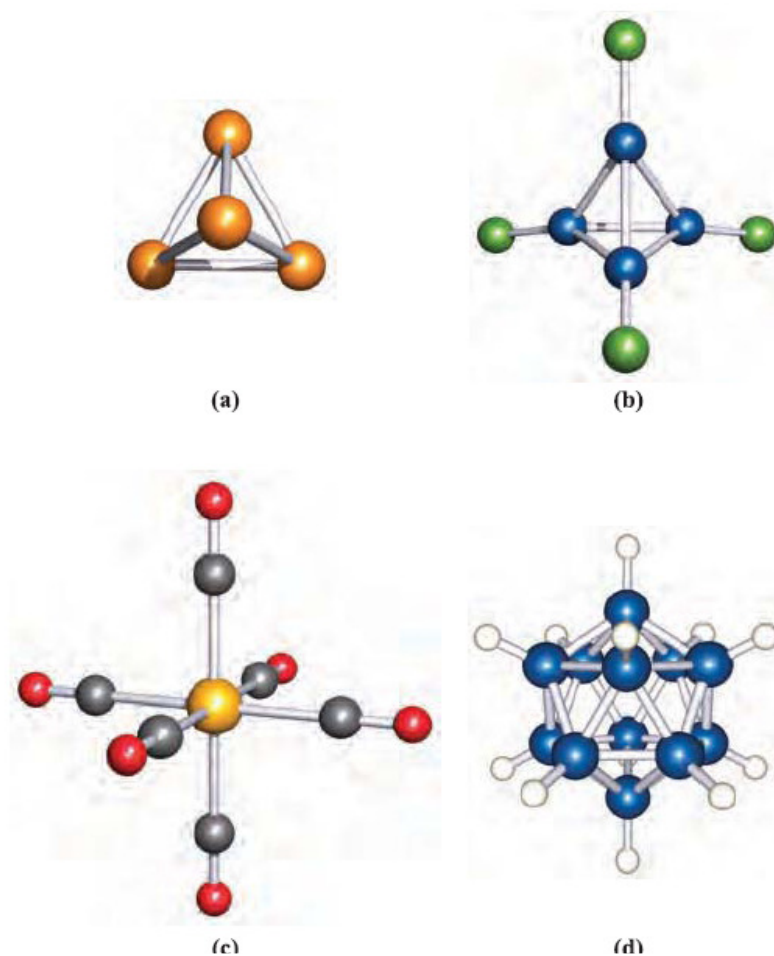


**Figure 11:** The molecular structures of (a)  $\text{P}_4$ , (b)  $\text{B}_4\text{Cl}_4$  (c)  $[\text{W}(\text{CO})_6]$  and (d)  $[\text{B}_{12}\text{H}_{12}]^{2-}$

### 1.9 Determining the point group of a molecule or molecular ion

The application of a systematic approach is essential for the assignment of a point group, otherwise the symmetry elements will be missed, as a consequence an incorrect assignment is made. Figure 12 shows a procedure that may be adopted. Some of the less common point groups (e.g.  $S_n$ ,  $T$ ,  $O$ ) are omitted from this. Notice that it is not necessary to find all the symmetry elements (e.g. improper axes) in order to determine the point group.

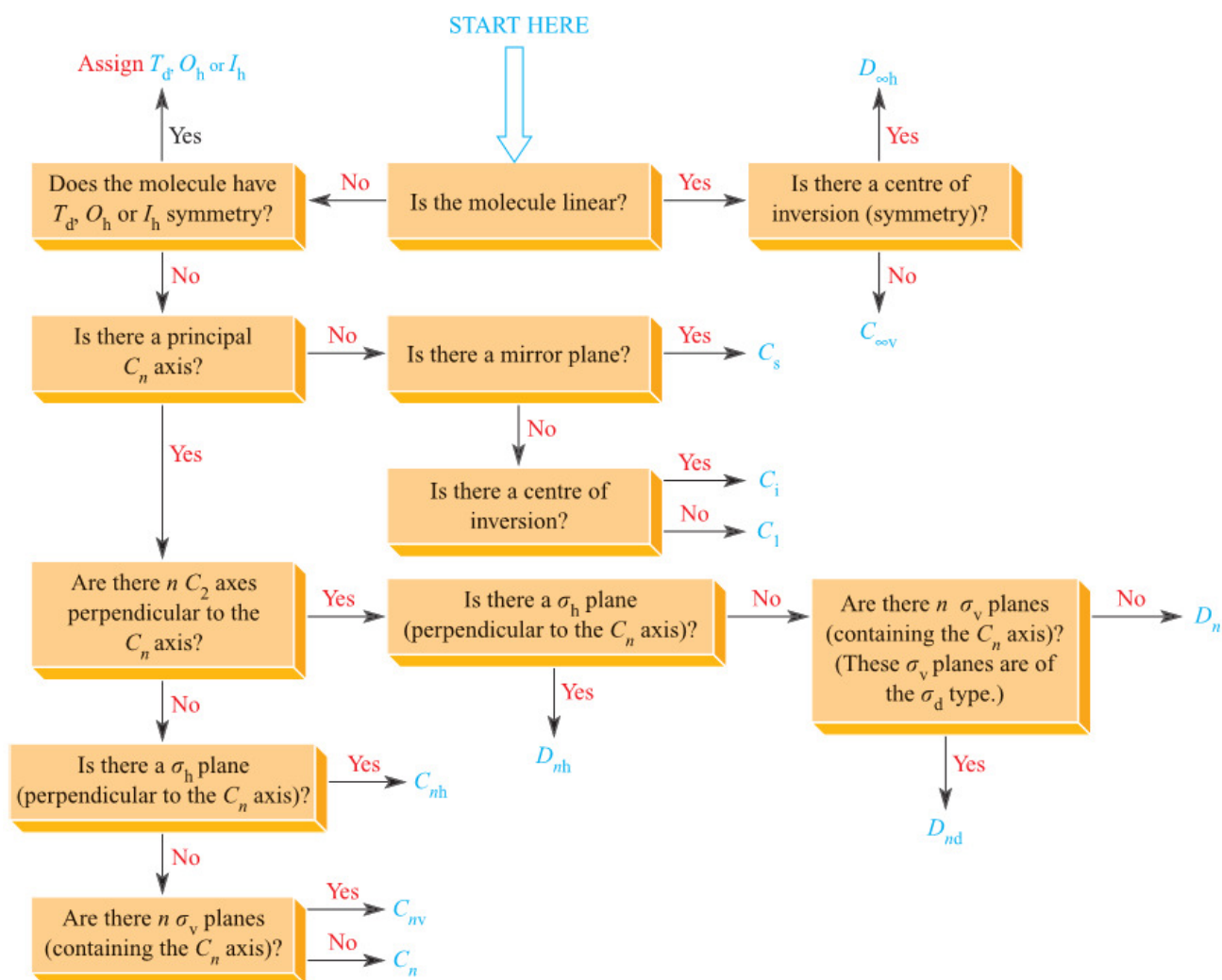


**Figure 12:** Scheme for assigning point groups of molecules and molecular ions. Apart from the cases of  $n = 1$  or  $\infty$ ,  $n$  most commonly has values of 2, 3, 4, 5 or 6.

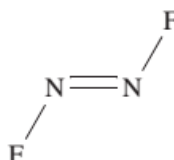
Let us illustrate the application of Figure 10 using some worked examples. Before assigning a point group to a molecule, it is necessary to determine its structure by microwave spectroscopy, or X-ray, electron or neutron diffraction, etc.... methods.

#### a) Determination of the point group for trans- $N_2F_2$ molecule

First draw the structure.

Apply the strategy shown in Figure 12

**START**

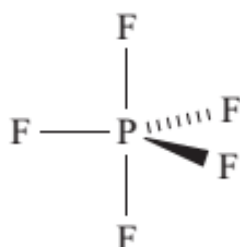


- 1) Is the molecule linear?  $\implies$  No
- 2) Does trans-N<sub>2</sub>F<sub>2</sub> have  $T_d$ ,  $O_h$  or  $I_h$  symmetry?  $\implies$  No
- 3) Is there a  $C_n$  axis?  $\implies$  Yes; ( a  $C_2$  axis perpendicular the plane of the paper and passing through the midpoint of the N=N bond)
- 4) Are there two  $C_2$  axes perpendicular to the principal axis?  $\implies$  No
- 5) Is there a  $\sigma_h$  plane (perpendicular to the principal axis)?  $\implies$  Yes **STOP**

*The point group is  $C_{2h}$ .*

**b) Determination of the point group for PF<sub>5</sub>**

First, draw the structure.



It is important to remember that in the trigonal bipyramidal arrangement, the three equatorial F atoms are equivalent, and the two axial F atoms are equivalent.

Apply the strategy shown in Figure 12

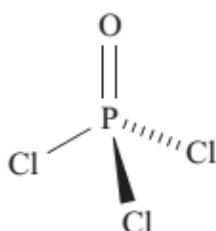
**START**

- 1) Is the molecule linear?  $\implies$  No
- 2) Does PF<sub>5</sub> have  $T_d$ ,  $O_h$  or  $I_h$  symmetry?  $\implies$  No
- 3) Is there a  $C_n$  axis?  $\implies$  Yes ( a  $C_3$  axis containing the P and two axial F atoms)
- 4) Are there three  $C_2$  axes perpendicular to the principal axis?  $\implies$  Yes (each lies along a P-Feq bond)
- 5) Is there a  $\sigma_h$  plane (perpendicular to the principal axis)?  $\implies$  Yes (it contains the P and three F eq atoms).  $\implies$  **STOP**

*The point group is  $D_{3h}$ .*

**c) Determination of the point group for POCl<sub>3</sub>**

First, draw the structure



Apply the strategy shown in Figure 12.

### START

- 1) Is the molecule linear?  $\implies$  No
- 2) Does  $\text{POCl}_3$  have  $T_d$ ,  $O_h$  or  $I_h$  symmetry?  $\implies$  No

(Remember that although this molecule is closely considered as being tetrahedral in shape, it does not possess tetrahedral symmetry)

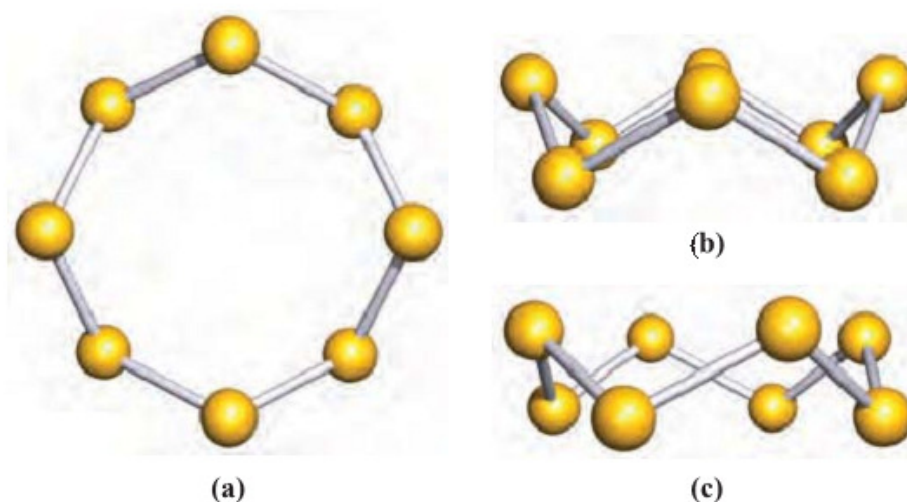
- 3) Is there a  $C_n$  axis?  $\implies$  Yes ( a  $C_3$  axis running along the O-P bond)
- 4) Are there 3  $C_2$  axes perpendicular to the principal axis?  $\implies$  No
- 5) Is there a  $\sigma_h$  plane (perpendicular to the principal axis)?  $\implies$  No
- 6) Are there n  $\sigma_v$  planes (containing the principal axis)?  $\implies$  Yes (each contains the one Cl and the O and P atoms.  $\implies$  **STOP**)

*The point group is  $C_{3v}$ .*

### d) Determination of the point group for cyclic structure of $S_8$

First, draw the structure

Three projections of the cyclic structure of  $S_8$  are shown below. All S-S bond distances and all S-S-S bond angles are equivalent.



### START

- 1) Is the molecule linear?  $\implies$  No
- 2) Does  $S_8$  have  $T_d$ ,  $O_h$  or  $I_h$  symmetry?  $\implies$  No
- 3) Is there a  $C_n$  axis?  $\implies$  Yes ( a  $C_4$  axis running through the centre of the ring, perpendicular to the plane of the paper in diagram (a))
- 4) Are there 4  $C_2$  axes to the principal axis?  $\implies$  Yes (these are most easily seen from diagram (c))
- 5) Is there a  $\sigma_h$  plane (perpendicular to the principal axis)?  $\implies$  No

- 6) Are there  $n$   $\sigma_d$  planes (containing the principal axis)?  $\implies$  Yes (these are most easily seen from diagrams (a) and (c)  $\implies$  STOP

*The point group is  $D_{4d}$ .*

### 1.10 Summary of the unit

The symmetry of molecules is important for understanding the structures and properties of compounds. In chemistry, many phenomena may be easily explained by consideration of symmetry. The systematic discussion of symmetry is called group theory.

Atoms or groups in molecules are called symmetry equivalent if they have the same atomic number or chemical constitution, and if they can be transposed into each other by the application of symmetry operations. This equivalency plays an important role in the chemical properties of these atoms or groups, and in the process of stereo differentiation of these positions.

Symmetry operations are geometrical operations applied to molecules. The application of a symmetry operation to a particular molecular geometry produces a spatial orientation which is indistinguishable from the initial orientation. For example, rotating a water ( $H_2O$ ) molecule by  $180^\circ$  about an axis bisecting the H-O-H bond angle will produce a orientation of that molecule which looks the same as its original orientation. In fact, this rotation leads to an exchange of both protons  $H_a$  and  $H_b$ , but as these two protons may not be distinguished from each other, the resulting orientation of the water molecule is equivalent to the initial one. Another rotation of  $180^\circ$  about this axis leads to an orientation which is identical to the starting geometry.

The five basic symmetry operations that need to be considered are identity, rotation, reflection (mirroring), inversion, and rotary reflection. The symmetry properties of molecules are described as the set (combination) of valid symmetry operations for its molecular geometry. For each symmetry operation there is a corresponding symmetry element, with respect to which the symmetry operation is applied. For example, the rotation (a symmetry operation) is carried out around an axis which is the corresponding symmetry element. Other symmetry elements are planes (for reflections) and points (for inversions). All spatial points along these symmetry elements (i.e. the symmetry plane, axis, or center of inversion) do not change their positions during the corresponding symmetry operation. Common to all symmetry operations is that the geometrical center of a molecule does not change its position, all symmetry elements must intersect in this center. In fact, out of the five symmetry operations mentioned above only two (rotation and rotary reflection) are sufficient to describe all symmetry properties of molecules.

### Identity Operation (E)

The identity operation does nothing and leaves any molecule unchanged, the corresponding symmetry element is the entire object (molecule) itself. The reason for including this symmetry operation is that some molecules have only this symmetry element and no other symmetry properties. Another reason is the logical completeness of the mathematical description of group theory.

All molecules which do not have any other symmetry element than the identity operation must belong to the  $C_1$  point group (see below), and thus must be chiral. Many natural compounds like carbohydrates and  $\alpha$ -amino acids belong to this group. However, all molecules belonging to the  $C_1$  point group must be chiral, but the reverse conclusion is not true. Chiral molecules may not necessarily be a member of the  $C_1$  point group family.

### Inversion (i)

The inversion (the symmetry operation) through a center of inversion (the symmetry element, which must be identical to the center of geometry of the molecule) takes any point in the molecule, moves it to the center, and then moves it out the same distance on the other side again (sometimes called point reflection). The benzene molecule, a cube, and spheres do have a center of inversion, whereas a tetrahedron does not.

At this point, it should be noted, that molecules which contain a center of inversion as the only symmetry element (except for the identity operation, which occurs in all molecules), belong to the  $C_i$  point group. However, if a center of inversion is present in a molecular geometry, the corresponding compound must be achiral, irrespective of any other type or number of symmetry elements (mirror planes, rotation or rotary-reflection axes) which may be present in addition.

### Reflection ( $\sigma$ )

The reflection (the symmetry operation) in a plane of symmetry or mirror plane  $\sigma$  (the corresponding symmetry element) produces a mirror image geometry of the molecule (this symmetry operation is not present in chiral molecules). The mirror plane bisects the molecule and must include its center of geometry. If this plane is parallel to the principal axis, it is called a vertical mirror plane denoted  $\sigma_v$ , if it is perpendicular to the principal axis, it is denoted a horizontal mirror plane  $\sigma_h$ . Vertical mirror planes bisecting the angle between two  $C_n$  axes are called dihedral mirror planes  $\sigma_d$ .

The benzene molecule features all three different types of mirror planes for benzene  $\sigma_v$  and  $\sigma_d$  planes coincide.

Molecules which contain a single mirror plane as the only symmetry element belong to the  $C_s$  point group, but any number of mirror planes will automatically result in achiral molecular geometries.

#### n-Fold rotation $C_n$

The n-fold rotation (the symmetry operation) about a n-fold axis of symmetry (the corresponding symmetry element) produces molecular orientations indistinguishable from the initial for each rotation of  $360^\circ/n$  (clockwise and counter-clockwise). A water molecule has a single  $C_2$  axis bisecting the H-O-H bond angle, and benzene has one  $C_6$  axis (amongst one  $C_3$  axis and seven  $C_2$  axes of which the  $C_3$  and one  $C_2$  axis coincide with the  $C_6$  axis). Linear molecules display a  $C_\infty$  axis (any infinitely small rotation about this axis produces unchanged orientations), and perfect spheres possess an infinite number of symmetry axes along any diameter with all possible integral values of n. If a molecule has one (or more) rotation axes  $C_n$  or  $S_n$ , the axis with the greatest n is called the principal axis.

#### n-Fold rotary reflection ( $S_n$ )

The n-fold rotary reflection (or n-fold improper rotation, the symmetry operation) about an n-fold rotary reflection axis (or n-fold axis of improper rotation) is composed of two successive geometry transformations: first, a rotation through  $360^\circ/n$  about the axis of that rotation, and second, reflection through a plane perpendicular (and through the molecular center of geometry) to that axis. Neither of these two operations (rotation or reflection) alone is a valid symmetry operation, but only the outcome of the combination of both transformations.

For example, a methane molecule has three  $S_4$ . Any molecule featuring a  $S_n$  axis must be achiral. In fact, the most general description of chirality is the absence of any  $S_n$  rotary reflection in a molecular geometry.

Out of the five symmetry operations mentioned above only two (rotation and rotary reflection) are sufficient to describe all symmetry properties of molecules. The identity operation is equivalent to a  $C_1$  axis of rotation, as rotation of all objects around  $360^\circ$  about any axis produces the initial orientation only. On the other hand, a mirror plane is equivalent to a  $S_1$  axis of rotary-reflection perpendicular to that plane. In addition, a center of inversion can be represented by a  $S_2$  axis of improper rotation with any arbitrary orientation of this axis. Symmetry operations may not be combined arbitrarily with each other, but only in a limited number of variations which are the so called point groups. Some symmetry operations implicitly imply others, as for example any  $S_4$  or  $C_4$  axis must be accompanied by a parallel  $C_2$  axis. For example in benzene, the principal  $C_6$  axis simultaneously must be a  $C_3$  and a  $C_2$



axis of symmetry, too. Similarly, any  $S_n$  axis with odd  $n$  is identical to a  $C_n$  axis in conjunction with a horizontal mirror plane  $\sigma_h$ .

However, certain combinations of some symmetry operations implicitly generate other symmetries. For example, the combination of any  $C_n$  axis with even  $n$ , together with a center of inversion  $i$  implicitly generates a horizontal mirror plane  $\sigma_h$  (which is perpendicular to the  $C_n$  axis and runs through the inversion center). Similarly, the combination of any  $C_n$  axis with a vertical mirror plane  $\sigma_v$  must imply  $(n - 1)$  additional vertical mirror planes  $\sigma_v$ .

In addition, combinations of two rotation axes or two rotary-reflection axes must imply a new rotation axis, and combining a rotation axis with a rotary-reflection generates another rotary-reflection axis.

### 1.11 Key words

Symmetry operations; Symmetry elements;  $n$ -fold axis of symmetry; Plane of symmetry (mirror plane); Centre of symmetry (inversion centre); Identity operator; Point groups;  $C_1$  point group;  $C_{\infty v}$  point group;  $D_{\infty h}$  point group;  $T_d$ ,  $O_h$  and  $I_h$  point groups

### 1.12 References for further studies

- 1) Group theory and Symmetry in Chemistry; Gurdeep Raj; Ajay Bhagi; Vinod Jain; *Krishna Prakashan Media*; **2012**.
- 2) Symmetry: An Introduction to Group Theory and Its Applications; R. McWeeny; *Courier Corporation*, **2002**.
- 3) Symmetry and Group theory in Chemistry; M Ladd; *Elsevier*, **1998**.
- 4) Molecular Symmetry and Group Theory; Robert L. Carter; *Wiley India Pvt. Limited*, **2009**.
- 5) Introduction to Symmetry and Group Theory for Chemists; Arthur M. Lesk; *Springer Science & Business Media*, **2007**.
- 6) Group Theory and Chemistry; David M. Bishop; *Courier Corporation*, **2012**.

### 1.13 Questions for self understanding

- 1) Benzene, borazine, pyridine and  $S_6$  contain a 6-membered ring. Explain why only benzene contains a 6-fold principal rotation axis?
- 2) Among the following, which molecule contain a 4-fold principal rotation axis:  $CF_4$ ,  $SF_4$ ,  $[BF_4]^-$  and  $XeF_4$ . Explain why?
- 3) Draw the structure of  $[XeF_5]^-$ . On the diagram, mark the  $C_5$  axis. The molecule contains five  $C_2$  axes. Where are these axes located?
- 4) Draw the structure of  $B_5H_9$ . Where is the  $C_4$  axis located in this molecule?
- 5)  $N_2O_4$  is planar. Show that it possesses three planes of symmetry.

- 6)  $B_2Br_4$  has the following staggered structure. Show that  $B_2Br_4$  has one less plane of symmetry than  $B_2F_4$  which is planar.
- 7)  $Ga_2H_6$  has the following structure in the gas phase. Show that it possesses three planes of symmetry.
- 8) Show that the planes of symmetry in benzene are one  $\sigma_h$ , three  $\sigma_v$  and three  $\sigma_d$ .
- 9) Draw the structures of each of the following species and confirm that each possesses a centre of symmetry.  $CS_2$ ,  $[PF_6]^-$ ,  $XeF_4$ ,  $I_2$ ,  $[ICl_2]^-$ .
- 10)  $[PtCl_4]^{2-}$  has a centre of symmetry, but  $[CoCl_4]^{2-}$  does not. One is square planar and the other is tetrahedral. Which is which? Explain why?
- 11) Why does  $CO_2$  possess an inversion centre, but  $NO_2$  does not?
- 12)  $CS_2$  and  $HCN$  are both linear. Explain why  $CS_2$  possesses a centre of symmetry whereas  $HCN$  does not?
- 13) Explain why  $BF_3$  possesses an  $S_3$  axis, but  $NF_3$  does not.
- 14)  $C_2H_6$  in a staggered conformation possesses an  $S_6$  axis. Show that this axis lies along the C–C bond.
- 15) The  $CH_4$  molecule has 3  $S_4$  axes. On going from  $CH_4$  to  $CH_2Cl_2$ , are the  $S_4$  axes retained? Justify your answer.
- 16) How do the rotation axes and planes of symmetry in cis- and trans- $N_2F_2$  and  $HFC=CHF$  differ?
- 17) How many planes of symmetry do (a)  $F_2C=O$ , (b)  $ClFC=O$  and (c)  $[HCO_2]$  possess?
- 18) The symmetry operators for  $NH_3$  are  $E$ ,  $C_3$  and  $3\sigma_v$ . (a) Draw the structure of  $NH_3$ . (b) What is the meaning of the  $E$  operator? (c) Draw a diagram to show the rotation and reflection symmetry operations.
- 19) What symmetry operators are lost in going from  $NH_3$  to  $NH_2Cl$ ?
- 20) Compare the symmetry operators possessed by  $NH_3$ ,  $NH_2Cl$ ,  $NHCl_2$  and  $NCl_3$ .
- 21) Draw a diagram to show the symmetry operators of  $NCIF_2$ .
- 22) Write a note on symmetry operations and symmetry elements
- 23) With an example explain the rotation about an n-fold axis of symmetry
- 24) With an example explain the reflection through a plane of symmetry (mirror plane)
- 25) With an example explain the reflection through a centre of symmetry (inversion centre)
- 26) What are identity operators?
- 27) What are successive operations?
- 29) What are Point groups?
- 30) Explain the followings with suitable example

- a)  $C_1$  point group.
  - b)  $C_{\infty v}$  point group
  - c)  $D_{\infty h}$  point group
  - d)  $T_d$ ,  $O_h$  and  $I_h$  point groups
- 31) Explain the procedure followed for determining the point group of a molecule.
- 32) Determine the point group for trans- $N_2F_2$  molecule.
- 33) Determine the point group for  $PF_5$  molecule.
- 34) Determine the point group for  $POCl_3$  molecule.

**UNIT-2****Structure**

- 2.0 Objectives of the unit
- 2.1 Introduction
- 2.2 Properties of a group
- 2.3 Abelian and non- abelian group
- 2.4 Oder of a group (h)
- 2.5 Group generating elements
- 2.6 Sub Group
- 2.7 Class of a Group [Classes in a group]
- 2.8 An important note on classes
- 2.9 Group multiplication tables for symmetry operation of simple molecules
- 2.10 Isomorphism
- 2.11.1 Similarity transformation
- 2.12 Classes
- 2.13 Group multiplication table
- 2.13 Important characteristics of a group multiplication table
- 2.14 Symmetry classification of molecules into point groups
- 2.15 Difference between point group and space group
- 2.16 Summary of the unit
- 2.17 Keywords
- 2.18 References for further studies
- 2.19 Questions for self understanding

## 2.0 Objectives of the unit

After studying this unit you are able to

- List the different properties of a group
- Explain the differences between abelian and non-abelian groups
- Calculate the order of given group (h)
- Recognize the group generating elements

## 2.1 Introduction

A subgroup is a “group within another group”- a subset of group elements. A supergroup is a group obtained by adding new elements to a group (to give a larger group). The order of any subgroup  $g$  of a group of order  $h$  must be a divisor of  $h$ :  $h/g = k$  where  $k$  is an integer.

$A$  is said to be conjugate with  $B$ , if there exists any element of the group,  $X$ , such that (i)  $A = X^{-1}BX$ . Every element is conjugate with itself. (ii) If  $A$  is conjugate with  $B$ , then  $B$  is conjugate with  $A$ . (iii) If  $A$  is conjugate with  $B$  and  $C$ , then  $B$  and  $C$  are conjugate with each other.

A complete set of elements that are conjugate to one another within a group is called a class of the group. The number of elements in a class is called its order. The orders of all classes must be integral factors of the order of the group

## 2.2 Properties of a group

The elements of all groups obey a simple set of rules. These rules are

1. The product of any two elements of a group must also be an element of the group.

Ex. Consider  $C_{2v}$  group

$$\sigma_v^1 \times \sigma_v = C_2$$

2. Products of elements are associative (Associative law).

Ex. Consider  $C_{2v}$  group

$$(\sigma_v^1 \times \sigma_v)C_2 = \sigma_v^1(\sigma_v \times C_2)$$

[Note: According to correction the multiplication inside the brackets is carried out first]

3. The group contain an element which when used to multiply any other element leaves it unchanged such an element is called identity and represent by the letter  $E$  (or  $I$ )

Ex.  $C_2 * E = E * C_2 = C_2$

4. Each element of a group has an inverse which is also an element of the group.

Ex. In  $C_{3v}$  group  $C_3$  and  $C_3^{-1}$  are inverse of one another.

$C_3 = C_3^{-1}$ ,  $E$  is its own inverse

### 2.3 Abelian and non-abelian group

An abelian group is one in which all the elements commute with each i.e for any two elements P and Q

$$P*Q = Q*P$$

Ex.  $C_{2v}$  group  $\rightarrow$  elements are E,  $C_2$  and  $\sigma_v, \sigma_v^1$

$$C_2 \times \sigma_v = \sigma_v^1 \sigma_v * C_2 = \sigma_v^1$$

$$\therefore C_2 * \sigma_v = \sigma_v * C_2$$

Similarly

$$\sigma_v * \sigma_v^1 = \sigma_v^1 * \sigma_v = C_2$$

$\therefore C_{2v}$  group an Abelian group

There are only a few abelian group. Some examples are:  $C_n, S_n, C_{nn}, C_{2v}, D_2$  and  $D_{2h}$ .  $D_{3h}$  is a non abelian group.

### 2.4 Oder of a group (h)

The order of the group is similarly the total number of elements in the group. For example, in  $C_{2v}$  group the order is four there are some elements namely E,  $C_2, \sigma_v$  and  $\sigma_v^1$ . In  $C_{3v}$  there are six elements E,  $C_3, C_3^2, \sigma_v, \sigma_v^1, \Delta\sigma_v^{11}$  therefore the ordering  $C_{3v}$  is six.

### 2.5 Group generating elements

In a given group there will be a small minimum number of elements called a 'subset'. The elements of this subset are called group generating elements or group generators. These group generators can generate all the elements of the group.

Example.

i)  $C_3$  group has the elements  $E, C_3^1, C_3^2, C_3^1$  is the group generate

$$C_3^1 * C_3^2 = C_3^2$$

$$C_3^1 * C_3^1 * C_3^1 * C_3^1 = E$$

ii) In  $C_{2v}$  group  $\sigma_v$  and  $\sigma_v^1$  are group generator elements

$$\sigma_v * \sigma_v = E, \quad \sigma_v * C_2 = \sigma_v, \quad \sigma_v * E = C_2$$

iii)  $D_{3h}$  has twelve elements of symmetry

$$E, C_3^1, C_3^2, C_2, C_2^1, C_2^{11}, \sigma_v, \sigma_v^1, \sigma_v^{11}, \sigma_n, S_3^1, S_3^5$$

The group generating elements are  $C_3^1, C_2$  perpendicular to  $C_3^1$  and  $\sigma_n$

[Group generating elements or group generators will be useful in arriving at the point group of a molecule.]

## 2.6 Sub Group

Smaller groups which can be found within a bigger group are called subgroups. The subgroup must obey all the condition to be called a group. There are two types of subgroups, they are

1) Trivial subgroup, in which there is only one element E and the order of this subgroup is one.

2) Non trivial subgroup, in which elements E is invariably present and order of these groups begin with two

If the order of the subgroup is 'g' and that of full group is 'h' then  $h/g=k$  where 'k' is an integer

Examples.

i.  $C_1$  group has no subgroup it has only element E.

ii.  $C_{2v}$  ( elements  $E, \sigma_n, \sigma'_v, C_2$ ) has trivial subgroup E and more subgroups

$$C_2 \rightarrow E, C_2$$

$$C_2 \rightarrow E, \sigma_v (\Delta C_s^1 \longrightarrow E, \sigma_v^1)$$

iii.  $C_{3v}$  (elements  $E, C_3, C_3^2, \sigma_v, \sigma'_v, \sigma''_v$ )  $h=6$  the subgroups are

	$g$	$h/g$
$C_1 \rightarrow E$	1	6
$C_3 \rightarrow E, C_3^1, C_3^2$	3	2
$C_s \rightarrow E, \sigma_v$	2	3
$C_s^1 \rightarrow E, \sigma_v^1$	2	3
$C_s^{11} \rightarrow E, \sigma_v^{11}$	2	3

Note:

1. All subgroup contain the element E.

2. The elements of a full group may or may not commute but elements of subgroup do necessarily commute. Therefore the subgroups are always Abelian.

## 2.7 Class of a Group [Classes in a group]

We have already seen how it is possible to select sets of elements constituting subgroup. There is another way of sorting out elements of a point group into what is called classes in order to understand how to rearrange elements into classes we need to know a new operation called '*similarity transformation*'

If A and B are the elements of a group and X is another elements of the same group such that  $X^{-1}AX = B$  where  $X^{-1}$  is the inverse X.

The product B is called 'similarity transform of A by X. A and B are called conjugate elements. the following are three elements is conjugate elements

1. Every element is conjugate with itself  $X^{-1}AX = A$ .
2. If A is conjugate with B then B is conjugate with  $AX^{-1}AX = B$ . B is the similarity transform of A by X. Also there must be an element Y in the group such that

$$Y^{-1}BY = A, \text{ i.e } A \text{ is the similarity transforms of B by Y.}$$

3. If A is conjugate with B and C then B and C conjugate with each other (Law of Associative conjugation)

$$\text{i.e if } X^{-1}AX = B \text{ and } Y^{-1}AY = C \text{ then } X^{-1}BX = C \text{ and } Y^{-1}CY = B.$$

A class of a group is now defined as 'a set of elements which are conjugate to one another'.

Example:  $C_{3v} \rightarrow E, C_3^1, C_3^2, \sigma_v, \sigma_v', \sigma_v''$

Work out the similarity transform of each of the above six elements with every other element. Also use the group multiplication table of  $C_{3v}$  group to work out the products of similarity information.

Since  $\sigma_v, \sigma_v', \sigma_v''$  are their own inverse and  $C_3^1$  and  $C_3^2$  are the inverse of each other the following similarity transformation can be written on E, to begin with

$$\begin{array}{c} \underline{\mathbf{E}} \\ E \quad E \quad E = E \\ C_3^2 \quad E \quad C_3^1 = E \\ C_3^1 \quad E \quad C_3^2 = E \\ \sigma_v \quad E \quad \sigma_v = E \\ \sigma_v' \quad E \quad \sigma_v' = E \\ \sigma_v'' \quad E \quad \sigma_v'' = E \end{array}$$

In all these transformation E has come out as its own similarity transformation i.e, E is self conjugate. Therefore the conclusion from this exercise is that E is in a class by itself and the order of this class is always one, irrespective of the point group it belongs to. This class is called 'trivial class'

The similar transformation of  $C_3^1, C_3^2$  can be worked out as given below



$C_3^1$			$C_3^2$		
$E$	$C_3^1$	$E = C_3^1$	$E$	$C_3^2$	$E = C_3^2$
$C_3^2$	$C_3^1$	$C_3^1 = C_3^1$	$C_3^2$	$C_3^2$	$C_3^1 = C_3^2$
$C_3^1$	$C_3^1$	$C_3^2 = C_3^1$	$C_3^1$	$C_3^2$	$C_3^2 = C_3^2$
$\sigma_v$	$C_3^1$	$\sigma_v = C_3^1$	$\sigma_v$	$C_3^2$	$\sigma_v = C_3^2$
$\sigma_v'$	$C_3^1$	$\sigma_v' = C_3^1$	$\sigma_v'$	$C_3^2$	$\sigma_v' = C_3^2$
$\sigma_v''$	$C_3^1$	$\sigma_v'' = C_3^1$	$\sigma_v''$	$C_3^2$	$\sigma_v'' = C_3^2$

From these two exercises it is clear that  $C_3^1$  and  $C_3^2$  are mutually conjugate hence they can be in one class. The order of this class is 2. We can similarly work through the exercises for  $\sigma_v, \sigma_v', \sigma_v''$  but the product transformation will not be that straight forward

$\sigma_v$			$\sigma_v'$			$\sigma_v''$		
$E$	$\sigma_v$	$E = \sigma_v$	$E$	$\sigma_v'$	$E = \sigma_v'$	$E$	$\sigma_v''$	$E = \sigma_v''$
$C_3^2$	$\sigma_v$	$C_3^1 = \sigma_v''$	$C_3^2$	$\sigma_v'$	$C_3^1 = \sigma_v$	$C_3^2$	$\sigma_v''$	$C_3^1 = \sigma_v'$
$C_3^1$	$\sigma_v$	$C_3^2 = \sigma_v'$	$C_3^1$	$\sigma_v'$	$C_3^2 = \sigma_v''$	$C_3^1$	$\sigma_v''$	$C_3^2 = \sigma_v$
$\sigma_v$	$\sigma_v$	$\sigma_v = \sigma_v$	$\sigma_v$	$\sigma_v'$	$\sigma_v = \sigma_v''$	$\sigma_v$	$\sigma_v''$	$\sigma_v = \sigma_v'$
$\sigma_v'$	$\sigma_v$	$\sigma_v' = \sigma_v''$	$\sigma_v'$	$\sigma_v'$	$\sigma_v' = \sigma_v'$	$\sigma_v'$	$\sigma_v''$	$\sigma_v' = \sigma_v$
$\sigma_v''$	$\sigma_v$	$\sigma_v'' = \sigma_v'$	$\sigma_v''$	$\sigma_v'$	$\sigma_v'' = \sigma_v$	$\sigma_v''$	$\sigma_v''$	$\sigma_v'' = \sigma_v''$

All the planes  $\sigma_v, \sigma_v', \sigma_v''$  are in one class of order three. While working out the similarity transformation on one of these planes say  $\sigma_v$ , if the product transformation occur as  $\sigma_v, \sigma_v', \sigma_v''$  then it is not really necessary to carry through the exercise on  $\sigma_v'$  and  $\sigma_v''$ . By recourse to property of associative conjugation one can conclude that the three planes can be put into one class i.e the plane ( $\sigma_v$ ) and its two products transforms.  $\sigma_v'$  and  $\sigma_v''$

Since similarity transformation involves the sequential operation of three elements, it is sometimes difficult to work out the product transforms. We can adopt one of the two following methods i.e,

- i) Use of groups multiplication tables and/or
- ii) Use of the molecular geometry for figurative illustration as shown below

Similarly transforms of  $C_3^1$

$$\sigma_v C_3^1 \sigma_v = C_3^2 \text{ or}$$

$$(\sigma_v C_3^1) \sigma_v = \sigma_v' \sigma_v = C_3^2$$

$C_3$  axes and  $\sigma_v$  planes are as in (I) planes always retain their orientation with respect to the original configuration (I) of the molecule. Axes and planes do not move with operation. It is rather easy to visualize the transforms of  $C_3^1$  and  $C_3^2$ . And for  $\sigma_v, \sigma'_v$  and  $\sigma''_v$  planes the transformation such as

$$\begin{array}{lll} E\sigma_v E = \sigma_v & E\sigma'_v E = \sigma'_v & E\sigma''_v E = \sigma''_v \\ \sigma_v\sigma_v\sigma_v = \sigma_v & \sigma'_v\sigma'_v\sigma'_v = \sigma'_v & \sigma''_v\sigma''_v\sigma''_v = \sigma''_v \end{array}$$

## 2.8 An important note on classes

A perusal of all the point groups reveals that there are only six types of Abelian groups and all others are non-Abelian. The Abelian groups are

$$C_n, C_{nh}, C_{2v}, D_2, D_{2h} \text{ and } S_n (n = \text{even})$$

Based on this information we can further state

- i. In all Abelian point groups each element is in a class by itself i.e the number of symmetry elements of order  $o$  of the group is equal to the number of classes.  
Number of classes =  $h$  (order of the group)
- ii. In non-Abelian groups the number of classes is always less than the order of a group.
- iii. No element of the group occurs in more than one class.

*Some hints on classes*

- i. E is always in a class by itself i.e, E is transformed into itself by all the elements of the group.
- ii. Inversion elements 'I' is in a class by itself.
- iii. All  $C_n^m$  axes are in a class.
- iv. Similar  $C_2$ s are in one class.
- v.  $S_n^m$  axes like  $C_n^m$  are in a class if there are two or more many such types, they are placed in as many classes.
- vi. Similar vertical planes ( $\sigma_v$ ) and similar dihedral planes ( $\sigma_d$ ) are in separate classes.
- vii. Horizontal plane is a special plane ( $\sigma_h$ ) and is always placed in a different class from other planes.

## 2.9 Group multiplication tables for symmetry operation of simple molecules

Group Multiplication Table (GMT) represents all possible products of elements of a group in the form of a table.

Consider a molecule having 'h' symmetry elements. Then there will be 'h<sup>2</sup>' products of symmetry elements. These can be presented as GMT. This consists of 'h' rows and 'h' columns. Each row and each column is tabulated with a group element. The entry in the table under a given column in a given row is the product of elements which head that column and that row. The operation which first applied is in the top of the column.

Example,  $C_{2v}$ ----- E,  $C_2$ ,  $\sigma_v$ ,  $\sigma_v'$

$C_{2v}$	E	$C_2$	$\sigma_v$	$\sigma_v'$
E	E	$C_2$	$\sigma_v$	$\sigma_v'$
$C_2$	$C_2$	E	$\sigma_v'$	$\sigma_v$
$\sigma_v$	$\sigma_v$	$\sigma_v'$	E	$C_2$
$\sigma_v'$	$\sigma_v'$	$\sigma_v$	$C_2$	E

$C_4$	E	$C_4^2 = C_2$	$C_4^1$	$C_4^3$
E	E	$C_2$	$C_4^1$	$C_4^3$
$C_4^2 = C_2$	$C_2$	E	$C_4^3$	$C_4^1$
$C_4^1$	$C_4^1$	$C_4^3$	$C_2$	E
$C_4^3$	$C_4^3$	$C_4^1$	E	$C_2$

This group with its GMTs written either way is isomorphic only with an abstract group  $G_2^4$  of the same order consisting of E A B and C elements. The one-to-one correlation of their elements is thus given as

$$A \longleftrightarrow C_2; B \longleftrightarrow C_4^1; C \longleftrightarrow C_4^3$$

Like A of  $G_2^4$ ,  $C_2$  is its own inverse and  $C_4^1$  and  $C_4^3$  have their inverse in each other, in much the same way as do B and C. similarly  $S_4$  group like  $C_4$  can also be shown as isomorphic with  $G_2^4$ . The GMT of  $S_4$  group is given as:

$S_4$	$E$	$C_2$	$S_4^1$	$S_4^3$
$E$	$E$	$C_2$	$S_4^1$	$S_4^3$
$C_2$	$C_2$	$E$	$S_4^3$	$S_4^1$
$S_4^1$	$S_4^1$	$S_4^3$	$C_2$	$E$
$S_4^3$	$S_4^3$	$S_4^1$	$E$	$C_2$

In  $G_1^4$  since each element A, B or C is its own inverse the above mentioned one-to-one correlation of its elements with those of  $G_2^4$  as well as  $C_4$  is found to be absent. Therefore  $G_1^4$  is not isomorphic with  $G_2^4$  and  $C_4$ . However a numerical group formed from a set of four elements 1, -1, I and -I is isomorphic with both  $C_4$  and  $G_2^4$ .

The only groups of order four that are isomorphic with  $G_1^4$  are  $C_{2h}$ ,  $C_{2v}$  and  $D_2$  whose multiplication tables are given below.

$C_{2h}$	$E$	$C_{2(z)}$	$\sigma_{xy}$	$i$
$E$	$E$	$C_{2(z)}$	$\sigma_{xy}$	$i$
$C_{2(z)}$	$C_{2(z)}$	$E$	$i$	$\sigma_{xy}$
$\sigma_{xy}$	$\sigma_{xy}$	$i$	$E$	$C_{2(z)}$
$i$	$i$	$\sigma_{xy}$	$C_{2(z)}$	$E$

One of the important uses of GMT is in grouping a set of elements into a class particularly in non-Abelian groups, where a class may contain more than one element in it. Abelian or cyclic groups however have only one element in each class. Consider the GMT for a non-Abelian group  $C_{3v}$  of order six.

$C_{2v}$	$E$	$C_{2(z)}$	$\sigma_{xz}$	$\sigma_{yz}$
$E$	$E$	$C_{2(z)}$	$\sigma_{xz}$	$\sigma_{yz}$
$C_{2(z)}$	$C_{2(z)}$	$E$	$\sigma_{yz}$	$\sigma_{xz}$
$\sigma_{xz}$	$\sigma_{xz}$	$\sigma_{yz}$	$E$	$C_{2(z)}$
$\sigma_{yz}$	$\sigma_{yz}$	$\sigma_{xz}$	$C_{2(z)}$	$E$

$D_2$	$E$	$C_{2(z)}$	$C_{2(x)}$	$C_{2(y)}$
$E$	$E$	$C_{2(z)}$	$C_{2(x)}$	$C_{2(y)}$
$C_{2(z)}$	$C_{2(z)}$	$E$	$C_{2(y)}$	$C_{2(x)}$
$C_{2(x)}$	$C_{2(x)}$	$C_{2(y)}$	$E$	$C_{2(z)}$
$C_{2(y)}$	$C_{2(y)}$	$\sigma_{xy}$	$C_{2(z)}$	$E$

The GMTs such as above can be used with lot of advantage for determining the product elements of similarity transformation.

### 2.10 Isomorphism

Two groups are supposed to be isomorphic if they obey the following rules.

1. Both have same order and structure.
2. There is a one-to-one correspondence in all respects between the members of the two groups.

If  $A_1, B_1, C_1, D_1$  and  $A_2, B_2, C_2, D_2$  are the members of the two isomorphic groups,  $A_1$  corresponds to  $A_2$ ,  $B_1$  corresponds to  $B_2$  and so on.

3. The relationship between the any two members of a group is exactly the same as the relationship between the corresponding members of the other group.

Let us take the three groups listed below:

(i)  $E, C_2$

(ii)  $E, i$

(iii)  $E, \sigma_h$

All the three are isomorphic groups.

$$E = C_2^2 ; C_2E = C_2$$

$$E = i^2 ; iE = i$$

$$E = \sigma_h^2 ; \sigma_hE = \sigma_h \text{ etc.}$$

### 2.11.1 Similarity transformation

Let  $A$  and  $X$  be the elements of a group and let us define  $B$  such that  $B = X^{-1}AX$ .  $B$  is called the similarity transform of  $A$  by  $X$ , or  $A$  is said to be subjected to similarity transformation with respect to  $X$ . If  $A$  and  $B$  are related by a similarity transformation they are called *conjugate* elements (Figure 1).

Take the  $\text{NH}_3$  molecule, for instance.  $Z$  axis is the  $C_3$  axis.

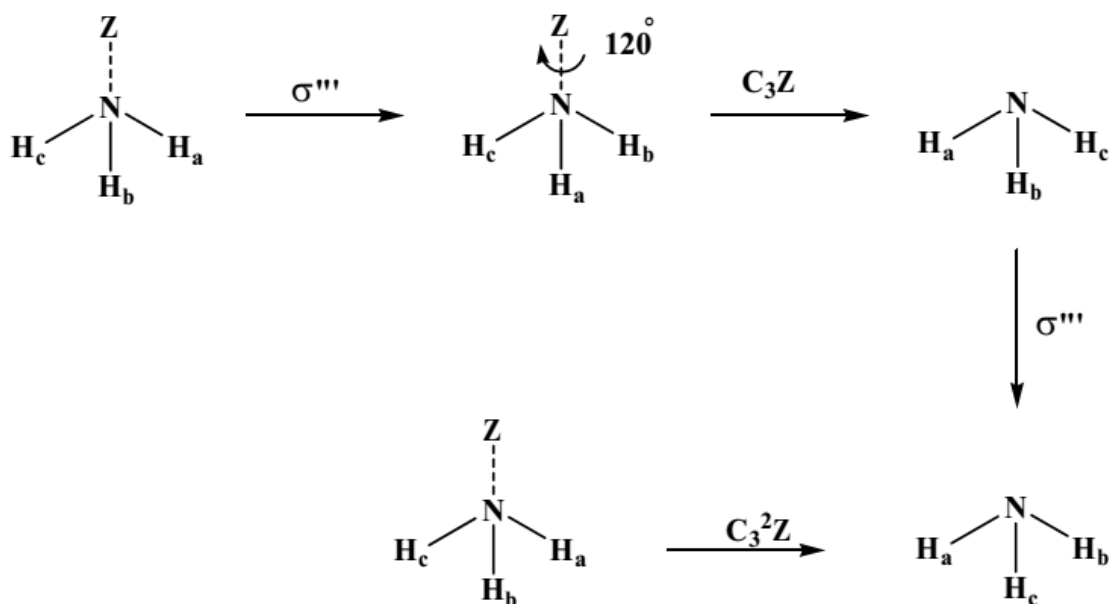


**Figure 1:** Illustration of similarity transformation on  $\text{NH}_3$

There are three reflection planes. These are usually designated as follows

1. Plane formed by z-axis and  $\text{NH}_a$  bond:  $\sigma'$  or  $\sigma_a$  or  $\sigma_v'$ .
2. Plane formed by z-axis and  $\text{NH}_b$  bond:  $\sigma''$  or  $\sigma_b$  or  $\sigma_v''$ .
3. Plane formed by z-axis and  $\text{NH}_c$  bond:  $\sigma'''$  or  $\sigma_c$  or  $\sigma_v'''$ .

Let us prefer the designation  $\sigma'$ ,  $\sigma''$  and  $\sigma'''$ .

Let us perform a reflection ( $\sigma'''$ ) with respect to the plane formed by  $\text{NH}_c$  and z-axis. Let us perform  $\sigma$  again.  $\sigma''''^2 = E$ .

Now let us find the similarity transform of  $C_3$  w.r.t.  $\sigma'''$ , i.e.,  $(\sigma''')^{-1}C_3\sigma''' = ?$

It is seen from the Fig. that  $(\sigma''')^{-1}C_3\sigma''' = C_3^2$ . Remember  $(\sigma''') = (\sigma''')^{-1}$ . Thus  $C_3$  and  $C_3^2$  are conjugate elements.

The following rules about conjugate elements are notable

1. Every element is conjugate of itself because every element is the similarity transforms of itself w.r.t. identity ( $E$ ):  $E = E^{-1}$  and  $A = E^{-1}AE$ .
2. If A is the conjugate of B then B is the conjugate of A. This means that if A is the similarity transform of B by X, B is the similarity transform of A by  $X^{-1}$ . We have  $A = X^{-1}BX$

But  $(X^{-1})^{-1}AX^{-1} = XAX^{-1} = X(X^{-1}BX)X^{-1}$   
 $= (XX^{-1})B(XX^{-1}) = B$  (associative law)

3. If A is the conjugate of B and B is the conjugate of C, then A, B and C are mutually conjugate.

## 2.12 Classes

A complete set of elements which are conjugate to one another is called a class of the group. Let us consider  $\text{NH}_3$ . Set up the coordinate system in such a manner that  $\text{ZNH}_a$  is in the  $yz$  plane. (Fig. 1)  $\sigma'$  is then  $\sigma_{yz}$ . Without disturbing the  $\text{NH}_3$  molecule rotate the coordinate system by  $120^\circ$  w.r.t  $z$  axis, i.e., subject the coordinate system to  $C_3$ . Now  $yz$  plane is  $\text{ZNH}_b$ .  $\sigma_{yz}$  is  $\sigma'$ ,  $\sigma''$  and  $\sigma'''$  are equivalent.  $\sigma'$  becomes same as that of  $\sigma''$  if we change the coordinate system by a symmetry operation ( $C_3$ ) of the point group.  $\sigma'$  and  $\sigma''$  are therefore in the same class.

Example:

Show that the three reflections of  $\text{NH}_3$  constitute a class. It is not difficult to show that

$$C_3^2 C_3 = E. \text{ Hence, } C_3^2 = (C_3)^{-1}$$

Let us perform the similarity transformation of  $\sigma'$  by  $C_3$  in  $\text{NH}_3$ .

$$C_3^{-1} \sigma' C_3 = C_3^2 \sigma' C_3 = \sigma''$$

Thus  $\sigma'$  and  $\sigma''$  are conjugate. Similarly we can show that  $\sigma'$ ,  $\sigma''$  and  $\sigma'''$  are mutually conjugate. Therefore  $\sigma'$ ,  $\sigma''$  and  $\sigma'''$  form a class.

## 2.13 Group multiplication table

Every group is characterized by a multiplication table. The relationship between the elements of the binary combinations is reflected in the multiplication table.

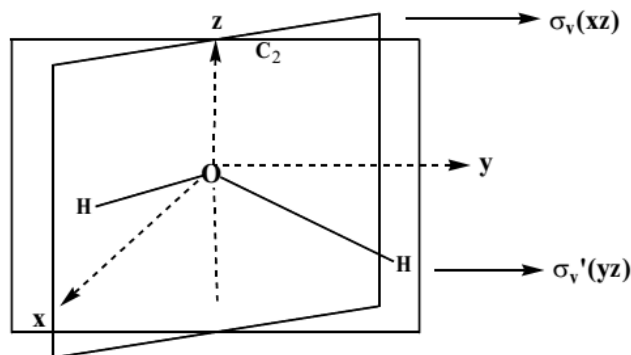


**Figure 2:** The Four symmetry elements of  $\text{H}_2\text{O}$  molecules

Consider a water molecule. It has four symmetry elements, viz.,  $E$ ,  $C_2(z)$ ,  $\sigma_v(xz)$  and  $\sigma_v'(yz)$  (Figure 2).

We can easily show that the product of any two symmetry elements is one of the four elements of the group. Thus, for instance,  $C_2(z)\sigma_v(xz) = \sigma_v'(yz)$ . Proceeding this way the symmetry operations of  $\text{H}_2\text{O}$  can be listed in a group multiplication table (GMT) as shown below

	E	$C_2(z)$	$\sigma_v(xz)$	$\sigma_v'(yz)$
E	E	$C_2(z)$	$\sigma_v(xz)$	$\sigma_v'(yz)$
$C_2(z)$	$C_2(z)$	E	$\sigma_v'(yz)$	$\sigma_v(xz)$
$\sigma_v(xz)$	$\sigma_v(xz)$	$\sigma_v'(yz)$	E	$C_2(z)$
$\sigma_v'(yz)$	$\sigma_v'(yz)$	$\sigma_v(xz)$	$C_2(z)$	E

### 2.13 Important characteristics of a group multiplication table

1. It consists of  $h$  rows and  $h$  columns where  $h$  is the order of the group.
2. Each column and row is labeled with group element.
3. The entry in the table under a given column and along given row is the product of the elements which head that column and the row (multiplication rule is strictly followed).
4. At the intersection of the column labeled by  $Y$  and the row labeled by  $X$ , we found the element which is the product  $XY$ .
5. The following rearrangement theorem holds good for every 'Group Multiplication Table'.  
"Each row and each column in the table lists each of the group elements once and only once. No two rows may be identical nor any two columns be identical. Thus each row and each column is a rearranged list of the group elements".

### 2.14 Symmetry classification of molecules into point groups

Molecules can be classified into point groups depending on the characteristic set of symmetry elements possessed by them. A molecular group is called a point group since all the elements of symmetry present in the molecule intersect at a common point and this point remains fixed under all the symmetry operations of the molecule. The symmetry groups of the molecules are denoted by specific symbols known as Schoenflies notations.

### 2.15 Difference between point group and space group

Symmetry operations do not alter the energy of the molecule. Further in all the above operations the centre of the molecule is not altered as none of the operations involve a total translational movement of the molecule. Whatever happens to the molecule, the centre (point) is not changed. At least one point is fixed. Hence these are classified as 'point group' operations.

In case of crystals operations such as 'screw rotations' and glide plane reflections can be additionally specified. Screw rotation involves a rotation with respect to an axis and then a translation in the direction of the same axis. Glide plane reflection is a reflection in a plane followed by a translation along a line in that plane. These are particular to crystals and the classification comes under what is known as space group. Note that here even the centre



changes. Thus in short, in point group, there is at least one point (centre) which is not altered after all operations while in space group it is not possible to identify such a stationary point.

### 2.16 Summary of the unit

A group is a complete set of members which are related to each other by certain rules. Each member may be called an element.

#### *Basic properties of a group*

Certain rules have to be satisfied by the elements so that they form a group. The rules are listed below

1. The product of any two elements and the square of any element must be elements of group. This property of the group is called closure property.
2. There must be one element in the group which commutes with every one of the elements and leaves it unchanged.
3. The associative law of multiplication should be valid.
4. For every element there must be a reciprocal (inverse) and this reciprocal is also an element of the group.

#### *Rule 1*

If  $A$  and  $B$  are the element of the group and if  $AB = C$ ,  $C$  must be a member of the group. Product  $AB$  means that we perform the operation  $B$  first and then operation  $A$  i.e., the sequence of operations is from right to left. It should be noted that the other product  $BA$  need not be same as  $AB$ .

$BA$  means doing  $A$  first and then performing the operation  $B$  later. Let  $BA = D$ .  $D$  must be a member of the group by rule 1. Usually  $AB \neq BA$  and so  $C \neq D$ . However, there may be some special elements  $A$  and  $B$  each that  $AB = BA$ . Then  $A$  and  $B$  are said to commute with each other or the multiplication of  $A$  and  $B$  is commutative. Such a group where any two elements commute is called an abelian group.

$H_2O$  belongs to an abelian group. The four symmetry operations for  $H_2O$  are  $E$ ,  $C_{2z}$ ,  $\sigma_{v(xz)}$  and  $\sigma'_{v(yz)}$ . The inter-relationships between these operations are given in the group multiplication table.

#### *Rule 2*

Each group must necessarily have an element which commutes with every other element of the group and leaves it unchanged.

Let  $A$  and  $B$  be the elements of the group. Let  $X$  be the element satisfying rule 2.

i.e.  $XA = AX = A$  and also  $XB = BX = B$ .

$BA = BX^2A$ ;  $BX^2 = B = BE$ , where we have set  $X^2 = E$  (identity)

It is clear  $BE^n = B$ ,  $n$  being any integer. This kind of element  $E$  which does not effect any change when multiplied with any element is a unique element and is called an identity operation  $E$ . For water,  $E$ , the identity operation satisfies this rule. It is so for all molecules.

#### *Rule 3*

Associative law of multiplication must be valid. This means  $ABCD$  is the same as  $(AB)(CD)$ ,  $(A)(BCD)$  or  $(ABC)(D)$ .  $ABC$  is the same as  $A(BC)$  or  $(AB)C$ .

#### *Rule 4*

Inverse of an element  $A$  is denoted by  $A^{-1}$  (this does not mean  $1/A$ ). It is simply an element of the group such that  $A^{-1} * A = E$ . In case of symmetry groups,  $A^{-1}$  is that element which undoes or annuls the effect of  $A$ . For  $H_2O$  we have, for example,  $C_2C_2 = E$ . Therefore  $C_2^{-1} = E$  i.e.,  $C_2$  is its own inverse. This is true of all other elements for  $H_2O$ . But this is not general. For example,  $C_6^2 = C_3 \neq E$ . Therefore  $C_6^{-1}$  is not  $C_6$ .

#### *Order of group*

The total number of elements present in a group is known as the order of the group. It is denoted by  $n$ .

Example:

1. Water molecule belongs to  $C_{2v}$  group of order 4 because it contains 4 elements namely  $E$ ,  $C_{2z}$ ,  $\sigma_v$  and  $\sigma'_v$ .
2. Ammonia belongs to  $C_{3v}$  group of order 6 as it contains 6 elements namely  $E$ ,  $C_3^1$ ,  $C_3^2$ ,  $\sigma_{v(1)}$ ,  $\sigma_{v(2)}$  and  $\sigma_{v(3)}$ .

#### *Abelian group*

A group is said to be abelian if for all pairs of elements of the group, the binary combination is commutative. That is  $AB = BC$ ;  $BC = CB$  and so on. Example: The elements of  $C_{2v}$  point group  $E$ ,  $C_{2z}$ ,  $\sigma_v$  and  $\sigma'_v$  form an abelian group as all the elements of this group commute with each other.

#### *Non-abelian group*

A group is said to be non-abelian if the commutative law does not hold for the binary combinations of the elements of the group, i.e.,  $AB \neq BA$ .

Example:

The elements of  $C_{3v}$  point group  $E$ ,  $C_3^1$ ,  $C_3^2$ ,  $\sigma_{v(1)}$ ,  $\sigma_{v(2)}$  and  $\sigma_{v(3)}$  do not constitute an abelian group since the elements do not follow commutative law.

### 2.17 Keywords

Group; Order of group; Abelian group; Non-abelian group; Isomorphism; Similarity transformation; Classes; Group multiplication table; point groups; Space group

### 2.18 References for further studies

- 1) Group theory and Symmetry in Chemistry; Gurdeep Raj; Ajay Bhagi; Vinod Jain; *Krishna Prakashan Media*; **2012**.
- 2) Symmetry: An Introduction to Group Theory and Its Applications; R. McWeeny; *Courier Corporation*, **2002**.
- 3) Symmetry and Group theory in Chemistry; M Ladd; *Elsevier*, **1998**.
- 4) Molecular Symmetry and Group Theory; Robert L. Carter; *Wiley India Pvt. Limited*, **2009**.
- 5) Introduction to Symmetry and Group Theory for Chemists; Arthur M. Lesk; *Springer Science & Business Media*, **2007**.

### 2.19 Questions for self understanding

- 1) Explain why a set of numbers cannot form a group by the process of division.
- 2) Explain why the set of integers between 0 and  $\mu$  do not form a group under the process of multiplication.
- 3) Construct the multiplication table for the  $C_{3v}$  point group to which  $NH_3$  molecule belongs.
- 4) Draw the structure of three distinct isomers of  $C_2H_2Cl_2$  and determine their point groups. Which of them is polar?
- 5) Discuss the general properties of a group.
- 6) What are Abelian and non-abelian group?
- 7) What is mean by order of a group (h)? Give one example.
- 8) Write a note on group generating elements.
- 9) What is mean by sub group?
- 10) What is mean by classes?
- 11) Write a note on group multiplication tables.
- 12) Explain Isomorphism.
- 14) What is similarity transformation?
- 15) Discuss the Important characteristics of a group multiplication table.
- 16) Discuss Symmetry classification of molecules into point groups.
- 17) Explain the differences between point group and space group.

**UNIT-3****Structure**

- 3.0 Objectives of the unit
- 3.1 Introduction
- 3.2 Representation
- 3.3 Reducible Representation
- 3.4 Block diagonal matrices
- 3.5 The trace of a matrix
- 3.6 Properties of irreducible representations
- 3.7 Symbols used for representing irreducible representation
- 3.8 Motions of H<sub>2</sub>O
- 3.9 Point Group Representations
- 3.10 Summary of the unit
- 3.11 Key words
- 3.13 References for further studies
- 3.14 Questions for self understanding

### 3.0 Objectives of the unit

After studying this unit you are able to

- Explain the different types of representation
- Identify the reducible and reducible representation in a character table
- Explain the block diagonal matrices
- Explain the trace of a matrix
- List the properties of irreducible representations
- Write the symbols used for representing irreducible representation

### 3.1 Introduction

The group representation plays a very important role in deducing the consequence of the symmetries of the system. Roughly speaking, representation of a group is just some way to realize the same group operation other than the original definition of the group. Of particular interest to most physical application is the realization of group operation by the matrices whose multiplication operation can be naturally associated with group multiplication.

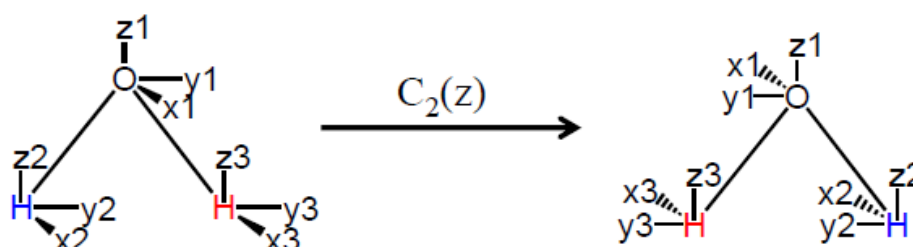
The basis is comprised by the labels attached to objects.

For molecules the objects can be:

1. Atoms
2. Coordinates
3. Orbitals
4. Bonds
5. Angles

The number of basic functions or labels is called the dimension.

For example, when considering molecular motions, we can assign coordinates  $x$ ,  $y$  and  $z$  to each atom. There are three coordinates for  $N$  atoms to give a total dimension of  $3N$ .



$C_2(z)$  gives  $(x_i \rightarrow -x_j)$ ,  $(y_i \rightarrow -y_j)$ , and  $(z_i \rightarrow +z_j)$  where  $i = j$  for O coordinates since the O lies along  $C_2$ . But  $i \neq j$  for the H since they do not lie along  $C_2$  and are therefore rotated into one another, e.g.,  $x_2 \rightarrow -x_3$ . We can represent this transformation in matrix notation where each atom will have a  $3 \times 3$  matrix,

$$\begin{pmatrix} x_i \\ y_i \\ z_i \end{pmatrix} = \begin{pmatrix} -1 & 0 & 0 \\ 0 & -1 & 0 \\ 0 & 0 & +1 \end{pmatrix} \begin{pmatrix} x_j \\ y_j \\ z_j \end{pmatrix} = \begin{pmatrix} -x_j \\ -y_j \\ +z_j \end{pmatrix} \quad \begin{matrix} (3r \times 3c)(3r \times 1c) \\ \text{gives a } (3r \times 1c) \end{matrix}$$

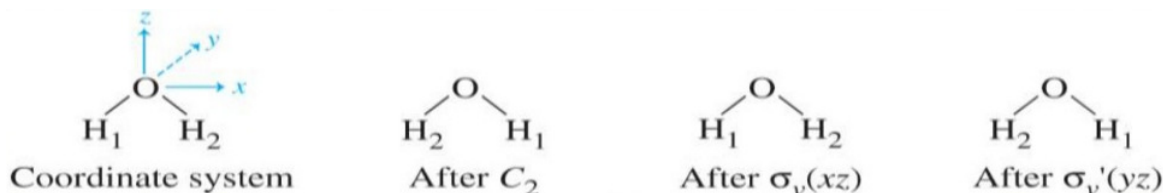
The trace of the matrix is the sum of the diagonal elements. In this case it is -1.

### 3.2 Representation

The set of matrices corresponding to the symmetry operations of a group is called its representation. Representations can be classified into

- Reducible representations (reps) and
- Irreducible representations (irreps).

Just watch what happens after the molecule undergoes each symmetry operation in the point group (E, C<sub>2</sub>, 2σ)



Let us consider the C<sub>2h</sub> point group as an example. E, C<sub>2</sub>, σ<sub>h</sub> and I are the four symmetry operations present in the group. The matrix representation for this point group is given below

$$E = \begin{bmatrix} 1 & 0 & 0 \\ 0 & 1 & 0 \\ 0 & 0 & 1 \end{bmatrix} \quad \sigma_h = \begin{bmatrix} 1 & 0 & 0 \\ 0 & 1 & 0 \\ 0 & 0 & -1 \end{bmatrix}$$

$$C_2 = \begin{bmatrix} -1 & 0 & 0 \\ 0 & -1 & 0 \\ 0 & 0 & 1 \end{bmatrix} \quad i = \begin{bmatrix} -1 & 0 & 0 \\ 0 & -1 & 0 \\ 0 & 0 & -1 \end{bmatrix}$$

In the case of C<sub>2h</sub> symmetry, the matrices can be reduced to simple matrices with smaller dimensions i.e., (1x1) matrices

### 3.3 Reducible Representation

A representation of a symmetry operation of a group, which can be expressed in terms of a representation of lower dimension is called reducible representation. Or

A representation of higher dimension which can be reduced in to representation of lower dimension is called reducible representation. They can be broken down into a simpler form and the characters can be further diagonalized.

Reducible representations are called block matrices. Example, each matrix in the  $C_{2v}$  matrix representation can be block diagonalized. To block diagonalize, make nonzero element into a  $1 \times 1$  matrix.

$$\begin{array}{cccc} \begin{bmatrix} [1] & 0 & 0 \\ 0 & [1] & 0 \\ 0 & 0 & [1] \end{bmatrix} & \begin{bmatrix} [-1] & 0 & 0 \\ 0 & [-1] & 0 \\ 0 & 0 & [1] \end{bmatrix} & \begin{bmatrix} [1] & 0 & 0 \\ 0 & [-1] & 0 \\ 0 & 0 & [1] \end{bmatrix} & \begin{bmatrix} [-1] & 0 & 0 \\ 0 & [1] & 0 \\ 0 & 0 & [1] \end{bmatrix} \\ E & C_2 & \sigma_v(xz) & \sigma_v(yz) \end{array}$$

### 3.4 Block diagonal matrices

A block diagonal matrix is a special type of matrices and it has blocks of number through its diagonal and has zeros elsewhere.

$$\begin{bmatrix} 6 & 3 & 4 & 0 & 0 & 0 \\ 1 & \sin\theta & 5 & 0 & 0 & 0 \\ \cos\theta & 2 & 4 & 0 & 0 & 0 \\ 0 & 0 & 0 & 9 & 0 & 0 \\ 0 & 0 & 0 & 0 & 12 & 2 \\ 0 & 0 & 0 & 0 & -\cos\theta & \sin\theta \end{bmatrix}$$

### 3.5 The trace of a matrix

The trace of a matrix ( $\chi$ ) is the sum of its diagonal elements. i.e,  $\chi(A) = \sum_i a_{ii}$

$$\begin{bmatrix} 6 & 3 & 4 & 0 & 0 & 0 \\ 1 & \sin\theta & 5 & 0 & 0 & 0 \\ \cos\theta & 2 & 4 & 0 & 0 & 0 \\ 0 & 0 & 0 & 9 & 0 & 0 \\ 0 & 0 & 0 & 0 & 12 & 2 \\ 0 & 0 & 0 & 0 & -\cos\theta & \sin\theta \end{bmatrix}$$

$$\chi = 31 + 2\sin\theta$$

Because the sub-block matrices cannot be further reduce, they are called irreducible representations. The original matrices are called reducible representations.

Irreducible representations

It is not possible to perform a similarity transformation matrix which will reduce the matrices of representation T, then the representation is called irreducible representation. In general all 1D representations are examples of irreducible representations.

The symbol  $\Gamma$  is used for representations

Where  $\Gamma^{\text{red}} = \Gamma^1 \Gamma^2 \Gamma^3 \dots \Gamma^n$

### 3.6 Properties of irreducible representations

Rule 1. The sum of the square of the dimensions of the IRs of a group is equal to the order of the group  $h$  (no proof).

$$\sum l_i^2 = l_1^2 + l_2^2 + \dots = h$$

Rule 1 can be written as  $\sum_i [x_i(E)]^2 = h$

Since  $[x_i(E)]$  the character of the representation of  $E$  in the  $i^{\text{th}}$  IR = order of the representation.

Rule 2. The sum of the square of the characters in any IR =  $h$

$$\sum_R [x_i(R)]^2 = h \text{ (simple test for irreducibility)}$$

Rule 3. The vectors whose components are the characters of two different IRs are orthogonal

$$\sum_R x_i(R)x_j(R) = 0$$

Rule 4. In a given reducible or irreducible representation the character of all matrices belong to the same class are identical

Rule 5. The number of IRs = number of classes in a group.

From rules 2 and 3.

$$\sum_R x_i(R)x_j(R) = h\delta_{ij}$$

Denote the number of elements in the  $m^{\text{th}}$  class by  $g_m$ , the number in the  $n^{\text{th}}$  class by  $g_n$  etc... and let there be  $k$  classes

$$\text{Then } \sum_p^k x_i(R_p)x_j(R_p)g_p = h\delta_{ij}$$

Here  $R_p$  is any one of the operations in the  $p^{\text{th}}$  class

This means  $kx_i(R_p)$  quantities in the  $\Gamma_i$  IR behave like components of a  $k$ -dimensional vector which is orthogonal to the  $k-1$  other vectors,

### 3.7 Symbols used for representing irreducible representation

1. Dimension of the irreducible representations

If it is uni dimensional (character of  $E = 1$ ), term A or B is used, for a two dimensional representation, term E is used. If it is three dimensional term T is used

2. Symmetry with respect to principle axis



If the 1-D irrep is symmetrical with respect to the principle axis (i.e, the character of the operation is + 1) the term A is used. However if the 1-D representation is unsymmetrical with respect to the principal axis (i.e, the character of is -1) the term B is used.

### 3. Symmetry with respect to subsidiary axis or plane

If the irrep is symmetrical with respect to the subsidiary axis, or in it absence to plane, subscript , , , are used if it is unsymmetrical subscript ,, are used.

4. Prime and double prime marks are used over the symbol of the irrep indicate its symmetry or anti symmetry with respect to the horizontal plane.

5. If there is a centre of symmetry in the molecule, subscripts g and u are used to indicate the symmetry or anti symmetry of irrep. Suppose the point group has no centre of symmetry, g or u subscripts are not used. The term g stands for gerade (centrosymmetric) and u stands for ungerade (non-centrosymmetric).

On the basis of the above symbols can be assigned to the irreducible representations of a point group.

This can be illustrated by considering water molecule

### 3.8 Motions of H<sub>2</sub>O

Since there are three atoms, the full matrix for H<sub>2</sub>O is a 9x9

$$C_2 \begin{pmatrix} x_1 \\ y_1 \\ z_1 \\ x_2 \\ y_2 \\ z_2 \\ x_3 \\ y_3 \\ z_3 \end{pmatrix} = \begin{pmatrix} -1 & 0 & 0 & 0 & 0 & 0 & 0 & 0 & 0 \\ 0 & -1 & 0 & 0 & 0 & 0 & 0 & 0 & 0 \\ 0 & 0 & +1 & 0 & 0 & 0 & 0 & 0 & 0 \\ 0 & 0 & 0 & 0 & 0 & 0 & -1 & 0 & 0 \\ 0 & 0 & 0 & 0 & 0 & 0 & 0 & -1 & 0 \\ 0 & 0 & 0 & 0 & 0 & 0 & 0 & 0 & +1 \\ 0 & 0 & 0 & -1 & 0 & 0 & 0 & 0 & 0 \\ 0 & 0 & 0 & 0 & -1 & 0 & 0 & 0 & 0 \\ 0 & 0 & 0 & 0 & 0 & +1 & 0 & 0 & 0 \end{pmatrix} \begin{pmatrix} x_1 \\ y_1 \\ z_1 \\ x_2 \\ y_2 \\ z_2 \\ x_3 \\ y_3 \\ z_3 \end{pmatrix}$$

The hydrogen atoms are not on the diagonal since the atoms themselves are moved as a result of the C<sub>2</sub> rotation. The trace of this matrix is -1. This is also called the character.

We can consider also the result of the σ<sub>v</sub> mirror plane, which is also a 9x9

$$\sigma \begin{pmatrix} x_1 \\ y_1 \\ z_1 \\ x_2 \\ y_2 \\ z_2 \\ x_3 \\ y_3 \\ z_3 \end{pmatrix} = \begin{pmatrix} -1 & 0 & 0 & 0 & 0 & 0 & 0 & 0 & 0 \\ 0 & +1 & 0 & 0 & 0 & 0 & 0 & 0 & 0 \\ 0 & 0 & +1 & 0 & 0 & 0 & 0 & 0 & 0 \\ 0 & 0 & 0 & -1 & 0 & 0 & 0 & 0 & 0 \\ 0 & 0 & 0 & 0 & +1 & 0 & 0 & 0 & 0 \\ 0 & 0 & 0 & 0 & 0 & +1 & 0 & 0 & 0 \\ 0 & 0 & 0 & 0 & 0 & 0 & -1 & 0 & 0 \\ 0 & 0 & 0 & 0 & 0 & 0 & 0 & +1 & 0 \\ 0 & 0 & 0 & 0 & 0 & 0 & 0 & 0 & +1 \end{pmatrix} \begin{pmatrix} x_1 \\ y_1 \\ z_1 \\ x_2 \\ y_2 \\ z_2 \\ x_3 \\ y_3 \\ z_3 \end{pmatrix}$$

None of the atoms are moved by the symmetry operation so all of the submatrices representing the vectors lie along the diagonal. For this operation the trace (also known as the character) is +3.

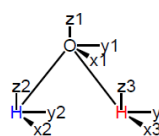
We can conclude with 2 general rules:

1. Only those atoms, which remain in the place following an operation can contribute to the trace.
2. Each atom contributes the same amount to the trace since all of the atoms have the same 3x3 matrix.

Using these principles we can see that  $\sigma_v$  has a character of +1.

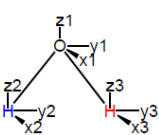
The identity always has a character equal to the number of basis functions. Here  $E = 9$ . Using the character of the 4 symmetry operations of the  $C_{2v}$  point group we can construct a representation  $\Gamma$ .

9x9 matrix for  $C_2$  rotation in  $H_2O$



$$C_2 = \begin{pmatrix} x_1 \\ y_1 \\ z_1 \\ x_2 \\ y_2 \\ z_2 \\ x_3 \\ y_3 \\ z_3 \end{pmatrix} = \begin{pmatrix} -1 & 0 & 0 & 0 & 0 & 0 & 0 & 0 & 0 \\ 0 & -1 & 0 & 0 & 0 & 0 & 0 & 0 & 0 \\ 0 & 0 & +1 & 0 & 0 & 0 & 0 & 0 & 0 \\ 0 & 0 & 0 & 0 & 0 & 0 & -1 & 0 & 0 \\ 0 & 0 & 0 & 0 & 0 & 0 & 0 & -1 & 0 \\ 0 & 0 & 0 & 0 & 0 & 0 & 0 & 0 & +1 \\ 0 & 0 & 0 & -1 & 0 & 0 & 0 & 0 & 0 \\ 0 & 0 & 0 & 0 & -1 & 0 & 0 & 0 & 0 \\ 0 & 0 & 0 & 0 & 0 & +1 & 0 & 0 & 0 \end{pmatrix} \begin{pmatrix} x_1 \\ y_1 \\ z_1 \\ x_2 \\ y_2 \\ z_2 \\ x_3 \\ y_3 \\ z_3 \end{pmatrix}$$

For  $\sigma_v(yz)$ , no atoms are moved so the matrix representation is



$$\sigma_v = \begin{pmatrix} x_1 \\ y_1 \\ z_1 \\ x_2 \\ y_2 \\ z_2 \\ x_3 \\ y_3 \\ z_3 \end{pmatrix} = \begin{pmatrix} -1 & 0 & 0 & 0 & 0 & 0 & 0 & 0 & 0 \\ 0 & +1 & 0 & 0 & 0 & 0 & 0 & 0 & 0 \\ 0 & 0 & +1 & 0 & 0 & 0 & 0 & 0 & 0 \\ 0 & 0 & 0 & -1 & 0 & 0 & 0 & 0 & 0 \\ 0 & 0 & 0 & 0 & +1 & 0 & 0 & 0 & 0 \\ 0 & 0 & 0 & 0 & 0 & +1 & 0 & 0 & 0 \\ 0 & 0 & 0 & 0 & 0 & 0 & -1 & 0 & 0 \\ 0 & 0 & 0 & 0 & 0 & 0 & 0 & +1 & 0 \\ 0 & 0 & 0 & 0 & 0 & 0 & 0 & 0 & +1 \end{pmatrix} \begin{pmatrix} x_1 \\ y_1 \\ z_1 \\ x_2 \\ y_2 \\ z_2 \\ x_3 \\ y_3 \\ z_3 \end{pmatrix}$$

9x9 matrices like those above could serve as the representations of the operations for the water molecule in this basis.

Fortunately, only the trace of this matrix is required. This sum is called the character,  $\chi(R)$ .

Here,  $\chi(\sigma_v) = 3$

For  $\chi(C_2) = -1$

$$C_2 \begin{pmatrix} x_1 \\ y_1 \\ z_1 \\ x_2 \\ y_2 \\ z_2 \\ x_3 \\ y_3 \\ z_3 \end{pmatrix} = \begin{pmatrix} -1 & 0 & 0 & 0 & 0 & 0 & 0 & 0 & 0 \\ 0 & -1 & 0 & 0 & 0 & 0 & 0 & 0 & 0 \\ 0 & 0 & +1 & 0 & 0 & 0 & 0 & 0 & 0 \\ 0 & 0 & 0 & 0 & 0 & 0 & -1 & 0 & 0 \\ 0 & 0 & 0 & 0 & 0 & 0 & 0 & -1 & 0 \\ 0 & 0 & 0 & 0 & 0 & 0 & 0 & 0 & +1 \\ 0 & 0 & 0 & -1 & 0 & 0 & 0 & 0 & 0 \\ 0 & 0 & 0 & 0 & -1 & 0 & 0 & 0 & 0 \\ 0 & 0 & 0 & 0 & 0 & +1 & 0 & 0 & 0 \end{pmatrix} \begin{pmatrix} x_1 \\ y_1 \\ z_1 \\ x_2 \\ y_2 \\ z_2 \\ x_3 \\ y_3 \\ z_3 \end{pmatrix}$$

**-1**

For a reflection through the plane bisecting the H-O-H bond angle,  $\chi(\sigma_v') = +1$  since only the O is unshifted and a plane contributes +1 for each unshifted atom. The character for the identity element will always be the dimension of the basis since all labels are unchanged. For water then,  $\chi(E) = 9$ . The representation ( $\Gamma$ ) for water in this Cartesian basis is

	E	C <sub>2</sub>	σ <sub>v</sub> (yz)	σ <sub>v</sub> '(xz)
Γ	9	-1	3	1

### 3.9 Point Group Representations

A point group representation is a basis set in which the irreducible representations are the basis vectors. The irreps form the a complete orthonormal basis for an m-dimensional space, where m is the number of irreducible representations and is equal to the number of classes in the group.

These considerations are summarized by the following rules.

1. The number of basis vectors or irreps (m) equals the number of classes.
2. The sum of the squares of the dimensions of the m irreps equals the order,

$$\sum_{i=1}^m d_i^2 = h \quad \boxed{\text{expect at least one } \chi(E) > 1 \text{ for } C_n (n > 2)}$$

The character of the identity operation equals the dimension of the representation,  $\chi(E) = d_i$  which is referred to as the degeneracy of the irrep. The degeneracy of most irreducible representations is 1 (nondegenerate representations are 1x1 matrices) but can sometimes be 2 or 3. No character in an irreducible representation can exceed the dimension of the representation. Thus, in non-degenerate representations, all characters must be  $\pm 1$ .

3. The member irreps are orthonormal, i.e., the sum of the squares of the characters in any irrep is equal to the order (row normalization), while the sum of the product of the characters over all operations in two different irreps is zero (orthogonality).

$$\sum_{\mathbf{R}} g(\mathbf{R}) \chi_i(\mathbf{R}) \chi_j(\mathbf{R}) = h \delta_{ij}$$

- $\delta_{ij}$  is the Kronecker delta (0 when  $i \neq j$  and 1 when  $i = j$ ), where the sum is over all of the classes of operations,

- $g(\mathbf{R})$  is the number of operations,  $\mathbf{R}$ , in the class,

- $\chi_i(\mathbf{R})$  and  $\chi_j(\mathbf{R})$  are the characters of the operation  $\mathbf{R}$  in the  $i^{\text{th}}$  and  $j^{\text{th}}$  irreps,

- $h$  is the order of the group.

4. The sum of the squares of the characters of any operation over all of the irreps times the number of operations in the class is equal to  $h$ , i.e., columns of the representation are also normalized.

$$\sum_{i=1}^m g(\mathbf{R}) \chi_i^2(\mathbf{R}) = h$$

where  $m$  is the number of irreducible representations

5. The sum of the products of the characters of any two different operations over all of the irreps is zero, i.e., columns of the representation are also orthogonal.

$$\sum_{i=1}^m \chi_i(\mathbf{R}') \chi_i(\mathbf{R}) = 0$$

6. The first representation is always the *totally symmetric* representation in which all characters are +1.

7. Any reducible representation in the point group can be expressed as a linear combination of the irreducible representations.

### 3.10 Summary of the unit

Mathematical techniques of group theory makes it possible to describe and analyze some of the molecule's chemically interesting properties. The approach we take, in general, is to define a set of imagined vectors on the molecule's various atoms to represent the properties of interest. In order to apply symmetry arguments to the solution of molecular problems, we

need an understanding of mathematical representations of groups - their construction, meaning, and manipulation.

Representation; a set of symbols that will satisfy the multiplication table for the group. The symbols themselves are called the characters of the representation. The characters may be positive or negative integers, numeric values of certain trigonometric functions, imaginary number, or even square matrices.

### 3.11 Key words

Representation; Reducible Representation; Block diagonal matrices; The trace of a matrix  
Properties of irreducible representations; Symbols used for representing irreducible representation; Motions of H<sub>2</sub>O; Point Group Representations

### 3.13 References for further studies

- 1) Group theory and Symmetry in Chemistry; Gurdeep Raj; Ajay Bhagi; Vinod Jain; *Krishna Prakashan Media*; **2012**.
- 2) Symmetry: An Introduction to Group Theory and Its Applications; R. McWeeny; *Courier Corporation*, **2002**.
- 3) Symmetry and Group theory in Chemistry; M Ladd; *Elsevier*, **1998**.
- 4) Molecular Symmetry and Group Theory; Robert L. Carter; *Wiley India Pvt. Limited*, **2009**.
- 5) Introduction to Symmetry and Group Theory for Chemists; Arthur M. Lesk; *Springer Science & Business Media*, **2007**.

### 3.14 Questions for self understanding

- 1) What is representation means?
- 2) What is reducible representation? Explain with example.
- 3) What are block diagonal matrices?
- 4) What is the trace of a matrix?
- 5) Explain the properties of irreducible representations.
- 6) Write the symbols used for representing irreducible representation.
- 7) Construct the representation table for H<sub>2</sub>O molecules.

**UNIT-4****Structure**

- 4.0 Objectives of the unit
- 4.1 Introduction
- 4.2 Character tables
- 4.3 Symmetry of orbitals and functions
- 4.4 Character Tables and Bonding
- 4.5 The  $\sigma$  bonding in dichloromethane,  $\text{CH}_2\text{Cl}_2$ .
- 4.6 The  $\sigma$  and  $\pi$  bonding in  $\text{SO}_3$
- 4.7 The  $\sigma$  and  $\pi$  bonding in  $\text{ClO}_4^-$
- 4.8 Summary of the unit
- 4.9 Key words
- 4.10 References for further studies
- 4.11 Questions for self understanding

## 5.0 Objectives of the unit

After studying this unit you are able to

- Construct the character tables for different symmetry elements
- Explain the symmetry of orbitals and functions
- Explain the character tables and bonding
- Write the character table for  $\sigma$  bonding in dichloromethane,  $\text{CH}_2\text{Cl}_2$ .
- Write the character table for  $\sigma$  and  $\pi$  bonding in  $\text{SO}_3$
- Write the character table for  $\sigma$  and  $\pi$  bonding in  $\text{ClO}_4^-$

## 4.1 Introduction

Each symmetry operation can be represented by a  $3 \times 3$  matrix that shows how the operation transforms a set of  $x$ ,  $y$ , and  $z$  coordinates. The set of four transformation matrices forms a matrix representation of the  $C_{2h}$  point group. These matrices combine in the same way as the operations. The sum of the numbers along each matrix diagonal (the character) gives a shorthand version of the matrix representation, called  $\Gamma$  (gamma), is a reducible representation b/c it can be further simplified. List of the complete set of irreducible representations (rows) and symmetry classes (columns) of a point group.

## 4.2 Character tables

The collection of irreducible representations for a group is listed in a character table, with the totally symmetric representation listed first. Thus each point group has a complete set of possible symmetry operations that are conveniently listed as a matrix known as a Character Table. As an example, we will look at the character table for the  $C_{2v}$  point group.

Point Group Label	Symmetry Operations – The <i>Order</i> is the total number of operations			
$C_{2v}$	E	$C_2$	$\sigma_v(xz)$	$\sigma'_v(yz)$
$A_1$	1	1	1	1
$A_2$	1	1	-1	-1
$B_1$	1	-1	1	-1
$B_2$	1	-1	-1	1

In  $C_{2v}$  the order is 4:  
1 E, 1  $C_2$ , 1  $\sigma_v$  and 1  $\sigma'_v$

← Character

← Representation of  $B_2$

↑ Symmetry Representation Labels

Representations are subsets of the complete point group – they indicate the effect of the symmetry operations on different kinds of mathematical functions. Representations are orthogonal to one another. The Character is an integer that indicates the effect of an operation in a given representation.

The effect of symmetry elements on mathematical functions is useful to us because orbitals are mathematical functions! Analysis of the symmetry of a molecule will provide us with insight into the orbitals used in bonding.

**Symmetry of Functions**

$C_{2V}$	E	$C_2$	$\sigma_v(xz)$	$\sigma'_v(yz)$		
$A_1$	1	1	1	1	$z$	$x^2, y^2, z^2$
$A_2$	1	1	-1	-1	$R_z$	$xy$
$B_1$	1	-1	1	-1	$x, R_y$	$xz$
$B_2$	1	-1	-1	1	$y, R_x$	$yz$

Notes about symmetry labels and characters:

“A” means symmetric with regard to rotation about the principle axis.

“B” means anti-symmetric with regard to rotation about the principle axis.

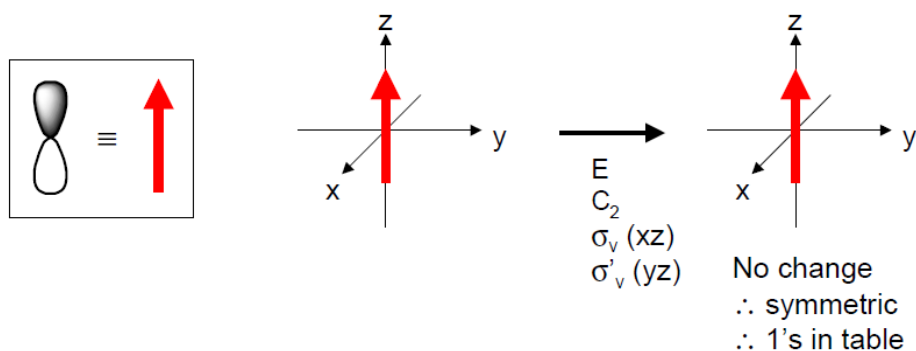
Subscript numbers are used to differentiate symmetry labels, if necessary.

“1” indicates that the operation leaves the function unchanged: it is called “symmetric”.

“-1” indicates that the operation reverses the function: it is called “anti-symmetric”.

### 4.3 Symmetry of orbitals and functions

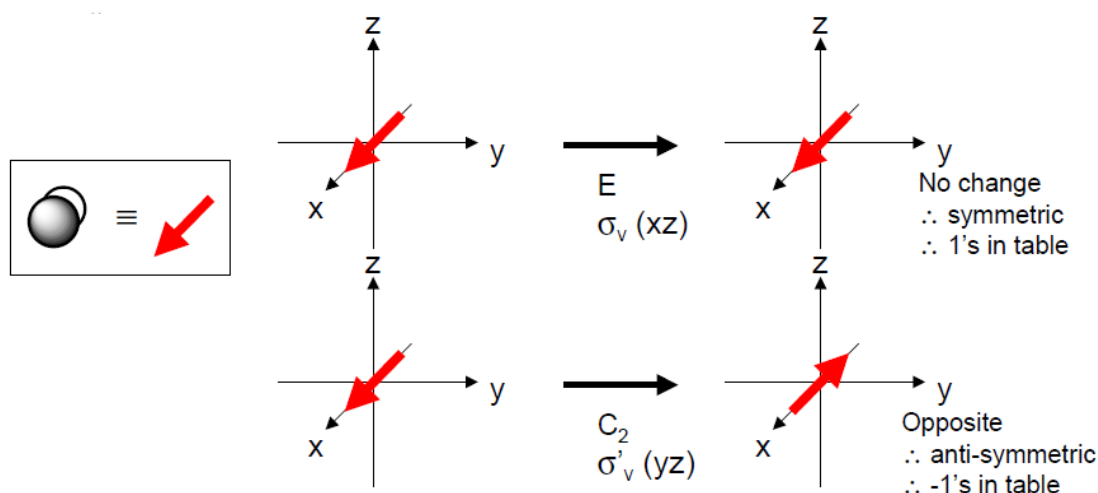
A  $p_z$  orbital has the same symmetry as an arrow pointing along the z-axis.



$C_{2V}$	E	$C_2$	$\sigma_v(xz)$	$\sigma'_v(yz)$		
$A_1$	1	1	1	1	$z$	$x^2, y^2, z^2$
$A_2$	1	1	-1	-1	$R_z$	$xy$
$B_1$	1	-1	1	-1	$x, R_y$	$xz$
$B_2$	1	-1	-1	1	$y, R_x$	$yz$

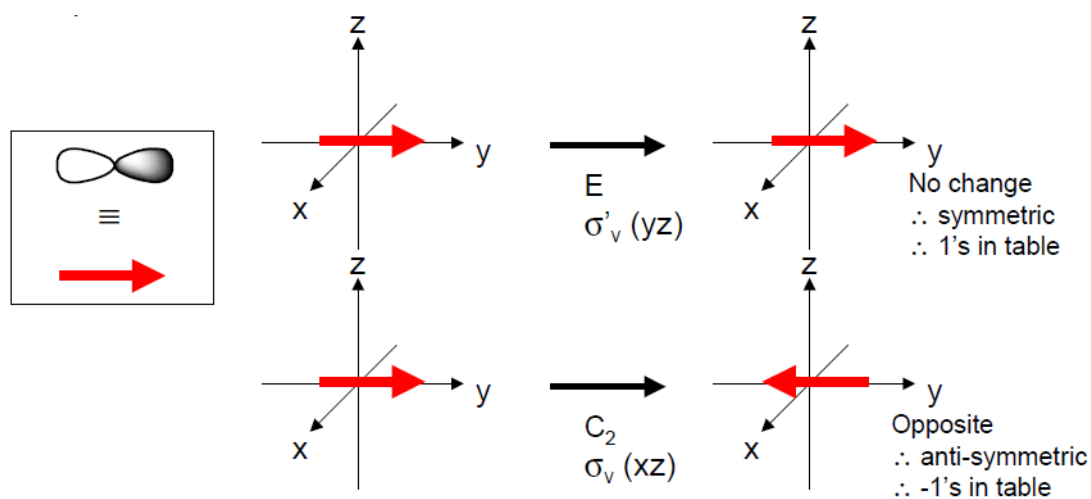


A  $p_x$  orbital has the same symmetry as an arrow pointing along the x-axis.



$C_{2v}$	E	$C_2$	$\sigma_v(xz)$	$\sigma'_v(yz)$		
$A_1$	1	1	1	1	z	$x^2, y^2, z^2$
$A_2$	1	1	-1	-1	$R_z$	xy
$B_1$	1	-1	1	-1	x, $R_y$	xz
$B_2$	1	-1	-1	1	y, $R_x$	yz

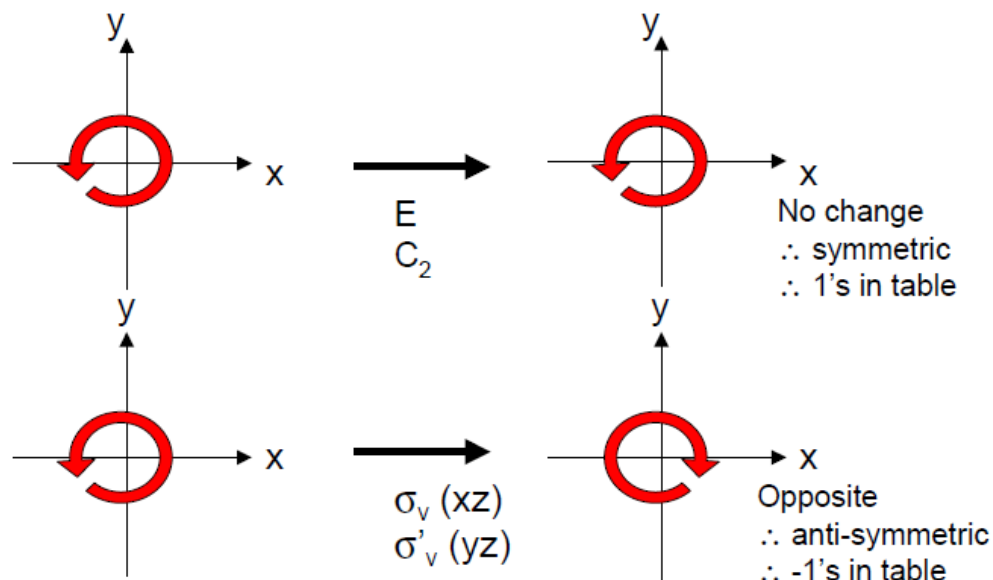
A  $p_y$  orbital has the same symmetry as an arrow pointing along the y-axis



$C_{2v}$	E	$C_2$	$\sigma_v(xz)$	$\sigma'_v(yz)$		
$A_1$	1	1	1	1	z	$x^2, y^2, z^2$
$A_2$	1	1	-1	-1	$R_z$	xy
$B_1$	1	-1	1	-1	x, $R_y$	xz
$B_2$	1	-1	-1	1	y, $R_x$	yz

Rotation about the  $n$  axis,  $R_n$ , can be treated in a similar way.

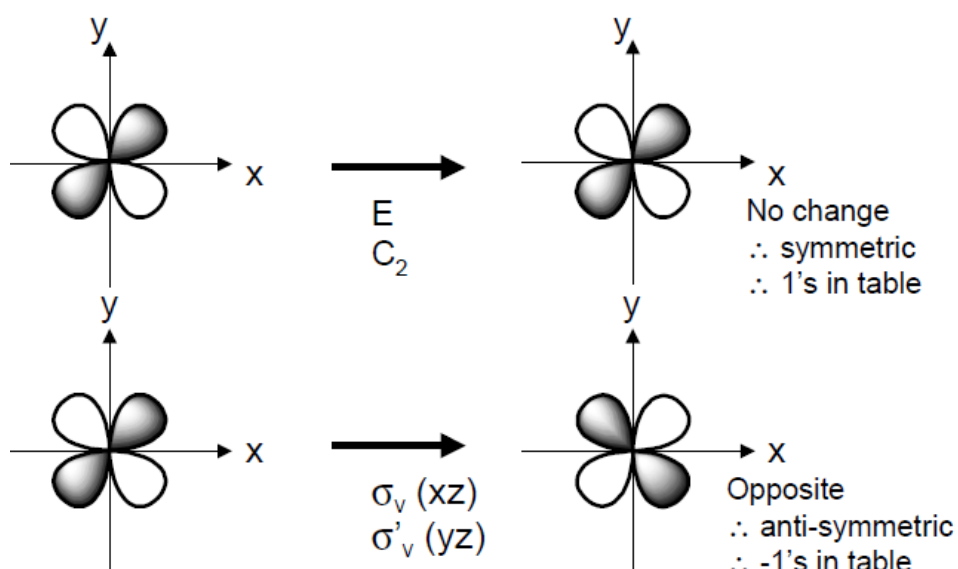
The  $z$  axis is pointing out of the screen. If the rotation is still in the same direction (e.g. counter clock-wise), then the result is considered symmetric. If the rotation is in the opposite direction (i.e. clock-wise), then the result is considered anti-symmetric.



$C_{2v}$	E	$C_2$	$\sigma_v(xz)$	$\sigma'_v(yz)$		
$A_1$	1	1	1	1	$z$	$x^2, y^2, z^2$
$A_2$	1	1	-1	-1	$R_z$	$xy$
$B_1$	1	-1	1	-1	$x, R_y$	$xz$
$B_2$	1	-1	-1	1	$y, R_x$	$yz$

$d$  orbital functions can also be treated in a similar way

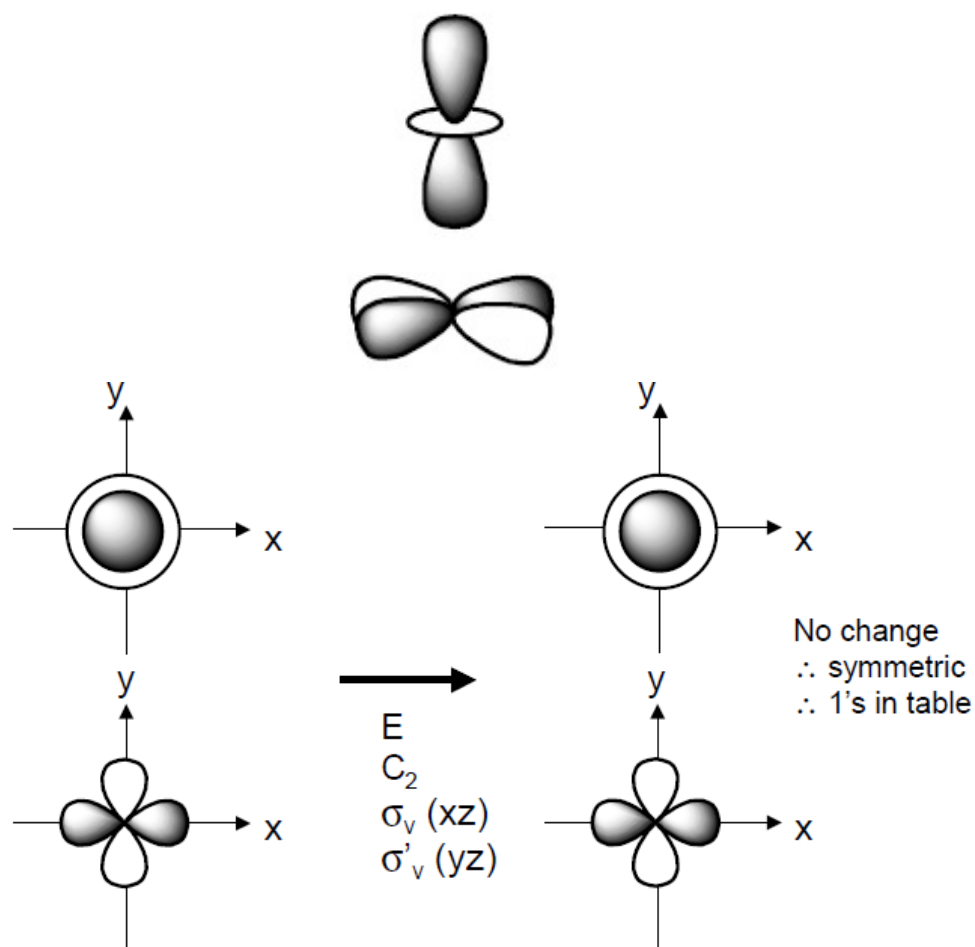
The  $z$  axis is pointing out of the screen.



$C_{2v}$	E	$C_2$	$\sigma_v(xz)$	$\sigma'_v(yz)$		
$A_1$	1	1	1	1	z	$x^2, y^2, z^2$
$A_2$	1	1	-1	-1	$R_z$	xy
$B_1$	1	-1	1	-1	x, $R_y$	xz
$B_2$	1	-1	-1	1	y, $R_x$	yz

d orbital functions can also be treated in a similar way

The z axis is pointing out of the screen. So these are representations of the view of the  $dz^2$  orbital and  $dx^2-y^2$  orbital down the z-axis.



$C_{2v}$	E	$C_2$	$\sigma_v(xz)$	$\sigma'_v(yz)$		
$A_1$	1	1	1	1	z	$x^2, y^2, z^2$
$A_2$	1	1	-1	-1	$R_z$	xy
$B_1$	1	-1	1	-1	x, $R_y$	xz
$B_2$	1	-1	-1	1	y, $R_x$	yz

Note that the representation of orbital functions changes depending on the point group – thus it is important to be able to identify the point group correctly.

$C_{2v}$	E	$C_2$	$\sigma_v(xz)$	$\sigma'_v(yz)$		
$A_1$	1	1	1	1	z	$x^2, y^2, z^2$ ←
$A_2$	1	1	-1	-1	$R_z$	xy
$B_1$	1	-1	1	-1	x, $R_y$	xz
$B_2$	1	-1	-1	1	y, $R_x$	yz

$D_{3h}$	E	$2 C_3$	$3 C_2$	$\sigma_h$	$2 S_3$	$3 \sigma_v$		
$A'_1$	1	1	1	1	1	1		$x^2 + y^2, z^2$ ←
$A'_2$	1	1	-1	1	1	-1	$R_z$	
$E'$	2	-1	0	2	-1	0	(x,y)	$(x^2 - y^2, xy)$ ←
$A''_1$	1	1	1	-1	-1	-1		
$A''_2$	1	1	-1	-1	-1	1	z	
$E''$	2	-1	0	-2	1	0	( $R_x, R_y$ )	(xz, yz)

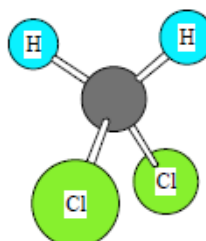
#### 4.4 Character Tables and Bonding

We can use character tables to determine the orbitals involved in bonding in a molecule. This process is done a few easy steps.

1. Determine the point group of the molecule.
2. Determine the Reducible Representation,  $\Gamma$ , for the type of bonding you wish to describe (e.g.  $\sigma$ ,  $\pi$ ,  $\pi_\perp$ ,  $\pi//$ ). The Reducible Representation indicates how the bonds are affected by the symmetry elements present in the point group.
3. Identify the Irreducible Representation that provides the Reducible Representation; there is a simple equation to do this. The Irreducible Representation (e.g.  $2A_1 + B_1 + B_2$ ) is the combination of symmetry representations in the point group that sum to give the Reducible Representation.
4. Identify which orbitals are involved from the Irreducible Representation and the character table.

Example,

#### 4.5 The $\sigma$ bonding in dichloromethane, $CH_2Cl_2$ .



The point group is  $C_{2v}$  so we must use the appropriate character table for the reducible representation of the sigma bonding,  $\Gamma_\sigma$ . To determine  $\Gamma_\sigma$  all we have to do is see how each symmetry operation affects the 4  $\sigma$  bonds in the molecule – if the bond moves, it is given a value of 0, if it stays in the same place, the bond is given a value of 1. Put the sum of the 1's and 0's into the box corresponding to the symmetry operation.

The E operation leaves everything where it is so all four bonds stay in the same place and the character is 4 (1+1+1+1). The  $C_2$  operation moves all four bonds so the character is 0.

Each  $\sigma_v$  operation leaves two bonds where they were and moves two bonds so the character is 2 (1+1). Overall, the reducible representation is thus:

$C_{2v}$	E	$C_2$	$\sigma_v(xz)$	$\sigma'_v(yz)$
$\Gamma_\sigma$	4	0	2	2

We now have to figure out what combination of symmetry representations will add up to give us this reducible representation. In this case, it can be done by inspection, but there is a simple equation that is useful for more complicated situations.

$C_{2v}$	E	$C_2$	$\sigma_v(xz)$	$\sigma'_v(yz)$
$\Gamma_\sigma$	4	0	2	2

$C_{2v}$	E	$C_2$	$\sigma_v(xz)$	$\sigma'_v(yz)$		
$A_1$	1	1	1	1	z	$x^2, y^2, z^2$
$A_2$	1	1	-1	-1	$R_z$	xy
$B_1$	1	-1	1	-1	x, $R_y$	xz
$B_2$	1	-1	-1	1	y, $R_x$	yz

Because the character under E is 4, there must be a total of 4 symmetry representations (sometimes called basis functions) that combine to make  $\Gamma_\sigma$ . Since the character under  $C_2$  is 0, there must be two of A symmetry and two of B symmetry. The irreducible representation is ( $2A_1 + B_1 + B_2$ ), which corresponds to: s,  $p_z$ ,  $p_x$ , and  $p_y$  orbitals – the same as in VBT. You can often use your understanding of VBT to help you in finding the correct basis functions for the irreducible representation.

$C_{2v}$	E	$C_2$	$\sigma_v(xz)$	$\sigma'_v(yz)$
$\Gamma_\sigma$	4	0	2	2

$C_{2V}$	E	$C_2$	$\sigma_v(xz)$	$\sigma'_v(yz)$		
$A_1$	1	1	1	1	z	$x^2, y^2, z^2$
$A_2$	1	1	-1	-1	$R_z$	xy
$B_1$	1	-1	1	-1	x, $R_y$	xz
$B_2$	1	-1	-1	1	y, $R_x$	yz

The formula to figure out the number of symmetry representations of a given type is

$$n_x = \frac{1}{\text{order}} \sum [(\# \text{ of operations in class}) \times (\text{character of RR}) \times (\text{character of X})]$$

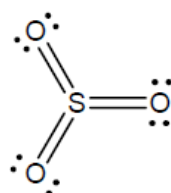
Thus, in our example:

$$n_{A_1} = \frac{1}{4} [(1)(4)(1) + (1)(0)(1) + (1)(2)(1) + (1)(2)(1)] \quad n_{B_1} = \frac{1}{4} [(1)(4)(1) + (1)(0)(-1) + (1)(2)(1) + (1)(2)(-1)]$$

$$n_{A_2} = \frac{1}{4} [(1)(4)(1) + (1)(0)(1) + (1)(2)(-1) + (1)(2)(-1)] \quad n_{B_2} = \frac{1}{4} [(1)(4)(1) + (1)(0)(-1) + (1)(2)(-1) + (1)(2)(1)]$$

Which gives: 2  $A_1$ 's, 0  $A_2$ 's, 1  $B_1$  and 1  $B_2$ .

#### 4.6 The $\sigma$ and $\pi$ bonding in $SO_3$



The point group is  $D_{3h}$  so we must use the appropriate character table to find the reducible representation of the sigma bonding,  $\Gamma_\sigma$  first, then we can go the representation of the  $\pi$  bonding,  $\Gamma_\pi$ . To determine  $\Gamma_\sigma$  all we have to do is see how each symmetry operation affects the 3  $\sigma$  bonds in the molecule.

The E and the  $\sigma_h$  operations leave everything where it is so all three bonds stay in the same place and the character is 3 (1+1+1). The  $C_3$  and  $S_3$  operations move all three bonds so their characters are 0. The  $C_2$  operation moves two of the bonds and leaves one where it was so the character is 1. Each  $\sigma_v$  operation leaves one bond where it was and moves two bonds so the character is 1. Overall, the reducible representation for the sigma bonding is

$D_{3h}$	E	2 $C_3$	3 $C_2$	$\sigma_h$	2 $S_3$	3 $\sigma_v$
$\Gamma_\sigma$	3	0	1	3	0	1

$D_{3h}$	E	$2 C_3$	$3 C_2$	$\sigma_h$	$2 S_3$	$3 \sigma_v$		
$A'_1$	1	1	1	1	1	1		$x^2 + y^2, z^2$
$A'_2$	1	1	-1	1	1	-1	$R_z$	
$E'$	2	-1	0	2	-1	0	$(x,y)$	$(x^2 - y^2, xy)$
$A''_1$	1	1	1	-1	-1	-1		
$A''_2$	1	1	-1	-1	-1	1	$z$	
$E''$	2	-1	0	-2	1	0	$(R_x, R_y)$	$(xz, yz)$

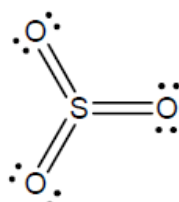
$$n_{A'_1} = \frac{1}{12} [(1)(3)(1) + (2)(0)(1) + (3)(1)(1) + (1)(3)(1) + (2)(0)(1) + (3)(1)(1)] \quad n_{A'_1} = \frac{12}{12} = 1$$

$$n_{A'_2} = \frac{1}{12} [(1)(3)(1) + (2)(0)(1) + (3)(1)(-1) + (1)(3)(1) + (2)(0)(1) + (3)(1)(-1)] \quad n_{A'_2} = \frac{0}{12} = 0$$

$$n_{E'} = \frac{1}{12} [(1)(3)(2) + (2)(0)(-1) + (3)(1)(0) + (1)(3)(2) + (2)(0)(-1) + (3)(1)(0)] \quad n_{E'} = \frac{12}{12} = 1$$

We can stop here because the combination ( $A'_1 + E'$ ) produces the  $\Gamma\sigma$  that we determined. None of the other representations can contribute to the  $\sigma$  bonding (i.e.  $n_{A''_1}$ ,  $n_{A''_2}$  and  $n_{E''}$  are all 0). The irreducible representation ( $A'_1 + E'$ ) shows us that the orbitals involved in bonding are the s and the  $p_x$  and  $p_y$  pair; this corresponds to the  $sp^2$  combination we find in VBT.

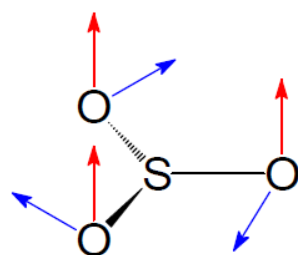
Now we have to determine  $\Gamma$  for the  $\pi$  bonding in  $SO_3$



To determine  $\Gamma\pi$  we have to see how each symmetry operation affects the  $\pi$  systems in the molecule. The treatment is similar to what we did for sigma bonding but there are a few significant differences:

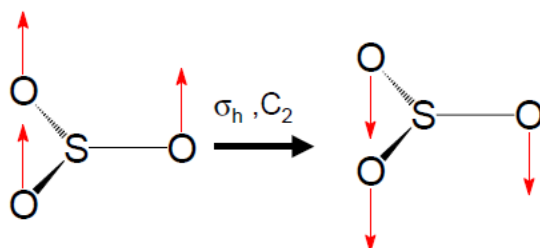
- 1) Pi bonds change sign across the inter-nuclear axis. We must consider the effect of the symmetry operation on the signs of the lobes in a  $\pi$  bond.
- 2) There is the possibility of two different  $\pi$  type bonds for any given  $\sigma$  bond (oriented  $90^\circ$  from each other). We must examine each of these.

To determine  $\Gamma\pi$  we have to see how each symmetry operation affects the  $\pi$  systems in the molecule. The treatment is similar to what we did for sigma bonding but there are a few significant differences: This means that we have to find reducible representations for both the  $\pi$  system perpendicular to the molecular plane ( $\pi_\perp$ , vectors shown in red) and the pi system in the molecular plane ( $\pi_{//}$ , vectors shown in blue).



Note: These are just vectors that are associated with each sigma bond (not with any particular atom) – they could also be placed in the middle of each SO bond. The vectors should be placed to conform with the symmetry of the point group (e.g. the blue vectors conform to the  $C_3$  axis).

First determine the reducible representation for the pi bonding perpendicular to the molecular plane,  $\Gamma_{\pi\perp}$ . The E operation leaves everything where it is so all three vectors stay in the same place and the character is 3. The  $C_3$  and  $S_3$  operations move all three vectors so their characters are 0. The  $C_2$  operation moves two of the vectors and reverses the sign of the other one so the character is -1. The  $\sigma_h$  operation reverses the sign of all three vectors so the character is -3. Each  $\sigma_v$  operation leaves one vector where it was and moves the two others so the character is 1. Overall, the reducible representation for the perpendicular  $\pi$  bonding is



$D_{3h}$	E	2 $C_3$	3 $C_2$	$\sigma_h$	2 $S_3$	3 $\sigma_v$
$\Gamma_{\pi\perp}$	3	0	-1	-3	0	1

$D_{3h}$	E	2 $C_3$	3 $C_2$	$\sigma_h$	2 $S_3$	3 $\sigma_v$		
$A'_1$	1	1	1	1	1	1		$x^2 + y^2, z^2$
$A'_2$	1	1	-1	1	1	-1	$R_z$	
$E'$	2	-1	0	2	-1	0	(x,y)	$(x^2 - y^2, xy)$
$A''_1$	1	1	1	-1	-1	-1		
$A''_2$	1	1	-1	-1	-1	1	z	
$E''$	2	-1	0	-2	1	0	$(R_x, R_y)$	$(xz, yz)$

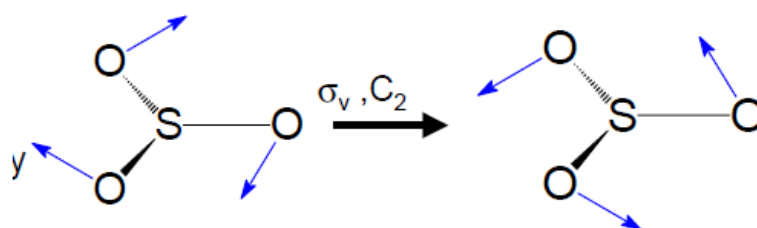


$$n_{A'_1} = \frac{1}{12} [(1)(3)(1) + (2)(0)(1) + (3)(-1)(1) + (1)(-3)(1) + (2)(0)(1) + (3)(1)(1)] \quad n_{A'_1} = \frac{0}{12} = 0$$

$$n_{A''_2} = \frac{1}{12} [(1)(3)(1) + (2)(0)(1) + (3)(-1)(-1) + (1)(-3)(-1) + (2)(0)(-1) + (3)(1)(1)] \quad n_{A''_2} = \frac{12}{12} = 1$$

$$n_{E''} = \frac{1}{12} [(1)(3)(2) + (2)(0)(-1) + (3)(-1)(0) + (1)(-3)(-2) + (2)(0)(1) + (3)(1)(0)] \quad n_{E''} = \frac{12}{12} = 1$$

Going through all the possible symmetry representations, we find that the combination ( $A''_2 + E''$ ) produces the  $\Gamma_{\pi\perp}$  that we determined. The irreducible representation shows us that the possible orbitals involved in perpendicular  $\pi$  bonding are the  $p_z$  and the  $d_{xz}$  and  $d_{yz}$  pair. This is in agreement with the  $\pi$  bonding we would predict using VBT.



First determine the reducible representation for the  $\pi$  bonding in the molecular plane,  $\Gamma_{\pi//}$ . The E operation leaves everything where it is so all three vectors stay in the same place and the character is 3. The  $C_3$  and  $S_3$  operations move all three vectors so their characters are 0. The  $C_2$  operation moves two of the vectors and reverses the sign of the other one so the character is -1. The  $\sigma_h$  operation leaves all three vectors unchanged so the character is 3. Each  $\sigma_v$  operation reverses the sign one vector where it was and moves the two others so the character is -1. Overall, the reducible representation for the parallel  $\pi$  bonding is:

$D_{3h}$	E	2 $C_3$	3 $C_2$	$\sigma_h$	2 $S_3$	3 $\sigma_v$
$\Gamma_{\pi//}$	3	0	-1	3	0	-1

$D_{3h}$	E	2 $C_3$	3 $C_2$	$\sigma_h$	2 $S_3$	3 $\sigma_v$		
$A'_1$	1	1	1	1	1	1		$x^2 + y^2, z^2$
$A'_2$	1	1	-1	1	1	-1	$R_z$	
$E'$	2	-1	0	2	-1	0	(x,y)	$(x^2 - y^2, xy)$
$A''_1$	1	1	1	-1	-1	-1		
$A''_2$	1	1	-1	-1	-1	1	z	
$E''$	2	-1	0	-2	1	0	$(R_x, R_y)$	$(xz, yz)$

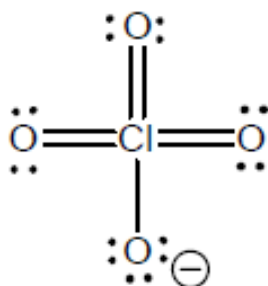
$$n_{A_1} = \frac{1}{12}[(1)(3)(1) + (2)(0)(1) + (3)(-1)(1) + (1)(3)(1) + (2)(0)(1) + (3)(1)(-1)] \quad n_{A_1} = \frac{0}{12} =$$

$$n_{A_2} = \frac{1}{12}[(1)(3)(1) + (2)(0)(1) + (3)(-1)(-1) + (1)(3)(1) + (2)(0)(1) + (3)(-1)(-1)] \quad n_{A_2} = \frac{12}{12} =$$

$$n_{E'} = \frac{1}{12}[(1)(3)(2) + (2)(0)(-1) + (3)(-1)(0) + (1)(3)(2) + (2)(0)(-1) + (3)(-1)(0)] \quad n_{E'} = \frac{12}{12} =$$

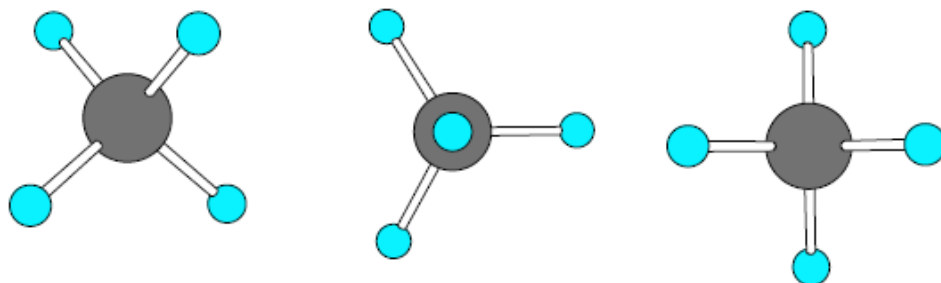
Going through all the possible symmetry representations, we find that the combination ( $A'_2 + E'$ ) produces the  $\Gamma_{\pi//}$  that we determined. The possible orbitals involved in parallel  $\pi$  bonding are only the  $dx^2-y^2$  and  $d_{xy}$  pair. The  $A'_2$  representation has no orbital equivalent. Note: Such analyses do not mean that there is  $\pi$  bonding using these orbitals – it only means that it is possible based on the symmetry of the molecule.

#### 4.7 The $\sigma$ and $\pi$ bonding in $\text{ClO}_4^-$



The point group is  $T_d$  so we must use the appropriate character table to find the reducible representation of the sigma bonding,  $\Gamma_\sigma$  first, then we can go the representation of the  $\pi$  bonding,  $\Gamma_\pi$ .

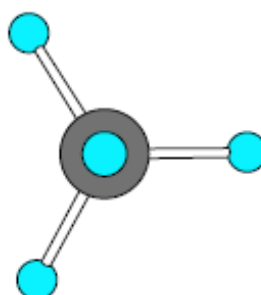
The  $E$  operation leaves everything where it is so all four bonds stay in the same place and the character is 4. Each  $C_3$  operation moves three bonds leaves one where it was so the character is 1. The  $C_2$  and  $S_4$  operations move all four bonds so their characters are 0. Each  $\sigma_d$  operation leaves two bonds where they were and moves two bonds so the character is 2.



$T_d$	E	8 $C_3$	3 $C_2$	6 $S_3$	6 $\sigma_d$
$\Gamma_\sigma$	4	1	0	0	2

$T_d$	E	8 $C_3$	3 $C_2$	6 $S_4$	6 $\sigma_d$		
$A_1$	1	1	1	1	1		$x^2 + y^2 + z^2$
$A_2$	1	1	1	-1	-1		
E	2	-1	2	0	0		$(2z^2 - x^2 - y^2, x^2 - y^2)$
$T_1$	3	0	-1	1	-1	$(R_x, R_y, R_z)$	
$T_2$	3	0	-1	-1	1	$(x, y, z)$	$(xy, xz, yz)$

The irreducible representation for the  $\sigma$  bonding is ( $A_1 + T_2$ ), which corresponds to the s orbital and the ( $p_x, p_y, p_z$ ) set that we would use in VBT to construct a the  $sp^3$  hybrid orbitals suitable for a tetrahedral arrangement of atoms. To get the representation for the  $\pi$  bonding, we must do the same procedure that we did for  $SO_3$ , except that in the point group  $T_d$ , one cannot separate the representations into parallel and perpendicular components. This is because the three-fold symmetry of the bond axis requires the orthogonal vectors to be treated as an inseparable pair.



The analysis of how the 8 vectors are affected by the symmetry operations gives

$T_d$	E	8 $C_3$	3 $C_2$	6 $S_3$	6 $\sigma_d$
$\Gamma_\pi$	8	-1	0	0	0

$T_d$	E	8 $C_3$	3 $C_2$	6 $S_4$	6 $\sigma_d$		
$A_1$	1	1	1	1	1		$x^2 + y^2 + z^2$
$A_2$	1	1	1	-1	-1		
E	2	-1	2	0	0		$(2z^2 - x^2 - y^2, x^2 - y^2)$
$T_1$	3	0	-1	1	-1	$(R_x, R_y, R_z)$	
$T_2$	3	0	-1	-1	1	$(x, y, z)$	$(xy, xz, yz)$

$dx^2-y^2$  and  $d_{xy}$  pair for E and either the ( $p_x, p_y, p_z$ ) set or the ( $d_{xy}, d_{xz}, d_{yz}$ ) set for  $T_2$ , since  $T_1$  does not correspond to any of the orbitals that might be involved in bonding. Because the ( $p_x,$

$p_y, p_z$ ) set has already been used in the  $\sigma$  bonding, only the ( $d_{xy}, d_{xz}, d_{yz}$ ) set may be used for  $\pi$  bonding.

#### 4.8 Summary of the unit

Each molecule has a point group, the full set of symmetry operations that describes the molecule's overall symmetry. We can use the decision tree to assign point groups character tables show how the complete set of irreducible representations of a point group transforms under all of the symmetry classes of that group. The tables contain all of the symmetry information in convenient form. We can use the tables to understand bonding and spectroscopy.

#### 4.9 Key words

Character tables; Symmetry of orbitals; Character Tables and Bonding; The  $\sigma$  bonding in dichloromethane,  $\text{CH}_2\text{Cl}_2$ ; The  $\sigma$  and  $\pi$  bonding in  $\text{SO}_3$ ; The  $\sigma$  and  $\pi$  bonding in  $\text{ClO}_4^-$

#### 4.10 References for further studies

- 1) Group theory and Symmetry in Chemistry; Gurdeep Raj; Ajay Bhagi; Vinod Jain; *Krishna Prakashan Media*; **2012**.
- 2) Symmetry: An Introduction to Group Theory and Its Applications; R. McWeeny; *Courier Corporation*, **2002**.
- 3) Symmetry and Group theory in Chemistry; M Ladd; *Elsevier*, **1998**.
- 4) Molecular Symmetry and Group Theory; Robert L. Carter; *Wiley India Pvt. Limited*, **2009**.
- 5) Introduction to Symmetry and Group Theory for Chemists; Arthur M. Lesk; *Springer Science & Business Media*, **2007**.

#### 4.11 Questions for self understanding

- 1) What is meant by character tables?
- 2) Discuss the symmetry of orbitals and functions
- 3) Discuss the character tables and bonding
- 4) Explain the formation of the  $\sigma$  bonding in dichloromethane,  $\text{CH}_2\text{Cl}_2$  using character table construction.
- 5) Explain the formation the  $\sigma$  and  $\pi$  bonding in  $\text{SO}_3$  using character table construction.
- 6) Explain the formation the  $\sigma$  and  $\pi$  bonding in  $\text{ClO}_4^-$  using character table construction.

**UNIT-5****Structure**

5.0 Objectives of the unit

5.1 Introduction

5.2 Infra-Red spectroscopy of inorganic compounds

5.3 Di atomic molecule of the type AB or A<sub>2</sub>

5.4 Tri atomic molecules of the type AB<sub>2</sub> or ABC

5.5 Tetra atomic molecules of the types AB<sub>3</sub>

5.6 Penta atomic molecules of the types AB<sub>4</sub>

5.7 Hexa atomic molecules of the types AB<sub>5</sub>

5.8 Hepta atomic molecules of the types AB<sub>6</sub>

5.9 IR spectral study of Lattice water and aquo and hydroxo complexes

5.9.1 *Lattice Water*

5.9.2 *Aquo (H<sub>2</sub>O) Complexes*

5.10 IR spectral study of sulfate and carbonate complexes

5.10.1 Sulfato (SO<sub>4</sub>)<sup>2-</sup> complexes

5.11 Carbonato (CO<sub>3</sub>) complexes

5.12 Mono and multinuclear carbonyl complexes

5.13 Diketonate complexes

5.14 IR spectra of Nitro and nitrate complexes

5.14.1 *Chelating Nitrite Complexes*

5.15 IR spectral study of thiocyanato complex

5.16 Applications in Coordination Chemistry

5.17 Complexes of ethylenediamine and related ligands

5.19 Study of isomerism

5.20 Metal Carbonyls

5.21 Organometallic Compounds

5.22 Summary of the unit

5.23 Key words

5.24 References for further studies

5.25 Questions for self understanding

## 5.0 Objectives of the unit

After studying this unit you are able to

- Explain the application of Infra-Red spectroscopy for inorganic compounds
- Explain the IR spectral study of Lattice water and aquo and hydroxo complexes
- Explain the IR spectral study of sulfate and carbonate complexes
- Explain the IR spectral study Mono and multinuclear carbonyl complexes
- Explain the IR spectral study Diketonate complexes
- Explain the IR spectra of Nitro and nitrate complexes

## 5.1 Introduction

The metal-ligand bond vibrations are sensitive to nature of ligand and metal. The stretching and bending vibration of metal-ligand bond appears in the low frequency region due to also the heavy mass of the metal ion/atom. Thus IR spectra studies of co-ordination compounds provide information about nature of metal ligand bond and the special distribution of the ligand atoms around metal atom/ion. The most common linkages in co-ordination compounds are M-O, M-N, M-X (halogens) and M-S. In general M-O stretching vibration gives a more intense and broad band than M-N stretching vibration. This is because large dipole moment change taking place in M-O bond than M-N bond (O is more electronegative than N). The M-S stretching vibration is generally of weak to medium intensity and this vibration occurs at much lower frequencies relative to M-O and M-N stretching vibrations. The M-X stretching vibration is usually medium to strong in infrared spectra. Compounds with bridge halogen atoms, it is expected that a bridging vibration is located at lower frequencies than those found for terminal vibrations. This is due to the fact that sharing of halogen between two metals in a bridged structure causes the bond to be weaker than a terminal halogen bond

Vibrations such as M-S, M-Se, M-P, M-C (this occurs in organometallic compounds) etc.... are expected to show only a slight change in the dipole moment, therefore such vibrations would be of weak to medium intensity

The most important factors which are responsible for affecting the metal-ligands vibration are

- i) Higher the oxidation state of the metal, higher is the frequency of vibration
- ii) Greater the mass of the metal and ligand, lower is the frequency
- iii) Higher the co-ordination number of the metal, lower is the frequency
- iv) Greater the basicity of the ligand, the greater the frequency for sigma bonding
- v) Non bridging ligands have higher frequency than bridging ligands
- vi) Greater the size of counter ion smaller is the frequency

- vii) Higher the ligand field stabilizing energy (LFSE) higher the frequency of vibration

### 5.2 Infra-Red spectroscopy of inorganic compounds

Characterization of compounds via infrared spectroscopy is not limited to organic compounds. Any inorganic compound that forms bonds of a covalent nature within a molecular ion fragment, cation or anion, will produce a characteristic absorption spectrum, with associated group frequencies.

Simple inorganic compounds, such as NaCl, do not produce any vibrations in the mid-infrared region, although the lattice vibrations of such molecules occur in the far-infrared region. This is why certain simple inorganic compounds, such as NaCl, KBr and ZnSe, are used for infrared windows. A slightly more complex inorganic, such as CaCO<sub>3</sub>, contains a complex anion. These anions produce characteristic infrared bands.

The cations in the complex inorganic compounds like KNO<sub>2</sub>, K<sub>2</sub>CO<sub>3</sub>, Na<sub>2</sub>SO<sub>4</sub> etc... generally has negligible effect on the wavenumber of the complex anion because of the crystal structure formed by such molecules. For example, in KNO<sub>2</sub> crystal, ionic lattice contains K<sup>+</sup> ions and NO<sub>2</sub><sup>-</sup> ions arranged in a regular array. The crystal structure consists of essentially isolated K<sup>+</sup> and NO<sub>2</sub><sup>-</sup> ions. Hence the infrared bands of the cation and anion are independent. K<sup>+</sup> is monatomic therefore does not produce vibrations and, consequently no infrared bands are absorbed. However, heavier cations cause a lower wavenumber shift for anionic vibration band. This effect is more common for the bending vibrations.

### 5.3 Di atomic molecule of the type AB or A<sub>2</sub>

The examples of di atomic molecules of the type A<sub>2</sub> are H<sub>2</sub>, Cl<sub>2</sub>, O<sub>2</sub>, N<sub>2</sub>, etc... These are called homonuclear di atomic molecules. The vibration of a homonuclear di atomic molecule like A<sub>2</sub> is infrared inactive. The examples of di atomic molecules of the type AB are, CO, HCl, HBr, etc.... these are called heteronuclear di atomic molecules.

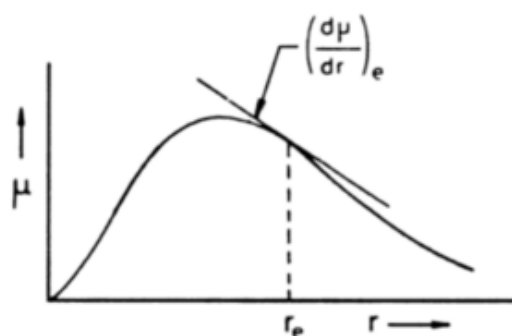


**Figure 1:** Variation of the dipole moment ( $\mu$ ) with internuclear distance  $r$  for a di atomic molecule AB

Heteronuclear diatomic molecule AB will necessarily have a permanent dipole moment because of asymmetry in its electron distribution. Hence the dipole moment occurs along the bond axis. The vibration of the dipole moment with inter nuclear distance is shown in figure 1.

Obviously the dipole moment is zero both for zero and infinitely large internuclear separations. The magnitude and sign of the dipole moment derivative depends on the particular molecule. Thus the stretching vibration of a heteronuclear diatomic molecule is infrared inactive

Table 1: Characteristic infrared bands of diatomic inorganic molecules

Wavenumber ( $\text{cm}^{-1}$ )	Assignment <sup>a</sup>
2250–1700	M–H stretching
800–600	M–H bending
750–100	M–X stretching
1010–850	M=O stretching
1020–875	M≡N stretching

<sup>a</sup>M, metal; X, halogen.

#### 5.4 Tri atomic molecules of the type AB<sub>2</sub> or ABC

Example of this type of molecules is CO<sub>2</sub>, NO<sub>2</sub>, SO<sub>2</sub>, ONCl, HCN, etc... Tri atomic molecules of the general formula AB<sub>2</sub> or ABC may have either a bent or a linear structure. Therefore first we have to look whether molecule is linear or non-linear. In case of linear, then we have to look whether it is symmetrical (B-A-B) or asymmetrical (B-B-A) Molecules such as H<sub>2</sub>O, SO<sub>2</sub>, NO<sub>2</sub>, ONCl etc..... are examples of bent tri atomic molecules. Molecules such as CO<sub>2</sub>, CS<sub>2</sub>, HCN etc.... Linear triatomic molecules.

Bent tri atomic molecules have three normal modes of vibration. Two of the vibrations are stretching modes and the remaining one vibration is a bending mode. These are shown in figure 2,

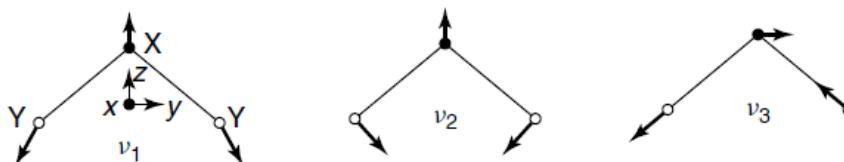


**Figure 2:** Normal modes of vibration of bent AB<sub>2</sub> {or XY<sub>2</sub>} molecules (+ and – denote vibrations moving upwards and downwards, respectively, in the direction perpendicular to the plane of the paper)

During each of the three normal vibrations of a bent triatomic molecule, there is change in the dipole moment of the molecule. Hence all the three vibrations are infrared active. The



intensity of the infrared absorption band is directly proportional to the square of the dipole moment changes during the vibration. Hence normally polar molecules are anticipated to give more intense infrared absorption band than non-polar molecules. It is not necessary for a molecule to possess permanent dipole moment for infrared activity, although bent triatomic molecules do possess permanent dipole moment.

A linear triatomic molecule of  $AB_2$  and  $ABC$  types has 4 normal vibrations. For example,  $CO_2$  molecule is a typical  $B_2A$  type molecule. The vibrations of  $CO_2$  molecule are depicted in figure 3, wherein observed frequencies are also indicated. The bending vibration ( $\nu_2$ ) shown in the plane of the paper and perpendicular to it are two distinct normal vibrations but they occur at same frequency. Such vibrations are said to be degenerate. Degenerate vibrations are found in molecules of higher symmetry.

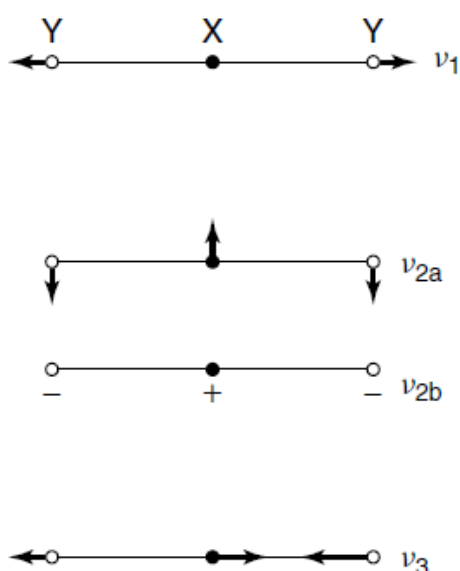


**Figure 3:** Normal modes of vibration of bent  $AB_2$  {or  $XY_2$ } molecules (+ and – denote vibrations moving upwards and downwards, respectively, in the direction perpendicular to the plane of the paper)

Another example is the vibration of  $NCS^-$  as in  $KNCS$ . The figure 4 shows the vibrations of  $NCS^-$  wherein the observed frequencies for the potassium compound are also given. The bending mode of  $NCS^-$  is again doubly degenerate. Appropriately one of the stretching vibrations is termed as  $N\equiv C$  stretching and other as C-S stretching.

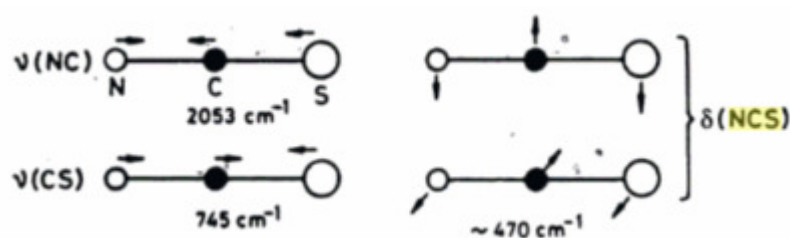


**Figure 4:** Normal vibrations of  $NCS^-$  ion

There is no dipole moment change during the symmetric stretching vibration of a linear symmetric tri atomic molecule such as  $\text{CO}_2$ . However, there is change in the dipole moment during bending and asymmetric stretching vibration. The symmetric stretching vibrations is hence infrared inactive and other two vibrations are infrared active.

Linear unsymmetrical triatomic molecules such as  $\text{HCN}$   $\text{NCS}^-$  etc... have three infrared bands, all the normal modes being infrared active since there is a change in the dipole moment during each of the vibrations.

Figure 5 depict the comparison of the bending vibration of a linear triatomic molecules with that of a nonlinear tri atomic molecules. It is clearly visible in the figure that for a non-linear molecules the vibrations corresponding to the terminal atoms moving downwards perpendicular to the plane of the molecule and the central atom moving upwards also perpendicular to the plane of the molecule. It is simply a rotational motion of the molecule as whole but this corresponding to a bending vibration in a linear triatomic molecule.

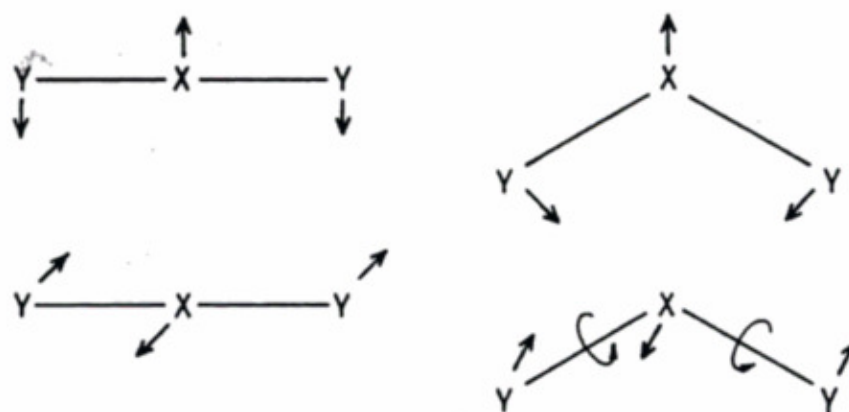


**Figure 5:** Comparison between degenerate bending vibrations in a linear triatomic molecules with the corresponding modes in a bent triatomic molecules

Table 2: Characteristic infrared bands ( $\text{cm}^{-1}$ ) of triatomic inorganic molecules

Molecule	$\nu_1$	$\nu_2$	$\nu_3$
<i>Linear</i>			
OCO	1388, 1286	667	2349
HCN	3311	712	2097
$\text{NCS}^-$	2053	486, 471	748
CICN	714, 784	380	2219
$\text{MgCl}_2$	327	249	842
<i>Bent</i>			
$\text{H}_2\text{O}$	3657	1595	3756
$\text{O}_3$	1135	716	1089
$\text{SnCl}_2$	354	120	334

### 5.5 Tetra atomic molecules of the types AB<sub>3</sub>

Tetra atomic molecules of the type AB<sub>3</sub> possess either pyramidal or planar geometry. The normal modes of 'infrared-active' vibrations of planar and pyramidal AB<sub>3</sub> molecules are illustrated in Figure 6.

The infrared absorption bands of some of the planar and pyramidal tetra atomic molecules are given in Table 3. Ligands may also adopt pyramidal and planar structures and the nature of the coordination also affects the resulting infrared bands of these ligands.

Table 3: Characteristic infrared bands (cm<sup>-1</sup>) of four-atom inorganic molecules

<i>Planar</i>	$\nu_2$	$\nu_3$	$\nu_4$	
BF <sub>3</sub>	719	1506	481	
CaCO <sub>3</sub>	879	1492–1429	706	
KNO <sub>3</sub>	828	1370	695	
SO <sub>3</sub>	498	1390	530	
<i>Pyramidal</i>	$\nu_1$	$\nu_2$	$\nu_3$	$\nu_4$
PF <sub>3</sub>	893	487	858	346
SO <sub>3</sub> <sup>2-</sup>	967	620	933	469
ClO <sub>3</sub> <sup>-</sup>	933	608	977	477
IO <sub>3</sub> <sup>-</sup>	796	348	745	306

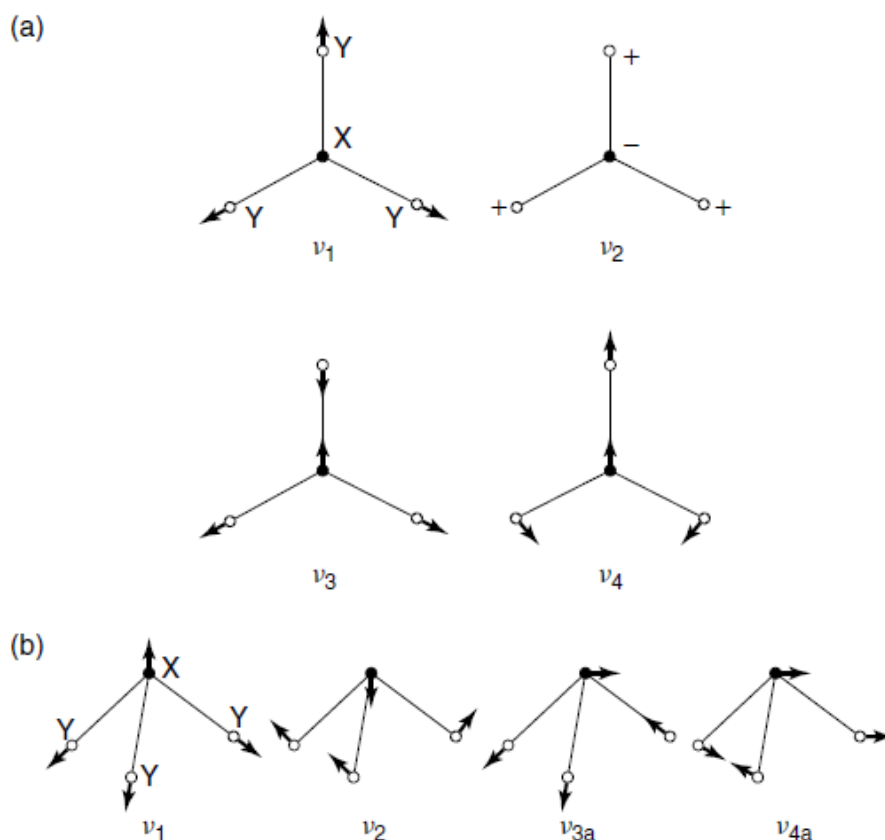


**Figure 6:** Normal modes of vibration of (a) planar and (b) pyramidal AB<sub>3</sub> molecules.

### 5.6 Penta atomic molecules of the types AB<sub>4</sub>

The five-atom penta atomic molecule of the type AB<sub>4</sub> and ligands commonly adopt tetrahedral and square-planar shapes. The normal modes of tetrahedral and square-planar AB<sub>4</sub> are shown in Figure 7. The tetrahedral AB<sub>4</sub> molecules show two ‘infrared-active’ normal modes of vibration, while the square-planar AB<sub>4</sub> molecules show three infrared-active’ normal modes of vibration.

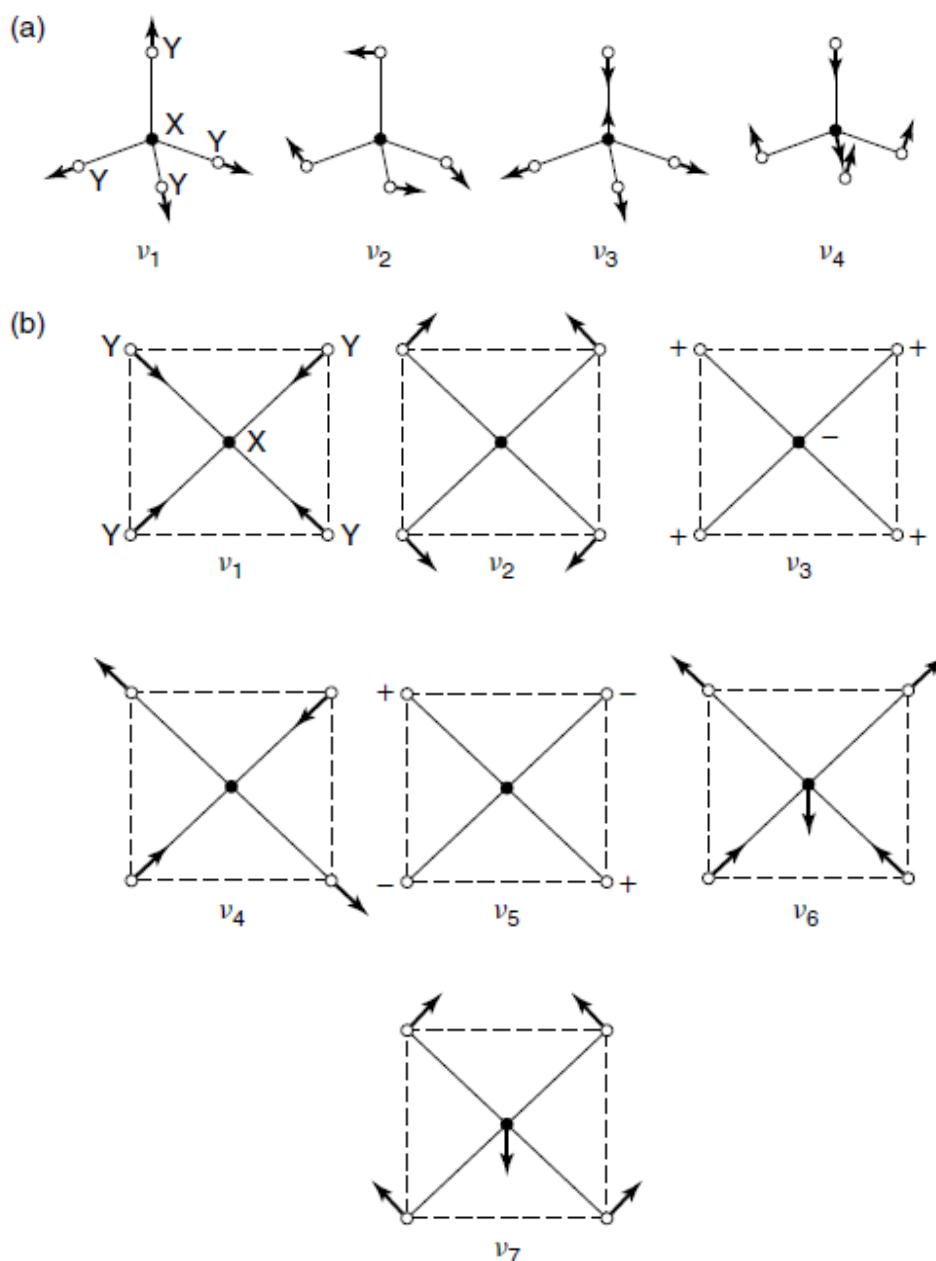


**Figure 7:** Normal modes of vibration of (a) tetrahedral and (b) square-planar AB<sub>4</sub> molecules. Table 4 summarizes the infrared bands of some common five-atom molecules.

Table 4: Characteristic infrared bands ( $\text{cm}^{-1}$ ) of five-atom inorganic molecules

<i>Tetrahedral</i>	$\nu_3$	$\nu_4$	
$\text{CH}_4$	3019	1306	
$\text{NH}_4^+$	3145	1400	
$\text{SnCl}_4$	408	126	
$\text{PO}_4^{3-}$	1017	567	
$\text{CrO}_4^{2-}$	890	378	
$\text{MnO}_4^-$	902	386	
<i>Square-planar</i>	$\nu_3$	$\nu_6$	$\nu_7$
$\text{XeF}_4$	291	586	161
$\text{PtCl}_4^{2-}$	147	313	165
$\text{PdCl}_4^{2-}$	150	321	161

### 5.7 Hexa atomic molecules of the types $\text{AB}_5$

Six atom molecules of the  $\text{AB}_5$  type have received considerable attention vibrational spectroscopic point of study. An  $\text{AB}_5$  molecule may adopt a trigonal bipyramidal, a square pyramidal or a planar-pentagonal structure. The trigonal bipyramidal, (e.g.  $\text{SF}_5^-$  or  $\text{BrF}_5$ ), shows six normal ‘infrared-active’ vibrations, while square (planar)-pentagonal  $\text{AB}_5$  molecules (e.g.  $\text{XeF}_5^-$ ) show three ‘infrared-active’ normal vibrations.

The normal modes of vibration of an  $\text{AB}_5$  molecule in the trigonalbipyramidal and square pyramidal geometry are depicted in Figure 8 and Figure 9 respectively.

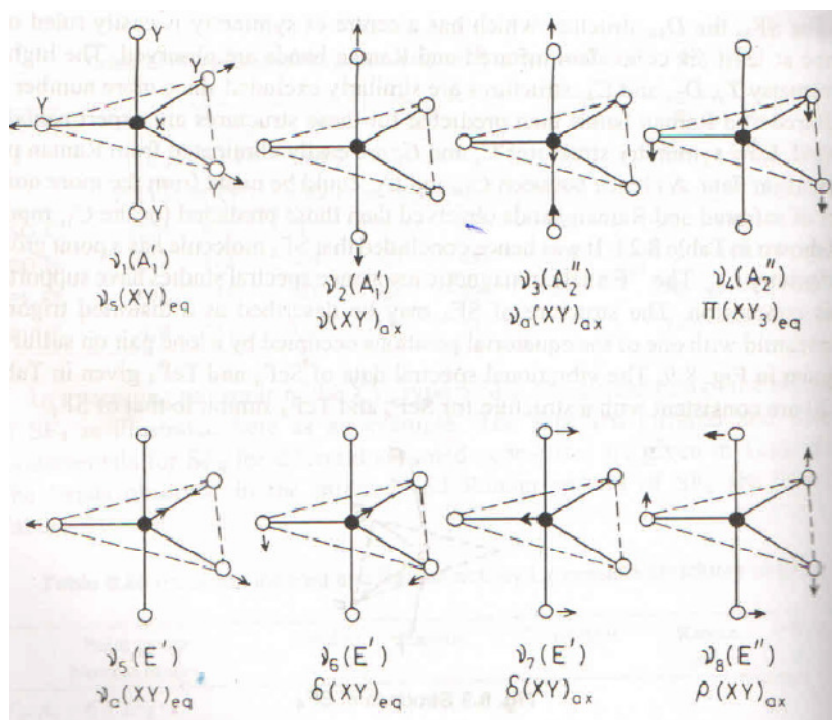


**Figure 8:** Normal modes of vibration of a trigonal bipyramidal  $\text{AB}_5$  molecule

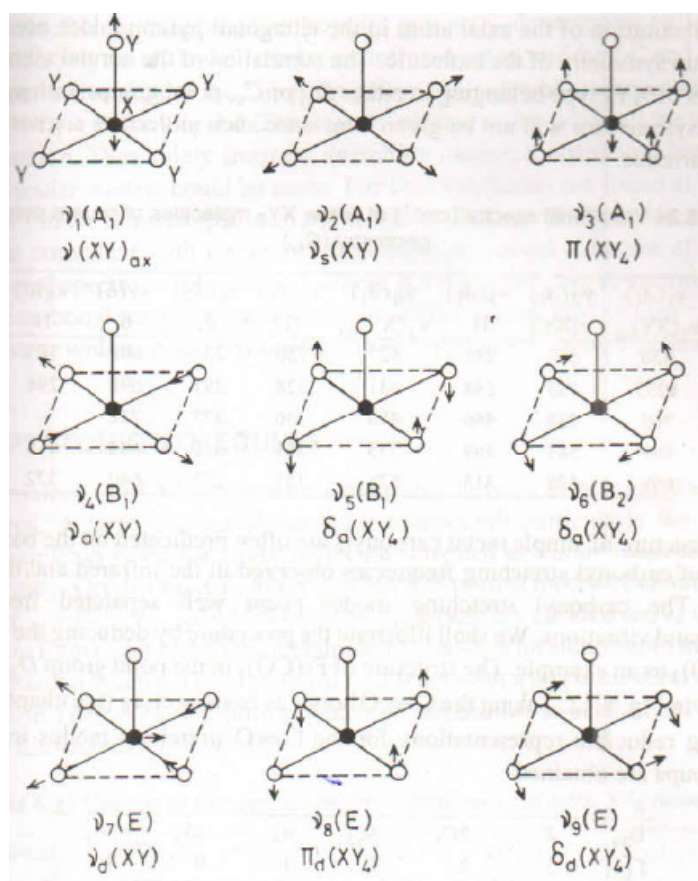


**Figure 9:** Normal modes of vibration of a square pyramidal  $AB_5$  molecule

### 5.8 Hepta atomic molecules of the types $AB_6$

$AB_6$  type of molecules invariably has an octahedral structure. A large number of inorganic compounds particularly transition metal complexes comes under this category. Octahedral  $AB_6$  molecules show 15 normal modes of vibration, but only two of these are 'infrared-active'. The normal modes of vibration of an octahedral  $AB_6$  molecule are illustrated in Figure 10.

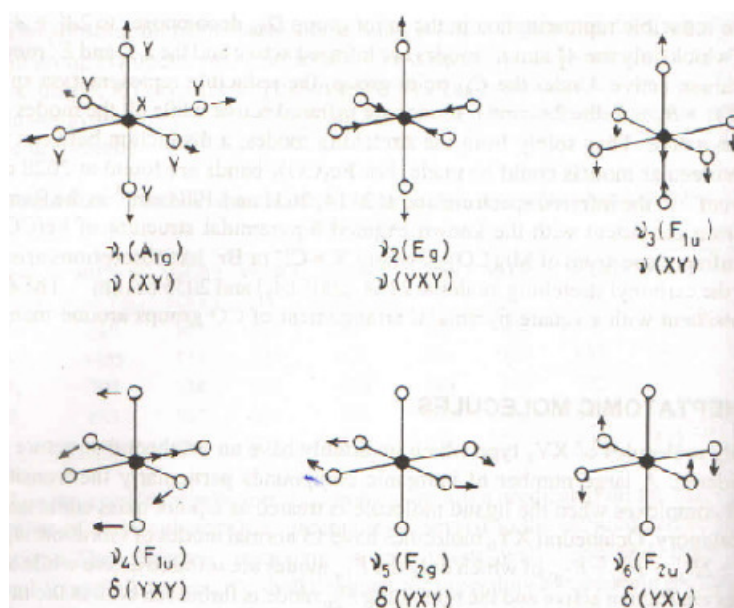


**Figure 10:** Normal modes of vibration of an octahedral  $AB_6$  molecule

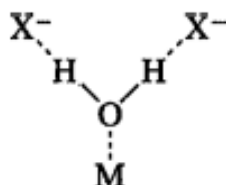
Table 5 summarizes the infrared bands of some hexahalo molecules which show an octahedral structure.

Table 5: Characteristic infrared bands ( $\text{cm}^{-1}$ ) of octahedral inorganic molecules

Molecule	$\nu_3$	$\nu_4$
$\text{AlF}_6^{3-}$	568	387
$\text{SiF}_6^{2-}$	741	483
$\text{VF}_6^{2-}$	646	300
$\text{PtCl}_6^{2-}$	343	183

### 5.9 IR spectral study of Lattice water and aquo and hydroxo complexes

Water in inorganic salts may be classified as lattice or coordinated water. There is, however, no definite borderline between the two. The former term denotes water molecules trapped in the crystalline lattice, either by weak hydrogen bonds to the anion or by weak ionic bonds to the metal, or by both



The latter term denotes water molecules bonded to the metal through partially covalent bonds.

Although bond distances and angles obtained from X-ray and neutron diffraction data provide direct information about the geometry of the water molecule in the crystal lattice, studies of vibrational spectra are also useful for this purpose. It should be noted, however, that the spectra of water molecules are highly sensitive to their surroundings.

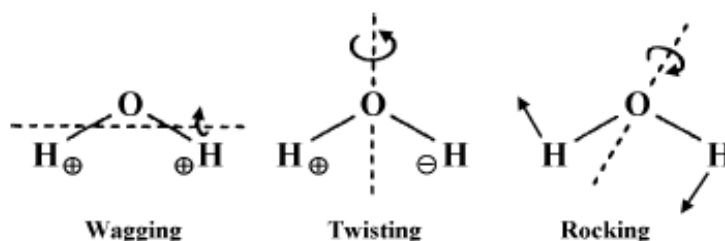


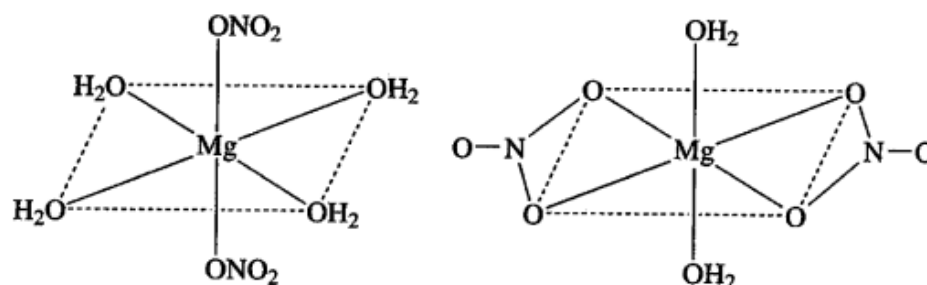
Figure 11: The three rotational modes of  $\text{H}_2\text{O}$  in the solid state

### 5.9.1 Lattice Water

In general, latticewater absorbs at  $3550\text{--}3200\text{ cm}^{-1}$  (anti-symmetric and symmetric -OH stretchings) and at  $1630\text{--}1600\text{ cm}^{-1}$  (H-O-H bending). If the spectrum is examined under high resolution, the fine structure of these bands is observed. For example,  $\text{CaSO}_4 \cdot 2\text{H}_2\text{O}$  exhibits eight peaks in the  $3500\text{--}3400\text{ cm}^{-1}$  region and its complete vibrational analysis can be made by factor group analysis. In the low-frequency region ( $600\text{--}200\text{ cm}^{-1}$ ) lattice water exhibits “librational modes” that are due to rotational oscillations of the water molecule, restricted by interactions with neighboring atoms. As shown in Figure 11, they are classified into three types depending on the direction of the principal axis of rotation. It should be noted, however, that these librational modes couple not only among themselves but also with internal modes of water (H-O-H bending) and other ions ( $\text{SO}_4^{2-}$ ,  $\text{NO}_3^-$ , etc.) in the crystal.

### 5.9.2 Aquo ( $\text{H}_2\text{O}$ ) Complexes

In addition to the three fundamental modes of the free water molecule, coordinated water exhibits other modes. Vibrational spectroscopy is very useful in elucidating the structures of aquo complexes. For example,  $\text{TiCl}_3 \cdot 6\text{H}_2\text{O}$  should be formulated as  $\text{trans}[\text{Ti}(\text{H}_2\text{O})_4\text{Cl}_2]\text{Cl} \cdot 2\text{H}_2\text{O}$  since it exhibits one TiO stretching ( $500\text{ cm}^{-1}$ ) and one TiCl stretching ( $336\text{ cm}^{-1}$ ) mode. Chang and showed from infrared and Raman studies that the structures of the tetrahydrates and dehydrates resulting from the dehydration of  $\text{Mg}(\text{NO}_3)_2 \cdot 6\text{H}_2\text{O}$  are as follows



## 5.10 IR spectral study of sulfate and carbonate complexes

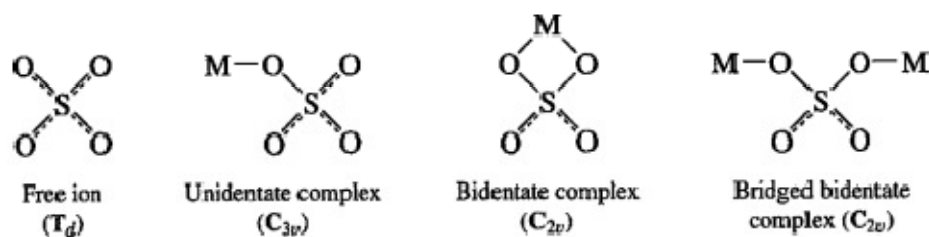
When a ligand of relatively high symmetry coordinates to a metal, its symmetry is lowered and marked changes in the spectrum are expected because of changes in the selection rules. This principle has been used extensively to determine whether acido anions such as  $\text{SO}_4^{2-}$  and  $\text{CO}_3^{2-}$  coordinate to metals as unidentate, chelating bidentate, or bridging bidentate ligands. Although symmetry lowering is also caused by the crystalline environment, this effect is generally much smaller than the effect of coordination.

### 5.10.1 Sulfato ( $\text{SO}_4^{2-}$ ) complexes

The free sulfate ion belongs to the high-symmetry point group  $T_d$ . Of the four fundamentals, only  $\nu_3$  and  $\nu_4$  are infrared-active. If the symmetry of the ion is lowered by complex

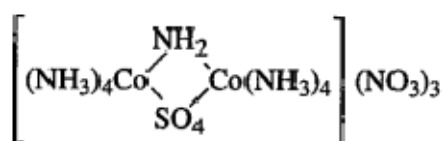


formation, the degenerate vibrations split and Raman-active modes appear in the infrared spectrum. The lowering of symmetry caused by coordination is different for the unidentate and bidentate complexes, as shown below



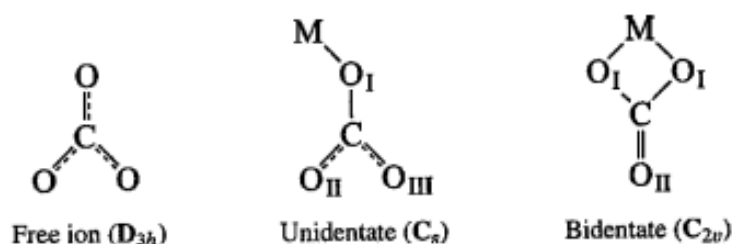
In  $[\text{Co}(\text{NH}_3)_6]_2(\text{SO}_4)_3 \cdot 5\text{H}_2\text{O}$  complex the  $\nu_3$  and  $\nu_4$  do not split and  $\nu_2$  does not appear, although  $\nu_1$  is observed, it is very weak. , Therefore it is concluded that the symmetry of the  $\text{SO}_4^{2-}$  ion is approximately  $T_d$ . In  $[\text{Co}(\text{NH}_3)_5\text{SO}_4]\text{Br}$ , both  $\nu_1$  and  $\nu_2$  appear with medium intensity. Moreover,  $\nu_3$  and  $\nu_4$  each splits in to two bands. This result can be explained by assuming a lowering of symmetry from  $T_d$  to  $C_{3v}$  (unidentate coordination).

In both  $\nu_1$  and  $\nu_2$  appear with medium intensity, and  $\nu_3$  and  $\nu_4$  each splits into three bands. These results suggest that the symmetry is further lowered and probably reduced to  $C_{2v}$ , Thus, the  $\text{SO}_4^{2-}$  group in this complex is concluded to be a bridging bidentate as depicted in the diagram.



### 5.11 Carbonato ( $\text{CO}_3$ ) complexes

The unidentate and bidentate (chelating) coordinations shown below are found in the majority of carbonato complexes



In  $C_{2v}$  and  $C_s^*$ , the  $\nu_1$  vibration, which is forbidden in the free ion, becomes infrared-active and each of the doubly degenerate vibrations,  $\nu_3$  and  $\nu_4$ , splits into two bands. Although the number of infrared-active fundamentals is the same for  $C_{2v}$  and  $C_s$ , the splitting of the degenerate vibrations is larger in the bidentate than in the unidentate complex. For example,  $[\text{Co}(\text{NH}_3)_5\text{CO}_3]\text{Br}$  exhibits two CO stretchings at 1453 and 1373  $\text{cm}^{-1}$ , whereas  $[\text{Co}(\text{NH}_3)_4\text{CO}_3]\text{Cl}$  shows them at 1593 and 1265  $\text{cm}^{-1}$ . In organic carbonates such as dimethyl carbonate,  $(\text{CH}_3\text{O})_2\text{CO}^{\text{II}}$ , this effect is more striking because the  $\text{CH}_3\text{O}$  bond is strongly

covalent. Thus, the C=O stretching is observed at  $1870\text{ cm}^{-1}$ , whereas the C-O stretching is at  $1260\text{ cm}^{-1}$ . Gatehouse and co-workers showed that the separation of the CO stretching bands increases along the following order:

Basic salt < carbonato complex < acid < organic carbonate

### 5.12 Mono and multinuclear carbonyl complexes

The carbonyl groups can have two modes of stretching vibrations. Both of these modes result in change in dipole moment as shown in figure 12. Thus two bands are expected in the infrared spectra of a terminally ligated carbon monoxide. The infrared and Raman spectroscopy together can be used to determine the geometry of the metallic carbonyls.

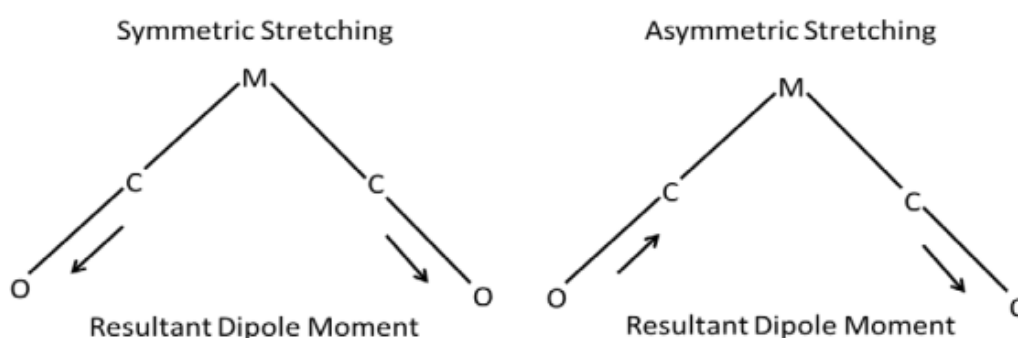


**Figure12:** Stretching modes of carbonyl ligand

A mono nuclear pentacarbonyl can exist both in square pyramidal and trigonal bipyramidal geometry. Performing infrared spectra after calculating the IR active and Raman active bands in both the possible geometries can provide information about the actual geometry of the molecule. Infrared spectroscopy of metallic carbonyls helps in determining the bond order of ligated carbon monoxide.

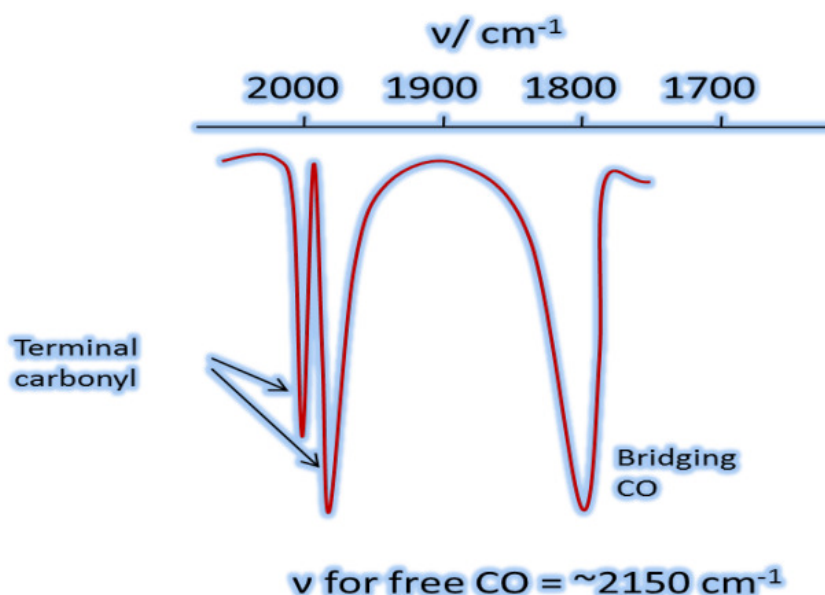
The C-O bond order and the frequency related to its absorption are directly proportional. Thus, it can be predicted that the frequencies of absorption will be in the order shown below  
Free CO > metal carbonyl cation > neutral metal carbonyl > metal carbonyl anion.

Table 6: Comparison C-O stretching in representative metal carbonyls

Carbonyl	Type	C-O stretching frequency ( $\text{cm}^{-1}$ )
Carbon monoxide	Free	~2150
$\text{Mn}(\text{CO})_6^+$	Cation	~2090
$\text{Cr}(\text{CO})_6$	Neutral	~2000
$\text{V}(\text{CO})_6^-$	Anion	~1850

It is also used to distinguish the terminal and bridging carbonyl groups. The C-O bonding in terminal carbonyl groups is stronger than the bridged carbonyl groups. Therefore, it is possible to differentiate the terminal carbonyls which absorb in the region of 2050–1900  $\text{cm}^{-1}$  from the bridged carbonyls absorbing below 1900  $\text{cm}^{-1}$  as illustrated in figure 13.

The change in the intensity of bands related to carbonyl group can provide information for the kinetic studies of the substitution reactions involving replacement of carbonyls.



**Figure 13:** A partial infrared spectrum showing terminal and bridged carbonyl

### 5.13 Diketonate complexes

The  $\beta$ -diketones or 1,3-diketones bear two carbonyl groups that are separated by one carbon atom. This carbon atom is the  $\alpha$ -carbon. In most  $\beta$ -diketones, the substituents on the  $\alpha$ -carbon are hydrogen atoms. The substituent on the carbonyl function can be an alkyl group, a fluorinated alkyl group, an aromatic or an heteroaromatic group. The simplest  $\beta$ -diketone is acetylacetone (Hacac), where the substituents on both carbonyl groups are methyl groups. All other  $\beta$ -diketones can be considered as derived from acetylacetone by substitution of the  $\text{CH}_3$  groups by other groups as shown in Figure 14.

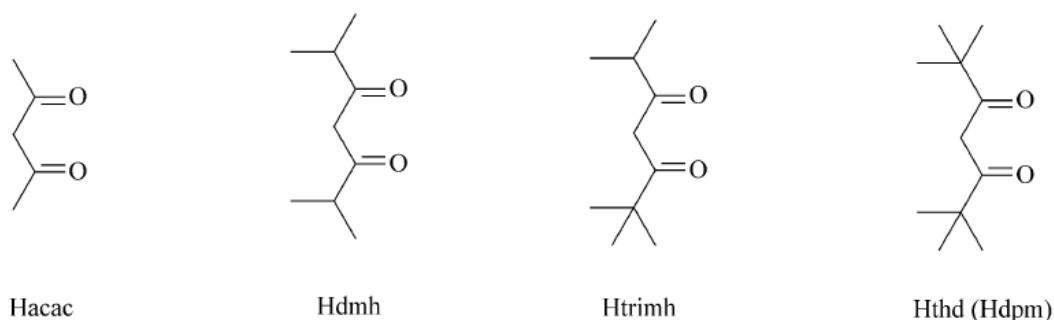


**Figure 14:** Structures of  $\beta$ -diketones with aliphatic substituents

The  $\beta$ -diketones exhibit keto–enol tautomerism (Figure 15). In the enol form the H-atom of the alcohol function is hydrogen-bonded to the carbonyl O-atom.



**Figure 15:** Keto-enol equilibrium in acetylacetone

Three main types of  $\beta$ -diketonate complexes with metal ion have found, they are, tris complexes, Lewis base adducts of the tris complexes (ternary rare-earth  $\beta$ -diketonates) and tetrakis complexes.

The neutral tris complexes or tris( $\beta$ -diketonates) have three  $\beta$ -diketonate ligands for each metal ion and they can be represented by the general formula  $[M(\beta\text{-diketonate})_3]$ . Because the coordination sphere of the metal ion is unsaturated in these six-coordinate complexes, the metal ion can expand its coordination sphere by oligomer formation (with bridging  $\beta$ -diketonates ligands), but also by adduct formation with Lewis bases, such as water, 1,10-phenanthroline, etc... It is also possible to arrange four  $\beta$ -diketonate ligands around a single metal ion and in this way tetrakis complexes or tetrakis( $\beta$ -diketonates) with the general formula  $[M(\beta\text{-diketonate})_4]^-$  are formed. These complexes are anionic and the electric neutrality is achieved by a counter cation. The cation can be an alkali-metal ion ( $\text{Li}^+$ ,  $\text{Na}^+$ ,  $\text{K}^+$ ,  $\text{Cs}^+$ ,  $\text{Rb}^+$ ).

Over the years, there has been a lot of dispute about the assignment of some absorption bands in the infrared (IR) spectra of metal complexes of  $\beta$ -diketonates, including the rare-earth  $\beta$ -diketonates. More particularly, the polemic was about the positions of the C=O and C=C stretching vibrations in the infrared spectra. The bands at  $1580\text{ cm}^{-1}$  and  $1520\text{ cm}^{-1}$  is assigned to the C=O and C=C stretching modes respectively.

The absorption bands observed in the infrared spectrum of  $[\text{Eu}(\text{acac})_3(\text{H}_2\text{O})_2]$  at  $1600\text{ cm}^{-1}$  and  $1515\text{ cm}^{-1}$  to the C=O and C=C stretching vibrations respectively. Replacement of a methyl group by a trifluoromethyl group strengthens the C=O and C=C bonds, but weakens the Eu–O bond. The former two bands are therefore shifted to higher wavenumbers, while the latter is shifted to lower wavenumbers.

Misumi and Iwasaki (1967) studied the infrared spectra of the tris acetylacetonate complexes of praseodymium(III), neodymium(III), europium(III), gadolinium(III), dysprosium(III) and erbium(III). Their assignments of the C=O and C=C stretching vibrations should be corrected, according to the findings of Pinchas et al. (1967). The M–O vibrations were found

in the regions  $420\text{--}432\text{ cm}^{-1}$  and  $304\text{--}322\text{ cm}^{-1}$ . The M–O stretching vibrations shift to higher wavenumbers from praseodymium(III) to erbium(III).

#### 5.14 IR spectra of Nitro and nitrate complexes

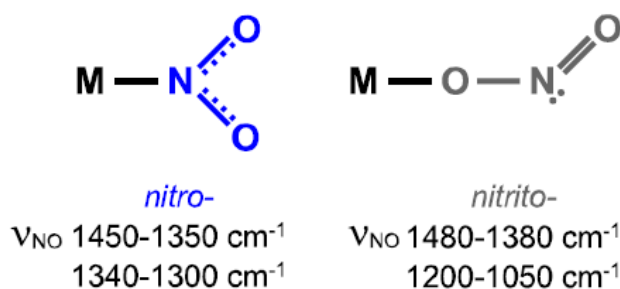
Many ligands are ambidentate, meaning they have the ability to bond a central atom in more than one way. Examples of this include  $\text{NCS}^-$ , which can coordinate via the N or S atom and  $\text{NO}_2^-$  which can coordinate via the N or O atom. For example, the  $\text{NO}_2^-$  ligand is can form a coordination complex with cobalt through the N atom or O atom to yield two structural isomers as shown in figure 16, a nitrito or the more stable nitro.



**Figure 16:** The two ways that  $\text{NO}_2^-$  can form coordination complexes to Co

In the nitrito complex, metal-to-ligand bonding is through one of the oxygen atoms while the metal-to-ligand bonding for the nitro complex takes place through the nitrogen. The nitro complex is the thermodynamically stable product while the nitrito complex is the kinetic product and over time will transform into the more stable thermodynamic product. The two complexes are distinguishable from one another based upon their individual IR spectrum. The nitro complex will give a significantly different peak than that of the nitrito complex due to the differences in the bonding of the two structures.

If the  $\text{NO}_2$  group is bonded to a metal through one of its O atoms, it is called a nitrito complex. The two  $\nu(\text{NO}_2)$  of nitrito complexes are well separated,  $\nu(\text{N}=\text{O})$  and  $\nu(\text{NO})$  with at  $1485\text{--}1400$  and  $1110\text{--}1050\text{ cm}^{-1}$  respectively. Distinction between the nitro and nitrito coordination can be made on this basis. It is to be noted that nitrito complexes lack the wagging modes near  $620\text{ cm}^{-1}$  that appear in all nitro complexes. The  $\nu(\text{MO})$  of nitrito complexes were assigned in the  $360\text{--}340\text{ cm}^{-1}$  region for metals such as Cr(III), Rh(III), and Ir(III).



### 5.14.1 Chelating Nitrito Complexes

If the nitrito group is chelating, the  $\nu(\text{N}=\text{O})$  and  $\nu(\text{NO})$  of the nitrito group will be shifted to a lower and a higher frequency, respectively, relative to those of unidentate nitrito complexes. As a result, the separation between these two modes ( $\Delta$ ) becomes much smaller than those of unidentate complexes. It should be noted that the  $\Delta$  value depends on the degree of asymmetry of the coordinated nitrito group; it is expected that the  $\Delta$  value is the smallest when the two N-O bonds are equivalent and increases as the degree of asymmetry increases. Suppose we record IR spectrum for the nitrito complex several days later, the spectrum nearly identical to the nitro complex. This is explained by the natural degradation of the kinetic product, nitrito, into the thermodynamically stable product, nitro.

### 5.15 IR spectral study of thiocyanato complex

Many of the associated group frequencies can be used diagnostically for characterization. The structure and orientation of the ion or complex, both as an isolated entity or within a crystal lattice, are important factors that affect the appearance and nature of the infrared spectrum. Hydration of compounds (water of crystallization) also has a large effect on the spectrum, and often adds a lot of complexity, in the form of additional absorption bands and structure to existing bands. A few example group frequencies are included here (Table 7).

Table 7: Example group frequencies for common inorganic ions

Group frequency ( $\text{cm}^{-1}$ )	Functional group/assignment
1490–1410/880–860 <sup>a</sup>	Carbonate ion
1130–1080/680–610 <sup>a</sup>	Sulfate ion
1380–1350/840–815 <sup>a</sup>	Nitrate ion
1100–1000	Phosphate ion
1100–900	Silicate ion
3300–3030/1430–1390 <sup>a</sup>	Ammonium ion
2200–2000	Cyanide ion, thiocyanate ion, and related ions

<sup>a</sup> Typically, the first absorption is intense and broad, and the second has weak to medium intensity and is narrow. Both often exist as multiple band structures, and this may be used to characterize individual compounds.

The degree of hydration of an inorganic compound is also a factor when interpreting spectra. The water molecules that are incorporated into the lattice structure of a crystalline compound produce characteristic sharp bands in the 3800–3200 and 1700–1600  $\text{cm}^{-1}$  regions, due to O–H stretching and bending, respectively. The lattice environment of the water molecules determines the position of the infrared bands of water and whether they are single or split.

The hydroxy stretching bands in the 3800–3200  $\text{cm}^{-1}$  range show unique patterns that may be used to characterize the compositions of hydrated inorganic compounds.

### 5.16 Applications in Coordination Chemistry

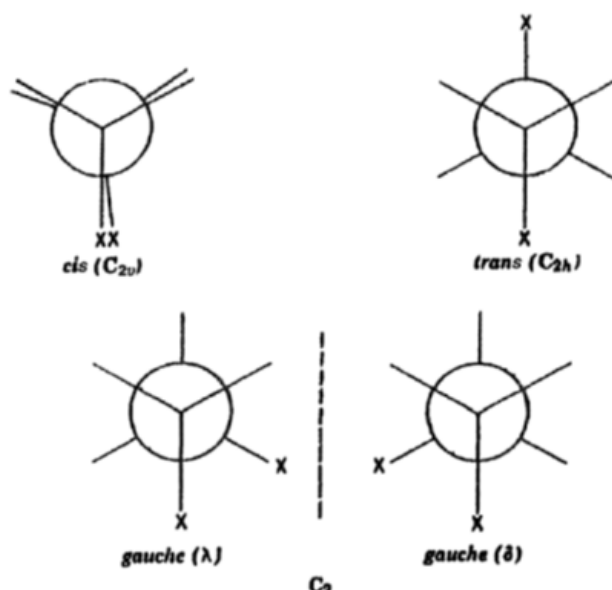
Metal complexes or chelates are largely covalent in nature and the spectra of such compounds are dominated by the contribution of the ligand and its coordination chemistry. The ligands may be small species, such as water or ammonium molecules, or large complex species, such as porphyrins.

### 15.17 Complexes of ethylenediamine and related ligands

#### *Chelating Ethylenediamine*

When ethylenediamine(en) coordinates to a metal as a chelating ligand, it may take a gauche ( $\delta$  and  $\lambda$ ) or a cis conformation, as shown in Figure 18. Then, there are eight different conformations are probable for the  $[\text{M}(\text{en})_3]^{n+}$  ion if we consider all possible combinations of conformations of the three chelate rings ( $\delta$  or  $\lambda$ ) around the chiral metal centre. They are designated as  $\Lambda(\delta\delta\delta)$ ,  $\Lambda(\delta\delta\lambda)$ ,  $\Lambda(\delta\lambda\lambda)$ ,  $\Lambda(\lambda\lambda\lambda)$ ,  $D(\lambda\lambda\lambda)$ ,  $\Delta(\lambda\lambda\delta)$ ,  $\Delta(\lambda\delta\delta)$ , and  $\Delta(\delta\delta\delta)$ . According to X-ray analysis, all the en ligands in the  $[\text{Co}(\text{en})_3]^{3+}$  ion take the gauche conformation ( $\delta$ ), and the configuration of the whole ion is  $\Lambda(\delta\delta\delta)$ . Although it is rather difficult to obtain such information from vibrational spectra, some of these conformers can be distinguished by the number of IR-active C-C stretching vibrations.

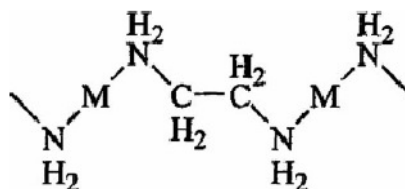
For example,  $[\text{Cr}(\text{en})_3]\text{Cl}_3 \cdot 3.5\text{H}_2\text{O}$  [ $\Lambda(\delta\delta\delta)$ ,  $D_3$  symmetry] exhibits only one band at 1003  $\text{cm}^{-1}$  whereas  $[\text{Cr}(\text{en})_3][\text{Ni}(\text{CN})_5] \cdot 1.5\text{H}_2\text{O}$  [ $\Lambda(\delta\delta\lambda)$ ,  $\delta\lambda\lambda$ ,  $C_2$  symmetry] exhibits three bands at 1008, 1002 (shoulder), and 995  $\text{cm}^{-1}$ . Racemic ( $\delta\lambda$ ) and optically active ( $\delta$ ) forms of  $[\text{Co}(\text{en})_3]\text{Cl}_3$  can be distinguished in the crystalline state by comparing vibrational spectra below 200  $\text{cm}^{-1}$ .



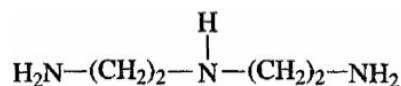
**Figure 18:** Rotational isomers of 1,2-disubstituted ethane. X=  $\text{NH}_2$  for en.

*Bridging Ethylenediamine*

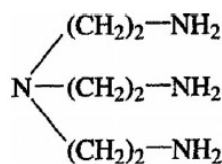
Ethylenediamine takes the *trans* form when it functions as a bridging group between two metal atoms. The *trans* configuration of ethylenediamine was found in  $(\text{AgCl})_2\text{en}$ ,  $(\text{AgSCN})_2\text{en}$ ,  $(\text{AgCN})_2\text{en}$ ,  $\text{Hg}(\text{en})\text{Cl}_2$ , and  $\text{M}(\text{en})\text{Cl}_2$  ( $\text{M} = \text{Zn}$  or  $\text{Cd}$ ). The structure of these complexes may be depicted as follows

*Complexes of Polyamines*

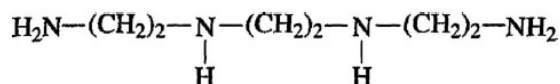
Polyamines such as Diethylenetriamine(dien), Triaminotriethylamine(tren), Triethylenetetramine(trien) shown below are coordinate to a metal as tridentate or tetradentate ligands. Diethylenetriamine(dien)



Triaminotriethylamine(tren)



Triethylenetetramine(trien)



The infrared spectra of diethylenetriamine (dien) complexes  $[\text{Pd}(\text{dien})\text{X}]\text{X}$  ( $\text{X} = \text{Cl}, \text{Br}, \text{I}$ ) and  $[\text{Co}(\text{dien})(\text{en})\text{Cl}]^{2+}$  reveals that the latter exists in the four isomeric forms as shown in Figure 19. 1.11. The  $\omega$  and  $\kappa$ -isomers contain dien in the *mer* configuration; the  $\pi$ - and  $\epsilon$ -isomers contain dien in the *fac* configuration. The *mer*- and *fac*-isomers of  $[\text{M}(\text{dien})\text{X}_3]$  [ $\text{M} = \text{Cr}(\text{III}), \text{Co}(\text{III}),$  and  $\text{Rh}(\text{III})$ ;  $\text{X}$ : a halogen] can also be distinguished by infrared spectra.

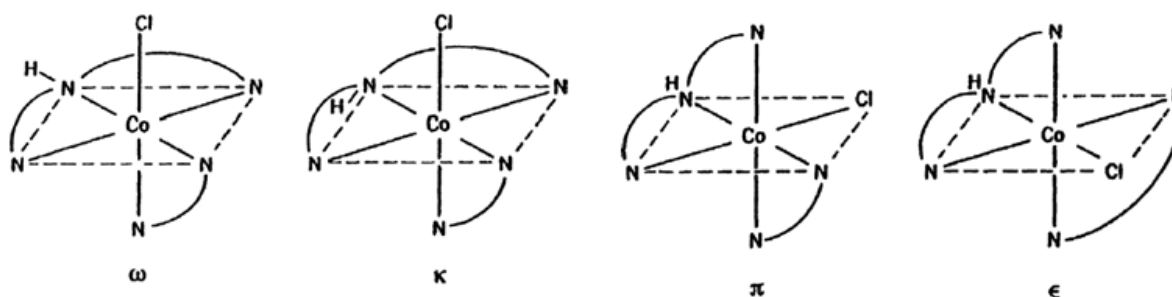


**Figure 19:** Structures of the  $[\text{Co}(\text{dien})(\text{en})\text{Cl}]^{2+}$  ion



The infrared spectra of  $\beta$ ,  $\beta^1$ ,  $\beta^{11}$ -triaminotriethylamine(tren) complexes with Co(III) and lanthanides give three isomers (Figure 20). For example the infrared spectra of  $[M(\text{tren})X_2]^+$ , where tren is triethylene-tetramine, M is Co(III), Cr(III), or Rh(III), and X is a halogen or an acido anion.

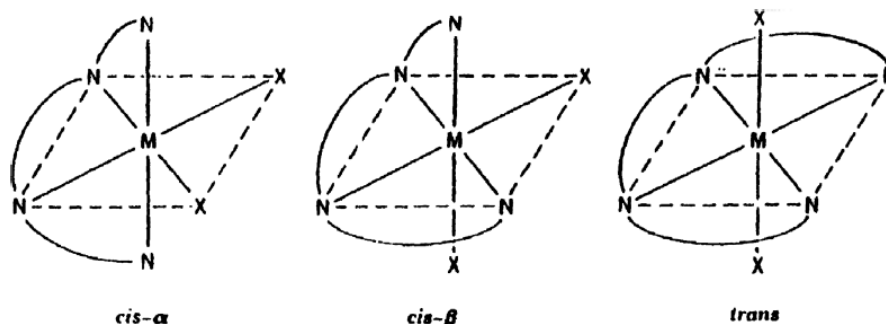


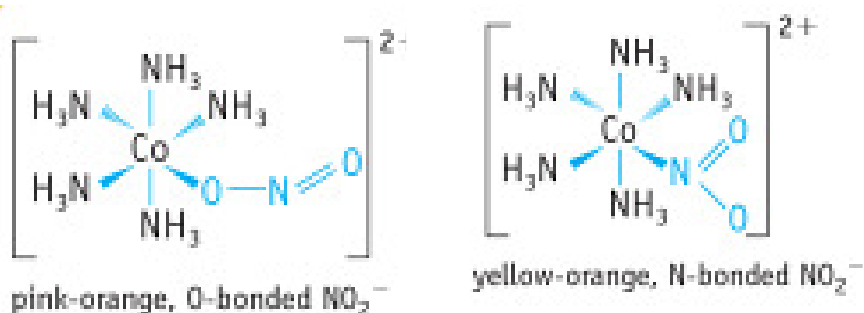
**Figure 20:** Structures of the  $[M(\text{tren})X_2]^+$  ions.

These compounds gave three isomers that can be distinguished by the  $\text{CH}_2$  rocking vibrations in the  $920\text{--}869\text{ cm}^{-1}$  region. For  $[\text{Co}(\text{tren})\text{Cl}_2]\text{ClO}_4$  complex, cis- $\alpha$ -isomer exhibits two strong bands at  $905$  and  $871\text{ cm}^{-1}$  and cis- $\beta$ -isomer shows four bands at  $918$ ,  $898$ ,  $868$ , and  $862\text{ cm}^{-1}$ ; trans-isomer gives only one band at  $874\text{ cm}^{-1}$  with a weak band at  $912\text{ cm}^{-1}$ .

### 5.19 Study of isomerism

Linkage and geometrical isomerisms are important issues in coordination chemistry, producing structures with differing properties. Linkage isomerism occurs when a ligand can coordinate to a central metal using either of two atoms within the ligand.

For example, the nitrite ion exhibits this type of isomerism. When the nitrite ion is attached to a central metal ion via the nitrogen atom, it is known as a nitro ligand. When one of the oxygen atoms is the donor, it is known as a nitritoligand.



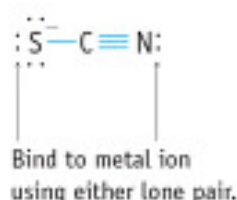
When  $\text{NO}_2^-$  bonds undergo bonding through an oxygen bond, one of the  $\text{NO}$  bonds is 'nearly' a double bond, while the other is a single bond. In the other coordination, both  $\text{NO}$  bonds are intermediate between single and double bonds. The infrared band of a bond increases as its strength increases and so it would be expected that the wavenumbers of the  $\text{NO}$  bonds in  $\text{NO}_2^-$  increase in the order:

Single-bond NO (in O-bonded) < NO (in N-bonded) < double-bond NO (in O-bonded).

It is observed that in complexes when  $\text{NO}_2^-$  is bonded through oxygen, N=O stretching appears in the  $1500\text{--}1400\text{ cm}^{-1}$  range while N–O stretching appears at  $1100\text{--}1000\text{ cm}^{-1}$ .

In complexes in which  $\text{NO}_2^-$  is bonded through nitrogen, the infrared bands appear at  $1340\text{--}1300\text{ cm}^{-1}$  and  $1430\text{--}1360\text{ cm}^{-1}$ , which are intermediate values when compared to the oxygen-bonded complex. This way it is possible to use infrared spectroscopy to determine whether a nitrite is coordinated and whether it is coordinated through a nitrogen or oxygen atom.

Similarly the linear thiocyanate group can be present in inorganic compounds as an anion or as a ligand. It can appear as a monodentate ligand coordinated through sulfur or nitrogen atom, or a bridging ligand.



This type of coordination ability and a variety of bonding modes of the thiocyanate group are responsible for the existence of a relatively large number of coordination compounds. Infrared spectroscopy is often used for approximative estimation of bonding modes.

Application of infrared spectroscopy for these purposes is based on the fact that the S- or N-coordinated thiocyanate and noncoordinated thiocyanate anion ligand gives significantly different shifts of absorption bands. Thus Infrared spectroscopy is use full for correlating the mode of coordination of thiocyanate ligand with changes of wavenumbers.

There are three vibrations occur, they are,

- i) The pseudosymmetric stretching vibration  $\nu(\text{CN})$   
The doubly degenerated deformation frequency  $\delta(\text{NCS})$ , and
- ii) The pseudosymmetric stretching vibration  $\nu(\text{CS})$ .

Vibrational frequencies (wavenumber) ranges of thiocyanate group with various bonding modes like  $\text{M—NCS}$ ,  $\text{M—SCN}$ , and  $\text{M—NCS—M}$  are listed in table 8.

Table 8: Vibrational frequencies (wavenumber) ranges of thiocyanate group

Mode of coordination	$\nu(\text{CN})$	$\nu(\text{CS})$	$\delta(\text{NCS})$ .
$(\text{NCS})^-$	2053	746	486, 471
$\text{M—NCS}$	2100—2050 s, b	870—820 w	485—475
$\text{M—SCN}$	2130—2085 s, sp	760—700 b	470—430
$\text{M—NCS—M}$	2165—2065	800—750	470—440

s — strong, b — broad, w — weak, sp — split.

However positions of the frequencies are slightly influenced by changes in the mass, charge, and size of the central atom.

From the above table it is concluded that among the reported values the wavenumber of the stretching frequency  $\gamma$  (CS) is the most suitable for distinguish of bonding mode.

Table 9 lists the main infrared bands observed for some common ligands capable of forming linkage isomers

Table 9: Infrared bands of some common ligands capable of forming linkage

Ligand	Wavenumber ( $\text{cm}^{-1}$ )
Nitro	1430–1360, 1340–1300
Nitrito	1500–1400, 1100–1000
Thiocyanato ( $-\text{S}-\text{C}\equiv\text{N}$ )	2140–2100, 720–680
Cyanato ( $-\text{O}-\text{C}\equiv\text{N}$ )	2210–2000, 1300–1150
Isothiocyanato ( $-\text{N}=\text{C}=\text{S}$ )	2100–2040, 850–800
Isocyanato ( $-\text{N}=\text{C}=\text{O}$ )	2250–2150, 1450–1300

Infrared spectroscopy can be used to determine both the coordination mode of a ligand and the geometrical arrangement of ligands around the metal atom. Thus geometrical isomers can also be differentiated by using infrared spectroscopy.

For example; The mid-infrared spectra of the cis–trans isomerism exhibited by tetrachlorobis(N,Ndimethylformamide) tin(IV) (abbreviated as  $\text{SnCl}_4(\text{DMF})_2$ ) show carbonyl stretching bands at 1651 and 1655  $\text{cm}^{-1}$  for the cis- and trans-isomers, respectively.

The nature of the ligand coordination can be determined by comparing these carbonyl bands with that of the isolated DMF molecules. The infrared spectrum of DMF in  $\text{CCl}_4$  shows a  $\text{C}=\text{O}$  stretching band at 1687  $\text{cm}^{-1}$ , a notably higher wavenumber. If coordination in the  $\text{SnCl}_4(\text{DMF})_2$  compound is through the nitrogen atom, the  $\text{C}-\text{O}$  bond order would be increased and the  $\text{C}=\text{O}$  stretching band will shift to a higher wavenumber. In comparison, coordination through the oxygen atom will decrease the  $\text{C}=\text{O}$  stretching wavenumber value. Thus, the positions of the carbonyl bands of cis- and trans- $\text{SnCl}_4(\text{DMF})_2$  indicate that the ligand coordinates via the oxygen atoms.

There are important differences in the far-infrared spectra of the trans- and cis- $\text{SnCl}_4(\text{DMF})_2$ . Both isomers show asymmetric  $\text{Sn}-\text{O}$  stretching at 425  $\text{cm}^{-1}$  and a ligand band near 400  $\text{cm}^{-1}$ . However, the trans-isomer shows a single band due to  $\text{Sn}-\text{Cl}$  stretching near 340  $\text{cm}^{-1}$ , the cis-isomer shows four  $\text{Sn}-\text{Cl}$  stretching bands in the 350–290  $\text{cm}^{-1}$  range as shown in figure 21. The cis-isomer also shows a symmetric  $\text{Sn}-\text{O}$  stretching band, which is not present in the spectrum of the trans-isomer. These notable differences are due to the different symmetries of the molecules.

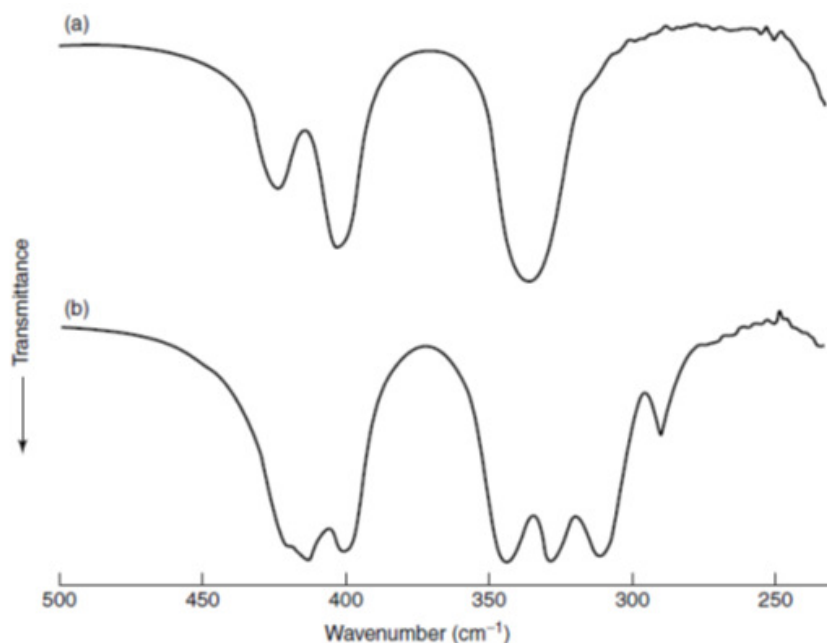


**Figure 21:** Far-infrared spectra of (a) *trans*- and (b) *cis*- $\text{SnCl}_4(\text{DMF})_2$ .

### 5.20 Metal Carbonyls

Infrared spectroscopy can be readily used to distinguish types of bonding in metal carbonyls. A useful band in the infrared spectra of carbonyl ligands in metal complexes is that due to C–O stretching which gives very strong sharp bands which are separated from the bands of other ligands that may be present. The strength of bonding between the d orbitals of the metal into the  $\pi^*$  anti-bonding orbitals of the CO ligand (known as backbonding) determines the band position. This back bonding weakens the C–O bond therefore appears at lower wavenumber compare to free CO. The carbonyl ligand present in either terminal (M–CO) and/or bridging (e.g. M–CO–M) types in metal carbonyls. *The bridging CO ligands appear at lower wavenumber values than those of the terminal ligands in complexes with the same metal and similar electron density.* Also the stretching wavenumber for a terminal carbonyl ligand in a complex correlates with the ‘electron-richness’ of the metal.

Terminal CO bands appear in the broad range from  $2130$  to  $1700\text{ cm}^{-1}$ , while bridging CO ligand bands appear in the  $1900$ – $1780\text{ cm}^{-1}$  range. However, care must be taken while assigning such carbonyl bands. A band appearing below  $1900\text{ cm}^{-1}$  may also be due to a terminal ligand, with a severe reduction of the carbonyl bond strength through  $d \rightarrow \pi^*$  bonding. However, if the complex also shows carbonyl bands well above  $1900\text{ cm}^{-1}$ , it may be assumed that such electronic effects are absent and that the lower-wavenumber CO stretching bands can be attributed to bridging ligands.

### 5.21 Organometallic Compounds

Organometallic compounds contain ligands directly bond to metal atoms or ions through carbon bonds. The metal–carbon stretching wavenumbers of organometallic compounds are observed in the 600–400  $\text{cm}^{-1}$  range. The lighter metals shows bands at higher values. The  $\text{CH}_3$  bending bands, arising from metal– $\text{CH}_3$  groups, appear in the 1210–1180  $\text{cm}^{-1}$  region in mercury and tin compounds, and at 1170–1150  $\text{cm}^{-1}$  in lead compounds. Aromatic organometallic molecules show a strong band near 1430  $\text{cm}^{-1}$ , due to benzene ring stretching for metals directly attached to the benzene ring.

### 5.22 Summary of the unit

Infrared spectroscopy is used to study the vibrational motions of molecules. As shall be described shortly, it turns out that different motion among different groups of atoms cause the molecule to absorb different amounts of energy. Studying these transitions can sometimes allow us to determine what kinds of atoms are bonded or grouped in an unknown compound, which in turn gives clues as to the molecular structure. Absorption of energy in the infrared region ( $\bar{\nu} = 4000 - 200 \text{ cm}^{-1}$ ) arises from changes in the vibrational energy of the molecules. There are two types of vibrations that cause absorptions in an IR spectrum. Stretching involves rhythmical displacement along the bond axis such that the interatomic distance alternately increases and decreases. Bending involves a change in bond angles between two bonds and an atom common to both.

One important condition is that only those vibrations that produce a change in the electric dipole moment of the molecule will be observed in the infrared spectrum. For example, stretching vibrations in homonuclear diatomic molecules like  $\text{O}_2$ ,  $\text{N}_2$ , and  $\text{Br}_2$  do not produce a change in dipole moment and hence these molecules do not give rise to an IR spectrum. On the other hand,  $\text{CO}$  and  $\text{IBr}$  produce IR spectra because these molecules contain a permanent dipole moment that will change as the bond is stretched or compressed.  $\text{CO}_2$ , a linear molecule that does not have a permanent electric dipole, nevertheless produces an IR spectrum because the two  $\text{C}=\text{O}$  bonds can stretch in an asymmetric fashion and also bend to produce changes in the dipole moment.

### 5.23 Key words

Infra-Red spectroscopy of inorganic compounds; Di atomic molecule of the type  $\text{AB}$  or  $\text{A}_2$ ; Tri atomic molecules of the type  $\text{AB}_2$  or  $\text{ABC}$ ; Tetra atomic molecules of the types  $\text{AB}_3$ ; Penta atomic molecules of the types  $\text{AB}_4$ ; Hexa atomic molecules of the types  $\text{AB}_5$ . Hepta atomic molecules of the types  $\text{AB}_6$ ; Lattice Water; Aquo ( $\text{H}_2\text{O}$ ) Complexes; Sulfato ( $\text{SO}_4$ )<sup>2-</sup>

complexes; Carbonato ( $\text{CO}_3$ ) complexes; Diketonate complexes; Chelating Nitrito Complexes.

#### 5.24 References for further studies

- 1) The characterization of a coordination complex using infrared spectroscopy: An inorganic or instrumental experiment; Lawrence C. Nathan *J. Chem. Educ.*, 1974, 51 (4), p 285. DOI: 10.1021/ed051p285
- 2) Infrared Spectroscopic Analysis of Linkage Isomerism in Metal–Thiocyanate Complexes; Carl Baer and Jay Pike *J. Chem. Educ.*, 2010, 87 (7), pp 724–726; DOI: 10.1021/ed100284z
- 3) Electronic Absorption Spectroscopy and Related Techniques; D. N. Sathyanarayana; *Universities Press*, 2001.
- 4) Infrared and Raman Spectra of Inorganic and Coordination Compounds, Applications in Coordination, Organometallic, and Bioinorganic Chemistry; 6<sup>th</sup> Ed, Kazuo Nakamoto; *John Wiley & Sons*; 2009.

#### 5.25 Questions for self understanding

- 1) Red and yellow isomers exist for the coordination complex  $[\text{Co}(\text{NH}_3)_5\text{NO}_2]\text{Cl}_2$ . The red isomer has  $\nu_{\text{NO}}$  bands at 1430 and  $1310\text{cm}^{-1}$  and  $\nu_{\text{NO}}$  bands at 1430 and  $1310\text{cm}^{-1}$ , what is the coordination mode of the  $\text{NO}_2$  ligand in each complex?
- 2) Explain the general conditions of Infra-Red spectroscopy of inorganic compounds
- 3) Explain the Infra-Red spectroscopy of Di atomic molecule of the type AB or  $\text{A}_2$
- 4) Explain the Infra-Red spectroscopy of Tri atomic molecules of the type  $\text{AB}_2$  or ABC
- 5) Explain the Infra-Red spectroscopy of Tetra atomic molecules of the types  $\text{AB}_3$
- 6) Explain the Infra-Red spectroscopy of Penta atomic molecules of the types  $\text{AB}_4$
- 7) Explain the Infra-Red spectroscopy of Hexa atomic molecules of the types  $\text{AB}_5$
- 8) Explain the Infra-Red spectroscopy of Hepta atomic molecules of the types  $\text{AB}_6$
- 9) Explain the Infra-Red spectroscopy of IR spectral study of Lattice water and aquo and hydroxo complexes
- 10) Explain the Infra-Red spectroscopy of *Lattice Water*
- 11) Explain the Infra-Red spectroscopy of *Aquo ( $\text{H}_2\text{O}$ ) Complexes*
- 12) Explain the Infra-Red spectroscopy of IR spectral study of sulfate and carbonate complexes
- 13) Explain the Infra-Red spectroscopy of Sulfato ( $\text{SO}_4$ )<sup>2-</sup> complexes
- 14) Explain the Infra-Red spectroscopy of Carbonato ( $\text{CO}_3$ ) complexes
- 15) Explain the Infra-Red spectroscopy of Mono and multinuclear carbonyl complexes

- 16) Explain the Infra-Red spectroscopy of Diketonate complexes
- 17) Explain the Infra-Red spectroscopy of Nitro and nitrate complexes
- 18) Explain the Infra-Red spectroscopy of *Chelating Nitrito Complexes*
- 19) Explain the IR spectral study of thiocyanato complex
- 20) Explain the applications of IR spectral study in Coordination Chemistry
- 21) Explain the applications of IR spectral study of complexes of ethylenediamine and related ligands
- 22) Explain the applications of IR spectral study of isomerism
- 23) Explain the applications of IR spectral study of Metal Carbonyls
- 24) Explain the applications of IR spectral study of Organometallic Compounds

**UNIT-6****Structure**

- 6.0 Objectives of the unit
- 6.1 Introduction
- 6.2 Basic theory of ESR spectroscopy
- 6.3 Characteristics of 'g'
- 6.4 Types of E.S.R. Instruments
- 6.5 Presentation of the Spectrum
  - 6.5.1 Normal mode
  - 6.5.2 Derivative mode
- 6.6 g-value for an electron and a complex
- 6.7 Factors affecting g-value in a complex
- 6.8 Sustaining effect
- 6.9 Combined effects of CFS and L-S coupling
- 6.10 g-value and structure
- 6.11 Zero- field splitting
- 6.12 Kramer's degeneracy
- 6.13 Consequences of ZFS
- 6.14 Break down of selection rules
- 6.15 Mixing of states
- 6.17 Magnitude of zero- field splitting and signal
- 6.18 Effective spin, S'
- 6.19 Mixing of States and Zero-Field Splitting
- 6.20 Hyperfine Splitting
- 6.21 Characteristics of A
- 6.22 Hyperfine Splitting in Various Structures
- 6.23 Spin-Lattice relaxation
- 6.24 Spin-Spin relaxation
- 6.25 Calculation of  $g_{||}$  and  $g_{\perp}$  for these two states
- 6.26 ESR and Jahn-Teller distortion
- 6.27 E.S.R. of Transition Metal Complexes
  - a)  $d^1$  system,  $^2T_{2g}$ ;  $S' = 1/2$ : octahedral
  - b)  $d^1$  tetrahedral
  - c)  $d^2$  system ;  $^3T_{1g}$



d)  $d^2$  tetrahedral

e)  $d^3$  system,  ${}^4A_{1g}$ ;  $S' = 1\frac{1}{2}$

f)  $d^4$  System;  ${}^5E_g$ ;  $S = 2$

g)  $d^5$  Spin- free,  ${}^6A_{1g}$ ; spin-paired,  ${}^2T_{2g}$

h) Spin-paired  $d^5$

6.28 Application of ESR spectroscopy of biological molecules

a) Iron proteins

b) Copper proteins

c) Manganese proteins

d) Cobalamin

6.29 The ESR spectrum of  $PH_4$  \*

6.30 Summary of the unit

6.31 Key words

6.32 References for further studies

6.33 Questions for self understanding

## 6.0 Objectives of the unit

After studying this unit you are able to

- Explain the basic theory of ESR spectroscopy
- Identify the Characteristics of 'g'
- Calculate the g-value for an electron and a complex
- Explain the conditions in which Zero– field splitting occurs
- Explain the conditions in which Kramer's degeneracy possible
- Draw the hyperfine splitting structure of various compounds
- Explain the ESR and Jahn-Teller distortion
- Explain the E.S.R. of Transition Metal Complexes
- Explain the Application of ESR spectroscopy of biological molecules
- Explain the The ESR spectrum of  $\text{PH}_4$  radical

## 6.1 Introduction

ESR or Electron Spin Resonance is a spectroscopic method for studies of paramagnetic species. This method and the related NMR or nuclear magnetic resonance technique were both established around 1945. Both methods make use of magnetic properties, in the first case of electrons in the second of nuclei. The microwave technique in the frequency range 109 Hz and higher that is normally employed in ESR instruments had been developed for Radar detection units during the Second World War. Systematic studies of transition metal salts began at the end of the 1940s. These studies have formed the basis for continued research on complex biochemical systems that is now one of the most active areas of applications. Other fields have been opened by the ongoing development of resolution and sensitivity. Free radicals – molecules with an unpaired electron have been tracked and identified and their reactions followed both in the liquid and the solid state in many instances. Such studies are still ongoing, nowadays more as one tool in conjunction with other methods to obtain chemical information.

## 6.2 Basic theory of ESR spectroscopy

When a paramagnetic molecule absorbs a quantum of electromagnetic radiation in the microwave region, electron is excited from one spin energy state to another spin energy state, which has higher energy. An electron has a spin,  $s = \frac{1}{2}$ . The spin – angular momenta,  $m_s \pm \frac{1}{2}$ , have equal energy in the absence of magnetic field. However, when a magnetic field is applied, the degeneracy is resolved, that is, removed. In the low energy state, the spin magnetic moment is aligned with the external magnetic field and hence,  $m_s = -\frac{1}{2}$ . In the high-

energy state, the magnetic moment is opposed to the external field and hence,  $m_s = +\frac{1}{2}$ . A transition will occur between these two states, when the energy of the quantum of radiation,  $\nu$ , is equal to the difference in energy,  $\Delta E$ , between the two spin states of the electron. That is,  $\Delta E = h\nu = g\beta H_0$

where, 'h' is the Planck's constant, ' $\nu$ ' is the frequency of radiation, ' $\beta$ ' is the Bohr magneton, ' $H_0$ ' is the external magnetic field strength and 'g' is the spectroscopic splitting factor.

### 6.3 Characteristics of 'g'

1. It is not a constant.
2. It is a tensor quantity. That is, it depends on three parameters, namely, magnitude, direction and arbitrary number of indices.
3. For a free electron,  $g = 2.00234$ . In metal ions, the 'g' values often greatly differ from the free electron value.
5. The magnitude of 'g' depends up on the orientation of the molecule containing the unpaired electron with respect to the magnetic field.
6. In solution or in the gas phase, 'g' is averaged over all orientations because of the free motion of the molecules.
7. If the paramagnetic radical or ion is located in a perfectly cubic crystal site (Oh or Td site), the 'g' value is independent of the orientation of the crystal and is said to be isotropic.
8. In a crystal of lower symmetry, the 'g' value depends up on the orientation of the crystal with respect to the magnetic field and is said to be anisotropic.
9. The 'z' direction coincides with the highest fold rotation axis, which can be determined by X-ray. When the z-axis is parallel with the external magnetic field, the 'G' value is called,  $g_{||}$ , and it is also known as  $g_z$ . The 'g' values along the x- and y-axes are called  $g_x$  and  $g_y$ . These are referred to as  $g_{\perp}$ . The reason is that the external magnetic field is perpendicular to the z-axis.
10. In a tetragonal site,  $g_x = g_y$ .
11. If ' $\theta$ ' is the angle between the magnetic field and the z-axis, the experimental 'g' value is given by the following equation for a system with axial symmetry:

$$g^2 = g_{||}^2 \cos^2 \theta + g_{\perp}^2 \sin^2 \theta$$

12. There will be inequality in 'g' values even if there are small distortions. These cannot be detected by X-ray. However, E.S.R can detect these small distortions from the inequalities in 'g' values.

## 6.4 Types of E.S.R. Instruments

There are two types of E.S.R. Spectrometers

1. X – band spectrometer
2. Q – band spectrometer

### *X – band spectrometer*

A frequency around 9400 mega cycles per second and a magnetic field strength around 3000 gauss are employed. The magnetic field strength can be varied in the range 1 – 10,000 gauss.

### *Q – band spectrometer*

A frequency around 35,000 mega cycles per second and a magnetic field strength around 12,500 gauss are used.

## 6.5 Presentation of the Spectrum

The spectrum can be presented in two ways

1. Normal mode
2. Derivative mode.

### 6.5.1 Normal mode

In this mode, the absorption intensity is plotted against the magnetic field and a curve as shown in Figure 1 is obtained.

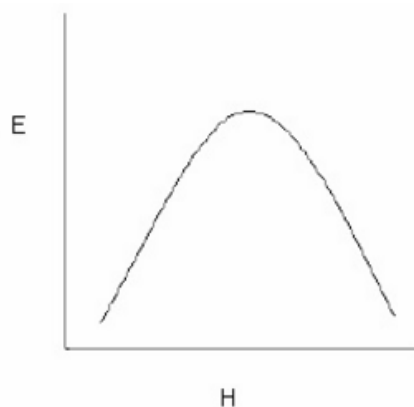


**Figure 1:** Normal mode

In this mode, the absorption intensity is plotted against the magnetic field and a curve as shown in Figure 1 is obtained. The disadvantage is that the absorption bands are broad. Therefore, the field at which maximum absorption occurs cannot be determined accurately.

### 6.5.2 Derivative mode

Here, the first derivative of the absorption intensity,  $dI/dH$  is plotted against  $H$ . The curve obtained is shown in Figure 2. The advantage of this curve is that this type of plot is more accurate. When the absorption intensity is maximum,  $dI/dH = 0$ . That is, the derivative curve crosses the x-axis. The number of peaks in an absorption curve corresponds to the number of maxima or minima in the derivative curve.

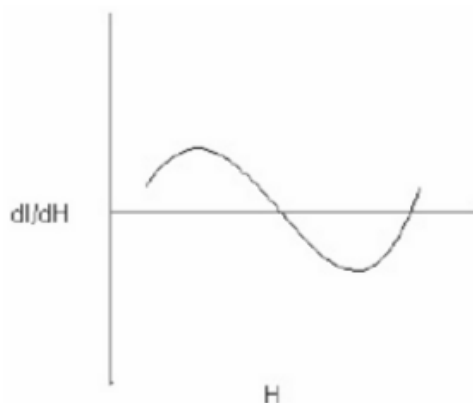


**Figure 2:** Derivative mode

### 6.6 g-value for an electron and a complex

It is an inherent property of a system containing an unpaired spin. Similar to the chemical shift observed in an NMR spectrum.

The  $g$  value for a single unpaired electron (free electron) has been calculated and experimentally determined. It is  $2.0023192778 \pm 0.0000000062$  ( $= g_e$ ). The  $g$  value for an  $S = 1/2$  system is usually near  $g_e$ , but it is not exactly at  $g_e$ . This is due to spin orbit coupling which determines both the value of  $g$  and its anisotropy (how far the 3  $g$  values are from  $g_{av}$ ). The  $g$  value can often be calculated and the value is characteristic for a particular spin system. The value of ' $g$ ' is given by the following expression

$$g = 1 + \frac{J(J+1) + S(S+1) - L(L+1)}{2J(J+1)}$$

For a free electron,  $S = 1/2$ ,  $L = 0$ , and  $J = S = 1/2$ . Therefore,  $g = 2.(J = L+S)$ .

The ' $g$ ' factor is a dimensionless constant and for a free electron,  $g = 2.0023$ . A free radical also has  $g = 2.0023$  because in a free radical, the unpaired electron can move about freely over orbitals and is not confined to a localized orbital. However, in a transition metal complex, the unpaired electron is localized in a particular orbital. In a complex, the orbital degeneracy is removed and spin-orbit coupling takes place. Therefore, the  $g$ -value for a complex is different from 2.0023.

### 6.7 Factors affecting g-value in a complex

The important factors affecting the  $g$ -value in a complex are

- 1) Nature of the metal
- 2) Geometry of the complex
- 3) The relative magnitude of spin-orbit coupling
- 4) The crystal field.

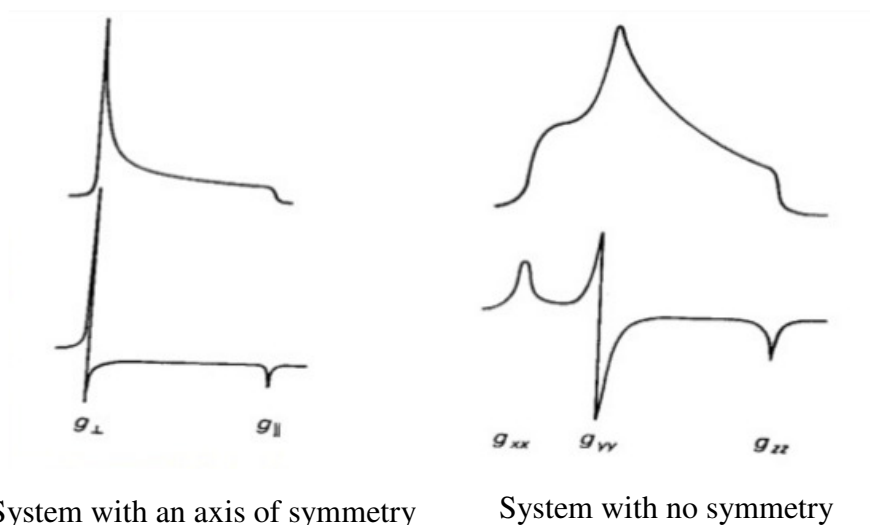
### 1) Nature of the metal

Science d metal ions have 5d orbitals situations are complicated. But the spectra are informative, in 4d and 5d series L-S/J-J coupling is stronger making the ESR hard to interpret.

### 2) Geometry of the complex

Ligands and their arrangement-CFS. CFS in turn affect the electronic levels hence the ESR transitions. The relative magnitude of CFS and L-S coupling is giving three situations.

If the complex ion is having cubic symmetry (octahedral or cubic)- g is isotropic. Complexes with at least one axis of symmetry show two g values. Ion with no symmetry element will show three values for g.



System with an axis of symmetry

System with no symmetry

This is clear from the following equation

$$g = 2 - \alpha k^2 \lambda / (10Dq)$$

Thus the spin-orbit contribution makes 'g' characteristic property of a transition metal ion and its oxidation state.

### 3) Effect of spin-orbit coupling

When the unpaired electron is placed in a chemical environment or in a transition metal complex, the 'g' value does not agree with the expected value. It is explained as follows

The chemical environment or the crystal field strongly perturbs the orbital motion of the electron. Therefore, the orbital degeneracy, if any, is partly removed or quenched. This called quenching. On the other hand, the spin-orbit coupling tends to sustain certain amount of orbital degeneracy. That is, complete removal of orbital degeneracy is prevented by spin-orbit coupling but higher fold degeneracies are often decreased by this effect. This sustaining effect implies that if an electron has orbital angular momentum, this is maintained by

coupling to the spin angular momentum and if it has a spin angular momentum this tends to generate orbital angular momentum. Because of this quenching and sustaining competition, the orbital degeneracy is partly but not completely removed and a net orbital magnetic moment results. Hence, g-value is different from 2.0023, which would be expected if the orbital degeneracy were completely removed.

#### 4) Crystal field effect

Crystal field is not affecting the 4f and 5f electrons so the ESR spectra of the lanthanides and actinides are quite simple. If an ion contains more than one unpaired electron ZFS may be operative.

The relative magnitudes of crystal field and spin-orbit coupling determine the properties of the transition metals to a large extent. These two have opposite effects on the orbital degeneracy (crystal field tries to remove while the spin-orbit coupling prevents the removal of orbital degeneracy). Three cases can be distinguished

- i) Spin-orbit coupling is very much greater than the crystal field.
- ii) Effect of crystal field is strong enough to break the coupling between L and S.
- iii) Effect of crystal field is very large so that L-S coupling is broken down completely.

#### Case i)

The effect of spin-orbit coupling is very much greater than that of the crystal field. (e.g.) rare earth ions:

The f-electrons are well shielded from the crystal field effects. Therefore, L-S coupling is not disturbed. 'J' is a good quantum number. Therefore, rare earth ions are very much like free ions. The magnetic moments calculated with the help of g-value obtained from the following equation agree with the experimental values.

$$g = 1 + \frac{J(J+1) + S(S+1) - L(L+1)}{2J(J+1)}$$

#### Case ii)

The effect of crystal field is strong enough to break the coupling between L and S. Now, 'J' is not a good quantum number. The splitting of  $m_L$  levels is large. That is, orbital degeneracy is quenched. The selection rule,  $m_S = \pm 1$ , is obeyed.

Example; I row transition elements.

The magnetic moment corresponds to more nearly to the spin-only value.

where  $g = 2$   $\mu_S = g\sqrt{S(S+1)}$ , where  $g = 2$

The orbital degeneracy is not completely removed because of the effect of spin-orbit coupling. Consequently, a net orbital magnetic moment results giving rise to a g-value expected if the orbital degeneracy were completely removed. Ions, which have an orbitally non-degenerate ground state such as  $\text{Fe}^{3+}({}^6\text{S})$  and  $\text{Mn}^{2+}({}^6\text{S})$ , give g-values nearly equal to the free electron value since there is practically no orbital angular momentum. The small deviation from the free electron value is due to slight spin-orbit coupling.

*Case iii)*

When the crystal field is very strong, the L-S coupling is broken down completely. This corresponds to covalent bonding and is applicable to the complexes of the 4d and 5d transition metals and to the strong field complexes of the 3d transition metals, such as cyanides. In many of these cases, M.O. description gives better results than the crystal field approximation.

Symmetry of the complex ion is important because ESR is recorded in frozen solutions. In such conditions the spins are locked. Lack of symmetry influences the applied field considerably. If the axis is not coinciding with Z axis, the sample is rotated about three mutually perpendicular axis and g is measured. Magnetically active nucleus causes hyperfine splitting. If more than one unpaired electrons present in the ion, more no of transitions are possible leads to fine structure in ESR spectrum.

In addition the following factors are also affect the g-value

- 1) Operating frequency of the instrument
- 2) Concentration of unpaired electrons
- 3) Ground term of the metal ion present
- 4) Direction and temperature of measurement
- 5) Inherent magnetic field in the crystals
- 6) Jahn-Teller distortion and ZFS

### 6.8 Sustaining effect

The g value for a gaseous atom or ion for which L-S coupling is applicable is given by the expression

$$g = 1 + [J(J+1) + S(S+1) - L(L+1)] / 2J(J+1)$$

For halogen atoms the g values calculate and experimental are equal, but for metal ions it varies from 0.2-8. The reason is the orbital motions of the electrons are strongly perturbed by the crystal field. Hence the L value is particularly or completely quenched. In addition to this ZFS and J-T distortion may also remove the degeneracy. The spin angular momentum S of electron tries to couple with the L. this partially retains the orbital degeneracy. The crystal



field tries to quench the L values and S tries to restore it. This phenomenon is called sustaining effect. Depending up on which effect dominate the L value deviates from the original value. So L and hence J is not a good quantum number to denote the energy of electrons hence the g value also.

### 6.9 Combined effects of CFS and L-S coupling

Three cases arises depending upon the relative magnitudes of strength of crystal field and L-S coupling

L-S coupling  $\gggg$  CFS

CFS  $>$  L-S coupling and

CFS  $\gggg$  L-S coupling

*L-S coupling  $\gggg$  CFS*

When L is not affected much by CFS then J is useful in determining the g value, example rare earth ions. 4f-electrons buried inside so not affected. G values falls in the expected regions.

All 4f-and 5f gives agreeing result other than Sm(III) and Eu(III)

*CFS  $>$  L-S coupling*

If CFS is larger enough to break L-S coupling then J is not useful in determining g values.

Now the transitions are explained by the selection rule and not by g values. The magnetic moment is given by  $\mu_s = [n(n + 2)]^{1/2}$

All 3d ions fall in this category. System with ground terms not affected by CFS ie L = 0 are not affected and the g values is close to 2.0036. There may be small deviation because of L-S coupling, spin-spin interaction and gs and es mixing.

CFS  $\gggg$  L-S coupling

In strong fields L-S coupling is completely broken and L = 0 which means there is covalent bonding. Applicable to 3d strong field, 4d and 5d series. In many cases MOT gives fair details than CFT

Example 1: Ni(II) in  $O_h$  field

For Ni(II) g calculation includes mixing  $^2A_{2g}(gs)$  and  $^3T_{2g}(es)$

$$g = 2 - [8\lambda/10Dq]$$

for Ni(II) the g values is 2.25 hence  $8\lambda/10Dq$  must be -0.25

From the electronic spectrum  $10Dq$  for Ni(II) in an  $O_h$  field is known to be  $8500\text{cm}^{-1}$ ,  $\lambda$  is  $-270\text{cm}^{-1}$ . For free Ni(III) ion the  $\lambda$  is about  $-324\text{cm}^{-1}$  the decrease is attributed to the es and gs mixing. This example shows how  $\lambda$  and  $10Dq$  can affect the g value.

Example 2: Cu(II) in a tetragonal field

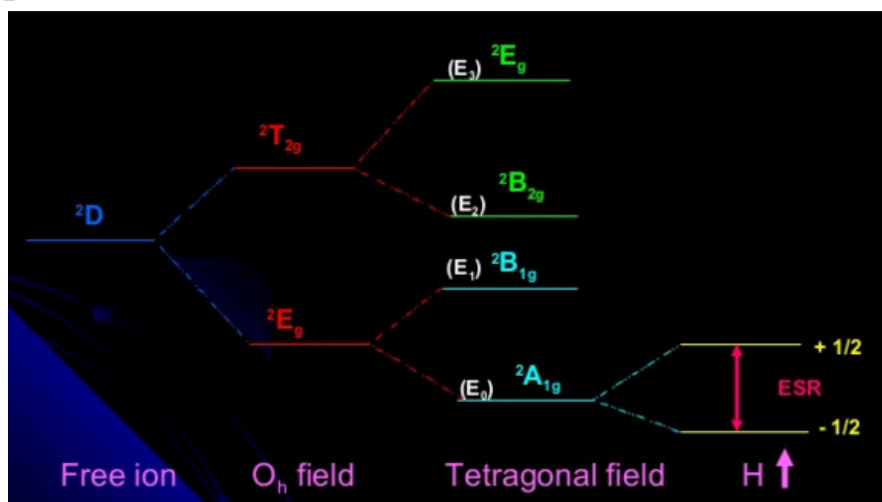
Cu (II) is a  $d^9$  system and its ground term symbol is  $2D$

$$2D \rightarrow {}^2E_g + {}^1T_{2g} \text{ (CFS)}$$

Since Cu(II) is a  $d^9$  system it must undergo J-T distortion. So the  $O_h$  field becomes tetragonal

$${}^2T_{2g} \rightarrow {}^2E_g + {}^2B_{2g}, {}^2E_g \rightarrow {}^2B_{2g} + {}^2A_{1g}$$

The unpaired electron is present in  ${}^2A_{1g}$ . On applying the magnetic field the spin levels are split and we get an ESR line.

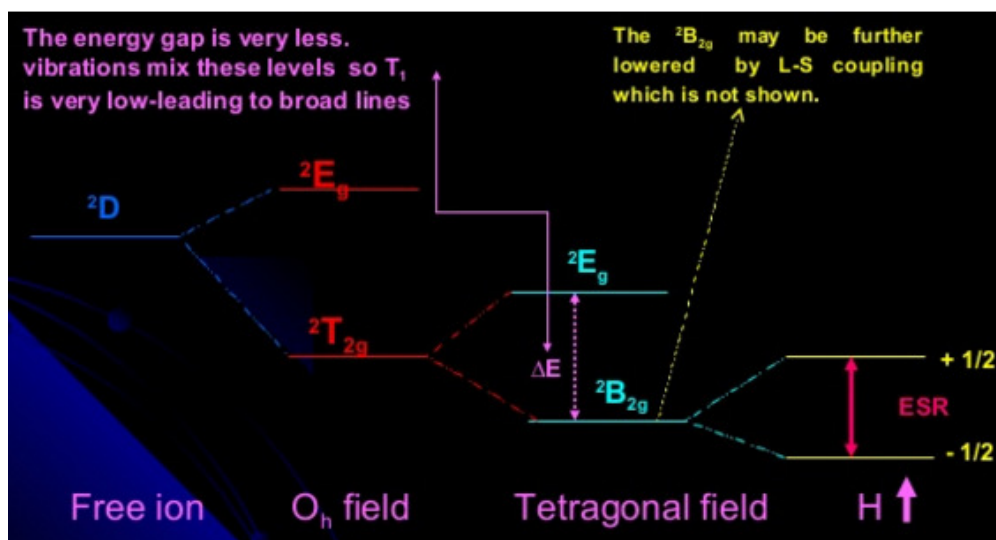


Cu(II) ion in various fields

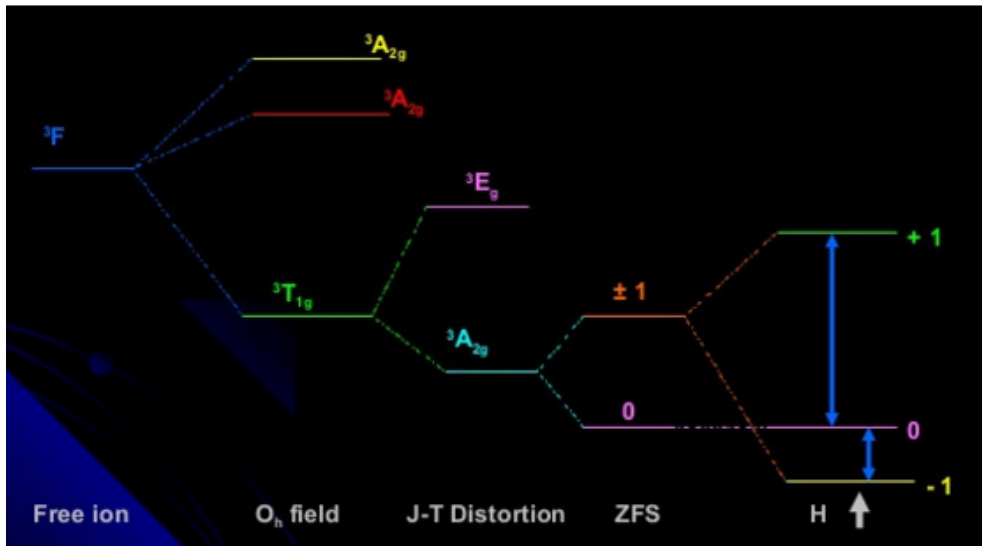
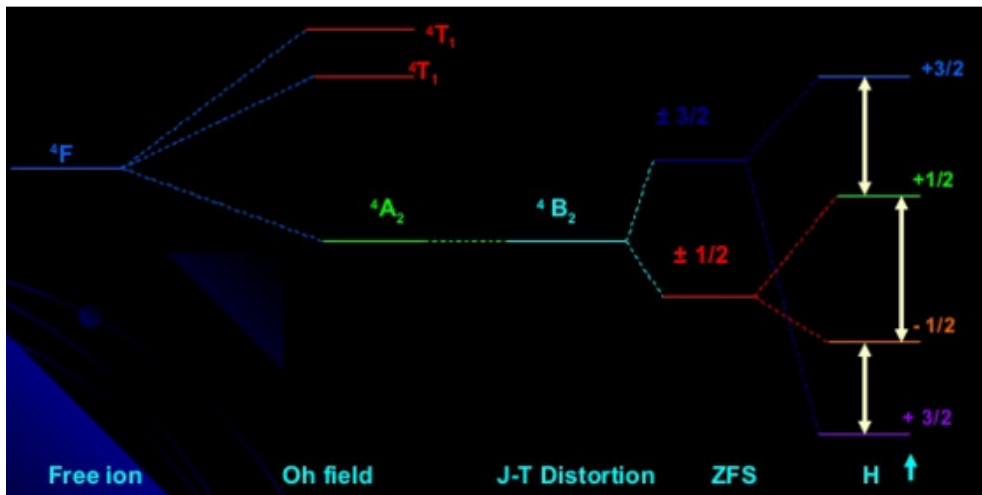
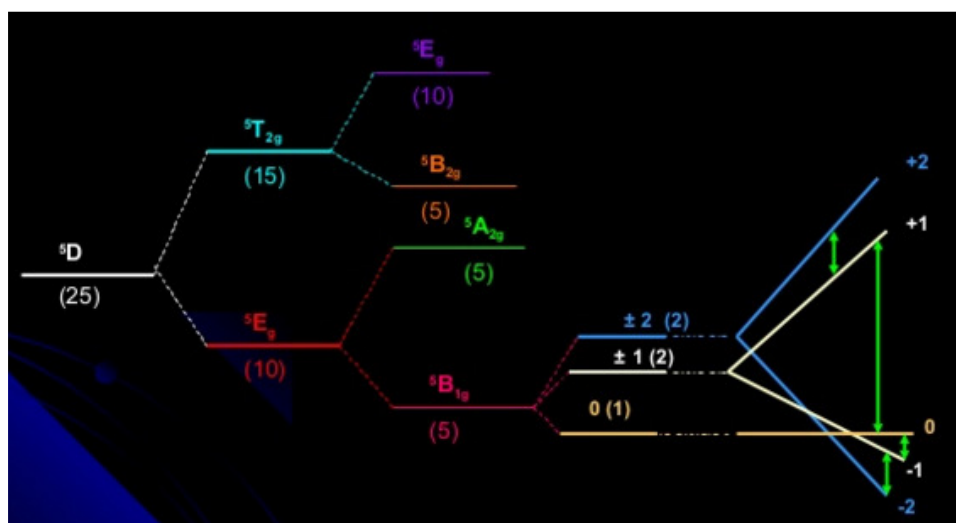
The  $g$  value is given by

$$g_{\parallel} = 2 - 8\lambda / (E_2 - E_0), \quad g_{\perp} = 2 - 2\lambda / (E_3 - E_0)$$

From electronic spectrum  $(E_2 - E_0)$  and  $(E_3 - E_0)$  can be calculated. From the above values  $\lambda$  can be calculated. It is seen that when splitting by distortion is high  $g$  values approaches 2. If the distortion splitting is lower, then resulting levels may mix with each other to give deviated  $g$  values.



$d^1$  system ( $Ti^{3+}$ ,  $VO^{2+}$ )

d<sup>2</sup> system ( $V^{3+}$  and  $Cr^{4+}$ )d<sup>3</sup> system ( $Cr^{3+}$ )d<sup>4</sup> system (weak field)

### 6.10 g-value and structure

From the g-value, we can obtain very important information about the structure of the complex. For a complex in solution, 'g' is averaged over all orientations because of the free motion of the molecules. However, in a crystal, the motion is restricted.

#### *Cubic field*

In a cubic crystal field, the metal–ligand bond lengths are the same along the three Cartesian axes and hence, 'g' remains the same. That is,  $g_x = g_y = g_z$ .

Now 'g' is said to be isotropic.

#### *Tetragonal field*

If the crystal field is tetragonal, the metal–ligand distances along the x- and y-axes are the same but different from the metal–ligand distances along the z-axis. The g-value of such a complex is not isotropic. The anisotropic 'g' may be expressed as  $g_x = g_y \neq g_z$ .

#### *Rhombic*

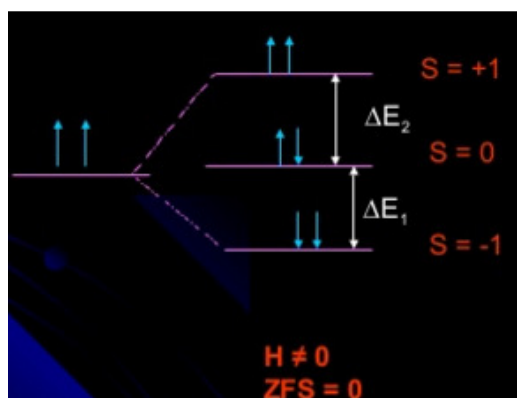
If the symmetry is rhombic, three different g-values are obtained. That is,  $g_x \neq g_y \neq g_z$ .

In bulk susceptibility measurements, a powdered sample is used and 'g' works out as an average,  $g_{av}$ . If a well formed single crystal is used, the E.S.R. measurements can provide the g-values based on the orientation of the crystal.

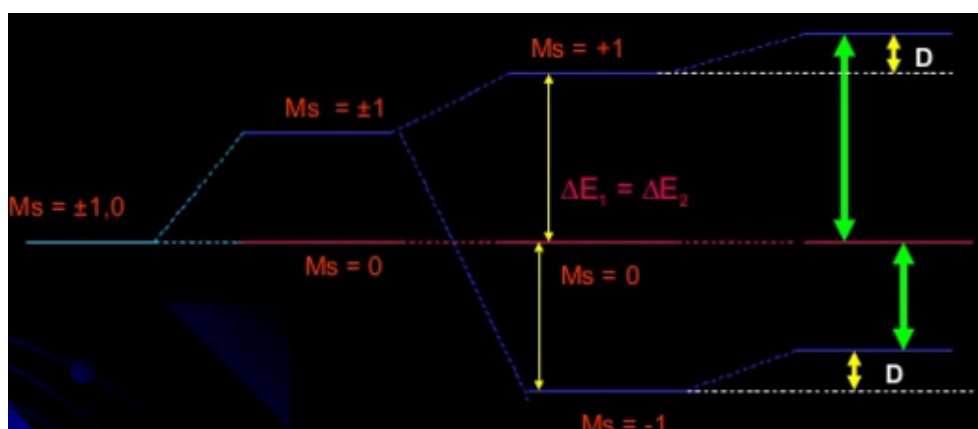
### 6.11 Zero– field splitting

When the spin levels are split even in the absence of magnetic field, it is called zero–field splitting. When a metal ion is placed in a crystal field, the degeneracy of the 'd' orbitals will be removed by the electrostatic interactions. That is crystal field removes the orbital degeneracy. However, the spin degeneracy is not removed until a magnetic field is applied. Nevertheless, when the species contains more than one unpaired electron, crystal field can also remove the spin degeneracy. Thus, the spin levels may be split even in the absence of a magnetic field. This phenomenon is called zero-field splitting.

Considering a system having two unpaired electrons, there are three combinations are possible for these electrons as shown in below figure. In the absence of external magnetic field all three states have equal energy. Under the influence of external field, the three levels are no longer with same energy. Hence two transitions are possible both with same energy

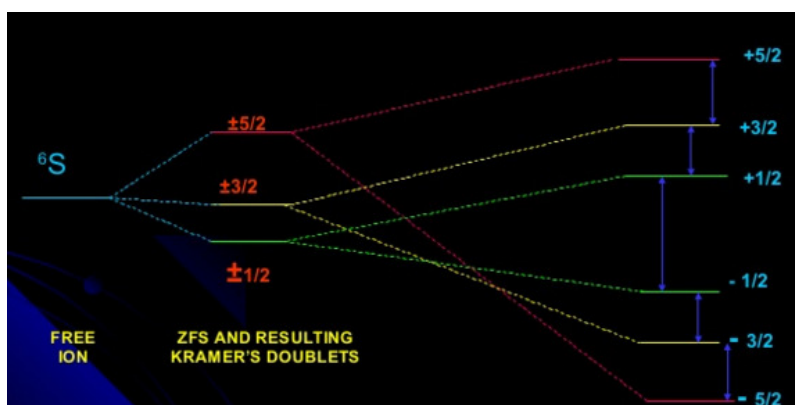


The splitting of electronic levels even in absence of external magnetic field is possible due to association of distortion and L-S coupling. And this is called zero field splitting (ZFS). The splitting may happen when there is strong dipolar interaction of the +1 level is raised in energy (Dipolar shift (D)) this dipolar shift reduces the gap between  $S = -1$  and  $S = 0$ . Now the two transitions do not have same energy resulting in two lines.



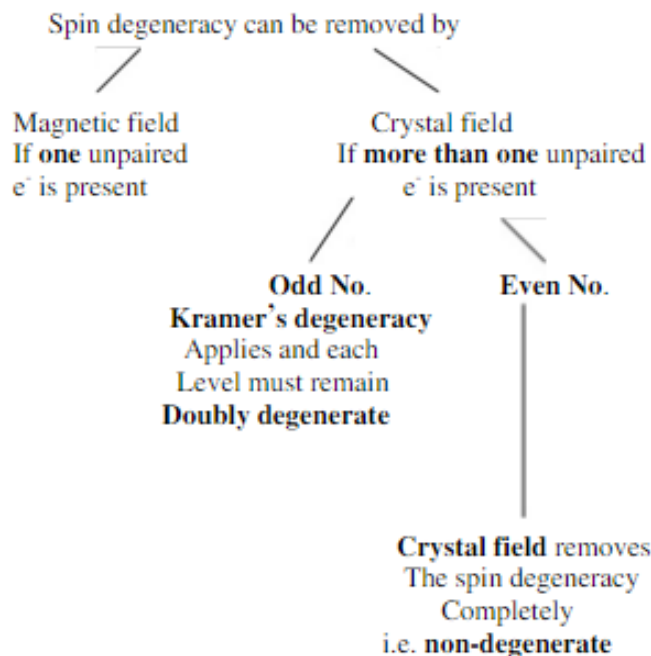
### 6.12 Kramer's degeneracy

System with even number of unpaired electrons will contain a state with  $S = 0$ . But in the case of odd electrons no state with  $S = 0$  is appears, since  $M_s = \frac{1}{2}$ . In such case even after ZFS the spin state with opposite  $M_s$  values remains degenerate which is called Kramer's degeneracy. The levels are called Kramer's doublets. In any system with odd number of unpaired electrons the ZFS leaves the ground state at least two fold degenerate.

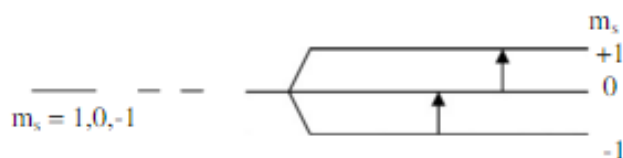


Effect of ZFS on Mn(II)

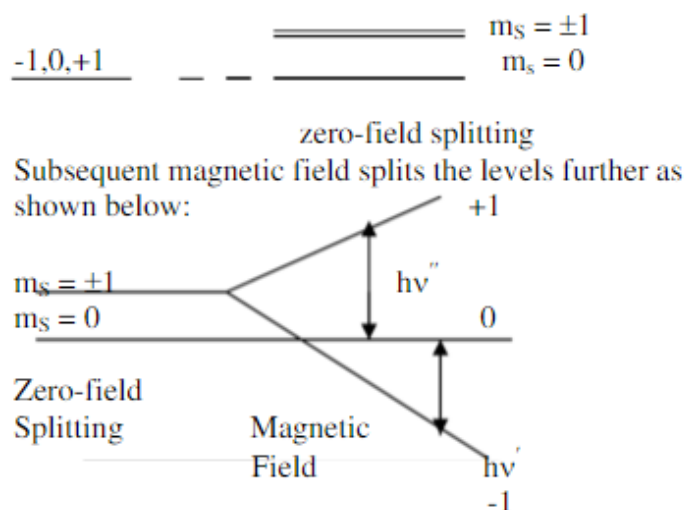
Thus when the species contains an odd number of unpaired electrons, the spin degeneracy of every level remains doubly degenerate. This is known as Kramer's degeneracy. (When the number of unpaired electrons is even, crystal field may remove the spin degeneracy entirely). This is schematically represented as follows



Example 1: Consider a molecule or ion with two unpaired electrons. Then  $S = +\frac{1}{2} + \frac{1}{2} = 1$ . Therefore,  $m_s = -1, 0, +1$ . In the absence of zero-field splitting, two transitions are possible as shown below



The first transition is  $m_s = 0$  to  $+1$  and the second transition is  $m_s = -1$  to  $0$ . These transitions have equal energy (i.e. degenerate) and only one signal is observed. This system has even number of unpaired electrons.



Hence, Kramer's degeneracy is not operative. That is, each level will not be doubly degenerate. If zero-field splitting is present, it removes the degeneracy in  $m_S$  as shown above. Now, the two transitions are not degenerate. Hence, two peaks are observed in the spectrum, when zero-field splitting is present but only one when it is absent.

Example 2:  $Mn^{2+}$  ( $d^5$  system). In this system, there are an odd number of unpaired electrons. Hence, Kramer's degeneracy must exist. The term symbol for the free ion ground state is  ${}^6S$ . The zero-field splitting produces three doubly degenerate spin states, namely,  $m_S = \pm 5/2, \pm 3/2, \pm 1/2$  (Kramer's degeneracy). Each of these is split into two singlets by the applied field producing six levels. As a result of this, five transitions are expected  $-5/2$  to  $-3/2$ ,  $-3/2$  to  $-1/2$ ,  $-1/2$  to  $+1/2$ ,  $+1/2$  to  $+3/2$ ,  $+3/2$  to  $+5/2$ .

The spectrum is further complicated by the hyperfine splitting due to the manganese nucleus ( $I = 5/2$ ). Thus each of the five peaks split into six hyperfine components as shown in Figure 3.

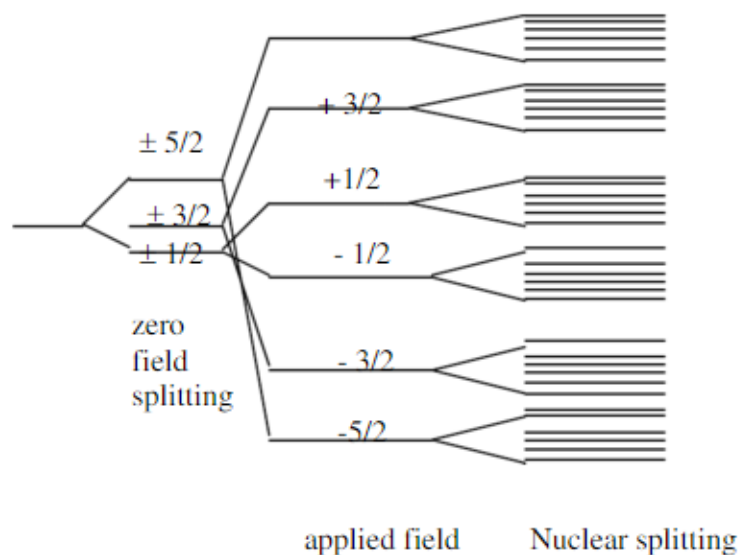
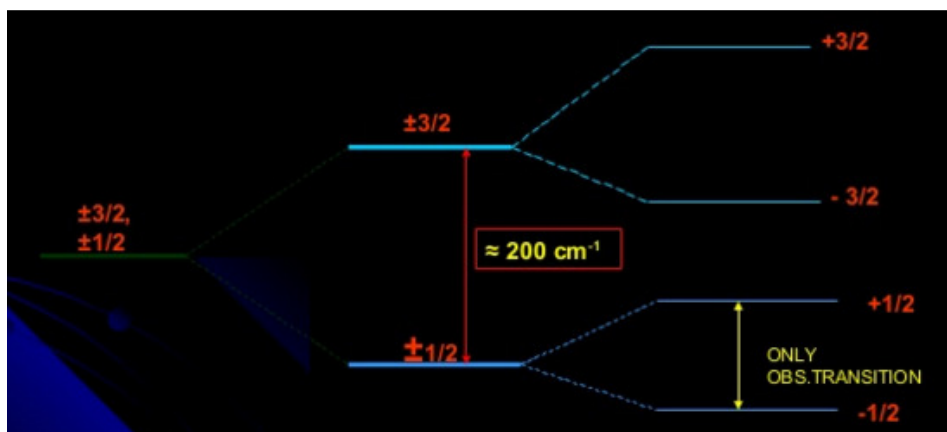


**Figure 3:** Zero-field splitting in  $Mn^{2+}$

### 6.13 Consequences of ZFS

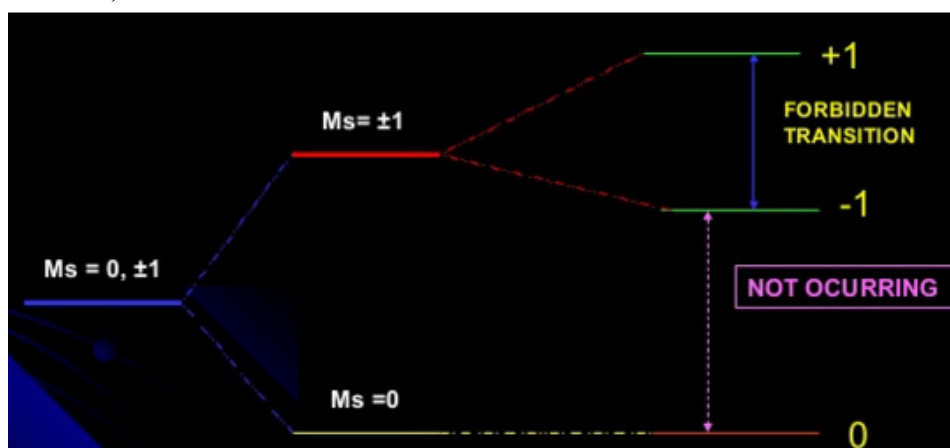
In some cases ZFS magnitude is very high than the splitting by external field. Then transition requires very high energy. Sometimes only one or no transitions occur. Example  $V^{3+}$  and  $Co^{2+}$

$Co(II)$  in cubic field has a ground term of  $4F$ , since it is a  $d^7$  system it have  $\pm 3/2$  and  $\pm 1/2$  levels. ZFS splits the levels by  $200\text{cm}^{-1}$ . Since the energy gap is higher only the transition  $-1/2$  to  $+1/2$  is seen. So it appears as if  $Co(II)$  has only unpaired electrons (Effective spin  $S = 1/2$ )



#### 6.14 Break down of selection rules

In some cases like V(III) the magnitude of ZFS is very high. Hence it exceeds the normal energy range of ESR transitions. In such system normal transitions occurs with  $\Delta M_s = \pm 1$ . But its energy exceeds the microwave region. Then the transition from  $-1$  to  $+1$  levels with  $\Delta M_s = \pm 2$  occurs, which is a forbidden one.



#### 6.15 Mixing of states

The magnitude of ZFS can be taken as originating from CFS. But orbitally singlet state  $S$  is not split by the crystal field even then Mn(II) shows a small amount of ZFS. This is attributed to the mixing of  $g$ - $s$  and  $e$ - $s$  because of L-S coupling. The spin-spin interaction is negligible. But for triplet states spin-spin terms are important and they are solely responsible for ZFS. Naphthalene trapped in durene in dilute states shows two lines as if it has ZFS. Since there is no crystal field or L-S coupling this is attributed to spin-spin interaction of the  $\pi$  electrons in the excited triplet state.

#### 6.17 Magnitude of zero- field splitting and signal

The effect of moderate zero-field splitting is shown in Figure 4 and that of large zero-field splitting in Figure 5. When the zero-field splitting is very large, the allowed transition,  $m_s = \pm 1$ , becomes too large to be observed in the microwave region. That is,  $m_s = 0$  to  $m_s = +1$



transition cannot be observed. However, it has been possible to observe a weak transition corresponding to  $m_S = \pm 2$ , that is, between the  $m_S = +1$  and  $m_S = -1$  levels. This transition will be weak because it is a forbidden transition. This is the case in  $V^{3+}$ . This signal is further split in to eight components ( $I = 7/2$  for  $V^{51}$ ).

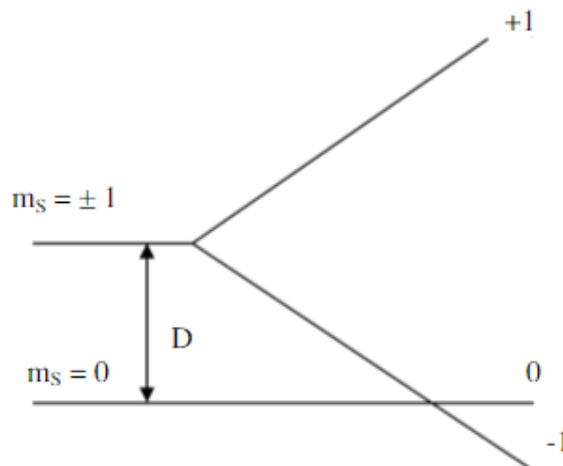


**Figure 5:** moderate Zero-field

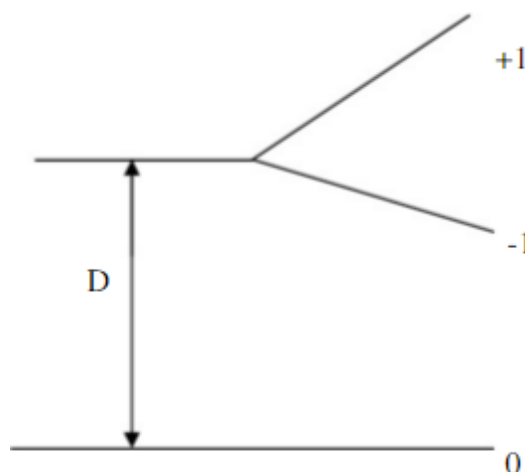


**Figure 6:** Large-Zero field splitting

### 6.18 Effective spin, $S'$

Consider a metal ion in a cubic crystal field and let the lowest state be an orbital singlet, that is, 'A' state. Now, the splitting of the degeneracy is generally small and the effective spin,  $S'$ , will be equivalent to the electronic spin. If zero-field splitting were operative 2S transitions would be expected. For example, consider  $Ni^{2+}$  ( $d^8$ ), which has  $^3A_{2g}$  ground state in an octahedral field and in some cases gives rise to two transitions in the e.p.r. spectrum. However, in the cubic field splitting, the ground state is an orbitally degenerate ground state like a 'T' state.

The effect of lower symmetry fields and the spin-orbit coupling will resolve this orbital degeneracy as well as the spin degeneracy. If an odd number of unpaired electrons is present, then the lowest spin state will be doubly degenerate according to Kramer's degeneracy. If the splitting is large, this doublet will be well isolated from higher lying doublets. Then transitions will be observed only in the low-lying doublet, and the effective spin will appear to have a value only  $\frac{1}{2}$  ( $S = \frac{1}{2}$ ).

Example,  $\text{Co}^{2+}$ : In an octahedral field, i.e., cubic field, the ground state is  ${}^4\text{F}$ . This is split by lower symmetry fields and spin-orbit coupling to six doublets (Kramer's degeneracy). The lowest doublet is separated from the next by about  $200\text{ cm}^{-1}$ . Thus, the effective spin has a value of  $\frac{1}{2}$  instead of  $\frac{3}{2}$  (three unpaired electron).

### 6.19 Mixing of States and Zero-Field Splitting

The magnitude of zero-field splitting in transition metal ions generally arises from the crystal field. But  $\text{Mn}^{2+}$  ( $d^5$  system) has a spherically symmetric electron distribution and has  ${}^6\text{S}$  ground state. It is not split by the crystal. However, this system also shows zero-field splitting.

#### Explanation

The spin-orbit coupling mixes the ground state with the excited states, which are split by crystal field. This mixing gives rise to a small zero-field splitting in  $\text{Mn}^{2+}$ .

### 6.20 Hyperfine Splitting

When the unpaired electron comes in the vicinity of a nucleus with a spin  $I$ , an interaction takes place, which causes the absorption signal to be split into  $2I+1$  components.

#### Reason

The nuclear spin-electron spin coupling arises mainly from the Fermi contact term. The two energy levels of a free electron in a magnetic field are given in Figure 6.

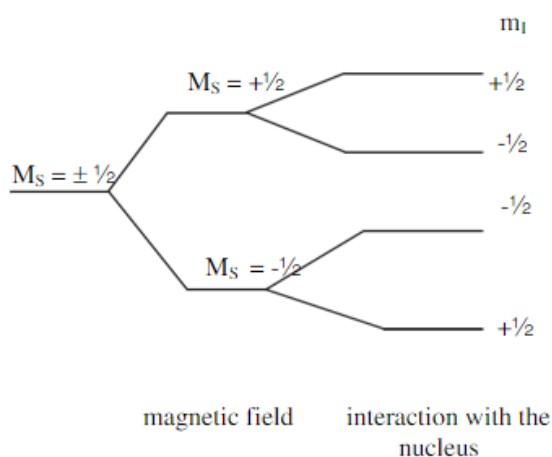


**Figure 6:** The two energy levels of a free electron in a magnetic field

From magnetic considerations, interaction of a proton nuclear moment corresponding to quantum number  $m_I = \frac{1}{2}$  with the electron spin moment corresponding to the quantum number  $m_S = -\frac{1}{2}$  will lead to lower energy than the interaction of moments of  $m_I = -\frac{1}{2}$  and  $m_S = -\frac{1}{2}$ . Similar theory applies to the other state. The energies of the levels are given by,

$$E = g\beta H m_S = A m_S m_I$$

where 'A' is the hyperfine coupling constant.

### Selection Rules

Only those transitions are allowed for which  $\Delta m_I = 0$  and  $\Delta m_S = \pm 1$ .

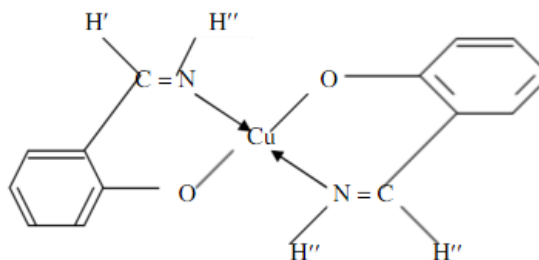
### 6.21 Characteristics of A

1. Positive 'A' means  $m_S = -\frac{1}{2}$ ,  $m_I = +\frac{1}{2}$  will have lower energy. Negative 'A' means  $m_S = -\frac{1}{2}$ ,  $m_I = -\frac{1}{2}$  will have lower energy.
2. Sign of A' cannot be determined from a simple spectrum.
3. Magnitude of splitting is expressed in terms of coupling constant 'A'.
4. The magnitude of 'A' depends on the following
  - a) The ratio of the nuclear magnetic moment to the nuclear spin.
  - b) Spin density in the immediate vicinity of the nucleus.
  - c) Anisotropic effect

### 6.22 Hyperfine Splitting in Various Structures

When an unpaired electron interacts with a nuclear spin, I, it will give rise to  $2I+1$  lines. All the lines will be of equal intensity and equal spacing. For example, for an unpaired electron on nitrogen, three lines are expected because  $I = 1$  for nitrogen and  $2I+1 = 2(1) + 1 = 3$ . When the absorption spectrum is split by 'n' equivalent nuclei of equal spin,  $I_i$ , the number of lines is given by  $2nI_i+1$ . When the splitting is caused by both a set of 'n' equivalent nuclei of spin  $I_i$  and a set of 'm' equivalent nuclei of spin  $I_j$ , the number of lines is given by  $(2nI_i+1)(2mI_j+1)$ . For example, if a radical contains 'n' non-equivalent protons on to which the electron is delocalised, a spectrum consisting of 2n lines will arise corresponding to the two spin states for 'n' protons. Instead, if the electron is delocalised over 'n' equivalent protons, a total of n+1 lines will appear in the spectrum.

Example. Bis(salicylaldimine)copper(II):



In the e.p.r. spectrum of the above complex, four main groups of lines are seen due to the coupling of the  $\text{Cu}^{63}$  nucleus ( $I = 3/2$ ) with the electron. Each group consists of eleven peaks due to hyperfine interaction with the two equivalent nitrogen atoms and two hydrogen atoms,  $\text{H}^{\beta}$ . The total number of peaks will be equal to  $(2n_{\text{N}}I_{\text{N}} + 1)(2n_{\text{H}}I_{\text{H}} + 1)$ . That is, the total number of peaks will be equal to,  $(2 \times 2 \times 1 + 1)(2 \times 2 \times 1/2 + 1) = 5 \times 3 = 15$ . However, only eleven peaks are seen due to overlap. The total number of peaks obtained shows that only two of the four hydrogens are involved in coupling. Therefore, we have to find out which set of the hydrogens,  $\text{H}'$  or  $\text{H}''$ , is involved in coupling. Deuteration of the  $\text{N}-\text{H}''$  produced a compound, which gave an identical spectrum. However, when the  $\text{H}'$  were replaced by methyl groups, the e.p.r. spectrum consisted of four main groups. Each group consisted of five lines resulting from nitrogen splitting only. This clearly proves that only the  $\text{H}'$  are involved in splitting. The spectrum furnishes conclusive evidence for the delocalisation of the odd electron in this complex between the metal and the ligand.

Line widths in Solid State e.p.r.

The line widths are determined by three factors

1. Spin–Lattice relaxation
2. Spin–Spin relaxation
3. Exchange processes

### 6.23 Spin–Lattice relaxation

Spin–Lattice relaxation causes line broadening. That is, the paramagnetic ion interacts with the thermal vibrations of the lattice leading to line broadening. The spin–lattice relaxation times vary for different systems. This variation in time in different systems is quite large. For some compounds, it is sufficiently long so that the spectra can be observed at room temperature while in others it is not possible. As the temperature decreases, the relaxation time increases. Hence, many salts of the transition metals are to be cooled to liquid nitrogen, hydrogen or helium temperature to observe good spectra.

### 6.24 Spin–Spin relaxation

This results from the small magnetic fields that exist on neighboring paramagnetic ions. As a result of these fields, the total field at the ions is slightly altered and the energy levels are shifted. A distribution of energies results which produces broadening of the signal. This effect depends on the distance between the ions,  $r$ , and the angle between the field and the symmetry axis  $\theta$ . These are clear from the expression,  $(1/r^3)(1 - 3\cos^2\theta)$ . This kind of broadening will show a marked dependence up on the direction of the field. This effect can

be reduced by increasing the distance between the paramagnetic ions by diluting the salt with an isomorphous diamagnetic material.

#### Exchange processes

Exchange processes alter line widths considerably. This effect can also be reduced by dilution. If the exchange occurs between equivalent ions, the lines broaden at the base and become narrower at the center. When exchange involves dissimilar ions, the resonances of the separate lines merge to produce a single broad line. Such an effect is observed for  $\text{CuSO}_4 \cdot 7\text{H}_2\text{O}$ , which has two distinct copper sites per unit cell.

#### Tetragonal distortion

In a tetragonally elongated octahedron, the energy of the  $d_z^2$  orbital will be lower than that of the  $d_{x^2-y^2}$  orbital. So, the unpaired ninth electron will stay in the  $d_{x^2-y^2}$  orbital. On the other hand, if the octahedron is compressed along the z-axis, then the energy of the  $d_z^2$  orbital will be higher than that of the  $d_{x^2-y^2}$  orbital. Hence, the unpaired electron will reside in the  $d_z^2$  orbital. These are shown in Figures 8 and 9.

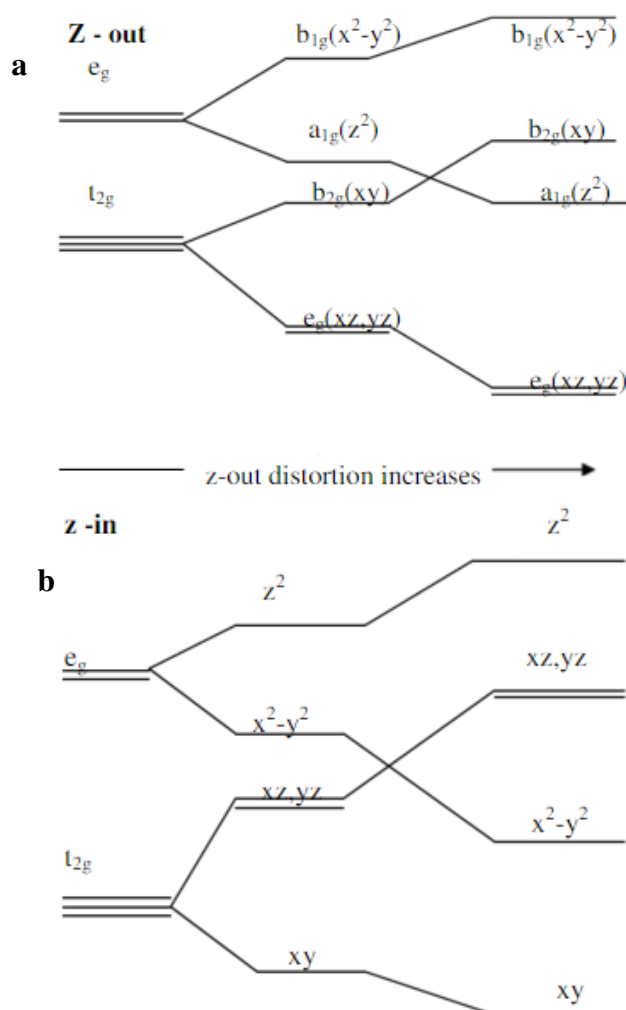


**Figure 8:** the energy levels in tetragonally elongated octahedron molecules

### 6.25 Calculation of $g_{\parallel}$ and $g_{\perp}$ for these two states

Ground state,  $d_z^2$

This means that the copper(II) unpaired electron is in the  $d_z^2$  orbital, that is, z-in distortion and compressed. Then,

$$g_{\perp} = 2 - \frac{6\lambda}{E(d_z^2) - E(d_{xz,yz})}$$

Where ' $\lambda$ ' is the spin-orbit coupling constant of the free ion. Here,  $\lambda$  is negative because the system is more than half-filled ( $d^9$  system). Hence ' $g$ ' will be greater than two. Therefore, for a tetragonally compressed copper(II) complex,  $g_{\perp} > g_{\parallel}$ , where  $g_{\parallel} = 2$ .

Ground state,  $d_{x^2-y^2}$

This means that the unpaired electron is in the  $d_{x^2-y^2}$  orbital. This orbital has the highest energy. This becomes the ground state in terms of the hole.

$$g_{\parallel} = 2 - \frac{8\lambda}{E(d_{x^2-y^2}) - E(d_{xy})}$$

Since  $\lambda$  is negative,  $g_{\parallel} > 2$

$$g_{\perp} = 2 - \frac{2\lambda}{E(d_{x^2-y^2}) - E(d_{xz,yz})}$$

Since  $\lambda$  is negative,  $g_{\perp}$  is also greater than two. Nevertheless, it is clear from the above equations that  $g_{\parallel} > g_{\perp}$ . Thus, for a tetragonally compressed copper(II) complex, (z-in distortion),  $g_{\perp} > g_{\parallel}$  and for a tetragonally elongated, (z-out distortion), copper(II) complex  $g_{\parallel} > g_{\perp}$ . These observations can be summarized as follows

Ground State	Distortion	Nature of g
$d_z^2$	Compressed (z-in)	$g_{\perp} > g_{\parallel}$
$d_{x^2-y^2}$	Elongated (z-out)	$g_{\parallel} > g_{\perp}$

### 6.26 ESR and Jahn-Teller distortion

Jahn-Teller theorem states any non-linear electronically degenerate system is unstable hence it will undergo distortion to reduce the symmetry, remove the degeneracy and hence increase its stability. But this theorem does not predict the type of distortion. Because of J-T distortion the electronic levels are split and hence the number of ESR lines may increase or decrease.

## 6.27 E.S.R. of Transition Metal Complexes

### a) $d^1$ system, ${}^2T_{2g}$ : $S = 1/2$ : octahedral

The ground term is  ${}^2T_{2g}$ . There is considerable spin-orbit coupling. Since it contains odd number of unpaired electrons, Kramer's degeneracy will operate.

All of the Kramer's doublets are close in energy. Hence, extensive mixing takes place by spin-orbit coupling. This leads to a short relaxation time. Therefore, the ESR signal may be obtained only at very low temperatures. (When the spin-orbit coupling is large, the degeneracy is maintained due to extensive mixing of the orbitals. Hence, the levels do not split and a signal is not obtained. However, at low temperatures, the mixing of orbitals does not take place readily due to the decrease in kinetic energy. Hence, the levels split and a signal is obtained.)

Example

1:CsTi(SO<sub>4</sub>)<sub>2</sub>.12H<sub>2</sub>O (undiluted)

In the above compound, Ti is present as Ti<sup>3+</sup>.  $g_{||} = 1.24$  and  $g_{\perp} = 1.14$ . The ESR signal may be obtained only at very low temperature. The ground state of the  ${}^2T_{2g}$  term is  $J = 1/2$  with  $g = 0$ . However, the above experimental  $g$ -values have been obtained due to a tetragonal or trigonal ligand field component of magnitude comparable to  $\lambda$  for the ion ( $\lambda_0 = 154 \text{ cm}^{-1}$ ).

Example 2: KTi(C<sub>2</sub>O<sub>4</sub>)<sub>2</sub>.2H<sub>2</sub>O.

For this compound,  $g_{||} = 1.86$  and  $g_{\perp} = 1.96$ . These results indicate that a large ligand field component compared to  $\lambda$  is present. The value is nearer to two and nearly isotropic. This indicates that the orbital angular momentum is almost quenched. Therefore, the electron is not restricted to any particular orbital and moves like a free electron. This is supported by the fact that the signal can be obtained at ordinary temperatures. The large ligand field component is due to the nonequivalence of the ligand groups.

### b) $d^1$ tetrahedral

In a tetrahedral ligand field, the ground state is  ${}^2E [(x^2-y^2); z^2]$ . It has no first order spin-orbit coupling. In this geometry, the ground state mixes with the nearby  ${}^2T_2$  excited states by second order spin-orbit coupling. This leads to a short spin relaxation time for the electron and broad absorption lines. The complexes must be usually studied near the liquid helium temperature. The  ${}^2T$  excited state is split by spin-orbit coupling. When the ligand field is distorted,

e.g. VO<sup>2+</sup>, the ground state becomes orbitally singlet and the excited states are well removed. Sharper lines are obtained at higher temperatures.

**c)  $d^2$  system ;  $^3T_{1g}$** 

The ground term is  $^3T_{1g}$ . Extensive spin-orbit coupling is present in this state. Therefore, ESR is usually not observed. The configuration approximates to cubic symmetry in an octahedral complex. Very few examples of ESR spectra of these ions in octahedral complexes have been reported because of this reason.  $V^{3+}$  in an octahedral environment in  $Al_2O_3$  gave  $g_{||} = 1.92$ ,  $g_{\perp} = 1.63$ ,  $D = +7.85$ , and  $A = 102$ .

**d)  $d^2$  tetrahedral**

Tetrahedral complexes have a  $^3A_2$  ground state and hence no spin-orbit coupling. The relaxation time will be longer and so the ESR signal is observed readily.

**e)  $d^3$  system,  $^4A_{1g}$ ;  $S' = 1\frac{1}{2}$** 

The ground term is  $^4A_{2g}$ .  $S' = 1\frac{1}{2}$ . Since more than one unpaired electron is present, zero field splitting will take place. The number of unpaired electron is odd and hence, Kramer's degeneracy will be applicable. That is, each level will remain doubly degenerate. As a result, Kramer's doublet will be the lowest in energy. When the zero field splitting is small as shown in Figure 9, sometimes three transitions can be observed. The zero field parameter can be obtained from the two effected transitions.

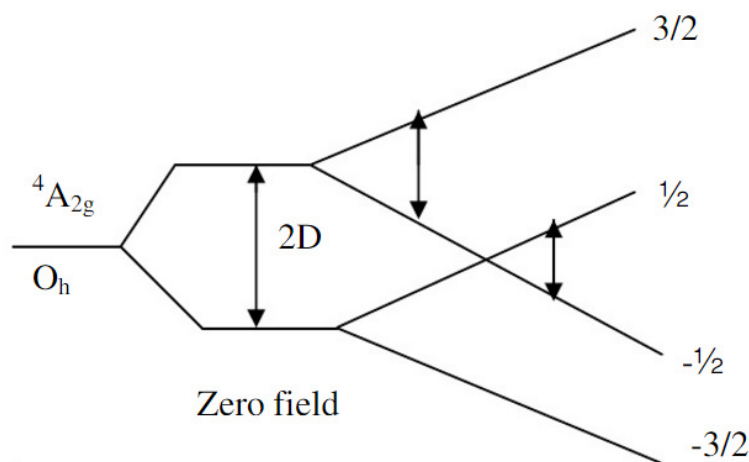


**Figure 9:** the zero field splitting of  $d^3$  system

When the zero field splitting is large compared to the spectrometer frequency, only one line will be observed. In octahedral complexes, the metal electrons are in  $t_{2g}$  orbitals, so that ligand hyperfine couplings are usually small. The  $g$ -value for this system is given according to the crystal field theory by the following expression

$$g = 2.0023 - \frac{8\lambda}{\Delta E(^4T_{2g} - ^4A_{2g})}$$

The ground state,  $^4A_{2g}$ , has no spin-orbit coupling. A small amount of this state is mixed with  $^4T_{2g}$  state.



For  $V(H_2O)_6$ ,  $\Delta E = 11800 \text{ cm}^{-1}$  and  $\lambda = 56 \text{ cm}^{-1}$ . These values give  $g = 1.964$ , which is close to the observed value of 1.972.

For  $Cr(H_2O)_6^{3+}$ ,  $\Delta E = 17400 \text{ cm}^{-1}$ ,  $\lambda = 91 \text{ cm}^{-1}$  and the predicted value of 'g' is smaller than the experimental value of 1.994. This is in agreement with the fact that the crystal field approximations are poorer and covalency becomes more important as the charge on the central ion increases.

In  $K_3MoCl_6$ , Mo is present as  $Mo^{3+}$ . When this is diluted in  $K_3InCl_6$ ,  $g = 1.93$  that is nearly isotropic. Zero field splitting, D, is very large. ('D' specifies the zero field due to a ligand field component of trigonal or tetragonal symmetry). The value of 'g' is in good agreement with the predicted by the following equation

$g = 2(1-4k^2\lambda_0)/10Dq$  for  $A_{2g}$  term. 'D' has a higher value relative to chromium compound because of the larger spin-orbit coupling constant for  $Mo^{3+}$  ( $\lambda_0 = 267 \text{ cm}^{-1}$ ).

#### f) $d^4$ System; ${}^5E_g$ ; $S = 2$

The ground term is  ${}^5E_g$  and  $S = 2$ . Very few spectra are reported for this 'd' electron configuration. In a weak crystalline  $O_h$  field, the ground state is  ${}^5E_g$ . This has no orbital angular momentum. The possible states are  $-2, -1, 0, +1, +2$ . The zero field splitting splits them in to three energy levels, namely,  $\pm 2, \pm 1, 0$ . That is, an non degenerate level, two fold degenerate levels lying higher by 'D' and two fold degenerate levels lying higher by 4D.

Example: undiluted  $CrSO_4 \cdot 5H_2O$

For this compound,  $g_{\parallel} = 1.95$  and  $g_{\perp} = 1.99$  and 'D' is fairly large. These results indicate an appreciably low symmetry ligand field component. The average value of 'g' is 1.98, which is in good agreement with predictions based up on the following equation

$$g = 2(1-2k^2\lambda_0)/10Dq$$

Since  $S = 2$ ,  $m_s = -2, -1, 0, +1, +2$ . The splitting of the energy levels is shown in Figure 10.

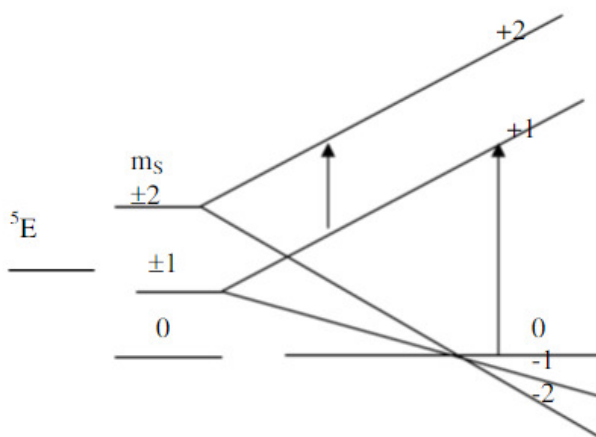


**Figure 10:** Splitting of energy levels in  $CrSO_4 \cdot 5H_2O$

When the splitting is large, no transition takes place because of large energy between the levels. The Jahn-Teller distortion and the accompanying large zero field splitting make it impossible to see a spectrum.

**g)  $d^5$  Spin-free,  ${}^6A_{1g}$ ; spin-paired,  ${}^2T_{2g}$**

For spin-free complexes,  $S' = 2\frac{1}{2}$  and for spin-paired complexes,  $S' = \frac{1}{2}$ . 'g' is isotropic. The very small zero field splitting is neglected. The absence of zero field splitting follows from the fact that there is no sextet term other than the ground  ${}^6A_{1g}$  term. The  ${}^4T_{1g}$  is the closest other term and second order spin-orbit coupling effects are needed to mix in this configuration, so the contributions are small. Hence, the electron lifetime is long and ESR signals are easily detected at room temperature in all symmetry crystal fields. Because of odd number of unpaired electrons, Kramer's degeneracy exists even when there is large zero field splitting. The energy levels of Mn(II) are shown in Figure 11.

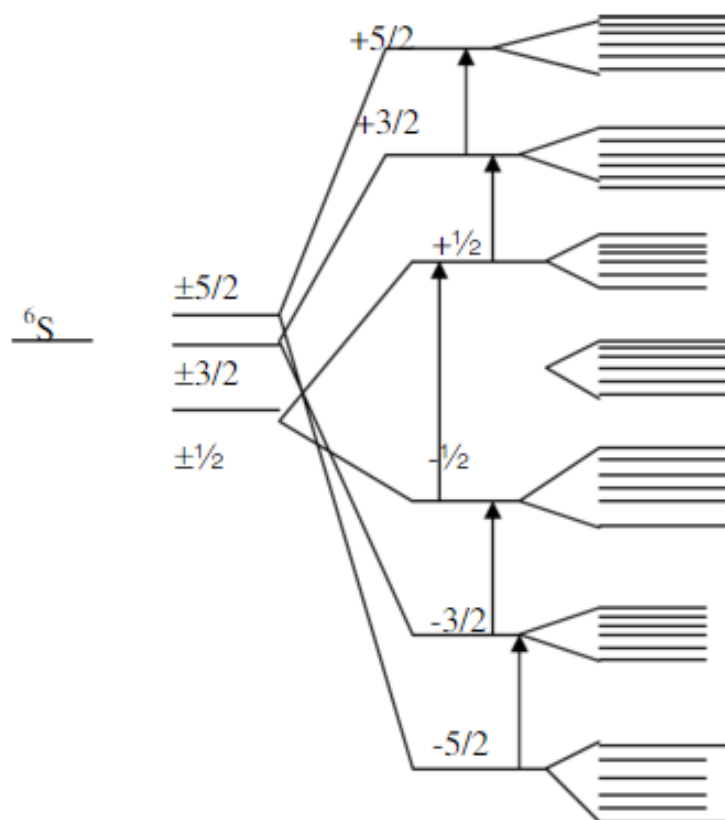


**Figure 11:** The energy levels of Mn(II)

The isotropy of 'g' also follows from the same fact. The different  $m_s$  values are  $-5/2$ ,  $-3/2$ ,  $-1/2$ ,  $0$ ,  $+1/2$ ,  $+3/2$ ,  $+5/2$ .

'g' is very nearly 2.00 in many salts of  $Mn^{2+}$  and of  $Fe^{3+}$ .

Examples are  $MnSO_4 \cdot 7H_2O$  diluted in  $ZnSO_4 \cdot 7H_2O$  and  $KFeSO_4 \cdot 12H_2O$  diluted in  $KAlSO_4 \cdot 12H_2O$ . These results are expected for the  ${}^6A_{1g}$  ( ${}^6S$ ) ground term.

**h) Spin-paired  $d^5$** 

In  $K_3Fe(CN)_6$ , diluted in  $K_3Co(CN)_6$ ,  $g_{\parallel}$  and  $g_{\perp}$  are 0.92 and 2.22 respectively. The signal may only be obtained at very low temperatures. These results indicate the presence of a ligand field component of low symmetry of magnitude less than the spin-orbit coupling constant ( $\lambda_0 = -460 \text{ cm}^{-1}$ ) together with a small amount of  $t_{2g}$  electron delocalisation. The splitting of the free ion doublet state by an  $O_h$  field, by  $D_3$  distortion, spin-orbit coupling, and a magnetic field are shown in Figure 12. Since we have non-integral spin, the double group representations are employed for the representations.

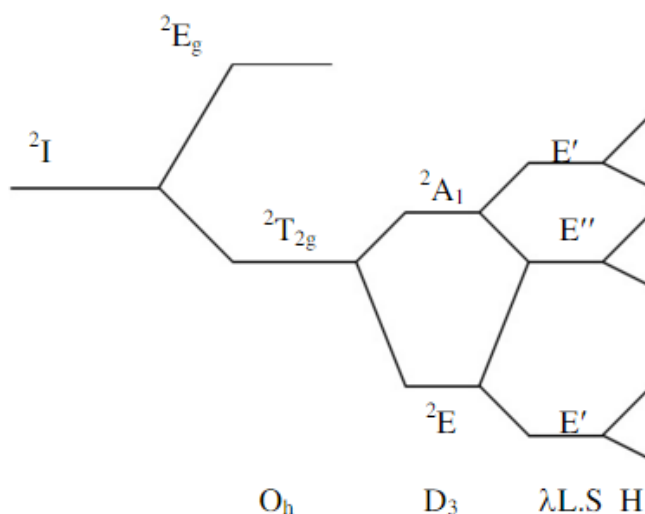


**Figure 12:** The splitting of the free ion doublet state by an  $O_h$  field, by  $D_3$  distortion, spin-orbit coupling, and a magnetic field

$K_4Mn(CN)_6 \cdot 3H_2O$  diluted in  $K_4Fe(CN)_6 \cdot 3H_2O$  has  $g_{\parallel} = 0.72$  and  $g_{\perp} = 2.41$ . The signal may be obtained only at very low temperatures. The results indicate that that ligand field component of low symmetry and of magnitude comparable to the spin-orbit coupling constant ( $\lambda_0 = -355 \text{ cm}^{-1}$ )

For  $Ru(NH_3)_6Cl_3$  diluted in  $Co(NH_3)_6Cl_3$ ,  $g_{\parallel} = 1.72$  and  $g_{\perp} = 2.04$ . The signal is obtained only at low temperatures. These results indicate a tetragonal or trigonal ligand field component, which is either smaller or large compared to the spin-orbit coupling parameter ( $\lambda_0 = -1180 \text{ cm}^{-1}$ ).

$K_2IrCl_6$  diluted in  $K_2PtCl_6$  gives  $g = 1.78$  and isotropic. The signal can be obtained only at low temperatures. The results indicate the presence of some  $t_{2g}$  electron delocalisation and that any low symmetry ligand field component must be much smaller than the spin-orbit coupling constant ( $\lambda_0 = -5000 \text{ cm}^{-1}$ ).

In a strong field, the ground state is  $^2T_{2g}$ . Spin-orbit coupling splits this term into three closely spaced Kramer's doublets. However, greater the spin-orbit coupling, shorter the relaxation time and hence the signal can be seen only at low temperatures. Due to Jahn-Teller distortions, the expected g-values are rarely obtained.

### 6.28 Application of ESR spectroscopy of biological molecules

Transition metal (d-group) ions are widespread in nature, essential for structural characteristics and mechanistic specificity of many proteins. Iron and copper are the two most prevalent metals in proteins responsible for the storage and transport of molecules, ions, and electrons. Electron paramagnetic resonance (EPR) spectroscopy has been extensively used for the determination of these metal ions without extensive disruption of the native protein moiety. It also detects variations in coordination geometry due to ligand substitutions as well as multiple valencies of the same metal.

#### a) Iron proteins

Iron is the single most abundant metal in biological systems, occurring mostly in respiratory proteins. Haemoglobin and myoglobin are two most abundant iron-containing proteins. The strategic presence of iron in the haem facilitates transportation and storage of oxygen by the two proteins, respectively. Reversible binding by carbon dioxide in the forms of carbonic acid and carbamino compounds in concert with a pH differential (Bohr effect) facilitate the gaseous exchange mechanisms through the lungs. Both proteins are structurally similar except that haemoglobin is a tetramer of the myoglobin-type structure. Other iron-containing proteins found in large amounts are ferritin, transferrin, and haemosiderin. Cytochromes and cytochrome oxidases are iron-containing proteins responsible for electron transport in the mitochondria.

Detection of iron by EPR spectroscopy depends on the presence of unpaired electrons in resting or intermediate reactive species. As a rule of thumb, electronic configurations of d-group metal ions which can be detected by EPR spectroscopy would contain  $d^1$ ,  $d^3$ ,  $d^5$ ,  $d^7$ , and  $d^9$  terms. The presence of an odd number of electrons results in at least one unpaired electron being available for EPR transitions.

Iron in the monovalent state  $Fe^I$  has the  $d^7$  configuration with spin value  $s = 1/2$  arising from a distribution into two sets of non-degenerate d-orbitals to give  $t_{2g}^6e_g^1$ . Promotion of the residual  $4s^1$  electron to the 3d-orbital however would require such a large amount of energy that constituent protein moiety close to the iron may be affected structurally. If at all possible, the EPR spectrum would comprise a doublet of lines arising from a spin value  $s = 1/2$ . Divalent  $Fe^{II}$  specie is a  $d^6$  configuration with two possibilities of spin states; a low spin

$t_{2g}^6e_g^0$  and a high spin  $t_{2g}^4e_g^2$  depending on crystal field splitting energy of associated ligands. Their respective spin values are hence  $s = 0$  and  $s = 2$ , both of which are not observable by EPR. Detection of nitrous oxide by binding to ferro-hemoproteins is due to formation of the Fe–N=O complex in which nitrogen p-orbital overlaps with the Fe d-orbital such that the unpaired electron is mainly localised on the NO ligand. The iron has a spin  $3/2$

The trivalent state  $Fe^{III}$  has  $d^5$ , a most stable configuration with possibilities of two spin states; low spin  $t_{2g}^3e_g^2$  and high spin  $t_{2g}^5e_g^0$ . Their respective spin values of  $5/2$  and  $1/2$  are both detectable by EPR, exhibiting many spectral characteristics depending on ligands, molecular environment, and solvent medium.

The tetravalent state  $Fe^{IV}$   $d^4$ ,  $t_{2g}^4e_g^0$  has a spin value  $s = 1$  which is not detectable by EPR. This is the form of Fe in the oxo- complex of haemoglobin after its reaction with hydrogen peroxide, known as ferryl species. Proof of formation of the ferryl [ $Fe^{IV}=O$ ] specie by EPR spectroscopy was obtained from its one-electron reduction to the easily detectable  $Fe^{III}$  derivative. The  $s = 2$  state may be expected from an energy equalisation of the  $t_{2g}$  and  $e_g$  levels so that four unpaired electrons are singly filled into four of the five degenerate energy levels  $\Delta = 0$ . This however is purely hypothetical. Pairing of the four electrons in two levels to give  $s = 0$  is also not possible. Figure 16 show typical EPR spectra for  $Fe^{III}$  derivatives of haemoglobin in high and low spin spectroscopic states.

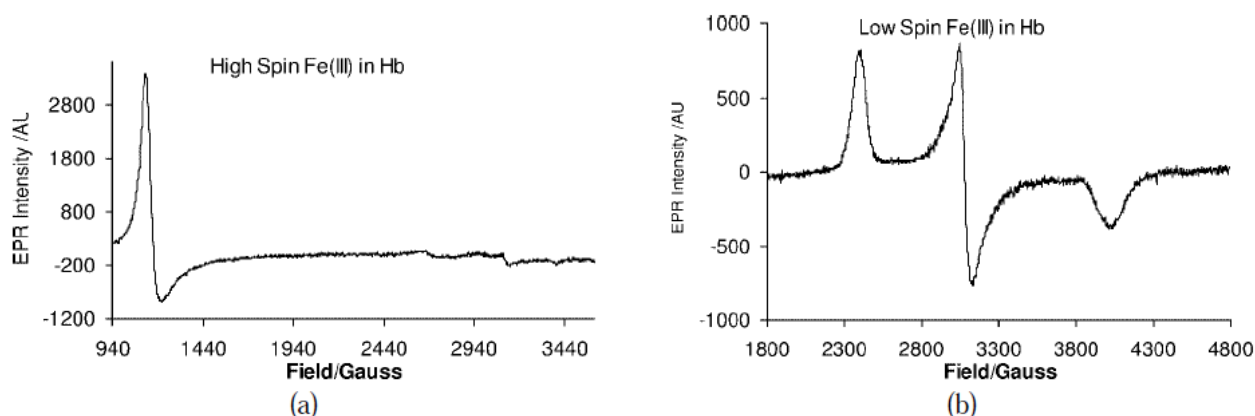


**Figure 16:** First derivative X-band EPR spectrum for methaemoglobin showing (a) high spin features of  $Fe^{III}$  at  $g = 6$ , low field, (b) low spin  $Fe^{III}$  features at  $g = 2.855$ ,  $2.226$ , and  $1.794$ , mid-field.

The distinguishing features are the field positions at which resonance occurs. More precisely these are translated to  $g$ -values, considering variations of frequencies of microwave applied. The X-band spectrum for high spin state shows strong features at  $g = 6$  and a complimentary weak absorption at close to free spin,  $g = 2$ . High spin  $Fe^{III}$  may also show up at  $g = 4.3$  due to quantum mechanical mixed states. For the low spin form three lines can be observed at  $g$ -values of  $2.82$ ,  $2.20$ , and

1.67, all of which arise from the same transition in axial symmetry exhibiting  $g_x$ ,  $g_y$ , and  $g_z$  orthogonal character of a tensor. As the ligand at the sixth coordination position changes, including pH effects, the symmetry of the central metal iron also changes creating distortions from rhombic to axial symmetry. This is a consequence of Jahn–Teller effect. If the  $g$ -values of low spin  $\text{Fe}^{\text{III}}$  spectra were plotted to display  $g_x$  in a linear format, the  $g_y$  and  $g_z$  have been shown to follow a trend as shown in Figure 17.

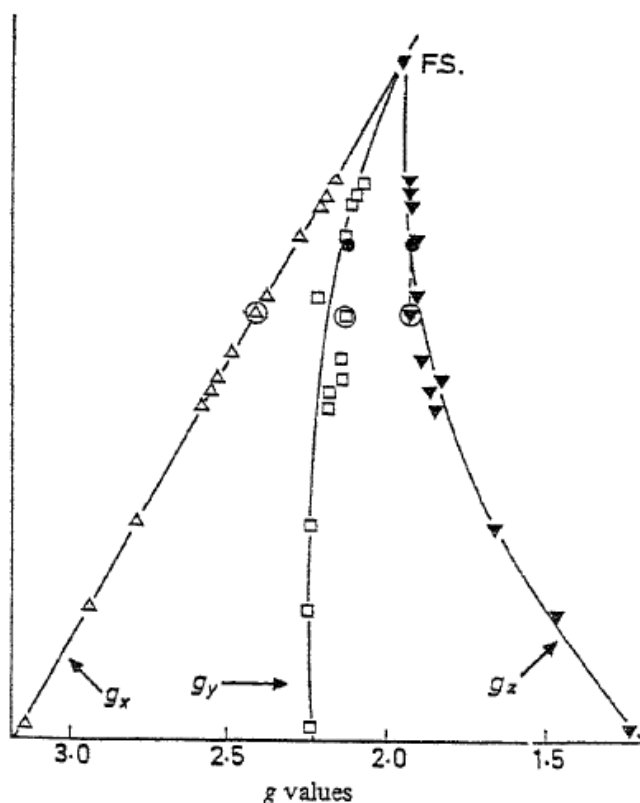


**Figure 17:** Trends in the  $g$ -values for a range of low spin  $\text{Fe}^{\text{III}}$  complexes showing convergence of  $g$ -values to 'free spin'.

The convergence point of all  $g$ -values is at 'free spin'. This therefore is a display of EPR spectroscopic parameters as geometry changes from axial to rhombic symmetry.

### b) Copper proteins

Naturally abundant copper proteins include ceruloplasmin, hemocyanin, and Cu/Zn superoxide dismutase.

The  $\text{Cu}^{\text{II}}$  is a  $d^9$  species contain an odd number of electrons to give a spin  $s = 1/2$  and therefore EPR transitions are absorbed. With a magnetic moment  $M_I = 3/2$ ,  $\text{Cu}^{\text{II}}$  gives a spectrum comprising a quartet of lines.

Major parameters for copper in proteins are the parallel and perpendicular features arising from an axial type spectrum defined by  $g_{\parallel}$  and  $g_{\perp}$  and  $A_{\parallel}$  and  $A_{\perp}$ . Typical spectra for  $\text{Cu}^{\text{II}}$  at 77 K are shown in Figure 18.

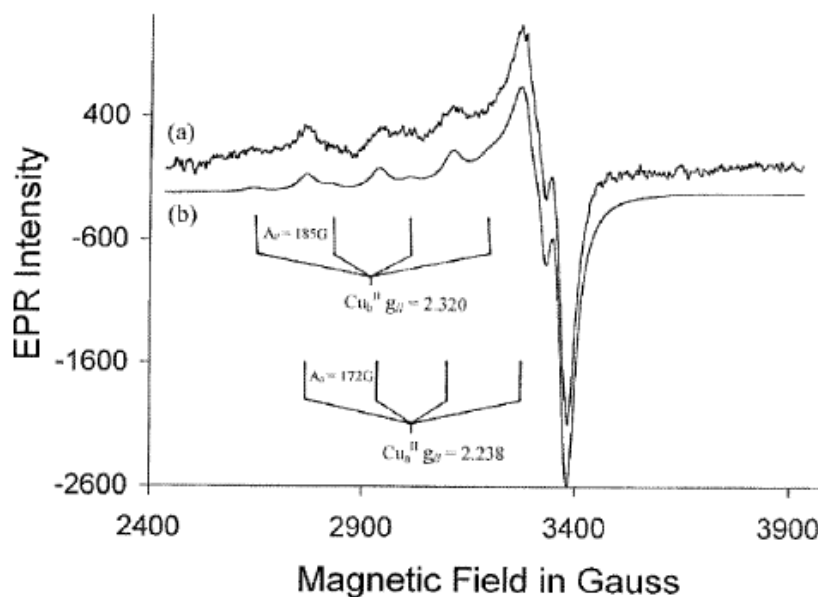


**Figure 18:** First derivative EPR spectra for  $\text{Cu}^{\text{II}}$  showing different  $g$ -values and  $A$ -values for different structural environments.

It is important to note differences in EPR parameters of the two copper species indicating different  $\text{Cu}^{\text{II}}$  centres by virtue of respective ligand environments. Some works have identified copper centres as type 1, type 2 and type 3. The type 1 has an intense blue coloration and a high extinction coefficient in its electronic absorption spectrum. The type 2 has a weaker absorption spectrum and higher hyperfine splitting constants ( $A$ -values) in its EPR spectrum than type 1. Type 3 comprises pairs of copper so close there is antiferromagnetic coupling and therefore not detectable by EPR spectroscopy. On a plot of  $A_{||}$  vs  $g_{||}$  types 1 and 2 are differentiated into groups as shown in Figure 4. Like iron the copper is complexed within protein moieties such that hydrated copper ion is not observed except where there has been denaturation in which the metal drops free of the protein. In such a case spectroscopic parameters would be different. A common ligand is nitrogen, usually from the side group of a histidine residue. Nitrogen hyperfines would therefore show on the copper peaks.

### c) Manganese proteins

Manganese occurs in much smaller amounts than iron and copper in nature. As a contributor to electron transfer in the oxygen evolving photosystem, manganese is widespread in plants. Its presence is easily determined by EPR, based on  $\text{Mn}^{\text{II}}$ ,  $d^5$ ,  $s = 5/2$ . On interaction with the nucleus  $M_I = 1$ , a characteristic set of six isotopic lines is obtained, centred close to free spin. Figure 6 shows  $\text{Mn}^{\text{II}}$  lines obtained from tobacco leaves at 77 K. The mitochondrial superoxide dismutase enzyme contains manganese, though this is far less abundant than the

copper-zinc enzyme. The EPR spectrum for MnSOD shows features ascribed to high spin.  $Mn^{III}$  and  $Mn^{IV}$  and probably higher oxidation states are reported to be present in catalases

#### d) Cobalamin

Cobalamin, also known as vitamin B<sub>12</sub>, is an organic molecule in which a cobalt is 4 coordinated at the centre of a corrin group, a smaller haem-type structure with 4 nitrogen donor positions. The fifth position is N-linked to a dimethylbenzimidazole to which is attached a ribose-3-phosphate O-linked to aminopropanol. The sixth position is occupied by 5-deoxyadenosyl, but can be replaced by other substitutes as in the different derivatives of cobalamin. The  $Co^{II}$  nucleus has a  $d^5$  configuration with spin  $s = 1/2$ , and a magnetic moment  $M_I = 7/2$ . The EPR spectrum comprises 8 lines as shown in Figure 19. In spite of apparent similarities of the haem and corrin structures iron and cobalt are not biologically interchangeable. This must be due to their redox potentials being different, an important discriminatory feature.

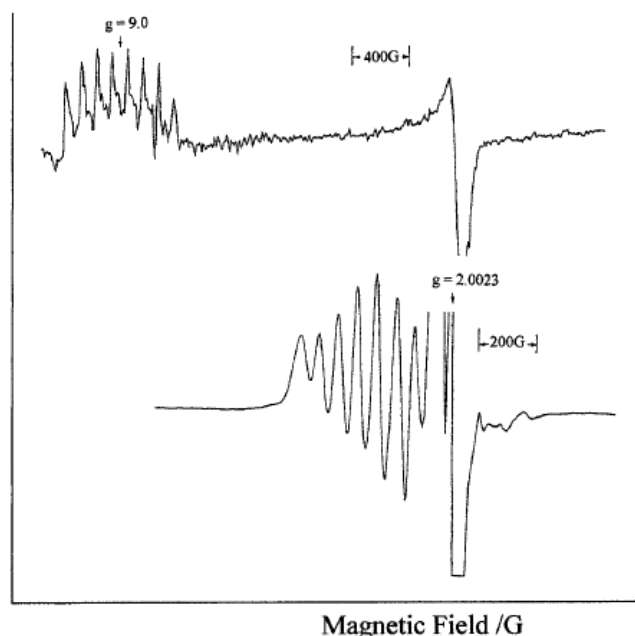


**Figure 19:** First derivative EPR spectrum for  $Co^{II}$  centres at 4 K, showing features assigned to spin  $s = 1/2$  and  $M_I = 7/2$ .

#### 6.29 The ESR spectrum of $PH_4^*$

The quantum-chemically calculated  $PH_4$  structure of minimum energy is a distorted trigonal bipyramid (TBP) with two axial (ax) and two equatorial (eq) hydrogen atoms. The unpaired electron is placed at the position of the missing equatorial ligand. From quantum-chemical calculations revealing significant odd-electron density to reside on the axial position it was shown that the metastable structure B as shown in Figure 20 is equally correct with dashed lines denoting three-electron three-centre bonding.



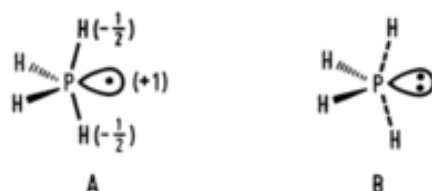


**Figure 20:** Structure of  $\text{PH}_4$

There is considerable evidence that the basic structure of free radicals derived from tetravalent phosphorus (phosphoranyl radicals) is that of a distorted trigonal bipyramid in which two ligand sites, apical and equatorial, are distinguished. ESR hyperfine interactions show a striking disparity between the unpaired spin densities at the two positions, and theoretical arguments favour the apical position as having the higher spin density.

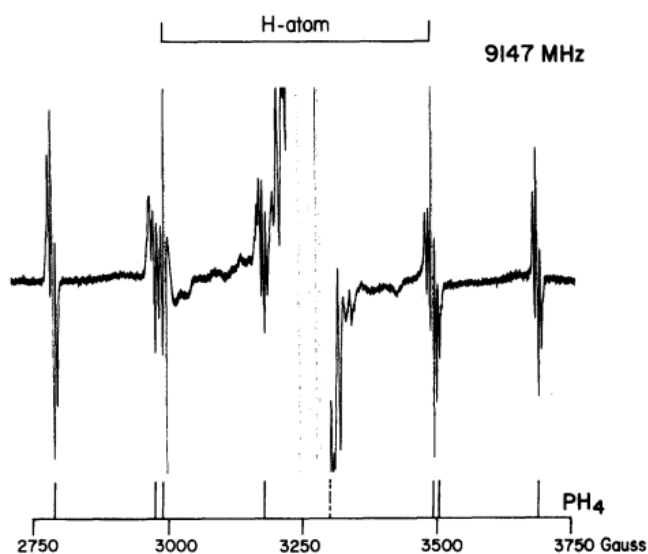


**Figure 21:** ESR spectrum  $\text{PH}_4$  in neopentane at 100

An analysis of the ESR spectra of  $\text{PH}_4$  (and deuterated species) in xenon and neopentane matrices confirmed the theoretically obtained TBP-eq structure of  $\text{PH}_4$ . The best resolved ESR spectrum of  $\text{PH}_4$  was obtained in a neopentane matrix. The ESR of  $\text{PH}_4$  consisted of eight 6.0 G, 1: 2: 1 triplets (Figure 21). It was conclusively shown by experiments with  $\text{PD}_3$  and neopentane- $\text{d}_{12}$  that a large interaction of - 500 G was due to a  $^{31}\text{P}$  nucleus, and that smaller (- 6 and 200 G) interactions were due to pairs of equivalent protons.

### 6.30 Summary of the unit

Electron Spin Resonance (ESR) spectroscopy, also referred to as Electron Paramagnetic Resonance (EPR) spectroscopy, is a versatile, non-destructive analytical technique based on the absorption of microwave radiation in presence of an applied field by paramagnetic species.

When any species that contains unpaired electron(s) is subjected to a static magnetic field, the interaction between the magnetic moment of the electron and the applied magnetic field splits

the spin energy levels (Zeeman splitting), and transitions between these spin levels are induced by applying suitable microwave radiation perpendicular to the magnetic field. Further interactions will depend on the presence of other factors such as the nuclear spins present in both the origin and other neighbours. The resulting absorption of the microwave radiation is modulated to record the first derivative of the absorption. Conventionally, EPR spectra are recorded as first derivative rather than absorption to improve the resolution. In fact, second derivative operation is also possible when needed to get better resolution of complex splitting patterns.

### 6.31 Key words

ESR spectroscopy; Characteristics of 'g'; Types of E.S.R. Instruments; g-value for an electron and a complex; Factors affecting g-value in a complex; Sustaining effect; Zero– field splitting; Kramer's degeneracy; Hyperfine Splitting; Spin–Lattice relaxation; Spin–Spin relaxation; E.S.R. of Transition Metal Complexes

### 6.32 References for further studies

- 1) Electron Spin Resonance: Analysis and Interpretation; Philip Henri Rieger; *Royal Society of Chemistry*, 2007.
- 2) Principles and Applications of ESR Spectroscopy; Anders Lund, Shigetaka Shimada, Masaru Shiotani; *Springer Science & Business Media*, 2011.
- 3) EPR Spectroscopy: Applications in Chemistry and Biology; Malte Drescher, Gunnar Jeschke; *Springer Science & Business Media*, 2012.
- 4) Biomolecular EPR Spectroscopy; Wilfred Raymond Hagen; *CRC Press*, 2008.
- 5) Foundations of Modern EPR; Gareth R. Eaton, Sandra S. Eaton; *World Scientific*, 1998.
- 6) Spectral Methods in Transition Metal Complexes; K. Sridharan; *Elsevier*, 2016.

### 6.33 Questions for self understanding

- 1) Explain the basic theory of ESR spectroscopy
- 2) Discuss the characteristics of 'g'
- 3) Write a note on g-value for an electron and a complex
- 4) Explain the factors affecting g-value in a complex
- 5) What is sustaining effect?
- 6) Discuss the combined effects of CFS and L-S coupling
- 7) Comment on g-value and structure of complex molecules
- 8) Write a note on Zero– field splitting and Kramer's degeneracy
- 9) Discuss the consequences of ZFS

- 10) Write a note on break down of selection rules
- 11) Discuss Mixing of states
- 12) Write a note on magnitude of zero- field splitting and signal
- 13) Explain the effective spin,  $S'$
- 14) Discuss mixing of states and Zero-Field splitting
- 15) Write a note on hyperfine Splitting
- 16) Discuss the characteristics of A
- 17) Write a note on calculation of  $g_{\parallel}$  and  $g_{\perp}$  for these two states
- 18) Write a note on ESR and Jahn-Teller distortion
- 19) With suitable example discuss the E.S.R. of transition metal complexes with following cases
  - a)  $d^1$  system,  ${}^2T_{2g}$ ;  $S' = 1/2$ : octahedral
  - b)  $d^1$  tetrahedral
  - c)  $d^2$  system ;  ${}^3T_{1g}$
  - d)  $d^2$  tetrahedral
  - e)  $d^3$  system,  ${}^4A_{1g}$ ;  $S' = 1/2$
  - f)  $d^4$  System;  ${}^5E_g$ ;  $S = 2$
  - g)  $d^5$  Spin- free,  ${}^6A_{1g}$ ; spin-paired,  ${}^2T_{2g}$
  - h) Spin-paired  $d^5$
- 20) Explain the application of ESR spectroscopy for following biological molecules
  - a) Iron proteins
  - b) Copper proteins
  - c) Manganese proteins
  - d) Cobalamin
- 21) Discuss the ESR spectrum of  $PH_4$  radical.

**UNIT-7****Structure**

7.0 Objectives of the unit

7.1 Introduction

7.2 NMR spectra of Inorganic compounds

7.3 Practical limitations to metal NMR spectroscopy

7.4 Favourable properties for high-resolution NMR spectroscopy are

7.5 Chemical Shift

7.6 Chemically equivalent nuclei

7.7 Integration

7.8 Spin-Spin Splitting (Coupling)

7.9  $^{31}\text{P}$  NMR spectroscopy

7.9.1 Differences between  $^1\text{H}$  and  $^{31}\text{P}$  NMR

7.9.2 Interpreting spectra

7.9.3 Different phosphorus environments and their coupling to  $^1\text{H}$

7.9.4  $^{31}\text{P}$ - $^1\text{H}$  coupling

7.9.5 Coupling to fluorine

7.9.6  $^{31}\text{P}$  NMR applications

7.10  $^{19}\text{F}$  NMR spectroscopy

7.10.1 Chemical shift in  $^{19}\text{F}$  NMR

7.11 Boron NMR spectroscopy

7.11.1 Chemical Shift

7.11.2 General Comments on the Boron Chemical Shifts

7.11.3 Spin-spin coupling between Boron and Nitrogen

7.11.4 Spin-spin coupling between boron and phosphorous

7.12 other NMR active nuclei

7.12.1 Lead

7.12.2 Platinum

7.12.3 Palladium

7.13  $^1\text{H}$  NMR spectroscopy organometallic

7.14 Summary of the unit

7.15 Key words

7.16 References for further studies

7.17 Questions for self understanding

## 7.0 Objectives of the unit

After studying this unit you are able to

- Explain the NMR spectra of Inorganic compounds
- Explain the practical limitations to metal NMR spectroscopy
- Identify the favourable properties for high-resolution NMR spectroscopy are
- Explain the Spin-Spin Splitting (Coupling)
- Explain the use of  $^{31}\text{P}$  NMR spectroscopy
- Explain the use of  $^{19}\text{F}$  NMR spectroscopy
- Explain the use of Boron NMR spectroscopy
- Explain the use of other NMR active nuclei
- Explain the use of  $^1\text{H}$  NMR spectroscopy for organometallic compounds

## 7.1 Introduction

Nuclear Magnetic Resonance (NMR) spectroscopy takes advantage of the magnetic properties of certain nuclei and records the absorption of energy between quantized nuclear energy levels. In an NMR experiment, the spectrometer is tuned to the frequency of a particular nucleus and the spectrum reveals all such nuclei in the molecule being investigated. It is thus a very powerful technique, the closest analogy being a powerful microscope that allows the chemist to "see" the structure of molecules in solution. Actually, the NMR experiment does not directly show how all the atoms are connected. Accordingly, it is up to the chemist to take the information provided by NMR spectra to build a model of the molecule. The analysis of NMR spectra is very much like putting a puzzle together. The structure of the molecule will be known when all of the pieces fit together.

## 7.2 NMR spectra of Inorganic compounds

Multinuclear NMR spectroscopy is the name given to the study of NMR active nuclei of elements other than  $^1\text{H}$  (proton) or  $^{13}\text{C}$  (carbon). The  $^{15}\text{N}$ ,  $^{11}\text{B}$ ,  $^{19}\text{F}$ ,  $^{31}\text{P}$ ,  $^{77}\text{Se}$ ,  $^{119}\text{Sn}$ ,  $^{199}\text{Hg}$ , etc nucleus have spin number  $I \geq \frac{1}{2}$  and are NMR active. The second most sensitive nucleus for NMR is  $^{19}\text{F}$ .

In addition to charge and mass, which all nuclei have, various nuclei also possess a property called nuclear spin, which means they were spinning. Since nuclei have a charge, they generate a magnetic field with an associated magnetic moment. NMR is possible owing to the magnetic properties of certain nuclei.

There are useful empirical rules relating mass number, atomic number (Z) and nuclear spin quantum number (I), which are shown in the Table 1:

**Table 1:** Empirical rules relating mass number, atomic number (Z) and nuclear spin quantum number (I)

Mass Number	Z	I
even	even	0
odd	even or odd	$1/2, 3/2, 5/2, \dots$
even	odd	1, 2, 3, ...

Since NMR depends on the existence of a nuclear spin, nuclei with  $I = 0$  have no NMR spectrum (e.g.,  $^{12}\text{C}$ ,  $^{16}\text{O}$ ,  $^{18}\text{O}$ ). The most important class of nuclei are those with  $I = 1/2$  are NMR active and give sharp NMR spectrum. Nuclei with  $I > 1/2$  (e.g.,  $^{11}\text{B}$ ,  $I = 3/2$ ;  $^{14}\text{N}$ ,  $I = 1$ ) have quadrupole moments, a non-spherical distribution of nuclear charge, which results in broad absorption lines and makes observation of spectra more difficult. The quadrupole moment can even affect the lineshape of neighbouring nuclei. For example, resonances of protons bonded to nitrogen or boron atoms are generally broad in  $^1\text{H}$  NMR spectra. We shall thus be primarily concerned with nuclei where  $I = 1/2$ , but the effect that quadrupolar nuclei can have on the NMR spectra of  $I = 1/2$  nuclei should be remembered. A listing of isotopes with  $I = 1/2$  is provided in the Table 2.

**Table 2:** Isotopes with  $I = 1/2$  and their natural abundance

Natural abundances of isotopes with  $I = 1/2$ .

Isotope	Natural Abundance (%)	Isotope	Natural Abundance (%)	Isotope	Natural Abundance (%)
$^1\text{H}$	100	$^{107}\text{Ag}$	51.35	$^{129}\text{Xe}$	26.44
$^{13}\text{C}$	1.108	$^{109}\text{Ag}$	48.65	$^{169}\text{Tm}$	100
$^{15}\text{N}$	0.365	$^{111}\text{Cd}$	12.75	$^{183}\text{W}$	14.4
$^{19}\text{F}$	100	$^{113}\text{Cd}$	12.26	$^{187}\text{Os}$	1.64
$^{29}\text{Si}$	4.71	$^{115}\text{Sn}$	0.34	$^{195}\text{Pt}$	33.8
$^{31}\text{P}$	100	$^{117}\text{Sn}$	7.57	$^{199}\text{Hg}$	16.84
$^{57}\text{Fe}$	2.17	$^{119}\text{Sn}$	8.58	$^{203}\text{Tl}$	29.50
$^{77}\text{Se}$	7.58	$^{123}\text{Te}$	0.87	$^{205}\text{Tl}$	70.50
$^{89}\text{Y}$	100	$^{125}\text{Te}$	6.99	$^{207}\text{Pb}$	21.7
$^{103}\text{Rh}$	100				

### 7.3 Practical limitations to metal NMR spectroscopy

The NMR spectroscopy study of metal (in particular transition metal) is very much unfavourable. This is because of the small number of nuclei with favourable nuclear properties for high-resolution NMR. As the technology evolves, more nuclei bond types are being brought into the spectroscopist's net. The NMR properties of the various nuclei tabulate in Table 3.

**Table 3:** The NMR properties of the various nuclei.

NMR properties of some elements of biological and/or medicinal interest

Isotope	Natural abundance (%)	Nuclear spin ( <i>I</i> )	Magnetogyric ratio ( $\gamma$ ) ( $\times 10^7$ rad T <sup>-1</sup> s <sup>-1</sup> )	Quadrupole moment ( <i>eQ</i> ) ( $\times 10^{28}$ C m <sup>-2</sup> )	Relative receptivity (to <sup>13</sup> C) <sup>a</sup>
<b>Non-metals</b>					
<sup>1</sup> H	99.98	1/2	26.7519	–	5666
<sup>13</sup> C	1.108	1/2	6.7283	–	1
<sup>14</sup> N	99.635	1	1.9338	$1.99 \times 10^{-2}$	5.69
<sup>15</sup> N	0.365	1/2	–2.712	–	0.022
<sup>17</sup> O	$3.7 \times 10^{-2}$	5/2	–3.6279	$-2.6 \times 10^{-2}$	0.06
<sup>19</sup> F	100	1/2	25.181	–	4761.5
<sup>31</sup> P	100	1/2	10.841	–	377
<sup>33</sup> S	0.76	3/2	2.055	$-5.5 \times 10^{-2}$	0.097
<sup>35</sup> Cl	75.53	3/2	2.624	–0.1	20.2
<sup>37</sup> Cl	24.47	3/2	2.1842	$-7.9 \times 10^{-2}$	3.8
<sup>77</sup> Se	7.58	1/2	5.12	–	2.98
<sup>79</sup> Br	50.54	3/2	6.7228	0.37	226
<sup>81</sup> Br	49.46	3/2	7.2468	0.31	277
<sup>127</sup> I	100	5/2	5.3817	–0.79	530
<b>Metalloids</b>					
<sup>10</sup> B	19.58	3	2.875	$8.5 \times 10^{-2}$	22.1
<sup>11</sup> B	80.42	3/2	8.584	$4.1 \times 10^{-2}$	754
<sup>29</sup> Si	4.7	1/2	–5.3188	–	2.09
<sup>73</sup> Ge	7.76	9/2	–0.9357	–0.18	0.617
<sup>75</sup> As	100	3/2	4.595	0.29	143
<sup>121</sup> Sb	57.25	5/2	6.4355	–0.28	520
<sup>123</sup> Sb	42.75	7/2	3.4848	–0.36	111
<sup>123</sup> Te	0.87	1/2	–7.049	–	0.89
<sup>125</sup> Te	6.99	1/2	–8.498	–	12.5
<b>Metals</b>					
<sup>6</sup> Li	7.42	1	3.9371	$-8 \times 10^{-4}$	3.58
<sup>7</sup> Li	92.58	3/2	10.3976	$-4 \times 10^{-2}$	1540
<sup>23</sup> Na	100	3/2	7.0801	0.1	525
<sup>25</sup> Mg	10.13	5/2	–1.639	0.22	1.54
<sup>27</sup> Al	100	5/2	6.976	0.15	1170
<sup>39</sup> K	93.12	3/2	1.2498	$4.9 \times 10^{-2}$	2.69
<sup>41</sup> K	6.88	3/2	0.686	$6 \times 10^{-2}$	0.033
<sup>43</sup> Ca	0.145	7/2	–1.8025	0.2	0.053
<sup>45</sup> Sc	100	7/2	6.5081	–0.22	1710
<sup>47</sup> Ti	7.28	5/2	–1.5105	0.29	0.864
<sup>49</sup> Ti	5.51	7/2	–1.5109	0.24	1.118
<sup>50</sup> V <sup>b</sup>	0.24	6	2.6717	$6 \times 10^{-2}$	0.755
<sup>51</sup> V	99.76	7/2	7.0453	$-5 \times 10^{-2}$	2150
<sup>53</sup> Cr	9.55	3/2	–1.512	$3 \times 10^{-2}$	0.49
<sup>55</sup> Mn	100	5/2	6.608	0.4	994
<sup>57</sup> Fe	2.19	1/2	0.8661	–	0.004
<sup>59</sup> Co	100	7/2	6.317	0.38	1570
<sup>61</sup> Ni	1.19	3/2	–2.394	0.16	0.24
<sup>63</sup> Cu	69.09	3/2	7.0974	–0.211	365
<sup>65</sup> Cu	30.91	3/2	7.6031	–0.195	201
<sup>67</sup> Zn	4.11	5/2	1.6768	0.16	0.67
<sup>69</sup> Ga	60.4	3/2	6.4323	0.19	237
<sup>71</sup> Ga	39.6	3/2	8.1731	0.12	319
<sup>85</sup> Rb	72.15	5/2	2.5909	0.26	43
<sup>87</sup> Rb	27.85	3/2	8.7807	0.13	277
<sup>89</sup> Y	100	1/2	–1.3155	–	0.668
<sup>95</sup> Mo	15.72	5/2	1.75	0.12	2.88
<sup>97</sup> Mo	9.46	5/2	–1.787	1.1	1.84
<sup>99</sup> Tc	100	9/2	6.0211	0.3	2134
<sup>99</sup> Ru	12.72	3/2	–1.234	$7.6 \times 10^{-2}$	0.83
<sup>101</sup> Ru	17.07	5/2	–1.383	0.44	1.56
<sup>103</sup> Rh	100	1/2	–0.846	–	0.177
<sup>105</sup> Pd	22.23	5/2	–0.756	0.8	1.41
<sup>107</sup> Ag	51.82	1/2	–1.087	–	0.195
<sup>109</sup> Ag	48.18	1/2	–1.25	–	0.276
<sup>111</sup> Cd	12.75	1/2	–5.6926	–	6.93

Isotope	Natural abundance (%)	Nuclear spin ( <i>I</i> )	Magnetogyric ratio ( $\gamma$ ) ( $\times 10^7 \text{ rad T}^{-1} \text{ s}^{-1}$ )	Quadrupole moment ( $eQ$ ) ( $\times 10^{28} \text{ C m}^{-2}$ )	Relative receptivity (to $^{13}\text{C}$ ) <sup>a</sup>
$^{113}\text{Cd}$	12.26	1/2	-5.955	-	7.6
$^{113}\text{In}$	4.28	9/2	5.8782	0.83	83.8
$^{115}\text{In}$	95.72	9/2	5.8908	0.83	1890
$^{115}\text{Sn}$	0.35	1/2	-8.801	-	0.70
$^{117}\text{Sn}$	7.61	1/2	-9.589	-	19.54
$^{119}\text{Sn}$	8.58	1/2	-10.0138	-	25.2
$^{133}\text{Cs}$	100	7/2	3.5277	$-3 \times 10^{-3}$	269
$^{183}\text{W}$	14.4	1/2	1.12	-	0.059
$^{187}\text{Os}$	1.64	1/2	0.616	-	0.001
$^{189}\text{Os}$	16.1	3/2	0.8475	0.8	2.13
$^{195}\text{Pt}$	33.7	1/2	5.768	-	19.1
$^{197}\text{Au}$	100	3/2	0.4625	0.59	0.06
$^{199}\text{Hg}$	16.84	1/2	4.8154	-	5.42
$^{201}\text{Hg}$	13.22	3/2	-1.7776	0.44	1.08
$^{203}\text{Tl}$	29.5	1/2	15.436	-	289
$^{205}\text{Tl}$	70.5	1/2	15.589	-	769
$^{207}\text{Pb}$	22.6	1/2	5.54	-	11.8
$^{209}\text{Bi}$	100	9/2	4.342	-0.38	777
$^{138}\text{La}$	0.089	5	3.5295	-0.47	0.43
$^{139}\text{La}$	99.91	7/2	3.801	0.22	336
$^{155}\text{Gd}$	14.73	3/2	-1.0152	n.a.	0.23
$^{157}\text{Gd}$	15.68	3/2	-1.2566	n.a.	0.46

#### 7.4 Favourable properties for high-resolution NMR spectroscopy are

- 1) Spin quantum number  $I = 1/2$  or, for  $I > 1/2$
- 2) A relatively small value of the nuclear electric quadrupole moment ( $eQ$ ) and
- 3) A large value of  $I$ , to minimize quadrupolar broadening.

Also necessary are a sufficiently large natural abundance ( $A$ ) and magnetogyric ratio ( $\gamma$ , effectively the ratio of the magnetic moment to the spin quantum number), to which the NMR frequency is proportional.

The intrinsic NMR receptivity, which is a measure of the intensity of signal, increases as  $| \gamma | AI(I+1)$ . Thus, larger values of  $I$  are more favorable by a factor of 33 from  $I = 1/2$  to  $9/2$ . Transition metal nuclei with natural abundance below 5% that may be usefully studied with enrichment are  $^{57}\text{Fe}$ ,  $^{61}\text{Ni}$ ,  $^{67}\text{Zn}$  and  $^{187}\text{Os}$ .

Spin  $I = 1/2$  nuclei with low  $\gamma$  values have a further problem of too slow relaxation, since the rate depends on  $\gamma$ , and long accumulation times or sensitivity enhancement techniques may be needed for adequate sensitivity; examples are  $^{89}\text{Y}$ ,  $^{183}\text{W}$ ,  $^{57}\text{Fe}$ ,  $^{187}\text{Os}$ ,  $^{103}\text{Rh}$  and  $^{109}\text{Ag}$ .

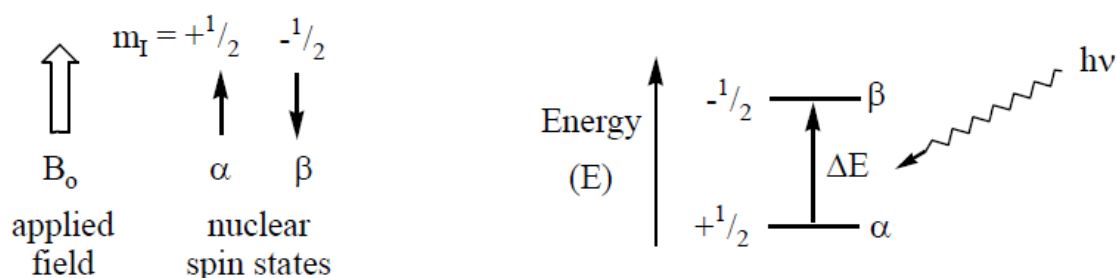
For the majority of metal nuclei, the spin quantum number  $I$  is greater than  $1/2$  and, therefore, they possess a nuclear electric quadrupole moment  $eQ$  (in addition to their magnetic moment), as the nuclear electric charge distribution is not spherically symmetric. The electric quadrupole is coupled to the spin (magnetic dipole), since transitions in the one change the magnetic environment of the other. Whereas the orientation of the spin dipole is quantized relative to the magnetic field, that of the electric quadrupole is quantized relative to the electric field gradient (EFG)  $eQ$  at the nucleus due to the electrons and the other nuclei.



Thus the interaction of the nuclear quadrupole moment with the electric field gradients arising from the local electronic environment provides a strong relaxation mechanism for the spin states, often resulting in short-lived states with broad resonance lines. In general, quadrupolar nuclei display broad resonances in NMR spectra, unless they are in highly symmetric electrical environments, which reduce the magnitude of the electric field gradients at the nuclei.

In an NMR experiment, the sample is placed in a strong magnetic field,  $B_0$ . Since the spins of the magnetic nuclei are quantized, they can have only certain well-defined values. If we have nuclei with  $I = 1/2$  (e.g.,  $^1\text{H}$ ,  $^{31}\text{P}$ ), the spins can orient only in two directions: ie, either with ( $m_I = +1/2$ ,  $\alpha$ ) or against ( $m_I = -1/2$ ,  $\beta$ ) the applied field. NMR transitions are allowed for cases where  $\Delta m_I = \pm 1$ . There is an energy difference,  $\Delta E$ , between the two states, and this is given by

$$\Delta E = h\nu = \frac{h}{2\pi}\gamma B_0 \quad \text{or} \quad \nu = \frac{1}{2\pi}\gamma B_0$$



where  $h$  is Planck's constant,  $\gamma$  is the gyromagnetic ratio (a constant characteristic of each nucleus), and  $B_0$  is the applied magnetic field. When the energy of the incoming radiation matches the energy difference between the spin states, energy is absorbed and the nucleus is promoted from the lower  $+1/2$  to the higher  $-1/2$  spin state. Since the sign of  $m_I$  changes, this is sometimes referred to as a "spin flip". NMR transitions occur in the radio frequency (rf) range of the electromagnetic spectrum. The absorption of rf energy is electronically detected and is displayed as an NMR spectrum.

The above equation is very important since it shows that  $\Delta E$  depends only on  $\gamma$  and  $B_0$ . The gyromagnetic ratio,  $\gamma$ , is an intrinsic property of the magnetic nucleus. Therefore, each type of nucleus has a distinct and characteristic value of  $\gamma$ . Accordingly, the NMR experiment must be tuned for a specific nucleus and one must record a different NMR spectrum for each NMR active nucleus of interest therefore not to worry about observing signals from different nuclei on the same NMR spectrum. In order to gather all NMR knowledge about a molecule such as  $\text{PH}_3$ , we would record two different NMR spectra - a  $^1\text{H}$  NMR spectrum to observe

the  $^1\text{H}$  nuclei and a  $^{31}\text{P}$  NMR spectrum to observe the  $^{31}\text{P}$  nucleus. We would not observe the  $^{31}\text{P}$  nucleus in a  $^1\text{H}$  NMR spectrum and vice-versa.

The above equation also reveals that  $\Delta E$  is directly proportional to  $B_0$ , the external magnetic field. The higher the external field, the greater is the energy separation between the  $\alpha$  ( $m_I = +1/2$ ) and  $\beta$  ( $m_I = -1/2$ ) spin states. Recalling that  $E = h\nu$ , another way of saying this is that the resonance frequency of the nucleus increases with increasing  $B_0$  since  $E$  increases, so also  $\nu$ . This is shown in the Table.

**Table 4:** The differences in resonance frequency of the nucleus under same  $B_0$

$B_0$ (tesla) <sup>‡</sup>	Resonance Frequency ( $\nu$ , MHz)				
	$^1\text{H}$	$^{13}\text{C}$	$^{11}\text{B}$	$^{19}\text{F}$	$^{31}\text{P}$
2.35	100	25.2	32.1	94.1	40.5
4.70	200	50.4	64.2	188.2	81.0

<sup>‡</sup>a *tesla* is a unit describing magnetic field strength

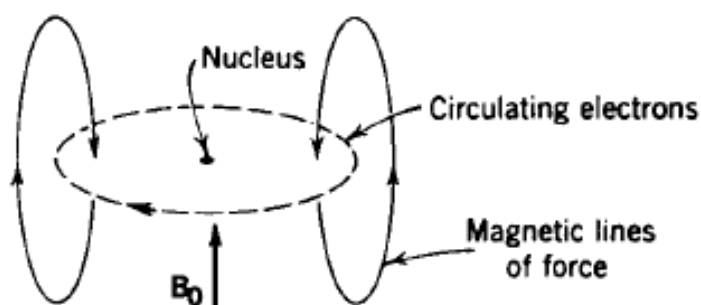
$$* \gamma = \frac{2\pi\mu}{hI} \text{ where } \mu \text{ is the magnetic moment of the nucleus.}$$

Note that all  $I = 1/2$  nuclei behave according to the same theoretical principles, although  $^1\text{H}$  NMR spectroscopy is the most commonly practiced,  $^{19}\text{F}$  and  $^{31}\text{P}$  NMR spectra are generated in exactly the same way as a  $^1\text{H}$  NMR spectrum. The main difference between the different  $I = 1/2$  nuclei is that the resonance frequency is changed when recording the spectrum.

### 7.5 Chemical Shift

From the previous equation it is clear that, the resonance frequency is determined only by  $\gamma$  and  $B_0$ . Therefore all atoms of a given nucleus in a molecule (e.g., all  $^1\text{H}$  nuclei) should resonate at the same frequency. If this were the case, the NMR could tell us whether a molecule contains NMR active nuclei ( $^1\text{H}$ ,  $^{31}\text{P}$ ,  $^{13}\text{C}$ , etc.) or not and how many different NMR active nuclei are present in the given molecule. Fortunately, the frequency of the NMR absorptions of a given nucleus also depends on the chemical environment of the nucleus. *The variation of the resonance frequency with chemical environment is termed the chemical shift*, and herein lies the power of the NMR method.

The origin of the chemical shift is traced by the electrons surrounding the nucleus and the interaction of the electron cloud with the applied field  $B_0$ . The reason for this is that circulating electrons also generate a magnetic field that orients itself in the opposite direction to the applied field.



The actual field ( $B_{\text{local}}$ ) “felt” by a nucleus is thus less than  $B_0$ , and the ability of the electrons to alter the field felt at the nucleus can be expressed by  $\sigma$ , the shielding constant.

$$B_{\text{local}} = B_0 (1 - \sigma) \text{ or } \nu_{\text{local}} = \frac{1}{2\pi} \gamma B_0 (1 - \sigma)$$

Nuclei are said to be shielded or deshielded depending on the presence or absence of electron density surrounding them. For example, the introduction of an electron withdrawing group (e.g., halogen, O, etc.) will reduce the electron density around a nucleus (deshielding;  $\sigma$  is small) and the resonance frequency will increase. Conversely, an electron donating substituent (e.g., CH<sub>x</sub>, SiH<sub>x</sub>) will cause increased shielding ( $\sigma$  is large) and lower the resonance frequency.

For reporting chemical shifts, one could use absolute field or absolute frequency, but this would be cumbersome and would result in the chemical shift being dependent upon the applied field. A simpler scale for chemical shifts has been devised. Chemical shifts ( $\delta$ ) are expressed in units of parts per million (ppm) of the spectrometer frequency with respect to a reference material whose position is arbitrarily assigned a value of 0.0 ppm.

$$\delta \text{ (ppm)} = \frac{\nu_{\text{sample}} \text{ (Hz)} - \nu_{\text{reference}} \text{ (Hz)}}{\nu_{\text{spectrometer}} \text{ (Hz)}} \times 10^6 = \frac{\Delta\nu \text{ (separation from reference in Hz)}}{\nu_{\text{spectrometer}} \text{ (in MHz)}}$$

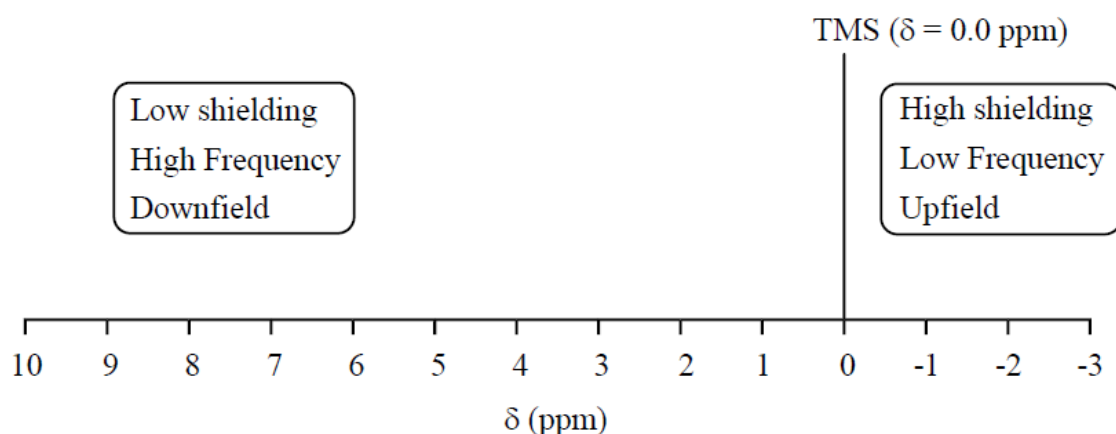
When expressed in such dimensionless units ( $\delta$  in ppm), the chemical shifts are invariant of the frequency of the spectrometer and can be used as molecular parameters. For example, 1.0 ppm at 60 MHz is equal to a separation of 60 Hz, and at 200 MHz, 1.0 ppm equals 200 Hz. Thus, the same two resonances that are separated by 1 ppm at 60 MHz are still 1 ppm apart at 200 MHz, because  $\delta = 60 \text{ Hz}/60 \text{ MHz} = 200 \text{ Hz}/200 \text{ MHz} = 1 \text{ ppm}$ . Therefore, if the same sample is run at two different spectrometer frequencies, the chemical shifts of the resonances will be identical.

Naturally, this statement is only true if the same reference material is used for each spectrum. Different references are used for different nuclei. The most widely accepted reference for  $^1\text{H}$

and  $^{13}\text{C}$  NMR is tetramethylsilane ( $\text{Si}(\text{CH}_3)_4 = \text{TMS}$ ). For  $^{11}\text{B}$  NMR,  $\text{F}_3\text{B}\cdot\text{OEt}_2$  is commonly used, as are  $\text{CFC}_{13}$  for  $^{19}\text{F}$  NMR and 85%  $\text{H}_3\text{PO}_4$  for  $^{31}\text{P}$  NMR spectroscopy.

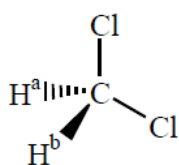
In the past, NMR spectra were obtained by varying the applied field and measuring the chemical shift as a function of the field strength. This gave rise to the terminology of a downfield shift for nuclei that were deshielded (as they required a lower applied field to bring the nucleus into resonance) and upfield shift for shielded nuclei. For example, one would say that a resonance at  $\delta$  8.0 ppm is downfield of one at  $\delta$  2.0 ppm, and conversely that the signal at  $\delta$  2.0 ppm was upfield of the signal at  $\delta$  8.0 ppm.

More modern NMR spectrometers generate spectra by varying the frequency,  $\nu$ , while keeping the magnetic field strength,  $B_0$ , constant. Nevertheless, the upfield/downfield terminology remains in common use. Unfortunately, this results in the confusing situation that  $\delta$  is positive in the downfield direction (to the left of the standard on spectra) where resonance frequencies are higher. Resonances that are upfield of the reference appear at lower frequencies and have negative  $\delta$  values.

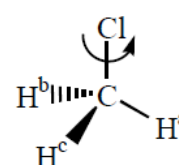
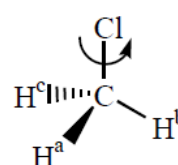
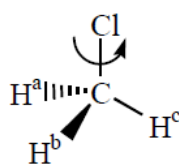


### 7.6 Chemically equivalent nuclei

One important consequence of chemical shift is that each chemically different type of NMR active nucleus in a molecule will give rise to its own signal in an NMR spectrum. Nuclei are thus referred to as chemically equivalent or chemically inequivalent in determining how many signals will be observed in an NMR spectrum. For example, both  $\text{CH}_3\text{Cl}$  and  $\text{CH}_2\text{Cl}_2$  provided one resonance each in the  $^1\text{H}$  NMR spectrum in below figure.



mirror in the plane of the page renders  $\text{H}^a = \text{H}^b$

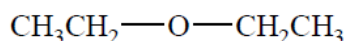


three-fold rotation axis demonstrates  $\text{H}^a = \text{H}^b = \text{H}^c$

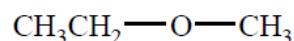
From this, we can infer that the individual hydrogens in each of these molecules are chemically equivalent. From the viewpoint of chemical structure, the reason for this is that hydrogens are related by symmetry elements (reflection through a mirror plane or rotation about an axis) and are thus identical.

Sometimes, determining chemical equivalence or inequivalence is straightforward. It would not take very much to convince you that the methyl hydrogens in ethanol ( $\text{CH}_3\text{CH}_2\text{OH}$ ) are different from the methylene hydrogens and that both of these are different than the hydroxyl hydrogen; we would thus anticipate three signals in the  $^1\text{H}$  NMR spectrum. Upon further reflection though, why should the hydrogens of the methyl group all be equivalent? The answer is simple when it is recognized that methyl groups rotate freely and rapidly, with the result that each hydrogen experiences the same overall chemical shift as it completes one rotation, a situation analogous to  $\text{CH}_3\text{Cl}$  described above. Therefore, all methyl groups generally give rise to one signal in  $^1\text{H}$  NMR spectra. This concept can generally be applied to analogous groups such as tert-butyl,  $\text{C}(\text{CH}_3)_3$ , trimethylsilyl,  $\text{Si}(\text{CH}_3)_3$ , and trifluoromethyl,  $\text{CF}_3$  (in  $^{19}\text{F}$  NMR spectra).

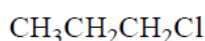
The most general method of determining whether nuclei are chemically equivalent to other nuclei in a molecule is to determine whether they are in the same environment, and whether one nucleus can be related to the other through a symmetry transformation such as rotation or reflection through a mirror plane. Some examples are provided below for illustration.



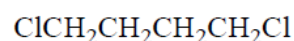
The  $\text{CH}_2$  groups are equivalent and the  $\text{CH}_3$  groups are equivalent.  $\Rightarrow$  2 signals in either the  $^1\text{H}$  or  $^{13}\text{C}$  NMR spectra



The  $\text{CH}_3$  groups are inequivalent.  $\Rightarrow$  3 signals in either the  $^1\text{H}$  or  $^{13}\text{C}$  NMR spectra

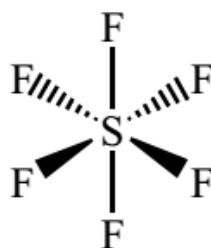


The  $\text{CH}_2$  groups are inequivalent.  $\Rightarrow$  3 signals in either the  $^1\text{H}$  or  $^{13}\text{C}$  NMR spectra

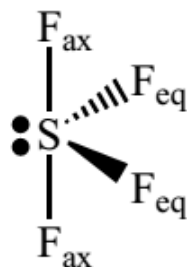


There are two distinct sets of  $\text{CH}_2$  groups.  $\Rightarrow$  2 signals in either the  $^1\text{H}$  or  $^{13}\text{C}$  NMR spectra

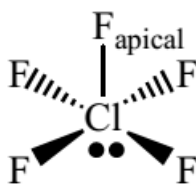
$\text{SF}_6$  is a highly symmetrical octahedral molecule it gives 1 signal in the  $^{19}\text{F}$  NMR spectrum



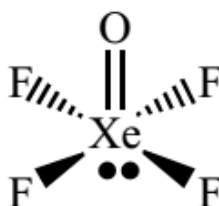
The axial (ax) and equatorial (eq) fluorines are chemically inequivalent hence there are 2 signals are seen in the  $^{19}\text{F}$  NMR spectrum



The apical fluorine is chemically distinct from the four fluorines in the square base hence 2 signals are seen in the  $^{19}\text{F}$  NMR spectrum



The four fluorine nuclei in the square base are chemically equivalent hence 1 signal is seen in the  $^{19}\text{F}$  NMR spectrum

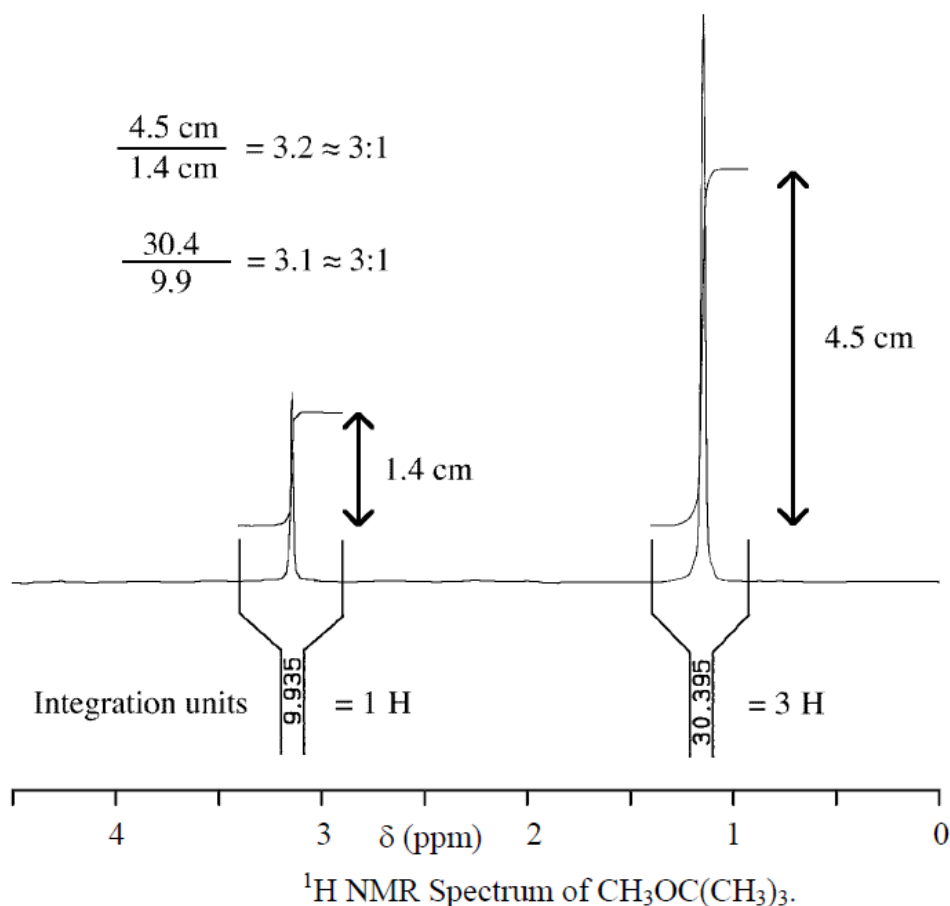


### 7.7 Integration

The area under each NMR absorption peak can be electronically integrated to determine the relative number of nuclei responsible for each peak. The integral of each peak can be provided numerically, and is often accompanied by a line that represents the integration graphically. Intensities of signals can be compared within a particular NMR spectrum only. For example,  $^1\text{H}$  intensities cannot be compared to those of  $^{19}\text{F}$  or  $^{31}\text{P}$  nuclei. It is important to note that the integration of a peak is a relative number and does not give the absolute number of nuclei that cause the signal. Thus, the  $^1\text{H}$  NMR spectrum of  $\text{H}_3\text{C-SiH}_3$  will show two peaks in a 1:1 ratio, as will the  $^1\text{H}$  NMR spectrum of  $(\text{H}_3\text{C})_3\text{C-Si}(\text{CH}_3)_3$ . This is simply because the ratios  $3:3 = 9:9 = 1:1$ .

The concept of integration, and also that of chemical shift, is illustrated in below Figure. Determining integration ratios is an exercise in finding the greatest common divisor for the series of peaks (the largest whole number divisor that will produce a whole number ratio). In the above example, this value is either 1.4 cm or 9.9 integration units. It should be remembered that integration is a measurement that is subject to error; it is common for the error in integrated intensity to approach 5 - 10 %. The ratio of the integrated peak intensities

is 1:3 = 3:9, allowing us to assign the resonance at  $\delta$  3.21 to the methyl group and that at  $\delta$  1.20 to the  $(\text{CH}_3)_3\text{C}$  group. It is important to note that the hydrogens of the  $(\text{CH}_3)_3\text{C}$  group are more shielded than the  $\text{CH}_3$  group. This occurs because the  $\text{CH}_3$  group is directly adjacent to the electron withdrawing oxygen, but the corresponding methyl protons in the  $(\text{CH}_3)_3\text{C}$  group are separated from oxygen by a second intervening carbon centre.

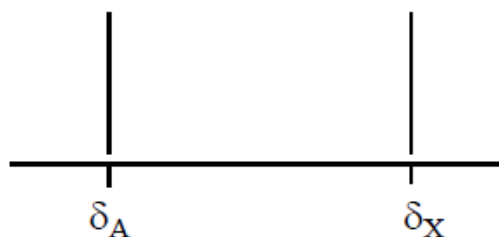


At this stage, we appreciate NMR resembles a molecular microscope. For example, at one frequency we could "see" the various protons, while the carbons, fluorines, phosphorus, and even certain metal nuclei could be observed at other frequencies. Within one spectrum, we can make use of the position (chemical shift) and integrated intensity of the different signals to assign particular molecular fragments responsible for them, and to build up a model of the molecule. There is one more aspect of NMR that is extremely helpful in determining how to connect the parts together.

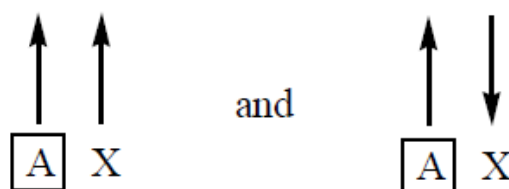
### 7.8 Spin-Spin Splitting (Coupling)

The appearance of a resonance may be very different when there are other neighbouring magnetic nuclei. The reason for this is that the nucleus under observation will interact with the magnetic spins of the different neighbouring nuclei.

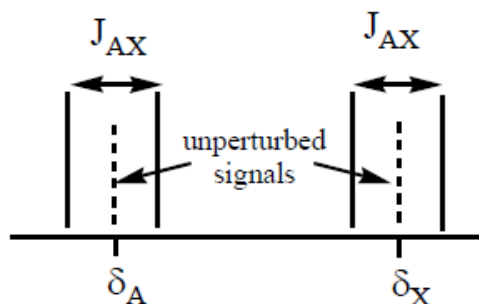
The simplest case is that of two protons having significantly different chemical shifts (designated A and X). Considering chemical shift and integration only, we could represent the spectrum as



Both protons have a spin of  $1/2$ , and both can exist in the  $+1/2$  and  $-1/2$  spin states. Now, it turns out that the magnetic environment of HA is slightly different when HX is in the  $+1/2$  state than when it is in the  $-1/2$  state. This can be represented pictorially with arrows (pointing either up or down) representing the two spin states of HX.



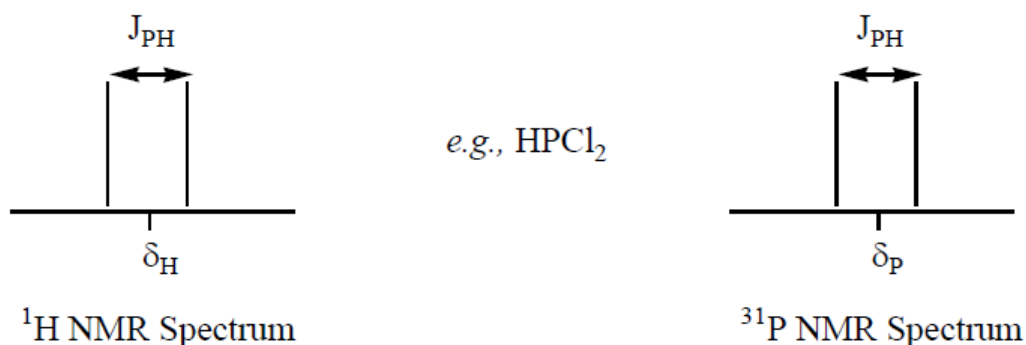
As a result, HA will split into two lines. Each half the intensity of the unperturbed signal. Similarly, HA will influence HX which becomes a doublet also. The splitting, or coupling, is symmetrical about the unperturbed resonances  $\delta_A$  and  $\delta_X$ , and is described by the means of a coupling constant,  $J_{AX}$ , which has units of Hz.



Note that the magnitude of  $J_{AX}$  is identical at both signals, coupled nuclei must share the same coupling constant.

In a similar way, the resonance of a proton attached to phosphorus will be a doublet, since the phosphorus nucleus has  $I = 1/2$  and may be in the  $+1/2$  or  $-1/2$  state. However, the key distinction here is that we are dealing with two different nuclei, and thus two different NMR spectra. Each NMR spectrum ( $^1\text{H}$  and  $^{31}\text{P}$ ) will show one doublet with a  $J_{\text{PH}}$  coupling constant that is identical in magnitude. It is important to remember that, we cannot "see" a  $^{31}\text{P}$  nucleus in a  $^1\text{H}$  NMR spectrum and vice-versa. Nonetheless, the splitting of the peaks into doublets in each spectrum tells us that the  $^1\text{H}$  and  $^{31}\text{P}$  nuclei are interacting.





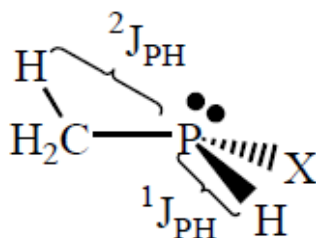
The influence of the neighbouring spins is called *spin-spin coupling* and NMR peaks are split into multiplets as a result. The separation between the two peaks is called the *coupling constant, J*, which is expressed in Hz.

Spin-spin coupling has the following characteristics

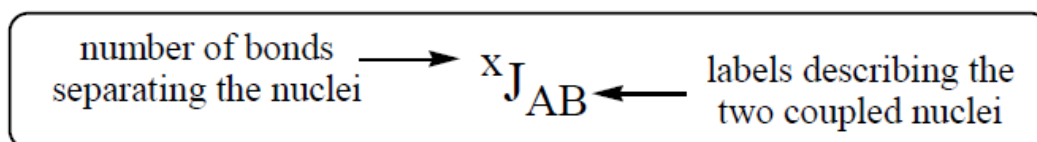
- The magnitude of J measures how strongly the nuclear spins interact with each other.
- Coupling is normally a through-bond interaction, and is proportional to the product of the gyromagnetic ratios of the coupled nuclei.

For example,  $^1J_{\text{CH}} = 124$  Hz for  $^1\text{H}$ - $^{13}\text{C}$  coupling in  $\text{CH}_4$ , and  $^1J_{\text{SnH}} = 1931$  Hz for  $^{119}\text{Sn}$ -H coupling in  $\text{SnH}_4$ . This happens because  $\gamma(^{119}\text{Sn})$  is much larger than  $\gamma(^{13}\text{C})$ .

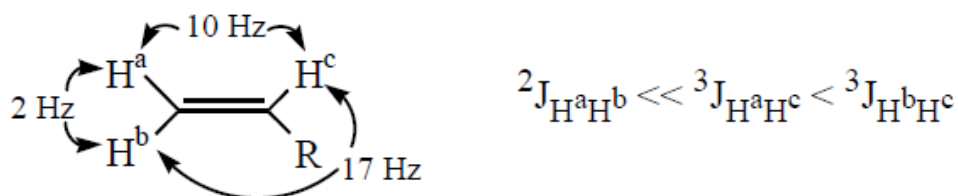
- Since coupling occurs through chemical bonds, the magnitude of J normally falls off rapidly as the number of intervening bonds increases. *e.g.*,  $^1J_{\text{PH}} \sim 700$ ;  $^2J_{\text{PH}} \sim 20$  Hz in



Coupling constants are thus labeled to show the types of nuclei and the number of bonds separating the nuclei that give rise to spin-spin splitting.



- Since spin-spin coupling is a through-bond interaction, it is sensitive to the orientation of the bonds between two interacting nuclei. This is particularly important for two-bond coupling constants. The influence of the orientation of the two coupled nuclei can occasionally render  $^2J < ^3J$ . For example,



${}^1J$  is not affected by the orientation of the coupled nuclei, so it is generally true that  ${}^1J \gg {}^2J$  or  ${}^3J$ , but it is not always true that  ${}^2J > {}^3J$ .

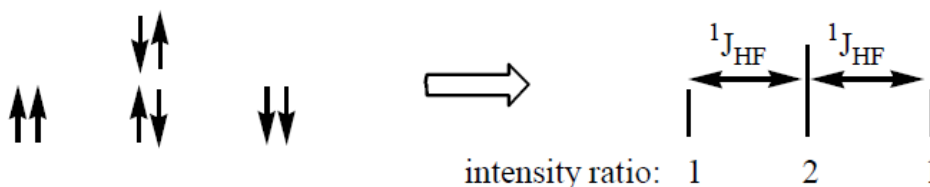
- Spin-spin interactions are independent of the strength of the applied field. The spacing (in Hz) between lines at two different field strengths will be the same if it is due to coupling, but will be proportional to the field strength if it is due to a difference in chemical shift.

#### Typical Coupling Constant Ranges (in Hz).

x	Coupled Nuclei (AB in ${}^xJ_{AB}$ )			
	HH	CH	PH <sup>b</sup>	PC <sup>b</sup>
1	–	115 - 250	630 - 710	120 - 180
2 <sup>a</sup>	2 - 30	5 - 60	7 - 13	5 - 40
3	2 - 17	2 - 20	6 - 11	5 - 11
4	–	–	0 - 1	–

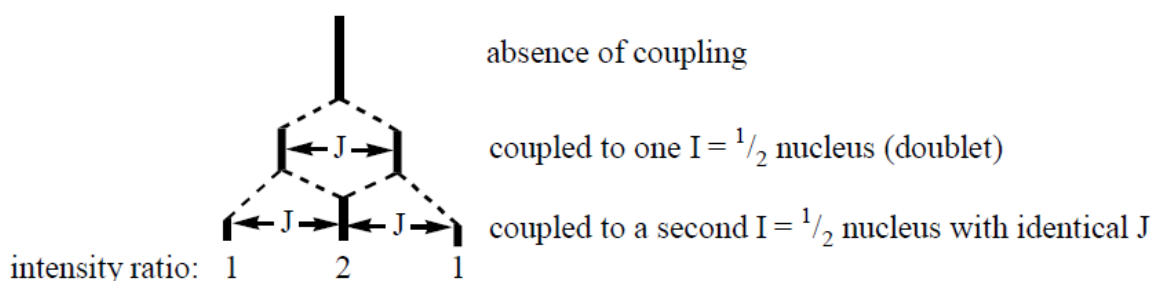
<sup>a</sup>Two bond couplings are particularly sensitive to the geometrical arrangement of the nuclei, which in some cases may render  ${}^2J_{AB} < {}^3J_{AB}$ . <sup>b</sup>Restricted to acyclic compounds.

Cases involving more than two nuclei with  $I = 1/2$  are direct extensions of the above. However, because there are more nuclear spins interacting, the pattern of lines observed in the NMR spectrum becomes more complicated. For example, let's consider the  ${}^1H$  NMR spectrum of the  $HF_2^-$  anion (i.e.,  $[F-H-F]^-$ ). We are observing the  ${}^1H$  nucleus, but it is coupled to two chemically equivalent  ${}^{19}F$  ( $I = 1/2$ ) nuclei. There are four ways that we can arrange the nuclear spins of the two fluorine nuclei, but only three different energy states are created, as is explained below

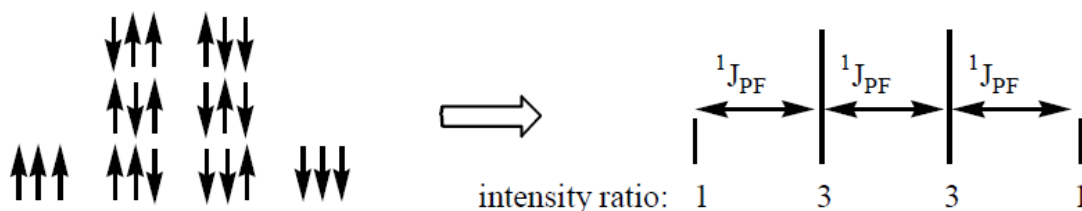


Extending what we learned about the generation of a doublet, we can clearly see that the  ${}^1H$  environment where both  ${}^{19}F$  spins are “up” is different from that where both  ${}^{19}F$  spins are “down”. However, we can also arrange things so that one  ${}^{19}F$  spin is “up” and the other is “down”. The latter case is degenerate; that is, there is more than one way of accomplishing an

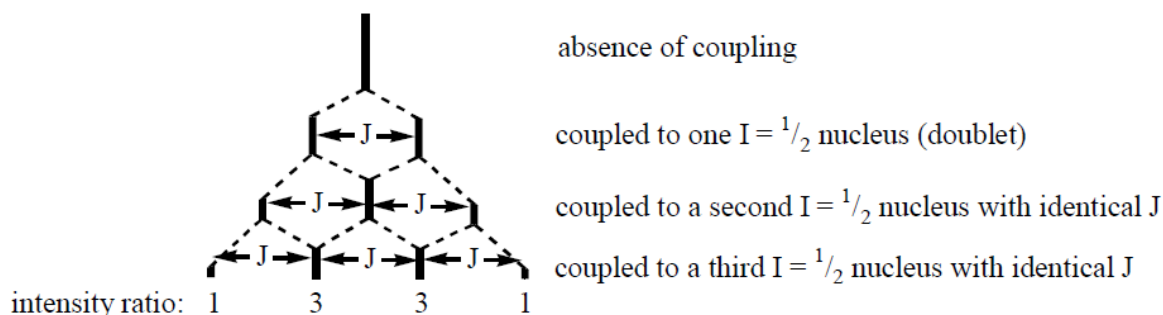
“up/down” arrangement of nuclei, but each “up/down” arrangement has the same energy. As a result, a pattern of three peaks (or triplet) with an intensity pattern of 1:2:1 is generated as shown above. It is important to note that each line in the triplet is separated by the same  $^1J_{\text{HF}}$  coupling constant. As we would expect, the  $^{19}\text{F}$  NMR spectrum of  $[\text{HF}_2]^-$  would show a doublet because the fluorine nuclei are chemically equivalent and couple to one  $^1\text{H}$  nucleus. Another way of looking at this is to begin with a singlet for the  $^1\text{H}$  nucleus and then couple each  $^{19}\text{F}$  nucleus one step at a time. The coupling of the first  $^{19}\text{F}$  nucleus generates a doublet. When each line in this doublet is split again into a doublet, they overlap identically at the centre of the signal, generating a single line of intensity two relative to each outer line of intensity one.



When a similar exercise is undertaken for the  $^{31}\text{P}$  NMR spectrum of  $\text{PF}_3$ , the nuclear spins of the three equivalent  $^{19}\text{F}$  nuclei can be arranged in four ways to generate a quartet



or we can split a singlet into doublets three times to accomplish the same transformation.



In this case, when each line at the triplet stage is split again into doublets, the intensity of the overlapping peaks is not identical; a signal of relative intensity two (from the middle peak) overlaps with a signal of intensity one (from the outer peak) to create a peak of intensity three.

Fortunately, the pattern of peaks generated by the interaction of  $I = 1/2$  nuclei can be easily generated by remembering that one nucleus is split by ( $n$ ) equivalent nuclei into ( $n+1$ ) peaks, each separated by the coupling constant,  $^xJ_{AB}$ . The number of peaks is referred as the multiplicity. The intensity pattern is a direct consequence of the number of combinations of the various nuclear spins that are possible and is described by a series of binomial coefficients. In practice, it is easiest to determine the intensity pattern by use of a mnemonic device such as Pascal's triangle.

$n$	$n+1$	Intensity	Multiplicity	Pattern	Example
0	1	1	singlet (s)		$CH_4$
1	2	1 : 1	doublet (d)		$(CH_3)_2CHCl$
2	3	1 : 2 : 1	triplet (t)		$CH_3CH_2Cl$
3	4	1 : 3 : 3 : 1	quartet (q)		$CH_3CH_2Cl$
4	5	1 : 4 : 6 : 4 : 1	quintet		$^{29}SiF_4$
5	6	1 : 5 : 10 : 10 : 5 : 1	sextet		$PF_5^*$
6	7	1 : 6 : 15 : 20 : 15 : 6 : 1	septet		$(CH_3)_2CHCl$

etc.

### 7.9 $^{31}P$ NMR spectroscopy

$^{31}P$  NMR spectroscopy is a simple technique that can be used alongside  $^1H$  NMR to characterize phosphorus-containing compounds. When used on its own, the biggest difference from  $^1H$  NMR is that there is no need to utilize deuterated solvents. This advantage leads to many different applications of  $^{31}P$  NMR, such as assaying purity and monitoring reactions.

Phosphorus-31 nuclear magnetic resonance ( $^{31}P$  NMR) is conceptually the same as proton ( $^1H$ ) NMR. The  $^{31}P$  nucleus is useful in NMR spectroscopy due to its relatively high gyromagnetic ratio ( $17.235 \text{ MHz T}^{-1}$ ). For comparison, the gyromagnetic ratios of  $^1H$  and  $^{13}C$  are ( $42.576 \text{ MHz T}^{-1}$ ) and ( $10.705 \text{ MHz T}^{-1}$ ), respectively. Furthermore,  $^{31}P$  has a 100% natural isotopic abundance. Like the  $^1H$  nucleus, the  $^{31}P$  nucleus has a nuclear spin of  $1/2$  which makes spectra relatively easy to interpret.  $^{31}P$  NMR is an excellent technique for studying phosphorus containing compounds, such as organic compounds and metal coordination complexes.

#### 7.9.1 Differences between $^1H$ and $^{31}P$ NMR

There are certain significant differences between  $^1H$  and  $^{31}P$  NMR. While  $^1H$  NMR spectra is referenced to tetramethylsilane [ $Si(CH_3)_4$ ], the chemical shifts in  $^{31}P$  NMR are typically

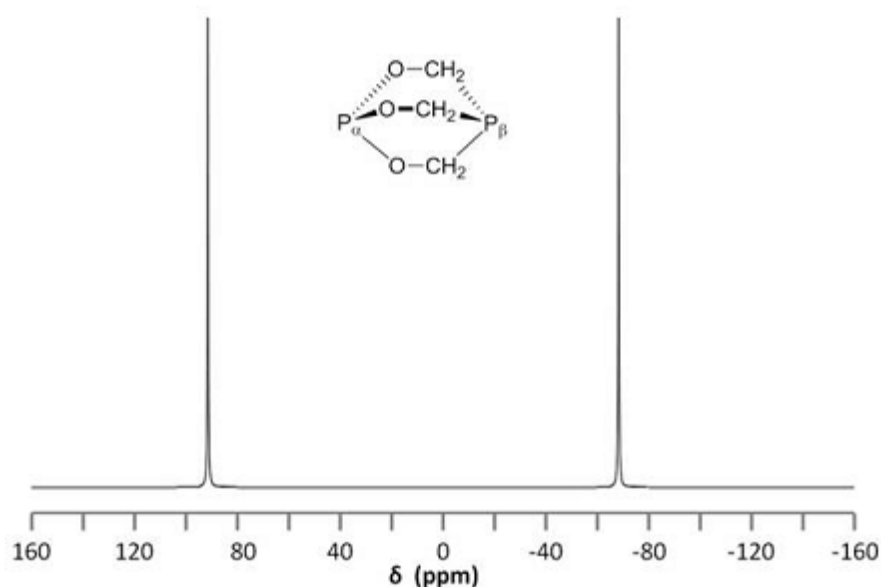
reported relative to 85% phosphoric acid ( $\delta = 0$  ppm), which is used as an external standard due to its reactivity. Trimethylphosphite,  $\text{P}(\text{OCH}_3)_3$ , is also used since unlike phosphoric acid its shift ( $\delta = 140$  ppm) is not dependent on concentration or pH. Chemical shifts in  $^{31}\text{P}$  NMR commonly depend on the concentration of the sample, the solvent used, and the presence of other compounds. This is because the external standard does not take into account the bulk properties of the sample. As a result, reported chemical shifts for the same compound could vary by 1 ppm or more, especially for phosphate groups ( $\text{P}=\text{O}$ ).  $^{31}\text{P}$ -NMR spectra are often recorded with all proton signals decoupled, i.e.,  $^{31}\text{P}\{-^1\text{H}\}$ , as is done with  $^{13}\text{C}$  NMR. This gives rise to single, sharp signals per unique  $^{31}\text{P}$  nucleus.

### 7.9.2 Interpreting spectra

As in  $^1\text{H}$ -NMR, phosphorus signals occur at different frequencies depending on the electron environment of each phosphorus nucleus. In this section we will study a few examples of phosphorus compounds with varying chemical shifts and coupling to other nuclei.

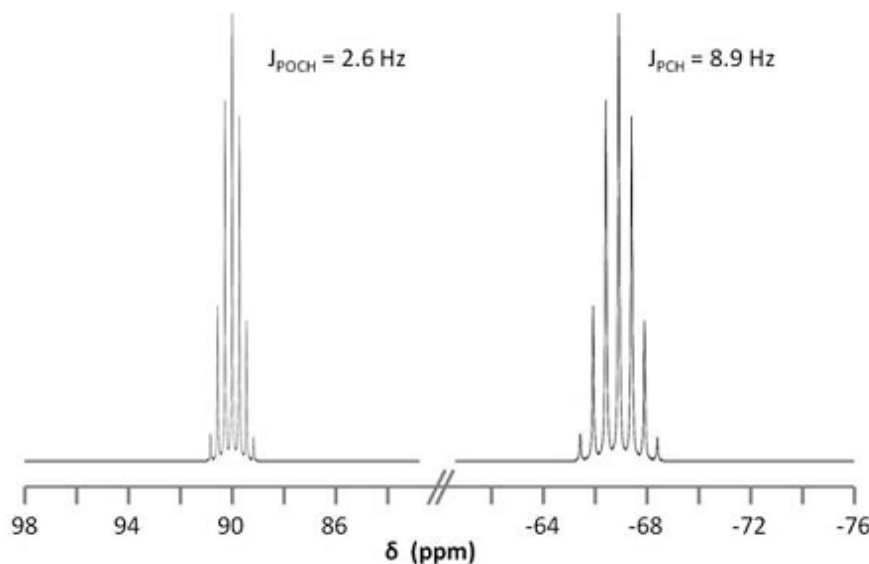
### 7.9.3 Different phosphorus environments and their coupling to $^1\text{H}$

Consider the structure of 2,6,7-trioxa-1,4-diphosbicyclo[2.2.2]octane [ $\text{P}_\alpha(\text{OCH}_2)_3\text{P}_\beta$ ] shown in below figure. The subscripts  $\alpha$  and  $\beta$  are used to differentiate the two phosphorus nuclei. According to Table 1, we expect the shift of  $\text{P}_\alpha$  to be downfield of the phosphoric acid standard, roughly around 125 ppm to 140 ppm and the shift of  $\text{P}_\beta$  to be up field of the standard, between -5 ppm and -70 ppm. In the decoupled spectrum shown in Figure 1, we can assign the phosphorus shift at 90.0 ppm to  $\text{P}_\alpha$  and the shift at -67.0 ppm to  $\text{P}_\beta$ .



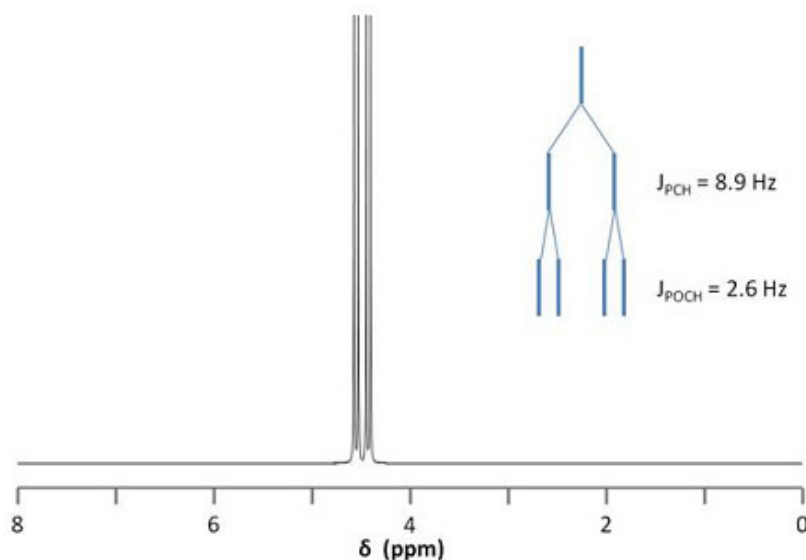
**Figure 1:** Structure and decoupled  $^{31}\text{P}$  spectrum ( $^{31}\text{P}\{-^1\text{H}\}$ ) of  $\text{P}_\alpha(\text{OCH}_2)_3\text{P}_\beta$ .

Figure 2 shows the coupling of the phosphorus signals to the protons in the compound. We expect a stronger coupling for  $P_\beta$  because there are only two bonds separating  $P_\beta$  from H, whereas three bonds separate  $P_\alpha$  from H ( $J_{PCH} > J_{POCH}$ ). Indeed,  $J_{PCH} = 8.9$  Hz and  $J_{POCH} = 2.6$  Hz, corroborating our peak assignments above.



**Figure 2:** The  $^{31}\text{P}$  spin coupled spectrum of  $\text{P}_\alpha(\text{OCH}_2)_3\text{P}_\beta$ .

Finally, Figure 3 shows the  $^1\text{H}$  spectrum of  $\text{P}_\alpha(\text{OCH}_2)_3\text{P}_\beta$  (Figure 5), which shows a doublet of doublets for the proton signal due to coupling to the two phosphorus nuclei.



**Figure 3:**  $^1\text{H}$  spectrum of  $\text{P}_\alpha(\text{OCH}_2)_3\text{P}_\beta$  and proton splitting pattern due to phosphorus.

As suggested by the data in Figure 1 we can predict and observe changes in phosphorus chemical shift by changing the coordination of P. Thus for the series of compounds with the

different chemical shifts corresponding to different phosphorus in compound is shown in Table 5.

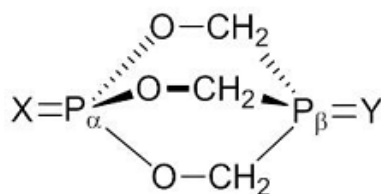


**Table 5:** Different chemical shifts corresponding to different phosphorus in the same compound

X	Y	$P_{\alpha}$ chemical shift (ppm)	$P_{\beta}$ chemical shift (ppm)
-	-	90.0	-67.0
O	O	-18.1	6.4
S	-	51.8	-70.6

#### 7.9.4 $^{31}\text{P}$ - $^1\text{H}$ coupling

Consider the structure of dimethyl phosphonate,  $\text{OPH}(\text{OCH}_3)_2$ , shown in Figure 4. As the phosphorus nucleus is coupled to a hydrogen nucleus bound directly to it, that is, a coupling separated by a single bond, we expect  $J_{\text{PH}}$  to be very high. Indeed, the separation is so large (715 Hz) that one could easily mistake the split peak for two peaks corresponding to two different phosphorus nuclei.

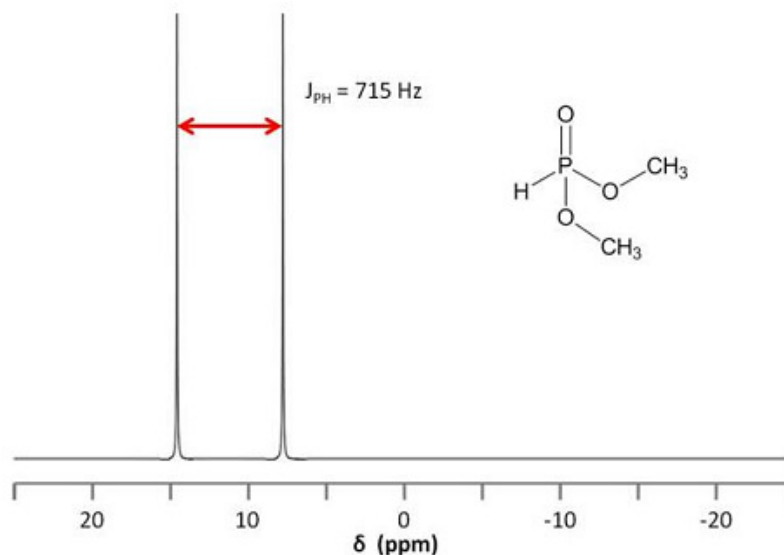


**Figure 4:**  $J_{\text{PH}}$  of phosphorus nucleus coupled to a hydrogen bound directly to it

This strong coupling could also lead us astray when we consider the  $^1\text{H}$  NMR spectrum of dimethylphosphonate (Figure 5). Here we observe two very small peaks corresponding to the phosphine proton. The peaks are separated by such a large distance and are so small relative

to the methoxy doublet (ratio of 1:1:12), that it would be easy to confuse them for an impurity. To assign the small doublet, we could decouple the phosphorus signal at 11 ppm, which will cause this peak to collapse into a singlet.

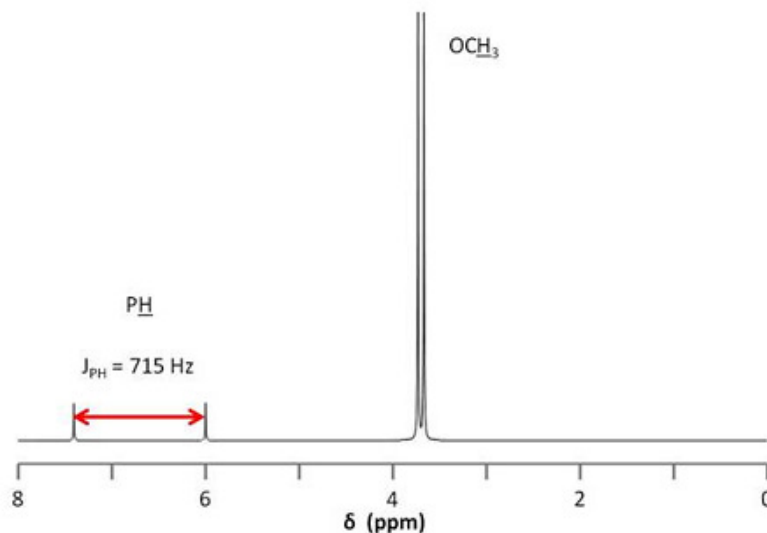


**Figure 5:**  $J_{PH}$  of phosphorus nucleus coupled to a hydrogen bound directly to it and separated by a large distance

### 7.9.5 Coupling to fluorine

<sup>19</sup>F NMR is very similar to <sup>31</sup>P NMR in that <sup>19</sup>F has spin 1/2 and is a 100% abundant isotope. As a result, <sup>19</sup>F NMR is a great technique for fluorine-containing compounds and allows observance of P-F coupling. The coupled <sup>31</sup>P and <sup>19</sup>F NMR spectra of ethoxybis(tri fluoromethyl)phosphine, P(CF<sub>3</sub>)<sub>2</sub>(OCH<sub>2</sub>CH<sub>3</sub>), are shown in Figure 6. It is worth noting the splitting due to  $J_{PCF} = 86.6$  Hz.

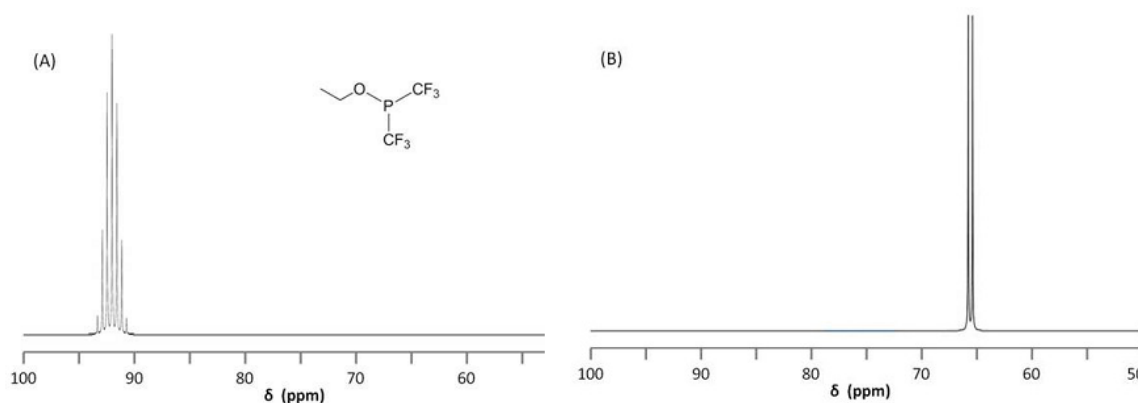


**Figure 6:** The coupled <sup>31</sup>P and <sup>19</sup>F NMR spectra of P(CF<sub>3</sub>)<sub>2</sub>(OCH<sub>2</sub>CH<sub>3</sub>),



### 7.9.6 $^{31}\text{P}$ NMR applications

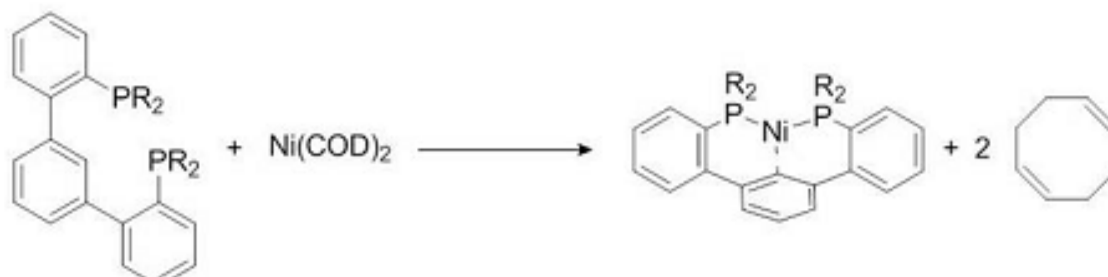
#### 1) Assaying sample purity

$^{31}\text{P}$  NMR spectroscopy gives rise to single sharp peaks that facilitate differentiating phosphorus-containing species, such as starting materials from products. For this reason,  $^{31}\text{P}$  NMR is a quick and simple technique for assaying sample purity. Beware, however, that a clean  $^{31}\text{P}$  spectrum does not necessarily suggest a pure compound, only a mixture free of phosphorus-containing contaminants.

$^{31}\text{P}$  NMR can also be used to determine the optical purity of a chiral sample. Adding an enantiomer to the chiral mixture to form two different diastereomers will give rise to two unique chemical shifts in the  $^{31}\text{P}$  spectrum. The ratio of these peaks can then be compared to determine optical purity.

#### 25) Monitoring reactions

As suggested in the previous section,  $^{31}\text{P}$  NMR can be used to monitor a reaction involving phosphorus compounds. Consider the reaction between a slight excess of organic diphosphine ligand and a nickel(0) bis-cyclooctadiene.



The reaction can be followed by  $^{31}\text{P}$  NMR by simply taking a small aliquot from the reaction mixture and adding it to an NMR tube, filtering as needed. The sample is then used to acquire a  $^{31}\text{P}$  NMR spectrum and the procedure can be repeated at different reaction times. The data acquired for these experiments is found in Figure 7. The changing in  $^{31}\text{P}$  peak intensity can be used to monitor the reaction, which begins with a single signal at  $-4.40$  ppm, corresponding to the free diphosphine ligand. After an hour, a new signal appears at  $41.05$  ppm, corresponding to the diphosphine nickel complex. The downfield peak grows as the reaction proceeds relative to the upfield peak. No change is observed between four and five hours, suggesting the conclusion of the reaction. There are a number of advantages for using  $^{31}\text{P}$  for reaction monitoring when available as compared to  $^1\text{H}$  NMR:

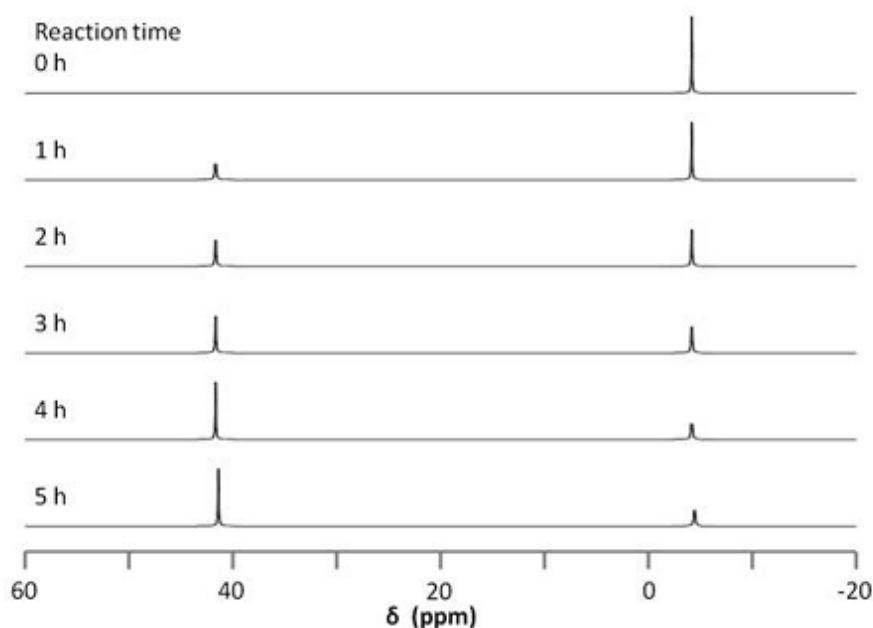


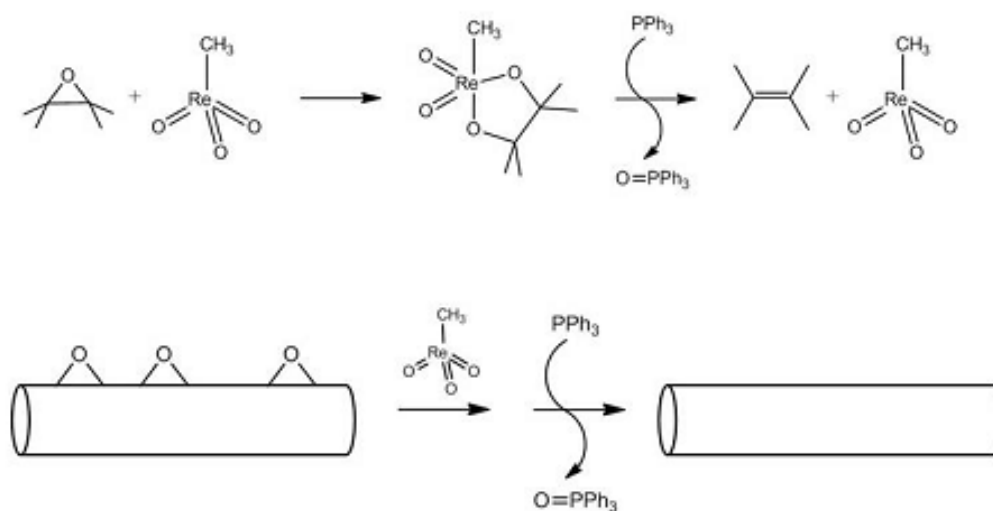
**Figure 7:**  $^{31}\text{P}$  NMR spectrum recorded at different reaction times

- There is no need for a deuterated solvent, which simplifies sample preparation and saves time and resources.
- The  $^{31}\text{P}$  spectrum is simple and can be analyzed quickly. The corresponding  $^1\text{H}$  NMR spectra for the above reaction would include a number of overlapping peaks for the two phosphorus species as well as peaks for both free and bound cyclooctadiene ligand.
- Purification of product is also easy assayed.

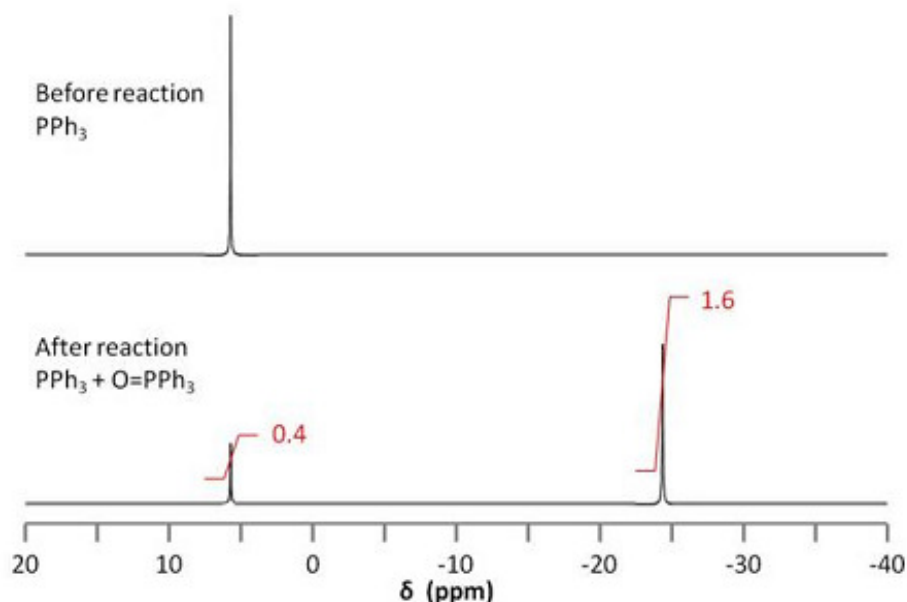
$^{31}\text{P}$  NMR does not eliminate the need for  $^1\text{H}$  NMR characterization, as impurities lacking phosphorus will not appear in a  $^{31}\text{P}$  experiment. However, at the completion of the reaction, both the crude and purified products can be easily analyzed by both  $^1\text{H}$  and  $^{31}\text{P}$  NMR spectroscopy.

#### 26) *Measuring epoxide content of carbon nanomaterials*

One can measure the amount of epoxide on nanomaterials such as carbon nanotubes and fullerenes by monitoring a reaction involving phosphorus compounds in a similar manner to that described above. This technique uses the catalytic reaction of methyltrioxorhenium. An epoxide reacts with methyltrioxorhenium to form a five membered ring. In the presence of triphenylphosphine ( $\text{PPh}_3$ ), the catalyst is regenerated, forming an alkene and triphenylphosphine oxide ( $\text{OPPh}_3$ ). The same reaction can be applied to carbon nanostructures and used to quantify the amount of epoxide on the nanomaterial. This way it is easy to illustrate the quantification of epoxide on a carbon nanotube.



Because the amount of initial PPh<sub>3</sub> used in the reaction is known, the relative amounts of PPh<sub>3</sub> and OPPh<sub>3</sub> can be used to stoichiometrically determine the amount of epoxide on the nanotube. <sup>31</sup>P NMR spectroscopy is used to determine the relative amounts of PPh<sub>3</sub> and OPPh<sub>3</sub>.



The integration of the two <sup>31</sup>P signals is used to quantify the amount of epoxide on the nanotube according to

$$\text{Moles of epoxide} = \frac{\text{area of OPPh}_3 \text{ peak}}{\text{area of PPh}_3 \text{ peak}} \times \text{moles PPh}_3$$

Thus, from a known quantity of PPh<sub>3</sub>, one can find the amount of OPPh<sub>3</sub> formed and relate it stoichiometrically to the amount of epoxide on the nanotube. Not only does this experiment allow for such quantification, it is also unaffected by the presence of the many different species present in the experiment. This is because the compounds of interest, PPh<sub>3</sub> and OPPh<sub>3</sub>, are the only ones that are characterized by <sup>31</sup>P NMR spectroscopy

## 7.10 $^{19}\text{F}$ NMR spectroscopy

$^{19}\text{F}$  NMR is similar to  $^1\text{H}$  NMR. After  $^1\text{H}$  and  $^{13}\text{C}$  NMR,  $^{19}\text{F}$  is the most common nucleus studied by this technique.  $^{19}\text{F}$  nuclei are spin  $\frac{1}{2}$  nuclei and have a high gyromagnetic ratio, which means that they have a high receptivity for NMR measurements. The  $^{19}\text{F}$  isotope has 100% natural abundance i.e.,  $^{19}\text{F}$  is the only naturally occurring isotope, giving high NMR sensitivity. The sensitivity is about 0.83 compared to H. The resonance frequency is slightly lower than  $^1\text{H}$  e.g. in the field of 1.4T  $^1\text{H}$  resonates at 60MHz,  $^{19}\text{F}$  resonates at 56.5MHz.

### 7.10.1 Chemical shift in $^{19}\text{F}$ NMR

$^{19}\text{F}$  chemical shift is more sensitive to solvent effects.  $\text{CFCl}_3$  is generally used as reference in  $^{19}\text{F}$  NMR (as TMS (Tetramethylsilane) is used in  $^1\text{H}$  NMR).  $\text{CFCl}_3$  is inert, volatile and gives rise to a sharp singlet. Figure 8 shows the  $^1\text{H}$  and  $^{19}\text{F}$  spectra of trifluorotoluene (TFT)

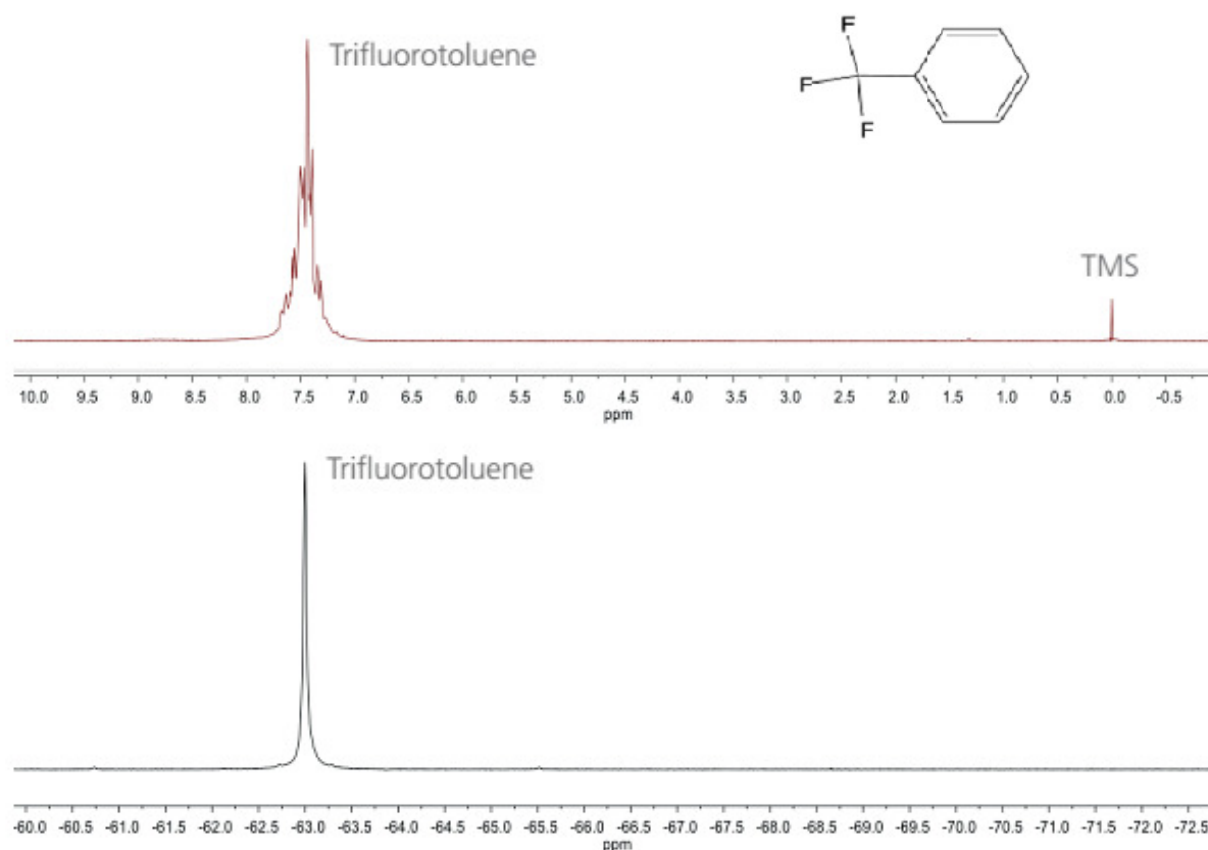


**Figure 8:**  $^1\text{H}$  (top) and  $^{19}\text{F}$  (bottom) spectra of trifluorotoluene

The chemical shift values span in wider range from 0 to 900ppm. The chemical shifts are sensitive to electronegativity, oxidation state and stereochemistry of the neighboring groups. For example, the chemical shift of equatorial and axial F's of  $\text{ClF}_3$  differ by 120 ppm. Ethyl and methyl F's differ by 60 ppm

For example,  $(\text{CH}_3)_2\text{PF}_3$  is a trigonal bipyramidal structure compound. The NMR spectra suggested that ( $J_{\text{P-F}} = 170 \text{ Hz}$ ) two methyl groups are equatorial and more electronegative groups are at apical positions.

Similarly in the  $(\text{CF}_3)_2\text{PF}_3$  compound, at low temperature NMR shows that two  $\text{CF}_3$  groups are apical position and at room temperature due to rapid exchange only one signal is appears.

For  $\text{BrF}_5$  molecule  $^{19}\text{F}$  NMR shows two peaks, one doublet and one quintet with intensity ration (1:4) this suggest that 4F atoms are equivalent and one is a different type. This is consistent with the assigned square pyramidal structure.

The  $^{19}\text{F}$  spectrum, shown in figure 3, consists of a single peak since the three F nuclei are in an equivalent chemical environment and are not in close proximity to any of the H nuclei in the molecule. The  $^1\text{H}$  spectrum is more complex since the H nuclei on the aromatic ring are not equivalent and the homonuclear couplings give rise to splitting of the aromatic peak.

The spectrum shown in Figure 9 is a mixture of two fluorinecontaining chemicals; Trifluorotoluene and trifluoroethanol. Trifluorotoluene (TFT) is often used as a reference material for  $^{19}\text{F}$  spectra. It appears as a strong, single peak with a chemical shift  $-63.72 \text{ ppm}$  with  $\text{CFCl}_3$  set at  $0 \text{ ppm}$ . It is a single peak as the structure consists of three equivalent F nuclei isolated from any other nuclei that would couple to it. By comparison the peak in the spectrum due to trifluoroethanol, at  $-77 \text{ ppm}$ , is split into a triplet. This is due to the fact that the  $^{19}\text{F}$  nuclei couples with the  $^1\text{H}$  nuclei on neighbouring carbon atoms in the molecule, just as  $^1\text{H}$  nuclei would couple with other neighbouring  $^1\text{H}$  nuclei in the molecule.

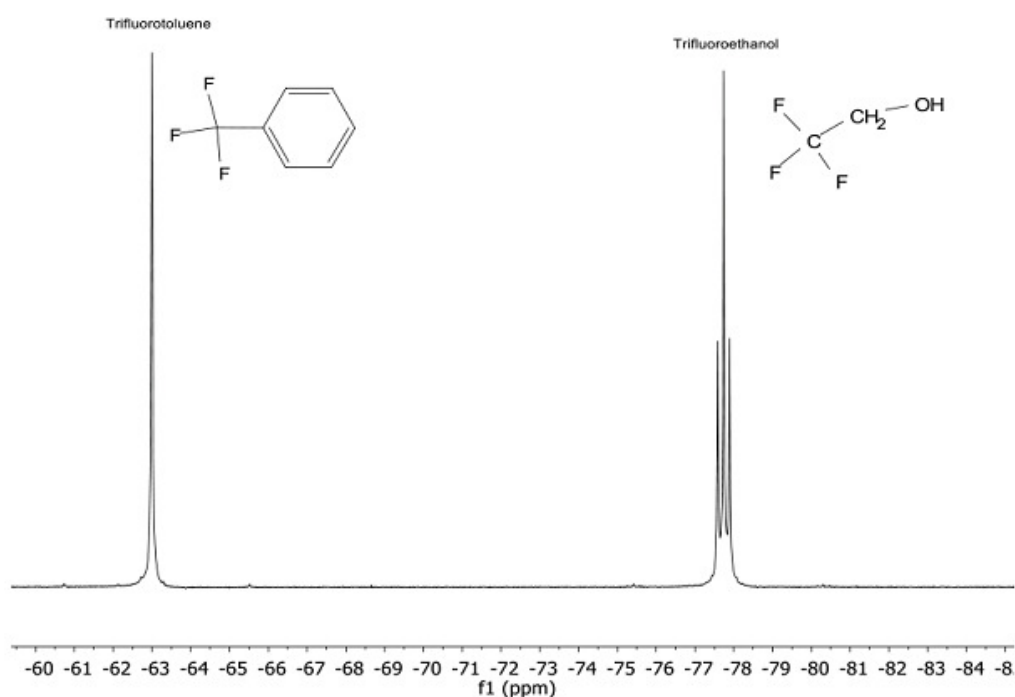


**Figure 9:**  $^{19}\text{F}$  spectrum of a mixture of trifluorotoluene and trifluoroethanol

Each of these resonances shows a complex coupling pattern due to the nuclei on the aromatic ring. Most easily recognisable is the triplet of triplet pattern at -162 ppm, arising because the fluorine at position 2 is coupled to two equivalent fluorines and two equivalent hydrogens. Any coupling between the fluorine and the bromine is too weak to be resolved in the spectrum. Finally, a comparison has been made of the  $^{19}\text{F}$  spectra of two different positional isomers of bromotrifluorobenzene. Figure 4 shows the  $^{19}\text{F}$  spectra of 5-bromo-1,2,3-trifluorobenzene and 1-bromo-2,4,5-trifluorobenzene. In contrast to the spectrum of 5-bromo-1,2,3-trifluorobenzene, the spectrum of 1-bromo-2,4,5-trifluorobenzene shows three  $^{19}\text{F}$  resonances because each of the fluorines on the ring are in different chemical environments. They all show complex coupling patterns since each has two different fluorines and two different hydrogens and potentially a bromine as coupled neighbours.

Figure 10 shows the  $^1\text{H}$  and  $^{19}\text{F}$  spectra of 5-Bromo-1,2,3-trifluorobenzene. The  $^1\text{H}$  spectrum consists of a single multiplet of peaks resulting from the two equivalent  $^1\text{H}$  nuclei and their couplings with,  $^{19}\text{F}$  and  $^{79}\text{Br}$  and  $^{81}\text{Br}$  nuclei within the molecule. The  $^{19}\text{F}$  spectrum consists of two resonances, each of which are multiplets due to the two different chemical environments of the  $^{19}\text{F}$  nuclei.

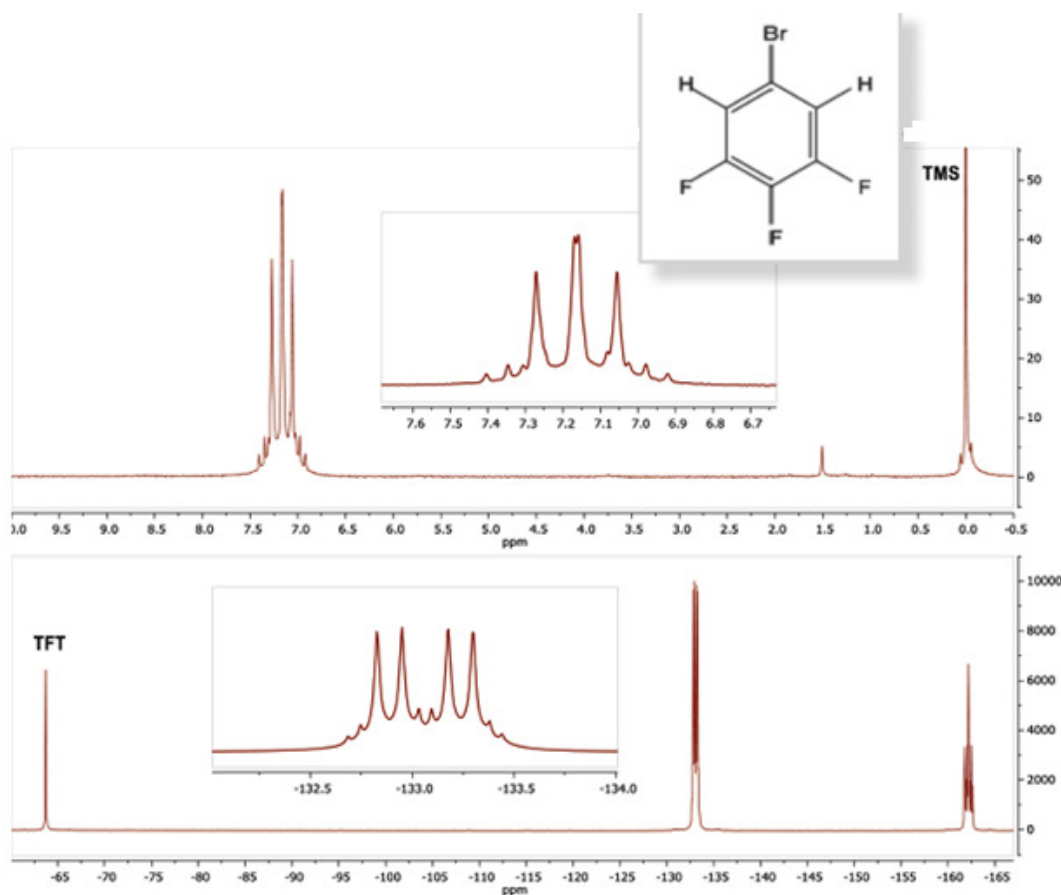


**Figure 10:**  $^1\text{H}$  and  $^{19}\text{F}$  spectra of 5-Bromo-1,2,3-trifluorobenzene

The resonance at  $\sim -133$  ppm arises from the fluorines in positions 1 and 3 on the molecule while the resonance at  $-162$  ppm arises from the fluorine in position 2.

Each of these resonances shows a complex coupling pattern due to the other nuclei on the aromatic ring. Most easily recognisable is the triplet of triplet pattern at  $-162$  ppm, arising because the fluorine at position 2 is coupled to two equivalent fluorines and two equivalent hydrogens. Any coupling between the fluorine and the bromine is too weak to be resolved in the spectrum.

Finally, a comparison has been made of the  $^{19}\text{F}$  spectra of two different positional isomers of bromotrifluorobenzene. Figure 6 shows the  $^{19}\text{F}$  spectra of 5-bromo-1,2,3-trifluorobenzene and 1-bromo-2,4,5-trifluorobenzene. In contrast to the spectrum of 5-bromo-1,2,3-trifluorobenzene, the spectrum of 1-bromo-2,4,5-trifluorobenzene shows three  $^{19}\text{F}$  resonances because each of the fluorines on the ring are in different chemical environments. They all show complex coupling patterns since each has two different fluorines and two different hydrogens and potentially a bromine as coupled neighbours.

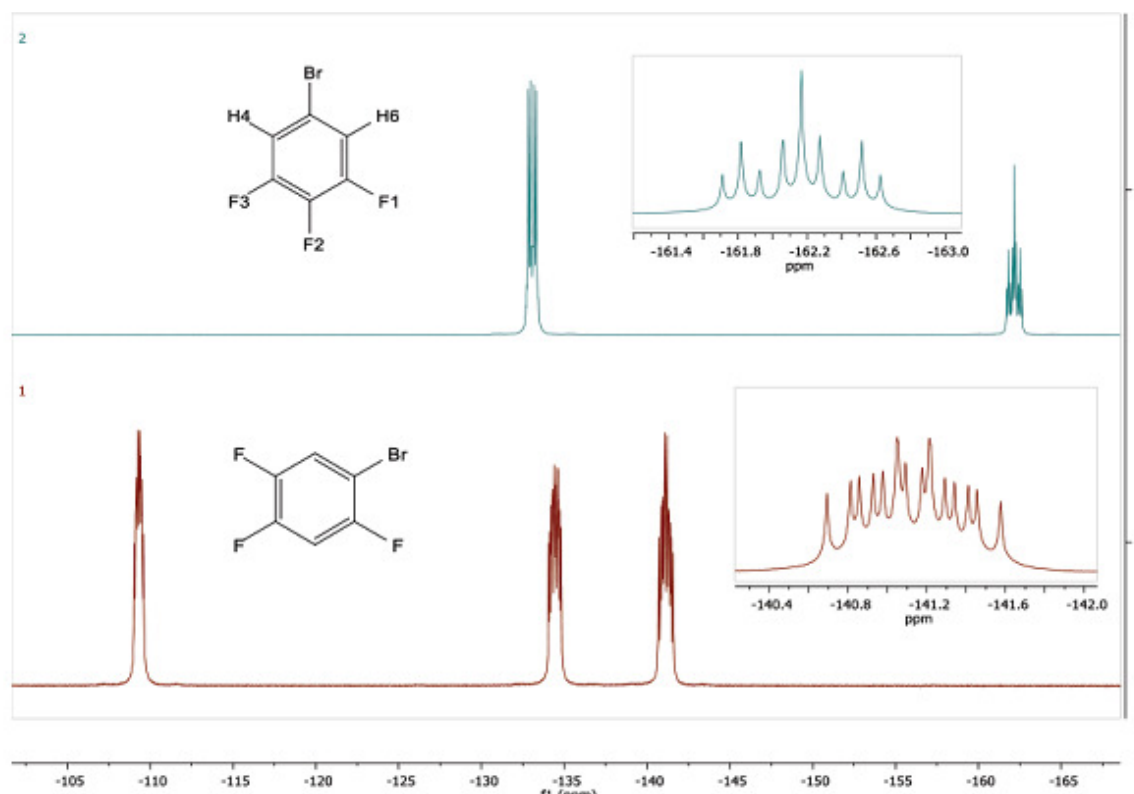


**Figure 11 :**  $^{19}\text{F}$  spectra of 5-bromo-1,2,3-trifluorobenzene (top) and 1-bromo-2,4,5-trifluorobenzene

The case of  $\text{PF}_5$ , The structure of  $\text{PF}_5$  has been found to be trigonal bipyramidal as shown in Figure 12. The trigonal bipyramidal polyhedron has two distinct sites, the axial site and the

equatorial site. The  $^{19}\text{F}$  NMR spectrum of this compound shows a doublet with the separation between the lines corresponding to the coupling constant  $J(\text{P-F})$ .

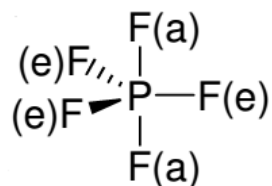


**Figure 12:** structure of  $\text{PF}_5$

However, for a trigonal bipyramidal structure we anticipate a more complex pattern as the axial fluorine atoms belong to one chemically equivalent set and the equatorial fluorines belong to another chemically equivalent set. Therefore the spectrum should have been more complicated as shown in Figure 13.

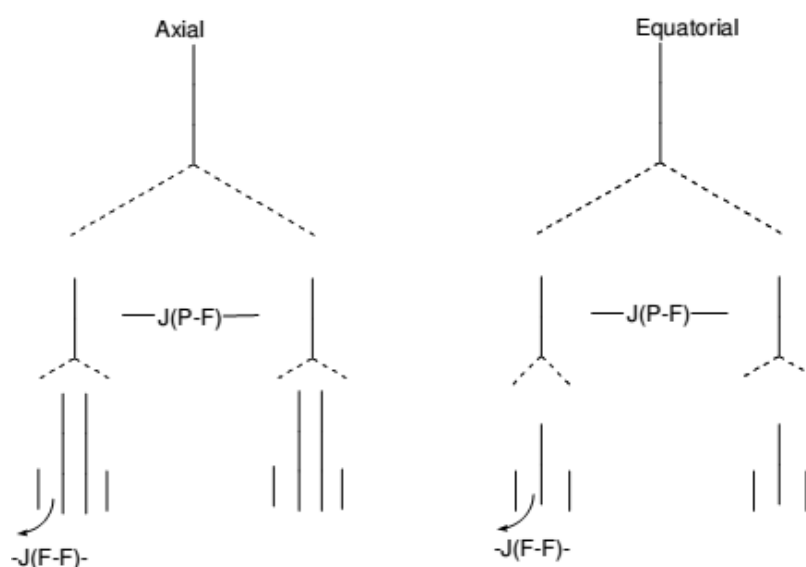
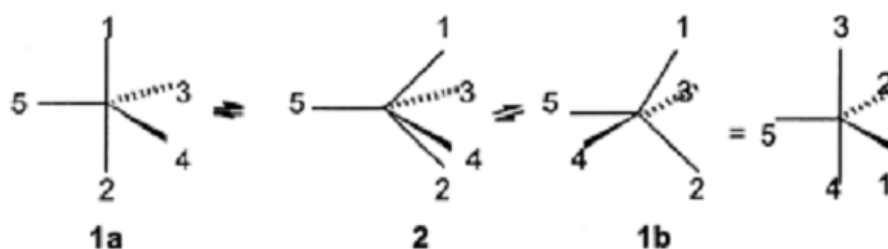


**Figure 13:** Anticipated spectrum for trigonal bipyramidal structure of  $\text{PF}_5$

The question is why is only a doublet seen?

The answer lies in the fact that the molecule is stereochemically non-rigid and is continuously changing its structure. This is known as fluxional behaviour. The mechanism that accounts for the behaviour of  $\text{PF}_5$  is known as Berry Pseudo Rotation and is shown below. In structure 1a the angle  $\text{F}_1\text{-P-F}_2$  is  $180^\circ$  and the  $\text{F}_3\text{-P-F}_4$  angle is  $120^\circ$ .





Imagine that the former is shrinking and the latter is expanding so that both the angles become nearly equal and structure 2, a square pyramid, is obtained. If this process is continued further such that the former  $F_1-P-F_2$  angle now becomes  $120^\circ$  and the former  $F_3-P-F_4$  angle becomes  $180^\circ$  we get the second trigonal bipyramidal structure 1b. Thus in reaching 1b from 1a through 2, we have essentially exchanged a pair of axial fluorine atoms with a set of equatorial fluorine atoms without breaking any bonds. In this whole process one  $PF_5$  does not change. If this process takes place faster than the NMR time scale in the NMR experiment only one set of fluorines is seen.

For the majority of five-coordinate main-group and transition metal compounds, the energy difference between the trigonal bipyramid (1) and tetragonal pyramid (2) structures is sufficiently low, so that Berry pseudorotation represents a widespread mechanism of stereochemical nonrigidity. No angular momentum is generated by this motion, this is the reason for the term. Important to note here that we single out one interchange path here, while in reality all atoms will rapidly occupy all possible positions in a very dynamic way.

Having bulky substituents such as chlorine or substituents that do not prefer to occupy axial positions can slow this process down. Accordingly in  $PCl_2F_3$ , although at room temperature all the fluorine atoms are still equivalent and only a doublet is seen in the fluorine NMR spectrum, at  $-143^\circ C$  the exchange is stopped and one sees two sets of peaks as shown in Figure 14(a doublet of doublet for the two axial fluorine atoms and a doublet of triplets for the equatorial fluorine atom).

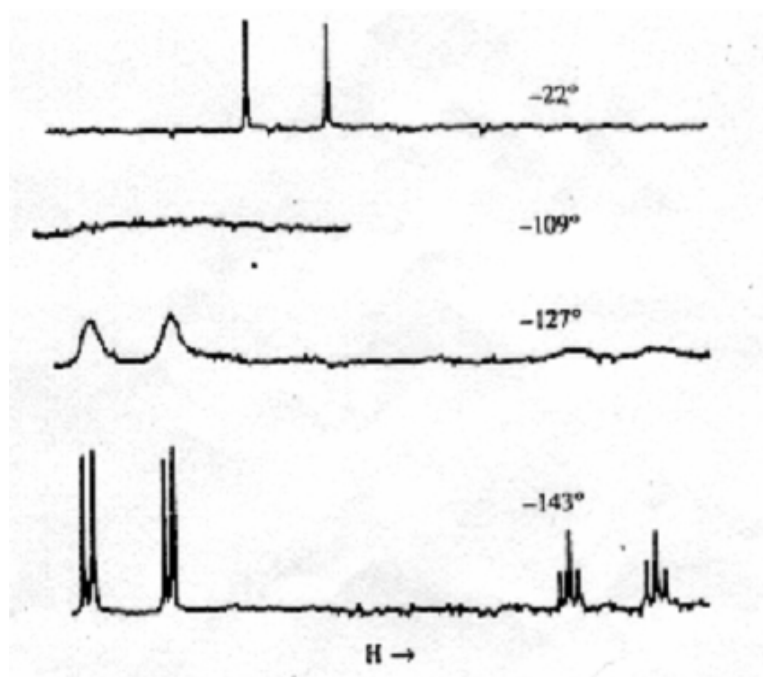


**Figure 14:**  $^{19}F$  NMR spectrum of  $PCl_2F_3$  molecule at different temperature

At temperature of  $-22^{\circ}\text{C}$  and above, the resonance of F is observed as a single doublet ( $^{31}\text{P}$ - $^{19}\text{F}$  coupling, 1048 Hz). However, as the temperature is lowered to  $-143^{\circ}\text{C}$ , a downfield doublet ( $\delta -67.4$ ) for the axial F atoms and an upfield doublet ( $\delta 41.5$ ) for the equatorial F atom. The single equatorial F atom is further split by the two axial F atoms ( $2nI+1$ ;  $n = 2$ ;  $J_{\text{F-F}} = 124$  Hz) into two triplets. The two axial F atoms is split into doublet by the single equatorial F atom ( $2nI+1$ ;  $n = 2$ ;  $J_{\text{F-F}} = 124$  Hz).

Also, the weighted average of the chemical shifts at  $-143^{\circ}\text{C}$   $\{2x(-67.4 \text{ ppm}) + 1x(41.5 \text{ ppm})\}$  is the same as that at  $-22^{\circ}\text{C}$   $\{3 \times (-31.1 \text{ ppm})\}$  indicating that the structure does not change on warming even though the F atoms exchanges positions.

### 7.11 Boron NMR spectroscopy

Boron is second only to carbon in its ability to bond to itself to form polyboron units. Boron has two naturally occurring NMR active nuclei. Both nuclei have spins of greater than  $\frac{1}{2}$  and are quadrupolar.  $^{11}\text{B}$  has a spin of  $3/2$  and  $^{10}\text{B}$  is spin 3.  $^{11}\text{B}$  is the better nucleus in all respects, having the lower quadrupole moment and being more sensitive. Both nuclei have the same wide chemical shift range. Each type of signal has a characteristic chemical shift range which is the same for both nuclei. In the immense field of chemistry,  $^{11}\text{B}$  NMR spectroscopy has been found to be the most economical, fastest, and most reliable method for the determination of structures of compounds with boron skeletons.

The informative value of  $^{11}\text{B}$  chemical shifts is very high for two reasons

- i) It helps significantly to analyze not only structures but also the centre of equilibrium in fluxional molecules, and
- ii) It can provide additional and significant insight into the distribution of valence-bond electrons in some fragments of a given molecule or/and in individual atomic orbitals, which is important for understanding both physical and chemical behaviour.

In many cases, analyses of individual  $^{11}\text{B}$  spectra from this point of view have indicated unexpected deviations that called for explanation. In this way, some new principles dominating the behaviour of B-cluster compounds have been revealed.

Both naturally occurring isotopes,  $^{10}\text{B}$  and  $^{11}\text{B}$ , are NMR active but the latter one is more advantageous for NMR investigations. The success of  $^{11}\text{B}$  NMR spectroscopy stems from several favourable factors

1. Strong signal of the  $^{11}\text{B}$  nucleus (0.133, i.e. 16% of the relative receptivity to  $^1\text{H}$ , or 754 relative to  $^{13}\text{C}$ ) and 80.4% natural abundance.
2. Resonance at relatively high frequency (32.1 MHz at 2.3 T, i.e. 100 MHz for  $^1\text{H}$ ).

3. Relative sensitivity of the  $^{11}\text{B}$  nucleus to different perturbations (bonding strains, substituents, heteroatoms, etc.).
4. In most cases a sufficient spectrum span in compounds with borane skeletons (Figure 1).
5. Optimum B-H coupling (BH, 120-190 Hz;  $\text{BH}_2$ , 110-130 Hz;  $\text{BH}_3$ , 90-110 Hz;  $\text{BH}_4$ , 70-80 Hz;  $\mu\text{H}$ , 5-60 Hz).
6. An acceptable width at half height of peaks (2-100 Hz, usually 30-60 Hz). Of the peak width, only a small part must be attributed to the influence of electric quadrupole moment (1-20 Hz), while further widening is due to the interactions of  $^{11}\text{B}$  with bridge hydrogens, the B---H long-range coupling (ca. 0-5 Hz), the  $^{11}\text{B}$ - $^{11}\text{B}$  (intramolecular, 5-40 Hz; exo-two-electron B-B bonds, 50-150 Hz), and  $^{11}\text{B}$ - $^{10}\text{B}$  couplings (ca. 3 times lower than the former one).
7. Short relaxation times of  $^{11}\text{B}$  nuclei (1-100 ms, commonly 10-50 ms, exceptionally a few seconds).

In contrast, the  $^{10}\text{B}$  nucleus is present in low natural abundance (19.58%), exhibits a low receptivity (22.1 relative to  $^{13}\text{C}$ ), and has 3 times higher quadrupole moment, which broadens its NMR signals.  $^{10}\text{B}$  is found at a lower resonance frequency on a given instrument (10.75 MHz in comparison with 32.08 MHz for  $^{11}\text{B}$ ). This results in 2.99 times lower resolution and coupling constants (in Hz). Despite these disadvantages, the measurement of  $^{10}\text{B}$  NMR spectra is exceptionally helpful in selected mechanistic studies including rearrangements and other reactions.

The introduction of higher magnetic fields and, especially, the progress in computational and programming techniques make it possible to obtain the following kinds of informations

- 1) The number of different types of boron atoms, their mutual ratios within a molecule, and the chemical shift of each signal (from  $^{11}\text{B}$  proton decoupled spec-)  $\delta(^{11}\text{B})$  relative to  $\text{BF}_3\cdot\text{OEt} = 0$  ppm with the '+' sign for signals at lower magnetic field, i.e. at higher frequencies;  $\delta(^{11}\text{B}) \text{B}(\text{OMe})_3 = 18.1$  ppm.
- 2) The number of terminal hydrogens on each boron atom, the position of each substituent, and the splitting or broadening of relevant signals by hydrogen bridges if present (via the comparison of undecoupled spectra with proton decoupled  $^{11}\text{B}$  spectra of equivalent intensity).
- 3) The number of terminal H(B) and H(C) and bridge hydrogens (from  $^1\text{H}$  or  $^1\text{H}(^{11}\text{B})$  spectra).
- 4) The number of different C atoms in the molecule, their mutual ratios, and the number of hydrogen atoms they bear (from  $^{13}\text{C}$  NMR spectra).

- 5) The structure of boron networks and the assignment of individual signals (from  $^{11}\text{B}$ - $^{11}\text{B}$ ( $^1\text{H}$ ) 2D COSY spectra).
- 6) The assignments of all H signals (from selective  $^1\text{H}$ ( $^{11}\text{B}$ ) spectra or from  $^1\text{H}$ - $^{11}\text{B}$ ( $^1\text{H}$ ) 2D spectra).
- 7) The presence of B-C links (from  $^{13}\text{C}$  NMR spectra decoupled by frequencies of individual B atoms).
- 8) The presence of fragments with H-B-C-H links (from  $^{11}\text{B}$ -decoupled  $^1\text{H}$ - $^1\text{H}$  2D spectra).
- 9) A relatively high  $J(^{11}\text{B}$ - $^1\text{H})$  of a  $\text{B}^*$  signal indicates a connection of the observed  $\text{B}^*$  atom with an adjacent heteroatom such as S.
- 10) The magnitude of electric field gradients around various B atoms (from high and low  $T_1$  of appropriate signals).

Practically all of this information can be obtained on commercially available FT spectrometers; the information under items 3,6,7, and 8 is obtained when using an inverse probe. An excellent tool for the elucidation of the skeletal connectivity is  $^{11}\text{B}$ - $^{11}\text{B}$  and  $^1\text{H}$ - $^1\text{H}$  2D NMR spectroscopy. This method is not a panacea in all cases. It fails to determine reliable structures in the following cases

- a) Symmetrical compounds in which the symmetry causes an insufficient number of cross-peaks to be observed.
- b) Missing cross-peak(s).
- c) A reduced number of cross-peaks due to overlapping signals.
- d) Heteroboranes, since these spectra do not provide information on the links of boron to the heteroatom(s).

### 7.11.1 Chemical Shift

The most informative characteristic of an NMR-active nucleus is its chemical shift which reflects

- 1) Its bonding surroundings, i.e. coordination, hybridization, bond angles,  $\pi$ -bonding, etc.
- 2) The charges on individual atoms originating from their positions in the skeleton, inductive, and mesomeric effects of terminal substituents, electronegativity of skeletal heteroatoms, etc.
- 3) The magnetic anisotropy of neighboring groups, i.e. the effect of heavy nuclei, "ring current", etc.

Hybridization is one of the most important factors influencing the chemical shift. This is well documented in compounds of carbon ( $^{13}\text{C}$  NMR), with which a change from  $sp^3$  to  $sp^2$  hybridization causes a shift of ca. 100 ppm to lower frequencies. A similar shift dependence

can also be observed for the  $^{11}\text{B}$  nucleus. In contrast to carbon, boron can form stable tricoordinated compounds  $\text{BX}_3$ , showing the  $\text{sp}^2$  arrangement of substituents. In the case that substituents X do not bear a free electron pair (e.g.  $\text{X} = \text{H}, \text{R}$ ), the fourth orbital can remain unoccupied (vacant), which results in a great "imbalance" of bonding electrons around the  $^{11}\text{B}$  nucleus and, consequently, a large shift to high frequency (-120 ppm).

In contrast, the same substituents in the tetraordinated anions  $\text{BX}_4^-$  exhibit a very symmetrical arrangement, i.e. the paramagnetic contribution vanishes, which results in minimum deshielding originating from this very important factor. The  $^{11}\text{B}$  chemical shift of  $\text{BX}_4^-$  anions depend therefore primarily on the shielding quality of substituents R lacking a free electron pair.

On the other hand, substituents possessing a free electron pair can interact with the unoccupied boron orbital, decreasing the "imbalance", i.e. lowering the "deshielding". The stronger the  $\text{p}-\pi$  interaction, the more the orbital electrons approximate the symmetry, and the signal of  $\text{BX}_3$  species in the spectrum approaches the signal of the related anions  $\text{BX}_4^-$ . With the first- and second-row elements as substituents, the differences  $\Delta = \delta(\text{sp}^2) - \delta(\text{sp}^3)$  very nicely reflect the measure of  $\text{p}-\pi$  interactions, due to the fact that other factors are here greatly eliminated.

### 7.11.2 General Comments on the Boron Chemical Shifts

#### *a) Coordination*

The addition of a ligand or base to the empty p-orbital on boron results in an upfield shift as compared to the tricoordinate borane. This effect is also seen with coordinating solvents such as THF. The chemical shift is dependent on the strength of the coordination complex, with the stronger complexes shifted to higher field. Borane dimers are also found upfield from the free monomer and may show a more complex coupled spectra due to the presence of both terminal and bridging hydrogens coupling to the boron. The addition complex with solvent or a basic ligand is generally found higher field than the dimer.

#### *b) Tricoordinate Boranes containing hydrogen*

The coupled  $^{11}\text{B}$  NMR spectra generally show a B-H coupling, unless there is a fast exchange of the hydrogens on the NMR time scale. Since the spin of hydrogen is 1/2, the number of peaks in the multiplet is one greater than the number of hydrogens attached to the boron. The magnitude of the B-H splitting increases with additional ligands and greater electronegativity of the ligand. The trivalent boranes tend to be dimeric, especially in non-coordinating solvents in the absence of sterically large groups. In a number of cases one may observe both

the monomeric borane (non-coordinated to the solvent or any another weak base such as dimethyl sulfide) and the dimeric borane. The chemical shifts of the trivalent organoboranes having a B-H bond are more variable than that of the trialkylboranes, and are dependent on the structure of the organic groups present.

*c) Trialkylboranes*

The trialkylboranes are found in a narrow low field region, 83-93 ppm. These chemical shifts are largely independent of the structure of the alkyl group. The exception are for the tertiary groups that shift the resonance ~ 3 ppm upfield. Cyclic boranes show a marked dependence on the size of the ring. Six membered rings have approximately the same chemical shifts as the acyclic compounds. The borolane compounds, five member rings, are shifted to lower field by ~ 6 ppm. The effect of the ring size is observed for all cyclic boranes independent of the substituents present.

*d) Substitution of Alkyl groups*

Substitution at the  $\alpha$ -carbon,  $R_2B-CH_2-X$ , with  $X = N_3, OH, NH_2, Cl, Br, I, PMe_3, AsMe_3, SMe, BR_2, SiR_3, Ph, vinyl$  results in an upfield shift of the borane. This effect may be attributed to inter- or intramolecular association of the lone pair electron with the empty p-orbital on the boron or a neighboring group anisotropic effect. The degree of upfield shift is variable, Cl is relatively small ~ +2.9 ppm while I is much larger ~ 15.4 ppm. Silyl and boryl groups shift upfield ~ 4-8 ppm. Similar explanation is made for phenyl and vinyl groups, ~ 0 - 6 ppm.

Boron compounds that are directly bonded to  $sp^2$  or  $sp$  carbons are shifted to higher field due to a pi-interaction between the two p-orbitals on the adjacent carbon and boron atoms. Steric effects are also very important, especially in the case of weaker pi-donors. The effects of acetylenic groups is larger than that of the alkenyl groups, probably due to anisotropic effects as opposed to pi-orbital interactions.

The presence of an OR' or OH group bonded to the boron results in  $^{11}B$  resonance at higher fields as compared to the corresponding alkylborane. The OR' and OH groups are strong pi-donors. In general, the structures of the alkoxy groups do not affect the boron chemical shifts for oxygen containing tricoordinate boranes. The exceptions to this are the tert-butyl, phenoxy and  $Me_3Si$  groups which give slightly higher upfield shift of ~ 2-4 ppm.

*e) Boroxines*

The cyclic anhydrides of the boronic acids are the boroxines,  $(RBO)_3$ . These compounds are found at slightly lower field, ~ 33 ppm, than the corresponding boronic esters or acids, ~ 30

ppm. Aryl and vinyl boroxines, are shifted upfield approximately 2-4 ppm from the alkyl derivatives.

#### *f) Borohydrides*

The parent borohydrides,  $\text{BH}_4^-$ , is a tetrahedral compound in which all hydrogens are magnetically equivalent. A quintet is observed in a 1:4:6:4:1 ratio. While the  $^1\text{H}$  NMR spectra shows a 1:1:1:1 resonance. The borohydrides may be ionic or covalent in nature and this may result in a more complex spectrum depending on the interactions of the cation with the borohydride hydrogens. In most cases, the exchange is fast and only one type of hydrogen is observed. The boron resonances are shifted to higher field, -26 to -45 ppm, more than most all other boron species. The solvent has a significant effect on the chemical shift due to solvation of the cation.

Replacement of an hydrogen with an alkyl group shifts the resonances downfield. The  $^{11}\text{B}$  NMR signal of these substituted alkylborohydrides,  $\text{R}_4\text{-nBH}_n$  overlap but the number of hydrogens present can readily be determined from the multiplicity of the proton coupled boron NMR.

#### *g) Tetraalkylborates*

The tetraalkylborates do not follow this pattern. These complexes are observed over a fairly narrow region, -15 to -22 ppm. The replacement with an aryl group shifts these tetraorganylborates downfield in a systemic manner. The tetraphenylborates are seen ca -6.0 ppm and in general all of these borates show a slight dependence on the cation and solvent.

### **7.11.3 Spin-spin coupling between Boron and Nitrogen**

The unfavourable nuclear magnetic properties of nitrogen isotopes  $^{14}\text{N}$  and  $^{15}\text{N}$  have not encouraged for spin-spin coupling between B-N atoms. The rapid quadrupole relaxation of  $^{14}\text{N}$  ( $I = 1$ ) is thought to be responsible for the fact that no  $^1\text{J}(^{11}\text{B}-^{14}\text{N})$  can be observed either by  $^{11}\text{B}$  or  $^{14}\text{N}$ . However  $^1\text{J}(^{11}\text{B}-^{15}\text{N})$  for several adducts  $\text{X}_3\text{BN}(\text{CH}_3)_2$  ( $\text{X} = \text{F}, \text{Cl}, \text{Br}$ ) have been reported and are too low (12-14Hz) and interesting thing is that the value is independent of nature of the X ligand.

### **7.11.4 Spin-spin coupling between boron and phosphorous**

Different situation exists for boron-phosphorus compounds. In many cases the coupling constants  $^1\text{J}(^{11}\text{B}-^{31}\text{P})$  were readily obtained either from  $^{11}\text{B}$  or  $^{31}\text{P}$  NMR spectra. While the sign of the  $^1\text{J}(^{12}\text{C}-^{31}\text{P})$  in organylphosphines is usually negative and changes to positive when phosphorus becomes tetracoordinated, the  $^1\text{J}(^{11}\text{B}-^{31}\text{P})$  in  $(\text{CH}_3)_3\text{P-B}[\text{N}(\text{CH}_3)\text{CH}_2]_2$  has been shown to be positive. In Phosphine-boranes(B-P)  $^{11}\text{B}-^{31}\text{P}$  coupling constant follows roughly the same trends as  $^1\text{J}(^{11}\text{B}-^1\text{H})$  and  $^1\text{J}(^{11}\text{B}-^{13}\text{C})$ .

## 7.12 other NMR active nuclei

### 7.12.1 Lead

Lead is a ubiquitous environmental contaminant. Although the use of lead (as [PbEt<sub>4</sub>]) in gasoline and paint has now been banned in most developed countries, lead is still one of the ten most common contaminants.

On the other hand, lead has been investigated for its potential applications in medicine. The potentially therapeutic radioisotope <sup>212</sup>Pb has a number of theoretical attractions including  $\alpha$ -emission by short-lived daughter radionuclides, and its application is encouraged by the development of a new generator system and the observation that when <sup>212</sup>Pb-conjugated antibodies are internalized, radioactivity is retained inside cells

There is one lead isotope with a nuclear spin that can be exploited for NMR spectroscopy, <sup>207</sup>Pb, I = 1/2. This isotope has an excellent receptivity (11.8 times greater than that of <sup>13</sup>C), high natural abundance (22.6%), and large chemical shift range (over 16000 ppm). Although <sup>207</sup>Pb NMR spectroscopy has been used extensively to characterize Pb(IV)-alkyl derivatives.

### 7.12.2 Platinum

Platinum is a relatively inert metal and has no natural biological role. Nevertheless, platinum complexes are now amongst the most widely used drugs for the treatment of cancer. The first and second generation compounds cis platin and carboplatin are in widespread use to treat a variety of cancers, either as single agents or in combination with other drugs.

<sup>195</sup>Pt (I = 1/2) is a reasonably sensitive nucleus for NMR detection having a natural abundance of 33.7% and receptivity relative to <sup>13</sup>C of 19.1. An attractive feature of <sup>195</sup>Pt NMR for studies of platinum anticancer drugs is the very large chemical shift range (>15000 ppm), which allows ready differentiation between Pt(II) and Pt(IV), which tend to have chemical shifts at the high-field and low-field ends of the range, respectively. The resonances for square-planar Pt(II) complexes span some 4000 ppm and ligand substitutions produce predictable chemical shift ranges. NMR methods have proved useful in the investigation of platinum drugs from the time that cisplatin was first introduced into the clinic more than 30 years ago. Both 1D <sup>195</sup>Pt and 2D [<sup>1</sup>H, <sup>15</sup>N] NMR techniques were used and made a major contribution in the understanding of the molecular mechanism of action of platinum-based anticancer drugs.

### 7.12.3 Palladium

Palladium is a non-essential element for life. Pharmaceutical interest in Pd(II) compounds is driven by analogy to antitumor Pt(II) complexes, as well as antiviral, antifungal and antimicrobial metallotherapeutics. Palladium has one naturally occurring NMR-active



isotope,  $^{105}\text{Pd}$ , with nuclear spin  $I = 5/2$ . Although it has high natural abundance (22.23%), this quadrupolar nucleus is characterized by a low sensitivity to detection by NMR, low resonance frequency and extremely fast relaxation times ( $<10^{-5}$  s). As far as we know, no  $^{105}\text{Pd}$  NMR studies in solution have been reported.

#### 7.12.4 Rhodium

Rhodium has no known biological function. Recently, rhodium complexes have been investigated for their possible applications in medicine as antitumor, antibacterial and antiparasitic agents. As a monoisotopic species with  $I = 1/2$  and a wide chemical shift range ( $\sim 8000$  ppm), the  $^{103}\text{Rh}$  nucleus is attractive for NMR studies. Unfortunately, low receptivity, negative magnetogyric ratio and very long relaxation times ( $>50$  s) are major drawbacks. A recent survey of  $^{103}\text{Rh}$  NMR spectroscopy has been published, but no studies of biological relevance appear to have been reported.

#### 7.12.5 Tungsten

$^{183}\text{W}$  is the only non-quadrupolar NMR-active nucleus in the Group 6 family, but it is characterized by low natural abundance (14.4%) and extremely low receptivity.

Thus, despite the interesting biological properties of molybdenum and tungsten, both  $^{95/97}\text{Mo}$  and  $^{183}\text{W}$  NMR spectroscopy have not often been used to investigate the biological chemistry of these two metals.  $^{183}\text{W}$  NMR has been used to characterize some heteropolytungstates tested as anti-HIV agents

### 7.13 $^1\text{H}$ NMR spectroscopy organometallic

The  $^1\text{H}$  NMR spectroscopy is among the extensively used techniques for the characterization of organometallic compounds. Of particular interest is the application of  $^1\text{H}$  NMR spectroscopy in the characterization of the metal hydride complexes, for which the metal hydride moiety appear at a distinct chemical shift range between 0 ppm to  $-40$  ppm to the high field of tetramethyl silane (TMS). This upfield shift of the metal hydride moiety is attributed to a shielding by metal d-electrons and the extent of the upfield shift increases with higher the  $d^n$  configuration. Chemical shifts, peak intensities as well as coupling constants from the through-bond couplings between adjacent nuclei like that of the observation of  $J_{\text{P-H}}$ , if a phosphorous nucleus is present within the coupling range of a proton nucleus, are often used for the analysis of these compounds. The  $^1\text{H}$  NMR spectroscopy is often successfully employed in studying more complex issues like fluxionality and diastereotopy in organometallic molecules. The paramagnetic organometallic complexes show a large range of chemical shifts, for example,  $(\eta^6\text{-C}_6\text{H}_6)_2\text{V}$  exhibits proton resonances that extend even up to 290 ppm.

### 7.14 Summary of the unit

Just as in organic chemistry, it is now routine to measure  $^1\text{H}$ ,  $^{13}\text{C}$ , and, often,  $^{19}\text{F}$  and  $^{31}\text{P}$  NMR spectra of diamagnetic organometallic and coordination compounds. Many NMR spectra are measured simply to see if a reaction has taken place as this approach can sometimes take less than 5 min. Having determined that something has happened, the most common reasons for continuing to measure are usually associated with

- 1) Confirmation that a reaction has taken place and, by simply counting the signals, deciding how to proceed
- 2) The recognition of new and/or novel structural features via marked changes in chemical shifts and/or J-values, and
- 3) The need for a unique probe with sufficient “structural resolution” to follow the kinetics or the development of a reaction.

When a P atom is present, proton-decoupled  $^{31}\text{P}$  NMR often represents one of the simplest analytical tools available as the spectra can be obtained quickly and do not normally contain many lines.

### 7.15 Key words

NMR spectra of Inorganic compounds; Chemical Shift; Spin-Spin Splitting ;  $^{31}\text{P}$  NMR spectroscopy;  $^{19}\text{F}$  NMR spectroscopy ; Boron NMR spectroscopy ; Other NMR active nuclei;  $^1\text{H}$  NMR spectroscopy organometallic.

### 7.16 References for further studies

- 1) NMR Spectroscopy in Inorganic Chemistry; Jonathan A. Iggo; *Oxford University Press*, **1999**.
- 2) Structural Methods in Molecular Inorganic Chemistry; D. W. H. Rankin, Norbert Mitzel, Carole Morrison; *John Wiley & Sons*, **2013**.
- 3) NMR in Organometallic Chemistry; Paul S. Pregosin; *John Wiley & Sons*, **2012**.
- 4) Phosphorus-31 NMR Spectroscopy: A Concise Introduction for the Synthetic Organic and Organometallic Chemist; Olaf Kühn; *Springer Science & Business Media*, **2008**.
- 5) Guide to Fluorine NMR for Organic Chemists; W. R. Dolbier; *John Wiley & Sons*, **2009**.

### 7.17 Questions for self understanding

- 1) Explain the practical limitations to metal NMR spectroscopy.
- 2) Discuss the favourable properties for high-resolution NMR spectroscopy.
- 3) Write a note on followings
  - a) Chemical Shift
  - b) Chemically equivalent nuclei

- c) Integration
- d) Spin-Spin Splitting (Coupling)
- 4) Discuss the  $^{31}\text{P}$  NMR spectroscopy.
- 5) Explain the Differences between  $^1\text{H}$  and  $^{31}\text{P}$  NMR.
- 6) With example explain the different phosphorus environments and their coupling to  $^1\text{H}$  in  $^{31}\text{P}$  NMR spectroscopy.
- 7) Write a note on coupling of  $^{31}\text{P}$  nucleus with
- a)  $^1\text{H}$
- b)  $^{19}\text{F}$
- 8) Explain the applications of  $^{31}\text{P}$  NMR as.
- 9) Discuss the  $^{19}\text{F}$  NMR spectroscopy.
- 10) Write a note on chemical shift in  $^{19}\text{F}$  NMR.
- 11) Discuss the Boron NMR spectroscopy.
- 12) Explain the chemical shift in Boron NMR spectroscopy.
- 13) Write a note on
- a) Spin-spin coupling between Boron and Nitrogen.
- b) Spin-spin coupling between boron and phosphorous.
- 14) Explain the possibility of NMR spectral study of following nuclei.
- a) Lead
- b) Platinum
- c) Palladium
- d) Rhodium
- d) Tungsten
- 15) Discuss the  $^1\text{H}$  NMR spectroscopy in study of organometallic compound structure.

**UNIT-8****Structure**

- 8.0 Objectives of the unit
- 8.1 Introduction
- 8.2 Recoil effect
- 8.3 Conditions for MB spectra
- 8.4 Fe is the most studied precursor
- 8.5 Recording the MB spectrum
- 8.6 Isomeric shift/centre shift/ chemical shift
- 8.7 Chemical Shift values for Fe compounds
- 8.8 Electric Quadrupole Interactions
- 8.9 Information's from quadrupole splitting
  - 8.10 Stereochemical activity of lone pair
- 8.11 Magnetic interactions
- 8.12 Application of Mossbauer spectra
- 8.13 Prussian blue and Turnbull's blue
- 8.14 Ferredoxin
- 8.15 Study of thermal spin-cross over
- 8.16 Summary of the unit
- 8.17 Key words
- 8.18 References for further studies
- 8.19 questions for self understanding

## 8.0 Objectives of the unit

After studying this unit you are able to

- Explain the Recoil effect
- Explain the required conditions for MB spectra
- Explain the Isomeric shift/centre shift/ chemical shift
- Identify the chemical shift values for Fe compounds
- Explain the Electric Quadrupole Interactions
- Explain the Information's extracted from quadrupole splitting
- Explain the application of Mossbauer spectra

## 8.1 Introduction

If a nucleus gives off radiation or any other form of energy (in this case, in the form of a  $\gamma$ -ray), the nucleus must recoil with an equal and opposite momentum to preserve its energy (E), in the same way that a gun (by analogy, the nucleus) recoils when a bullet (the  $\gamma$ -ray) is fired out of it.

We describe this general case in terms of energy by saying that:

$$E_{\gamma\text{-ray emission}} = E_{\text{transition}} - E_{\text{R}},$$

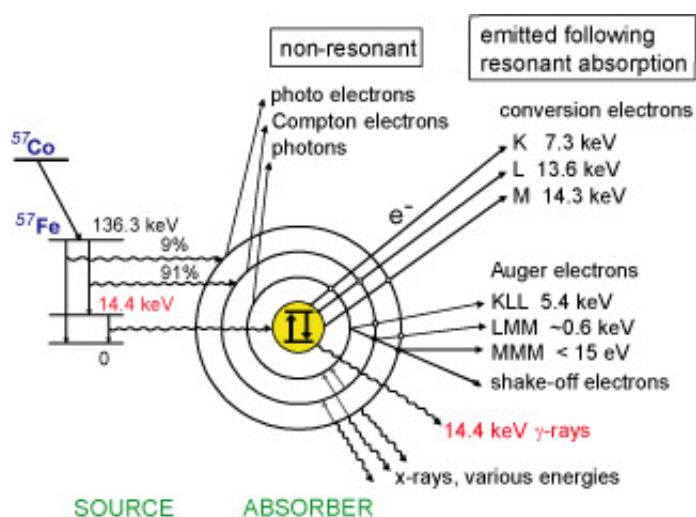
where

$E_{\gamma\text{-ray emission}}$  = the energy of the emitted  $\gamma$ -ray

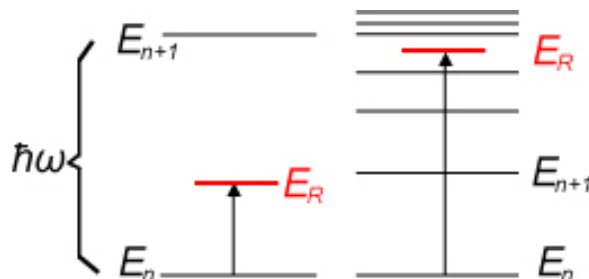
$E_{\text{transition}}$  = the energy of the nuclear transition and

$E_{\text{R}}$  = the energy of the recoil.

The  $^{57}\text{Fe}$  which is a decay product of  $^{57}\text{Co}$  is unstable.  $^{57}\text{Fe}$  decays by giving off a gamma ray ( $\gamma$ -ray), along with other types of energy. Below figure shows the nuclear decay scheme for  $^{57}\text{Co} \rightarrow ^{57}\text{Fe}$  and various backscattering processes for  $^{57}\text{Fe}$  that can follow resonant absorption of an incident gamma photon.

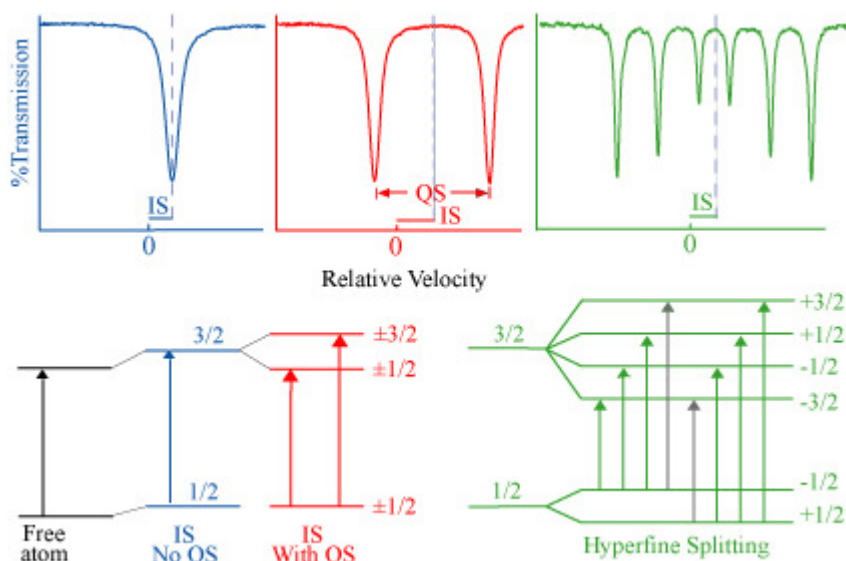


Below figure shows a schematic of the vibrational energy levels in a solid. On the left, the recoil energy  $E_R$  of an emitted gamma photon is less than what is needed to reach the next higher energy level, so that excitation of a vibrational mode has low probability. The probability that no excitation will occur is given the symbol  $f$ , which represents the fraction of recoil-free events.



A gamma ray would be emitted without losing energy to the solid, in what is called a zero-phonon transition. In other words, sometimes the nucleus absorbs the energy of the  $\gamma$ -ray and it doesn't recoil (instead, the entire structure, rather than just the nucleus, absorbs the energy). The variable  $f$  indicates the probability of this happening. This process of recoil-less emission forms the basis for Mössbauer spectroscopy. On the right,  $E_R$  is significantly greater in energy than the lowest excitation energy of the solid, which is  $E_{n+1} - E_n$ . Absorption of the recoil energy,  $E_R$ , by the solid thus becomes probable, and the photon emerges with energy reduced by  $E_R$  and with Doppler broadening. In the figure,  $\omega$  represents frequency, and  $\hbar$  is Planck's constant divided by  $2\pi$ .

The Mössbauer effect occurs because in solids, the value of  $f$  is high enough that recoil-free absorption is possible. Thus an atom of  $^{57}\text{Co}$  can decay to  $^{57}\text{Fe}$ , which gives off a  $\gamma$ -ray, and may be absorbed without recoil by a nearby  $^{57}\text{Fe}$ , which happens to have just the right splitting between the energy levels in its nucleus to absorb it.



This scenario will only happen if the decaying Co atom is surrounded by the same atoms as the absorbing Fe. If the receiving Fe atoms are in a different matrix (say, in a mineral) than in the emitter, then no absorption can occur.

### 8.2 Recoil effect

Whenever a high energy particle/projectile is released from a body at rest, the releasing body feels a back-kick ie, it is pushed backwards, this is true for absorption of high energy particles also. This phenomenon is called recoil effect. The recoil happens to conserve the momentum.

When a gaseous atom or molecule emits a quantum of energy, E then emitted quantum will always have the momentum  $E/C$  where C is the velocity of light

To conserve the momentum the emitter recoils with momentum P which is equal and in opposite direction. Therefore

$P = M \cdot V_R = -E/C$  where  $V_R$  recoil velocity [-ve sign shows that its direction is opposite]

$$E_R = P^2/2m = E^2/2MC^2$$

$$= (E_t - E_R)^2 / 2MC^2 \sim E_t/2MC^2$$

If M increases the recoil energy can be still lower, so the source and the absorber are fixed on a larger lattice to increase mass.

### 8.3 Conditions for MB spectra

The energy of nuclear transition must be larger enough to give useful  $\gamma$ -ray photon, but not enough to cause recoil effect.

The energy of the  $\gamma$ -ray photon must be in the range of 10-150keV.

A substantial amount of the nuclear decay must be with  $\gamma$ -ray emission.

The lifetime of the excited state must be long enough give a reasonably broad emission range.

Since, extremely narrow lines are not useful ( $\tau$  must be 001 to 100nS)

The excited state of the emitter should be having a long-lived precursor, and easy to handle.

The ground state of the isotope should be stable. Its natural abundance should be high or at least the enrichment of that isotope should be easy.

The cross section of for absorption should be high.

### 8.4 Fe is the most studied precursor

- i) The precursor of  $^{57}\text{Fe}$  is  $^{57}\text{Co}$  which decays to  $^{57}\text{Fe}^*$  with a half-life of 270days (highly stable precursor).
- ii) 9% of  $^{57}\text{Fe}$  decays to ground state directly with emission of  $\gamma$ -ray photon of energy 136.32keV.
- iii) 91% of  $^{57}\text{Fe}^*$  decays to another excited state with emission 121.91keV energy.
- iv) The lower excited state is having half-life times of 99.3nS (more stable).

- v) This decay to ground state with emission of 14.41keV.
- vi) This transition satisfies all the conditions for MB spectra except 2<sup>nd</sup> condition. But this is compensated by large absorption cross section.

Other elements that can be studied are <sup>119</sup>Sn, <sup>121</sup>Sb, <sup>125</sup>Te, <sup>129</sup>I, <sup>129</sup>Xe and <sup>197</sup>Au.

### 8.5 Recording the MB spectrum

Usually the standard emitter is used as the source. Sample under investigation is the absorber. Both the sample and absorber are embedded on a crystal lattice to minimize the recoil effect. The source for <sup>57</sup>Fe spectroscopy is commercially available <sup>57</sup>Co/Rh is mounted on the shaft of a vibrator. Source is generally kept at room temperature. Absorber (sample under study) may be cooled down to liquid nitrogen or liquid helium temperatures in cryostat, or for controlled heating in an oven.  $\gamma$ -rays are detected by a scintillation counter, gas proportional counter or a semi-conductor detector. A constant frequency clock synchronises a voltage waveform which serve as a reference signal to the servo-amplifier controlling the electro-mechanical vibrator. A difference between the monitored signal and the reference signal is amplified and drives the vibrator at the same frequency (typically 50s<sup>-1</sup>) as the channel address advance. Each channel corresponds to a certain relative velocity and is held open for a fixed time interval depending on the frequency and number of channels used. The incoming  $\gamma$ - counts are collected in their corresponding channels during the sequential accessing eg. 50 times per seconds, until satisfactory resolution is reached. The cryostat can be furnished with a superconducting solenoid for measuring the sample in an applied magnetic field. It is also possible to mount a pressure cell inside the cryostat for studying the sample properties under pressure.

### 8.6 Isomeric shift/centre shift/ chemical shift

The  $E_t$  values is affected by the interaction between the nucleus and the electrons present around it. This arises because of the different sizes of nucleus in ground and excited states.

The change in nuclear radius when going from gs to es is  $\Delta R$ . Z is the atomic number

The change in electrostatic energy on decay is given by (Chemical shift/ isomer shift)

$$\delta = (\epsilon_0/5)(Ze^2R^2)(\Delta R/R) [ |\Psi_s(\text{abs})|^2 - |\Psi_s(\text{source})|^2 ]$$

where

$\epsilon_0$ = permittivity of free space

Z = atomic number of the nucleus

e = electronic charge

$\Psi_s(\text{abs})$  = s orbital wave function of absorber

$\Psi_s(\text{source})$  = s orbital wave function of source.



Since s electron wave functions have their maxima at the nucleus, s electron density affect the isomer shift to a greater extent. But changes in p and d orbital occupancies affect the s electron through screening hence have a smaller effect on isomer shift. When  $\Delta R/R$  is positive the isomer shift is also positive and negative  $\Delta R/R$  reflected as negative shift. Isomer shift is related to the oxidation state of the metal. In  $^{119}\text{Sn}$  spectra Sn(II) shows a positive shift ( $\Delta R/R$ ) with respect to Sn whereas for Sn (IV) it is negative

Species	configuration	$\Delta R/R$	$\delta$
Sn(IV)	$5s^05p^0$	-ive	-ive
Sn	$5s^25p^2$	0	0
Sn(II)	$5s^25p^0$	+ive	+ive

s - electron density decreased so negative shift

s - electron density increased – p screening not present, so positive shift

In  $^{119}\text{Sn}$  compounds, the shift values depend on the ligand present and the coordination number of tin. Hence isomer shift values are useful in characterizing tin derivatives. My Sn compounds appears to contain Sn(II) from the formulae but on analysing with MB spectra Sn(IV) is present in them. Many of them are polymeric and contain Sn(IV). Generally Sn(II) compounds shows shift > than  $2.1\text{mmS}^{-1}$  and Sn(IV) shows shift <  $2.1\text{mmS}^{-1}$  (with relative to  $\text{SnO}_2$ ).

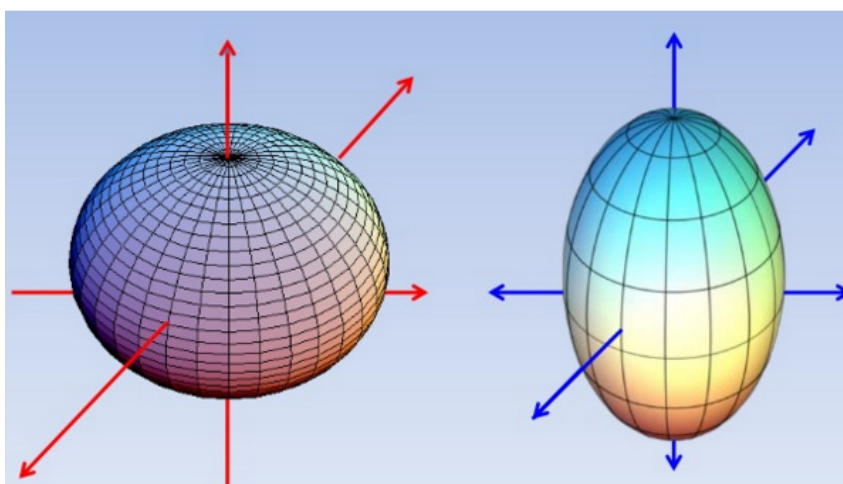
The isomer shift of  $(\text{SnPh}_2)_n$  is  $1.5\text{mm/S}$  clearly showing the presence of Sn(IV). Similarly formula  $\text{Sn}(\text{C}_5\text{H}_3)_2$  is having a momomeric structure in the solid state and shows a shift of  $3.74\text{mm/S}$ .

### 8.7 Chemical Shift values for Fe compounds

Fe isomer shift cannot be used for determining the oxidation state of Fe in a molecule. Fe shows oxidation state from 0 to 4 often differs in unit charge only. The electrons involved are from d orbital, so effect on the s electron is smaller. Varying spin states (which depend on the ligands present) also affect the shift values. Though some useful correlations had been drawn. Fe prophyrin complexes are very important biologically. Fe can be present in +2 or +3 state in them. The complexes can be easily reduced. The electron may be to the Fe or to the ligand. In that ambiguous case MB spectra is useful in determining the oxidation state.

### 8.8 Electric Quadrupole Interactions

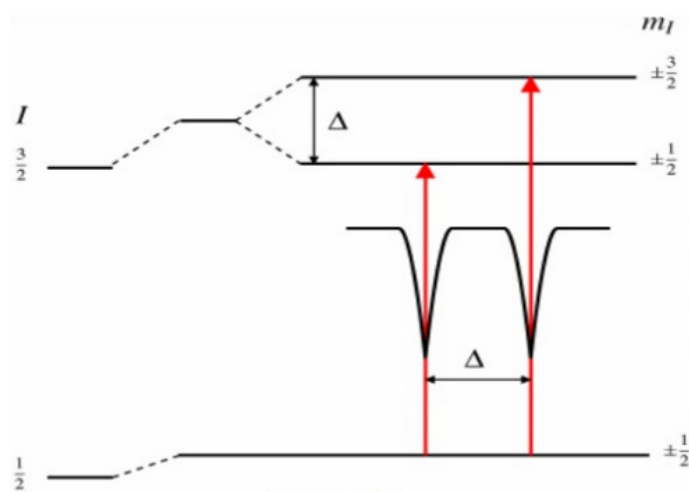
Nuclei in states with an angular momentum quantum number  $I > \frac{1}{2}$  have a non-spherical charge distribution. This produces a nuclear quadrupole moment. In the presence of an asymmetrical electric field (produced by an asymmetric electronic charge distribution of ligand arrangement) this split the nuclear energy levels. The charge distribution is characterized by a single quantity called the Electric Field Gradient (EFG)



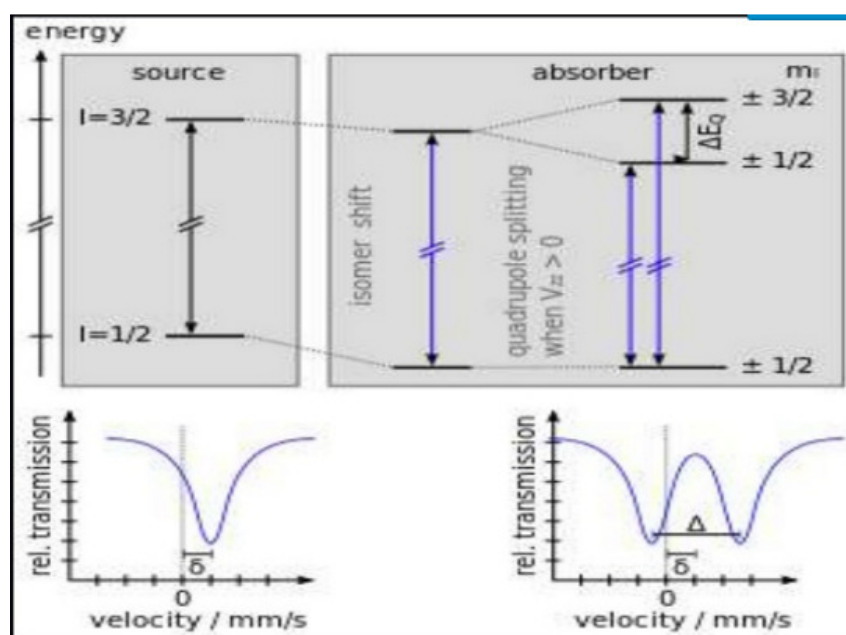
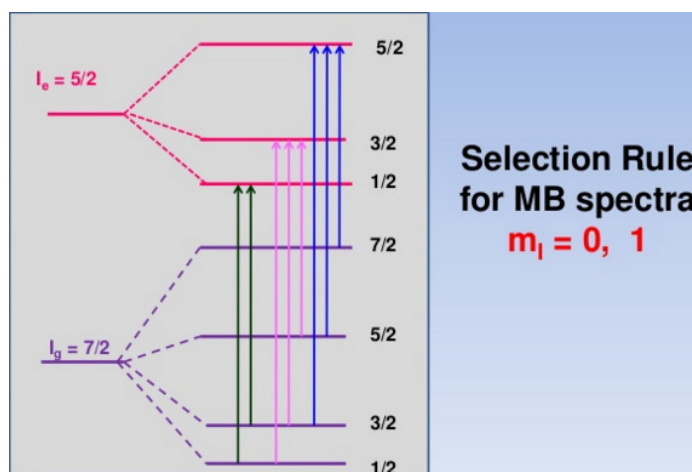
Oblate and Prolate nuclei

In the case of an isotope with  $I = \frac{3}{2}$  excited state, such as  $^{57}\text{Fe}$  or  $^{119}\text{Sn}$ , the excited state is split into two sub states  $m_I = \pm 1/2$  and  $m_I = \pm 3/2$ . This gave a two line spectrum or doublet. The magnitude of splitting,  $\Delta$ , is related to the nuclear quadrupole moment,  $Q$  and the principle component of the EFG,  $V_{ZZ}$ , by the relation

$$\Delta = \frac{eQV_{ZZ}}{2}$$



Quadrupole splitting for  $^{57}\text{Fe}$  and  $^{119}\text{Sn}$



### 8.9 Information's from quadrupole splitting

Appearance of quadrupole splitting shows the presence of *efg* at the nucleus. The *efg* may be created by the ligand field or by the electron distribution around the nucleus. Single crystal or application of magnetic field gives more information. If a nucleus with symmetric electron distribution is in  $O_h$  field *efg* is not expected.

### 8.10 Stereochemical activity of lone pair

Consider Te(IV) compounds with six ligands. If the lone pair of electron of Te is stereochemically active, then it will occupy one vertex of a pentagonal bipyramide (*pbp*). This will create an *efg* at the nucleus resulting in quadrupole splitting. But no quadrupole splitting is observed in these classes of compounds, hence it is clear that the lone pair is stereochemically inactive and occupies the 5s orbital.

Structure of the  $[\text{TeX}_4\text{Y}]^2-$  had not been crystallographically studied. The MB spectra of these species show no quadrupole splitting but this is not a conclusive evidence for absence

of  $efg$  at nucleus. The  $efg$  may not be enough to cause quadrupole splitting. But in  $\text{CsIF}_6$  substantial quadrupole splitting shows the stereochemical activity of the lone pair.

### 8.11 Magnetic interactions

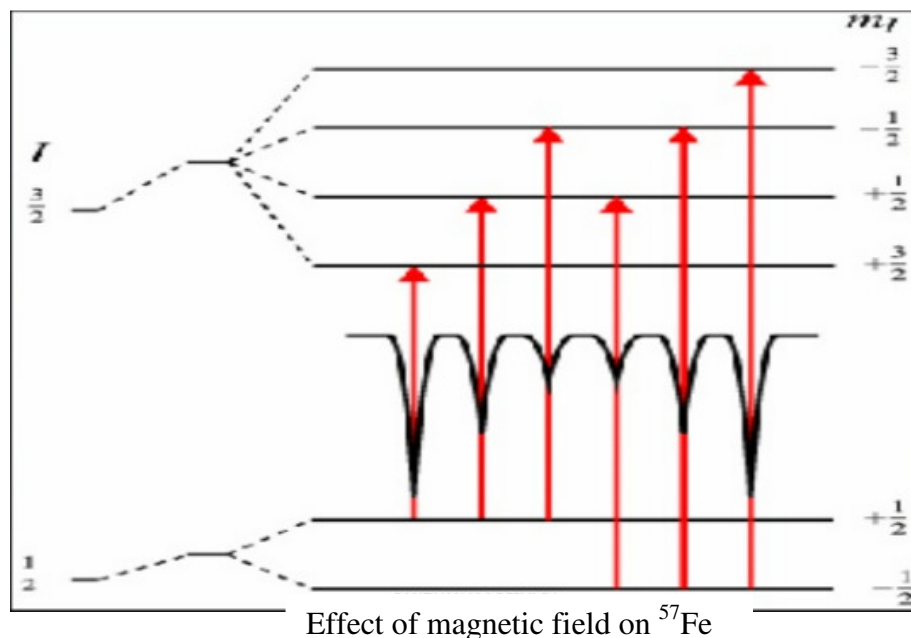
In the presence of a magnetic field the nuclear spin moment experiences a dipolar interaction with the magnetic field ie, Zeeman splitting. There are any sources of magnetic fields that can be experienced by the nucleus. The total effective magnetic field at the nucleus  $B_{\text{eff}}$  is given by

$$B_{\text{eff}} = (B_{\text{contact}} + B_{\text{orbital}} + B_{\text{dipolar}}) + B_{\text{applied}}$$

The first three terms being due to the atom's own partially filled electron shells.  $B_{\text{contact}}$  is due to the spin on those electrons polarizing the spin density at the nucleus.  $B_{\text{orbital}}$  is due to the orbital momentum on those electrons, and  $B_{\text{dipolar}}$  is the dipolar field due to the spin of those electrons.

Energy of the nuclear levels  $E_m = -g\mu_N B m_I$

This magnetic field splits nuclear levels with a spin of  $I$  in to  $(2I + 1)$  substates. Transitions between the excited state and ground state can only occur where  $m_I$  changes 0 or 1. This gives six possible transitions for a  $3/2$  to  $1/2$  transition, giving a sextet, with the line spacing being proportional to  $B_{\text{eff}}$ .



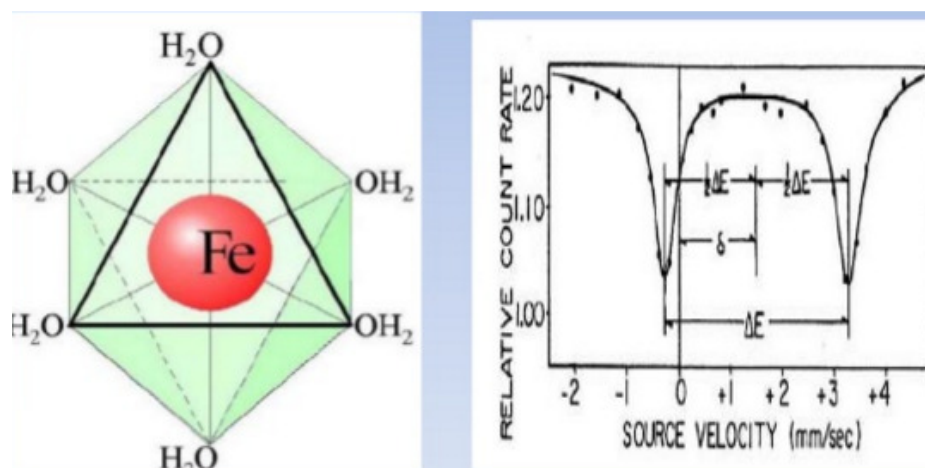
The line positions are related to the splitting of the energy levels, but the line intensities are related to the angle between the Mossbauer gamma-ray and the nuclear spin moment. Outer and inner lines are always in the same proportion. The middle lines can vary in relative intensity between 0 and 4 depending upon the angle the nuclear spin moments makes to the

gamma-ray. In polycrystalline samples with no applied field this value averages to 2. But in single crystals or under applied fields the relative line intensities can give information about moment orientation and magnetic ordering.

### 8.12 Application of Mossbauer spectra

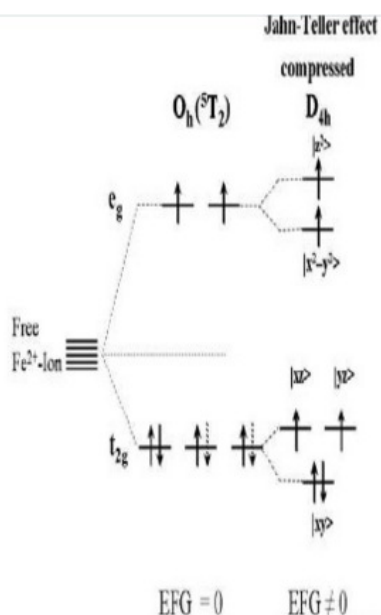
#### Spectra of spin free Fe(II) → FeSO<sub>4</sub>·7H<sub>2</sub>O

From the crystallographic data it was initially concluded that FeSO<sub>4</sub>·7H<sub>2</sub>O is having a perfect O<sub>h</sub> symmetry, with six H<sub>2</sub>O on each vertex. But the MB spectrum recorded showed a large quadrupole splitting which is not possible in a regular O<sub>h</sub> symmetry (for a perfect O<sub>h</sub> field *efg* is zero).



Spectra of spin free Fe(III) → FeSO<sub>4</sub>·7H<sub>2</sub>O

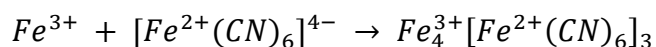
Fe(II) is a d<sup>6</sup> system, in weak field created by H<sub>2</sub>O an orbitally degenerate system results. This under goes J-T distortion (Z<sub>in</sub>) to remove the degeneracy and form a tetragonal field. This creates an *efg* at the nucleus and hence quadrupole splitting occurs. The structure assigned is a distorted O<sub>h</sub> with all angles 90° and *x* ≠ *y* ≠ *z*



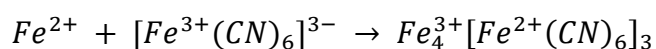
Ligand field splitting of <sup>5</sup>T<sub>2</sub> ground state in O<sub>h</sub> symmetry and Jahn-Teller effect leading to a compressed octahedron with D<sub>4h</sub> symmetry for [Fe(H<sub>2</sub>O)<sub>6</sub>]<sup>2+</sup>.

### 8.13 Prussian blue and Turnbull's blue

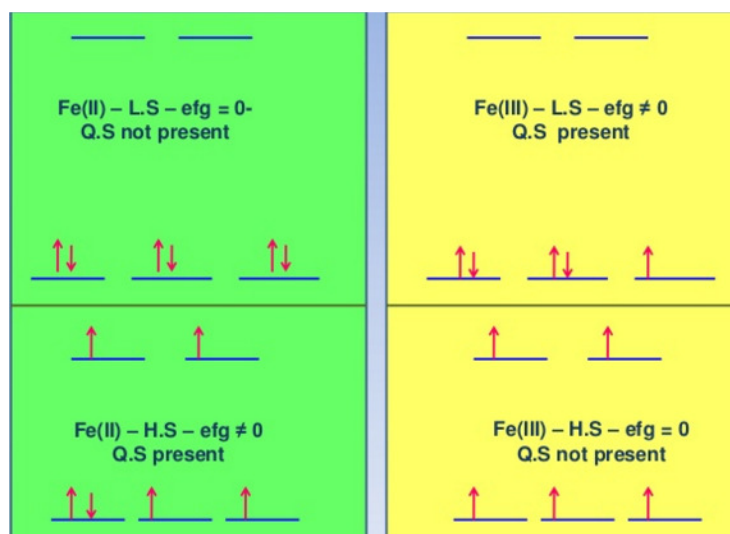
Prussian blue is a dark blue pigment with the idealized formula  $\text{Fe}_7(\text{CN})_{18}$ . It is prepared by adding a ferric salt to ferrocyanide.



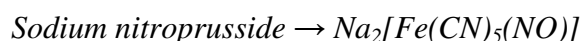
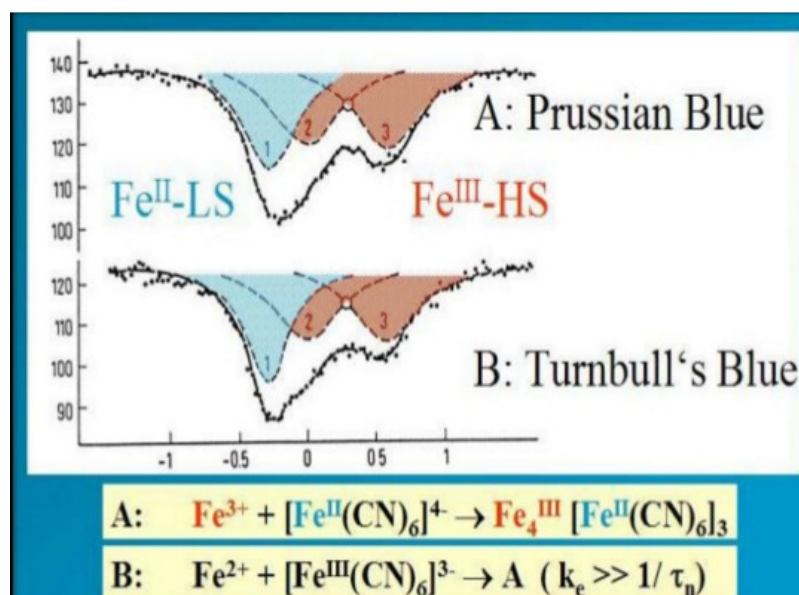
Turnbull's blue is the same substance but is made from different reagents, ie, addition ferrous salt to ferricyanide



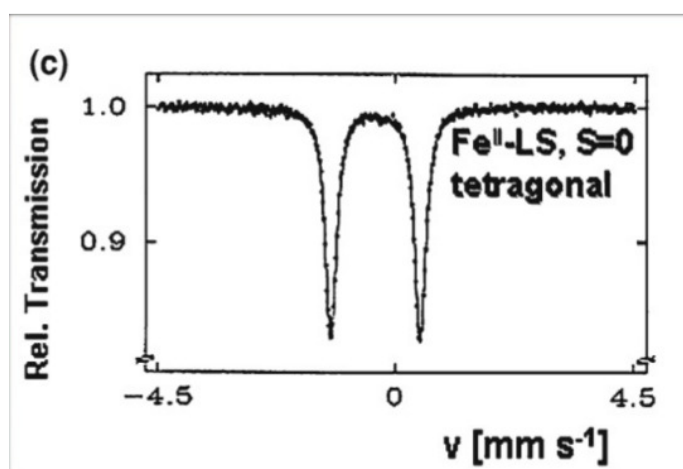
Its slightly different colour systems from different impurities. For a long time they considered as chemically different compounds. Prussian blue with  $[\text{Fe}^{\text{II}}(\text{CN})_6]^{4-}$  anions and Turnbull's blue with  $[\text{Fe}^{\text{III}}(\text{CN})_6]^{3-}$  anions, according to the different way of preparing them. However the Mossbauer were nearly identical for both PB and TB showing only the presence of  $[\text{Fe}^{\text{II}}(\text{CN})_6]^{4-}$  and  $\text{Fe}^{3+}$  in the high spin state. This was confirmed by use of  $\text{K}_4[\text{Fe}^{\text{II}}(\text{CN})_6]$  and  $\text{K}_3[\text{Fe}^{\text{III}}(\text{CN})_6]$  as a reference compounds. Immediately after adding a solution of  $\text{Fe}^{2+}$  to a solution of  $[\text{Fe}^{\text{III}}(\text{CN})_6]^{3-}$  a rapid electron transfer takes place from  $\text{Fe}^{2+}$  to the anion of the same material. A singlet for Fe(II) and a quadrupole doublet for Fe(III) were which confirmed Prussian blue and Turnbull's blue are identical.



The Fe(II) centres which are low spin are surrounded by six cyanide ligands in an octahedral configuration. The Fe(III) centres which are high spin are octahedrally surrounded on average by 4.5 nitrogen atoms and 1.5 oxygen atoms (the oxygen from the six coordinated water molecules). This introduces an  $efg$  at Fe(III) nucleus and hence quadrupole splitting occurs.

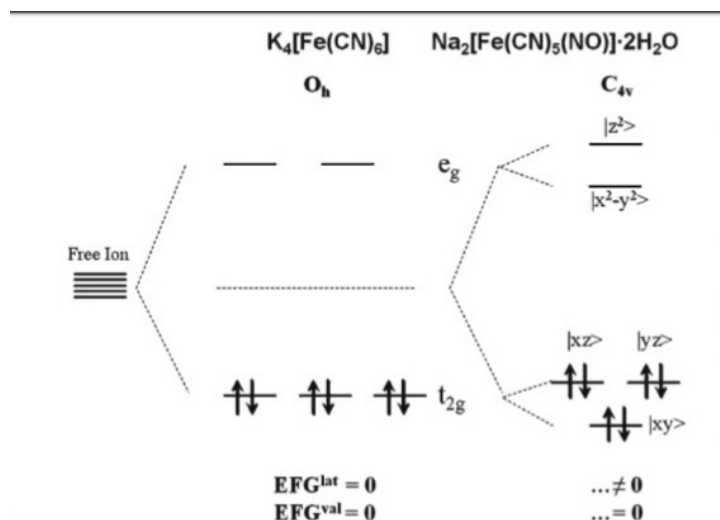


The oxidation state of Fe in nitroprusside was a matter of controversy for a long time. Initially it was assumed that it contained Fe(II) and <sup>+</sup>NO since it was diamagnetic. [Fe(II) is a d<sup>6</sup> and Fe(III) is a d<sup>5</sup> systems]. But the MB spectrum of the sample showed a doublet with  $\delta = -0.165 \text{ mm/S}$ . this value is too negative for a Fe(II) complex.



This suggests that the Fe may be in Fe(IV) state. The magnetism and MB spectrum are in consistent with the structure which has an extensive  $\pi$ -bonding with <sup>+</sup>NO ligand. The t<sub>2g</sub> orbital of Fe and the p-orbital of N present in <sup>+</sup>NO containing the off electron to form a  $\pi$ -bond. The Fe(II) is transferring the electrons from filled t<sub>2g</sub> level to an vacant  $\pi$ -antibonding orbital of NO. This makes the shift value to approach Fe(IV) values. Now because of this the shielding of s electrons by the d electrons decreases and hence the shift becomes more. This is supported by the decrease in N-O stretching frequency in IR since the anti-bonding levels is field.

$K_4[Fe(CN)_6]$  is a  $3d^6$  LS complex with  $O_h$  symmetry, where all six electrons are accommodated in the three  $t_{2g}$  orbitals. Both contributions  $(EFG)_{val}$  and  $(EFG)_{lat}$  vanish, there is no quadrupolar interaction.  $Na_2[Fe(CN)_5NO] \cdot 2H_2O$  has  $C_{4v}$  symmetry with d-orbital splitting as shown.



Its LS behaviour requires that all six electrons are accommodated in the lowest three orbitals arising from the tetragonal splitting of the former cubic  $t_{2g}$  ( $O_h$ ) subgroup.  $(EFG)_{val}$  is still zero but  $(EFG)_{lat} \neq 0$  arises from the ligand replacement in the iron coordination sphere. The isomer shift data for the pentacyano complexes of iron(II) with different sixth ligand X.

**Effect of  $\pi$ -Backdonation in  $[Fe(CN)_5X^{n-}]^{(3+n)-}$**

Ligand X	$\delta/mm\ s^{-1}$	$d_{\pi} \rightarrow p_{\pi}$	d-shield	$ \Psi_s(0) ^2$
$NO^+$	0.00			
CO	+0.15	↑	↓	↑
$SO_3^{2-}$	+0.22			
$P(C_6H_5)_3$	+0.23			
$NO_2^-$	+0.26			
$Sb(C_6H_5)_3$	+0.26			
$NH_3$	+0.26			
$As(C_6H_5)_3$	+0.29			
$H_2O$	+0.31			

$\delta \sim |\Psi_s(0)|^2 \frac{\Delta R}{R}$        $^{57}Fe: \frac{\Delta R}{R} < 0$

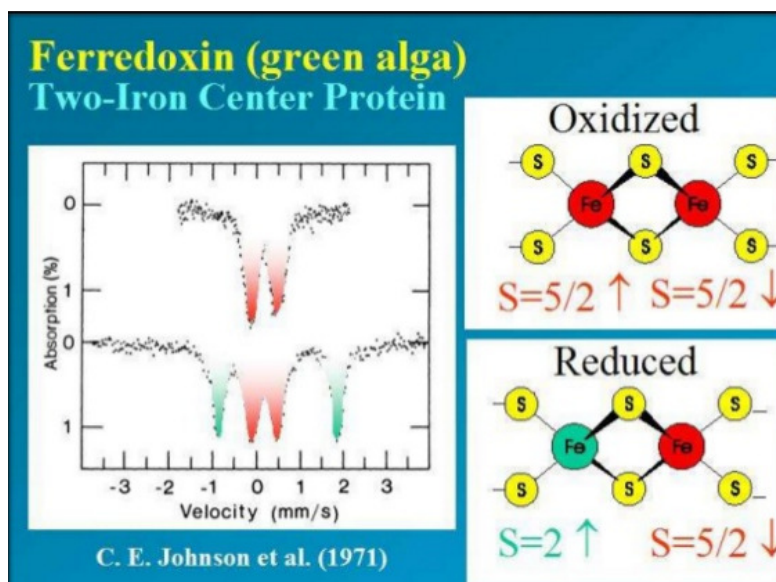
Normalizing the isomer shift to that of the pentacyanonitrosylferrate complex as zero point. The ordering expresses the varying effects of  $d_{\pi}-p_{\pi}$  back donation for the different sixth ligand X. the isomer shift values becomes more positive on going from  $^+NO$  to  $H_2O$ .

$d_{\pi}-p_{\pi}$  backdonation decrease causing an increasing d-electron density residing near the iron centre. Stronger shielding of s-electrons by d-electrons which finally creates lower s-electron density at the nucleus. The nuclear factor  $\Delta R/R$  is negative for  $^{57}Fe$  explains the increasingly positive isomer shift values in the given sequence from  $^+NO$  to  $H_2O$ .



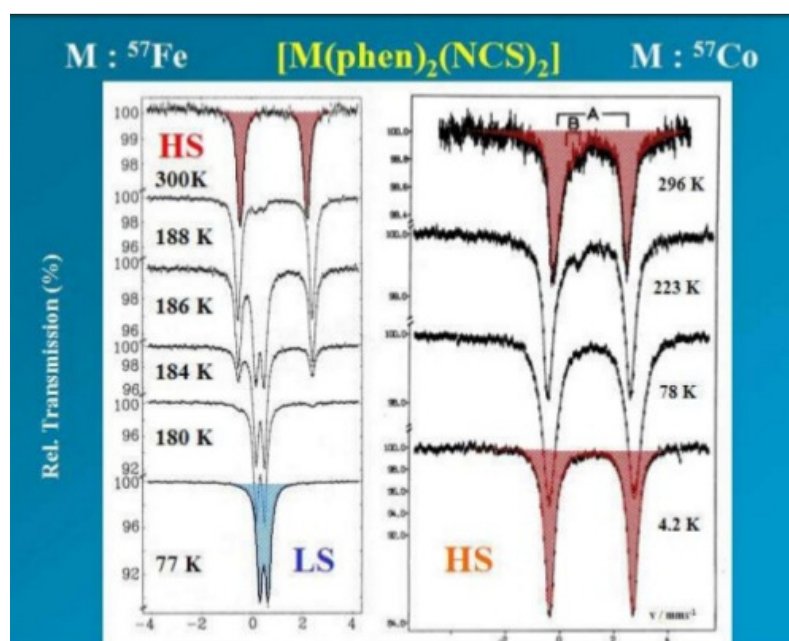
### 8.14 Ferredoxin

Study of ferredoxin a Fe-S protein which assists in in-vivo electron transfer reactions. The two-iron centres are not equivalent in the reduced form. The oxidized form with two Fe(III)-high spin centres can be distinguished from the reduced form with one Fe(III)-high spin centre only by using MB spectrum.



### 8.15 Study of thermal spin-cross over

Many coordination compounds possessing intermediate ligand field strengths show thermal spin crossover {ie, HS $\leftrightarrow$ LS}. For example  $[\text{Fe}(\text{phen})_2(\text{NCS})_2]$  undergoes thermal spin transition. The main result is that in the temperature region, where the MAS spectra reflect the transition to the LS state the MES spectra still show the typical HS signals arising from excited ligand field states.



### 8.16 Summary of the unit

Nearly fifty years ago Rudolf L Mössbauer discovered the recoilless nuclear resonance absorption of gamma rays and it is referred as Mössbauer spectroscopy. It gives very precise information about the chemical, structural, magnetic and time-dependent properties of a compound. Key feature of this technique is the recoilless gamma ray emission and absorption of a nucleus (referred as the 'Mössbauer Effect').

Nuclei in atoms undergo a variety of energy level transitions and these energy levels are influenced by their surrounding environment (both electronic and magnetic) which can change or split these energy levels. These changes in the energy levels can provide information about the atom's local environment within a system and ought to be observed using resonance-fluorescence. There are two major obstacles in obtaining this information they are

- i) The 'hyperfine' interactions between the nucleus and its environment (which are extremely small) and
- ii) The recoil of the nucleus as the gamma-ray is emitted or absorbed prevents resonance.

A nucleus with  $Z$  protons and  $N$  neutrons in an excited state of energy  $E_e$  undergoes transition to the ground state of energy  $E_g$  by emitting a gamma quantum of energy  $E_e - E_g$ . The gamma quantum may be absorbed by the nucleus of the same kind (same  $Z$  and  $N$ ) in its ground state, whereby transition to the excited state of energy  $E_e$  takes place (resonance absorption). The subsequent transition to the ground state emits a conversion electron  $e^-$  or a  $-\gamma$ -quantum (resonance fluorescence).

### 8.17 Key words

Recoil effect; Conditions for MB spectra; Isomeric shift/centre shift/ chemical shift; Chemical Shift values for Fe compounds; Electric Quadrupole Interactions; Magnetic interactions; Application of Mossbauer spectra ; Prussian blue and Turnbull's blue; Ferredoxin; Study of thermal spin-cross over

### 8.18 References for further studies

- 1) Mössbauer Spectroscopy: Tutorial Book; Yutaka Yoshida, Guido Langouche; *Springer Science & Business Media*, 2012.
- 2) Mössbauer Spectroscopy Applied to Inorganic Chemistry; G.J Long; *Springer Science & Business Media*, 2013.
- 3) Mossbauer Spectroscopy: Applications in Chemistry, Biology, and Nanotechnology; Virender K. Sharma, Gostar Klingelhofer, Tetsuaki Nishida; *John Wiley & Sons*, 2013.

- 4) Mössbauer Spectroscopy and Transition Metal Chemistry: Fundamentals and Applications; Philipp Gütlich, Eckhard Bill, Alfred X. Trautwein; *Springer Science & Business Media*, 2010.
- 5) Mössbauer Spectroscopy; Dominic P. E. Dickson, Frank J. Berry; *Cambridge University Press*, 2005.

### 8.19 questions for self understanding

- 1) What is Recoil Effect?
- 2) Explain the necessary Conditions for MB spectra
- 3) Why Fe is the most studied precursor in MB spectra?
- 4) Explain the recording of the MB spectrum
- 5) What is Isomeric shift/centre shift/ chemical shift?
- 6) Discuss the chemical shift values for Fe compounds
- 7) What is Electric Quadrupole interaction?
- 8) What are the informations obtained from quadrupole splitting?
- 9) Discuss the stereochemical activity of lone pair
- 10) Explain the magnetic interactions
- 11) Discuss the application of Mossbauer spectra for following cases
  - a) Prussian blue and Turnbull's blue
  - b) Ferredoxin
  - c) Study of thermal spin-cross over

---

**UNIT-9****Structure**

- 9.0 Objectives of the unit
- 9.1 Introduction
- 9.2 Thermogravimetric analysis (TGA)
- 9.3 Principle
- 9.4 Types of TGA
- 9.5 Instrumentation
- 9.6 Types of TGA instruments
- 9.7 Thermogravimetric curves
- 9.8 Sources of errors in TGA
- 9.9 Calibration of thermobalance for the measurement of mass
- 9.10 Interpretation of TG curves
- 9.11 Types of TG curves
  - 9.11.1 Plateau
  - 9.11.2 Procedural decomposition temperature
  - 9.11.3 Final temperature
  - 9.11.4 The reaction interval
  - 9.11.5 Isobaric mass change determination
  - 9.11.6 Evolved gas detection (EGD)
  - 9.11.7 Evolved gas analysis (EGA)
- 9.12 Information from TG curve
- 9.13 Factors affecting TG curve
- 9.14 Applications of thermogravimetric analysis
- 9.15 Analysis of inorganic and organic mixtures
  - 9.15.1 Binary mixtures
  - 9.15.2 Analysis of a mixture of calcium and magnesium carbonates
  - 9.15.3 Mixture of calcium and magnesium oxalates
  - 9.15.4 Analysis of a mixture of  $\text{AgNO}_3$  and  $\text{Cu}(\text{NO}_3)_2$
  - 9.15.5 Complex mixture
- 9.16 Summary
- 9.17 Key words
- 9.18 References for further studies

---

## 9.0 Objectives of the unit

After studying this unit you are able to

- Explain the principle of TGA,
- Describe the experimental setup of TGA,
- Interpret the analytical information from TGA curves
- Describe the applications of TGA in qualitative and quantitative analysis of inorganic, organic and polymer material.

## 9.1 Introduction

Thermogravimetric analysis (TGA) is the most widely used thermal method. It is based on the measurement of mass loss of material as a function of temperature. In thermogravimetry a continuous graph of mass change against temperature is obtained when a substance is heated at a uniform rate or kept at constant temperature. A plot of mass change versus temperature ( $T$ ) is referred to as the thermogravimetric curve (TG curve). For the TG curve, we generally plot mass ( $m$ ) decreasing downwards on the y axis (ordinate), and temperature ( $T$ ) increasing to the right on the x axis (abscissa). Sometime we may plot time ( $t$ ) in place of  $T$ . TG curve helps in revealing the extent of purity of analytical samples and in determining the mode of their transformations within specified range of temperature. In thermogravimetry, the term 'decomposition temperature' is a complete misnomer. In a TG curve of single stage decomposition, there are two characteristic temperatures; the initial  $T_i$  and the final temperature  $T_f$ .  $T_i$  is defined as the lowest temperature at which the onset of a mass change can be detected by thermo balance operating under particular conditions and  $T_f$  as the final temperature at which the particular decomposition appear to be complete. Although  $T_i$  has no fundamental significance, it can still be a useful characteristic of a TG curve and the term *procedural decomposition temperature* has been suggested. The difference  $T_f - T_i$  is termed as reaction interval. In a dynamic thermogravimetry a sample is subjected to continuous increase in temperature usually linear with time whereas in isothermal or static thermogravimetry the sample is maintained at a constant temperature for a period of time during which any change in mass is noted. Now we will take up the instrumentation commonly used to obtain TG Curve.

## 9.2 Thermogravimetric analysis (TGA)

*Thermogravimetric analysis (TGA) is an analytical technique used to determine a material's thermal stability and its fraction of volatile components by monitoring the weight change that occurs as a specimen is heated.* The measurement is normally carried out in air or in an inert

---

atmosphere, such as Helium or Argon, and the weight is recorded as a function of increasing temperature.

Sometimes, the measurement is performed in a lean oxygen atmosphere (1 to 5% O<sub>2</sub> in N<sub>2</sub> or He) to slow down oxidation. In addition to weight changes, some instruments also record the temperature difference between the specimen and one or more reference pans (differential thermal analysis, or DTA) or the heat flow into the specimen pan compared to that of the reference pan (differential scanning calorimetry, or DSC). The latter can be used to monitor the energy released or absorbed via chemical reactions during the heating process.

In the particular case of carbon nanotubes, the weight change in an air atmosphere is typically a superposition of the weight loss due to oxidation of carbon into gaseous carbon dioxide and the weight gain due to oxidation of residual metal catalyst into solid oxides.

### 9.3 Principle

Changes in the mass of a sample are studied is a subject of a program.

Changes in temperature affect the sample. Not all thermal changes/events brings a changes in mass of sample, i.e, melting, crystallization but some thermal events i.e, desorption, absorption, sublimation, vaporization, oxidation, reduction and decomposition brings changes in mass of sample

it is used in analysis of volatile products, gaseous products lost during the reaction in thermoplastics, thermosets, elastomers, composites, films, fibers, coatings, paints ect....

### 9.4 Types of TGA

There are three types of themogravimetry they are

Dynamic TGA: In this type of analysis, the sample is subjected to condition of continuous increase in temperature usually linear with time.

Isothermal or static TGA: in this type of analysis, sample is maintained at a constant temperature for a period of time during which change in weight is recorded.

Quasistatic TGA: in this technique sample is heated to a constant weight at each of a series of increasing temperature.

### 9.5 Instrumentation

The instrument used in thermogravimetry (TG) is called a *thermobalance*. It consists of following basic components in order to provide the flexibility necessary for the production of useful analytical data in the form of TGA Curve.

Basic components of a typical thermobalance are

i) Balance

- ii) Furnace (heating device)
- iii) Unit for temperature measurement and control (Programmer)
- iv) Recorder( automatic recording unit for the mass and temperature changes)

**a) Balance**

The essential requirements of an automatic recording thermobalance are accuracy, sensitivity, reproducibility, and capacity. The simple block diagram of thermobalance is shown in figure 1.

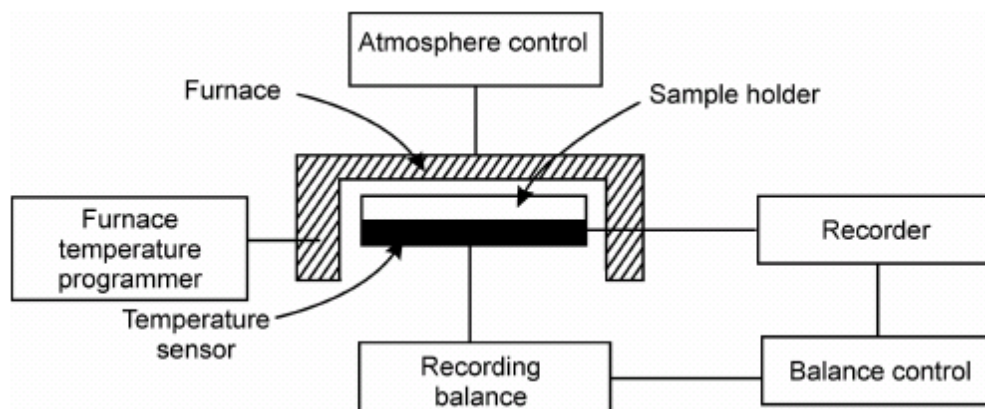


**Figure 1:** Block diagram of a thermobalance

Two types of recording thermobalances are generally used in thermogravimetry analysis they are null point type balance and deflection type balance.

The *null type balance*, are more widely used. A sensing element is incorporated to balance which detects a deviation of the balance beam from its null position. A sensor detects the deviation and triggers the restoring force to bring the balance beam to back to the null position. The restoring force is directly proportional to the mass change.

*Deflection balance* type involve the conversion of the balance beam deflection about the fulcrum into a suitable mass–change trace by

- a) Photographic recoding i.e change in path of a reflected beam of light available of photographic recording
- b) Recording electrical signals generated by an appropriate displacement measurement transducer and
- c) Using an electrochemical device.

The different balances used in TG instruments are having measuring range from 0.0001 mg to 1 g depending on sample containers used.

**b) Furnace**

The furnace and control system are designed to produce linear heating at over the whole working temperature range of the furnace and provision is made to maintain any fixed

temperature. A wide temperature range generally  $-150^{\circ}\text{C}$  to  $2000^{\circ}\text{C}$  of furnaces is used in different instruments. The range of furnace basically depends on the types of heating elements are used.

**c) Temperature measurement and control**

Temperature measurement are commonly done using thermocouples, chromal–alumel thermocouple are often used for temperature up to  $1100^{\circ}\text{C}$  whereas Pt/(Pt–10%Rh) is employed for temperature up to  $1750^{\circ}\text{C}$ . Temperature may be controlled or varied using a program controller with two thermocouple arrangement. The signal from one actuates the control system whilst the second thermocouple is used to record the temperature.

**d) Recorder**

Graphic recorders are preferred to meter type recorders. X-Y recorders are commonly used as they plot weight directly against temperature. The present instrument facilitate microprocessor controlled operation and digital data acquisition and processing using personal computer with different types recorder and plotter for better presentation of data.

### 9.6 Types of TGA instruments

The schematic TGA instrument is shown in Figure 2. The sample is heated under nitrogen or synthetic air with constant heat rate while the difference of the mass during this process is measured. A mass loss indicates that a degradation of the measured substance takes place. The reaction with oxygen from the synthetic air for example could lead to an increase of mass.

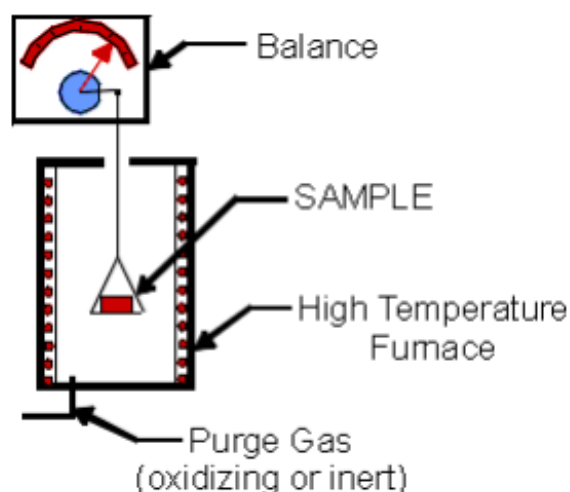


**Figure 2:** Schematic principle of TGA measurement

TGA instruments can be divided into two general types: vertical and horizontal balance. Vertical balance instruments have a specimen pan hanging from the balance. It is necessary to calibrate these instruments in order to compensate for buoyancy effects due to the variation



in the density of the purge gas with temperature. Vertical balance instruments generally do not have reference pan and are incapable of true DTA measurements.

Horizontal balance instruments normally have two pans (sample and reference) and can perform DTA and DSC measurements. They are considered free from buoyancy effects, but require calibration to compensate for differential thermal expansion of balance arms.

### 9.7 Thermogravimatic curves

TG curves represent the variation in the mass ( $m$ ) of the sample with the temperature ( $T$ ) or time ( $t$ ). Normally, plot of mass loss in downward and mass gain in upwards on the ordinate ( $y$ ) axis was done as shown in Figure 3.

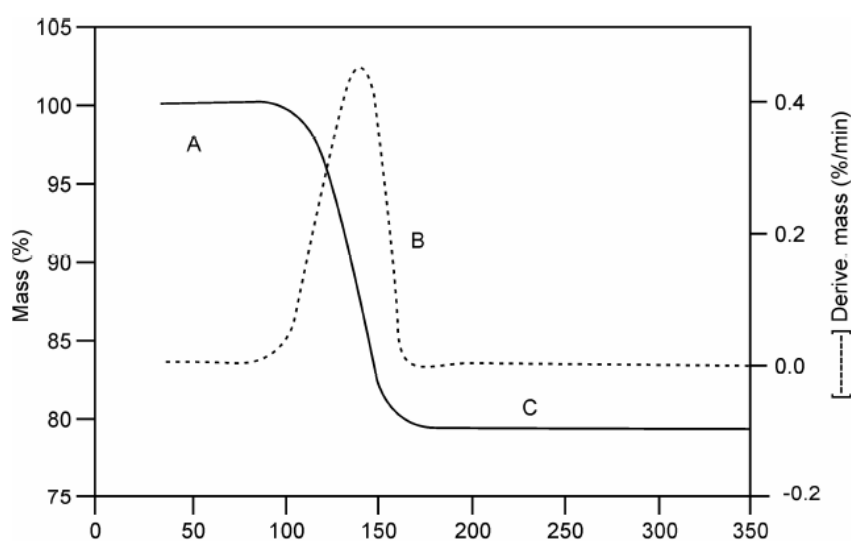


**Figure 3:** TG Curve. The plateau of constant weight (region A), the mass loss portion (region B), and another plateau of constant mass (region C)

Sometime (when substance is heated at uniform rate) a derivative thermogravimetric (DTG) curves is recorded. A DTG curve presents the rate of mass change ( $dm/dt$ ) as a function of temperature, or time ( $t$ ) against  $T$  on the abscissa ( $x$  axis) as shown in Figure 4. In this figure, the derivative of the curve is shown by dotted lines.

### 9.8 Sources of errors in TGA

There are a number of sources of error in TGA, and they can lead to inaccuracies in the recorded temperature and mass data. Some of the errors may be corrected by placing the thermobalance at proper place and handling it with great care.

#### *i) Buoyance effect*

If a thermally inert empty crucible is heated, there is usually an apparent weight change as temperature increases. This is due to effect of change in buoyancy of the gas in the sample

---

environment with the temperature, the increase convection and possible effect of heat from the furnace in the balance itself. In modern thermobalances, this effect is negligible. However, if necessary, a blank run with empty crucible can be performed over the appropriate temperature range. The resultant record can be used as a correction curve for subsequent experiment performed in the same condition.

i) *Condensation on balance suspension*

Condensation of the sample will also affect the mass of the sample and consequently the shape of TG curve. This can be avoided by maintaining a dynamic atmosphere around the sample in the furnace so that the entire condensable product may be driven by the flowing gases.

- ii) Random fluctuation of balance mechanism
- iii) Reaction between sample and container
- iv) Convection effect from furnace
- v) Turbulence effect from gas flow
- vi) Induction effect from furnace

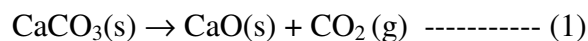
Errors of type (iii) can be avoided by proper placing of balance in the laboratory and error (v) can be avoided by sensible choice of sample container. Last three errors (v-vii) have to be considered in the design of the furnace, the balance and its suspension system. By avoiding excessive heating rate and proper gas flow rate some of above mentioned errors may be avoided.

### **9.9 Calibration of thermobalance for the measurement of mass**

It can be done by adding known mass of the sample container and noting the reading of the chart. Temperature calibration: ferromagnetic standards are used for this purpose. In a magnetic field these substances have shown detectable mass changes. The ferromagnetic standards are quite suitable for the temperature range from 242 to 771°C.

### **9.10 Interpretation of TG curves**

TG curves of a pure compound are characteristic of that compound. Using TG curve we can relate the mass changes to the stoichiometry involved. This can often lead us directly to the quantitative analysis of samples whose quantitative composition is known. To further illustrate, let's consider the example of TGA curve of  $\text{CaCO}_3$  shown in figure 5. This curve indicates that  $\text{CaCO}_3$  decomposes in a single step between 800°C and 950°C to form stable oxide  $\text{CaO}$  and the gas carbon dioxide. This can be explained the chemistry of  $\text{CaCO}_3$  when it is heated.



$$\text{Mr} \quad 100.1 \quad 56.1 \quad 44$$

Figure 4 indicates the % mass lost by the sample is 44 (100.1–56.1) between 800 and 950°C. This exactly corresponds to the mass changes calculations based on stoichiometry of the decomposition of CaCO<sub>3</sub>. The percentage weight loss of CaCO<sub>3</sub> will be

$$m\% = \frac{M_r(\text{CO}_2)}{M_r(\text{CaCO}_3)} \times 100$$

$$m\% = \frac{44}{100.1} \times 100$$

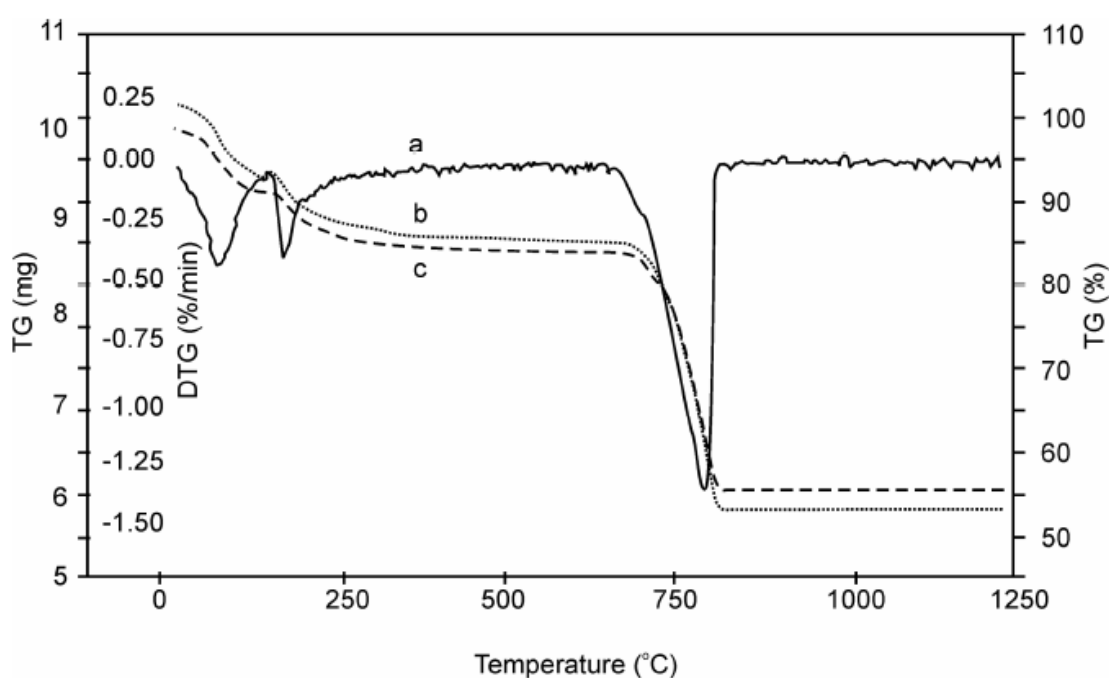


**Figure 4:** TG and DTG Curve of CaCO<sub>3</sub> at various heating rates (b = 10 °C, c = 3 °C)  
(DTG = Rate of Change of mass, dm/dt) curve

We have seen above how TG Curves is related to stoichiometry (quantitative interpretation). In next example we will see how it can be used to compare thermal stability of materials (qualitative interpretation). Such information can be used to select material for certain end-use application, predict product performance and improve product quality etc....

Figure 5 gives TG curves of some polymers. TG Curves clearly indicate that polymer (PVC) is the least thermally stable and polymer (PS) is most thermally stable. Polymer (PS) loses no weight at all below about 500°C and then decomposes abruptly by about 600°C. The other three polymers have all decomposed by about 450°C. Polymers (PMMA) decomposes more

slowly than the others as indicated by slopes of TG curves. TG curve of polymer (PMMA) has less slope than the others.

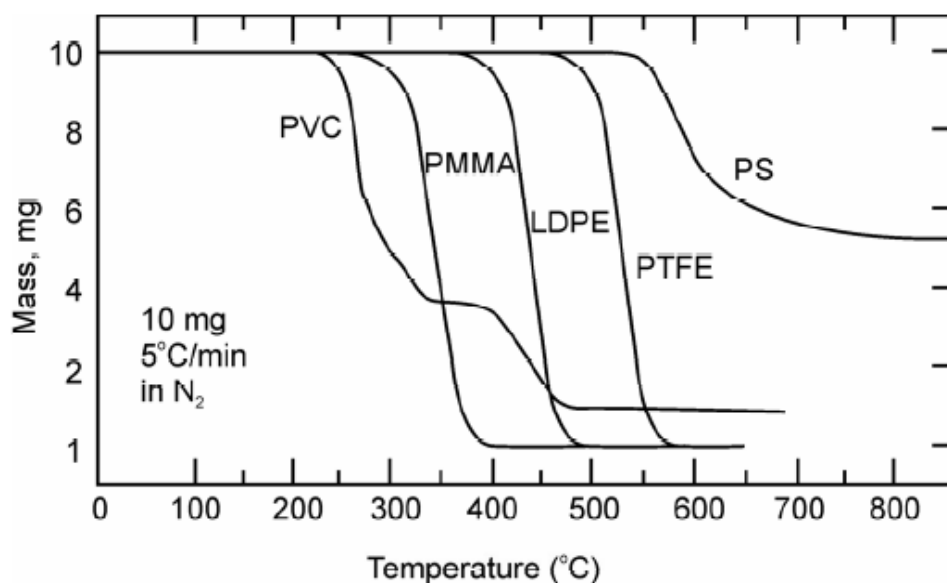


**Figure 5:** TG Curves of some polymers: PVC = polyvinyl chloride; PMMA = polymethyl methacrylate, LDPE = low density poly ethylene; PTFE = polytetra fluoroethylene; and PS = polystyrene.

### 9.11 Types of TG curves

TG curves are classified according to their shapes in to seven types as shown in Figure 6.

Type A: This curve shows no mass change over the entire range of temperature. It can be concluded that the decomposition temperature for a sample is greater than the temperature range of instrument.

Type B: this curve shows that there is large mass loss followed by mass plateau and is formed when evaporation of volatile product(s) during drying, desorption or polymerization takes place. If a non-interacting atmosphere is present in the chamber, type B curve will change in to type A curve.

Type C: this curve shows the single-stage decomposition temperatures ( $T_i$  and  $T_f$ ).

Type D: this curve shows the multi-stage decomposition processes where reaction is resolved.

Type E: this curve shows the multi-stage decomposition reaction where reaction is not resolved.

Type F: this curve shows the increase in mass in the presence of an interacting atmosphere, example, surface oxidation reaction.

Type G: this curve shows a multiple reaction one after the other, example, surface oxidation reaction followed by decomposition of reaction product(s)

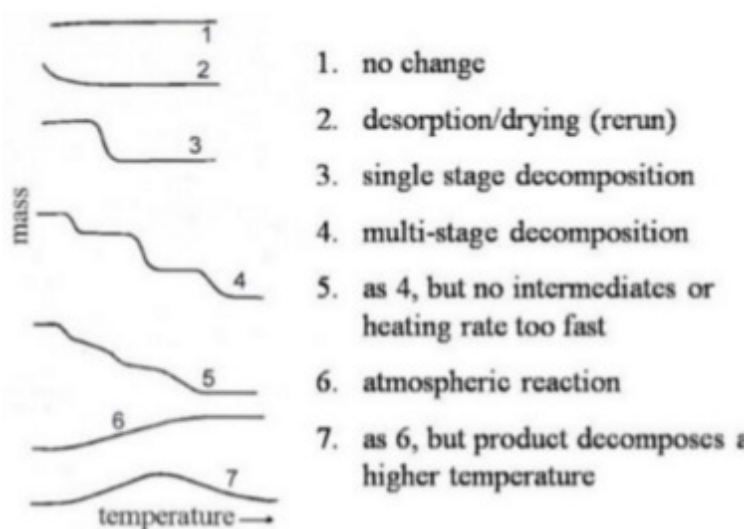


**Figure 6:** Classification of TG curves

### 9.11.1 Plateau

A plateau is the part of the TG curve where the mass is essentially constant or there is no change in mass.

### 9.11.2 Procedural decomposition temperature

The initial temperature  $T_i$  is that temperature at which the cumulative mass change reaches a magnitude that the thermobalance can detect.

### 9.11.3 Final temperature

The final temperature  $T_f$ , is that temperature at which the cumulative mass changes reaches maximum.

### 9.11.4 The reaction interval

The reaction interval is the temperature difference between  $T_f$  and  $T_i$ .

### 9.11.5 Isobaric mass change determination

A technique in which the equilibrium mass of a substance at constant partial pressure of the volatile product(s), is measured as a function of temperature while the substance is subjected to a controlled temperature program. The record is the isobaric mass change curve, the mass is plotted on Y-axis and temperature on X-axis increasing from the left to right.

### 9.11.6 Evolved gas detection (EGD)

A technique in which evolution of gas from a substance is detected as a function of temperature while the substance is subjected to a controlled temperature program.

### 9.11.7 Evolved gas analysis (EGA)

A technique in which the nature and/or amount of volatile product(s) released by a substance are measured as a function of temperature while the substance is subjected to a controlled temperature program. the method of analysis should be clearly stated.

### 9.12 Information from TG curve

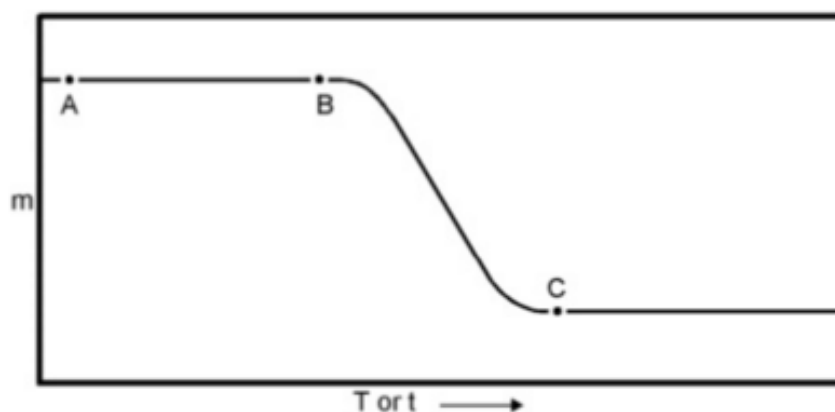


**Figure 7:** Formalized TG curve

Plot of weight/mass against temperature of time produced by a thermalgravimeter is called thermogram. The following features of TG curve should be noted from above figure 7.

*Plateau:* a region of no mass change indicates the thermal stability of the sample/substance. Thermal stability is the ability of a substance to maintain its properties as nearly unchanged as possible on heating. this information about the thermal stability is significant for engineers as they then know the temperature ranges of in which substances like alloy, building materials polymers etc.... can be used.

*Weight/mass loss:* heating a sample to given temperature causes it to lose weight/mass. Mass/weight loss is informative to inorganic chemist who can then determine the composition of substance/sample and understand the reaction involved in decomposition.

*Procedural decomposition temperature:* by looking at thermogram, one can determine the procedural decomposition temperature  $T_i$  indicating the decomposition or evaporation of sample/substance.

*Composition:* Weight/mass lost by heating helps determine the composition of substance/sample, also allows analytical chemist to identify unknown compound or determine the amount/percentage/weight of a compound in mixture of different compounds.

### 9.13 Factors affecting TG curve

We have already discussed that the lowest temperature,  $T_i$  at which the onset of a mass change can be detected by the thermobalance operating under particular conditions and  $T_f$  is the final temperature at which the decomposition completed. Actually in TGA experiments,

---

both  $T_i$  and  $T_f$  do not have fundamental significance, but they can still be a useful characteristic of a TG curve. The term *procedural decomposition temperature* is often used for the temperature at which mass change appears to commence. This indicates that procedural decomposition temperature does not have a fixed value, but depends on the experimental procedure employed to get it. Similar to this there are many factors which influence a TGA curve. These factors may be due to instrumentation or nature of sample. The main factors affect the shape precision and accuracy of the experimental results in thermogravimetry are listed below

1. Instrumental factors

- i) Furnace heating rate
- ii) Recording or chart speed
- iii) Furnace atmosphere
- iv) Geometry of sample holder/ location of sensors
- v) Sensitivity of recording mechanism
- vi) Composition of sample container

2. Sample Characteristics

- a) Amount of sample
- b) Solubility of evolved gases in sample
- c) Particle size
- d) Heat of reaction
- e) Sample packing
- f) Nature of sample
- g) Thermal conductivity.

a) *Furnace heating rate*

At a given temperature, the degree of decomposition is less in the case of slower heating rate. therefore the shape of the TG curve is influenced by the heating rate. For a single stage endothermic reaction it has been found that

- i)  $(T_i)_F > (T_i)_S$
- ii)  $(T_f)_F > (T_f)_S$
- iii)  $(T_f - T_i)_F > (T_f - T_i)_S$

where subscripts F and S indicate fast and slow heating rate respectively.

For example, calcium carbonate would not show any mass loss below 600 °C, when heated in a thermobalance at heating rate of 3°C per min., and yet it is known that CO<sub>2</sub> is evolved at

250 °C. Similarly, polystyrene decomposes 10% by mass when heating rate is 1°C per min by 357 °C and 10% by mass when heating rate is 5°C per min by 394°C. More specifically, it is observed that the procedural decomposition temperature  $T_i$ , and also  $T_f$  (the procedural final temperature) will decrease with decrease in heating rate and the TG curve will be shifted to the left. The appearance of an inflection in a TG curve at a fast heating rate may well be resolved into a plateau at a slower heating rate. Therefore, in TGA there is neither optimum no standard heating rate, but a heating rate of 3°C per min. gives a TG curve with maximum meaningful resolution.

b) *Recording or chart speed*

The chart speed on the recording of the TG curve of rapid or slow reaction has pronounced effect on the shape of the TG curves. For a slow decomposition reaction low chart speed is recommended for recording the TG curve because at high chart speed the curve will be flattened and it will not show the sharp decomposition temperature. For a slow reaction followed by a rapid one at the lower chart speed the curve will show less separation in the two steps than the higher chart speed curve. For fast-fast reaction followed by slower one similar observation was observed in shorter curve plateaus.

c) *Furnace atmosphere*

The effect of atmosphere on the TG curve depends on

- i) The types of the reaction
- ii) The nature of the decomposition products and
- iii) Type of the atmosphere employed.

The effect of the atmosphere on TG curve may be illustrated by taking the example of thermodecomposition of a sample of monohydrates of calcium oxalate in dry  $O_2$  and dry  $N_2$  as shown Figure 8.

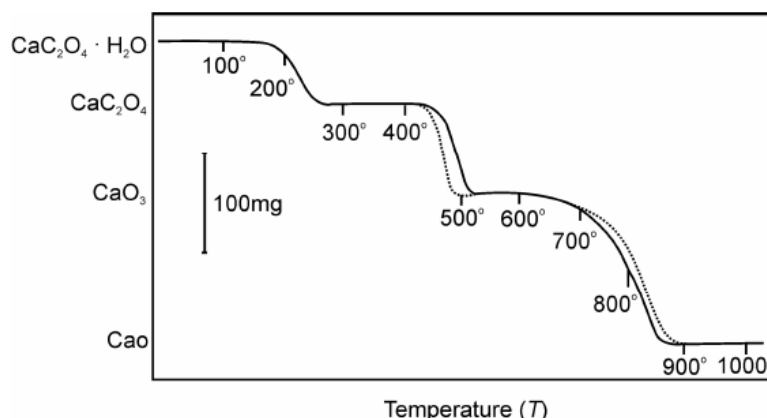
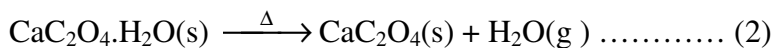


**Figure 8:** TG Curve of Calcium Oxalate in  $O_2$  and  $N_2$  atmosphere

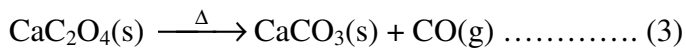
[ —————  $N_2$  , - - - - -  $O_2$  ]



The first step, which is dehydration is reversible reaction.

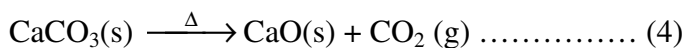


This is unaffected because both gases are equally effective in sweeping the evolved water vapours away from the sample surface. For the second step,



The curve diverges in O<sub>2</sub> atmosphere because the oxygen reacts with evolved CO, giving a second oxidation reaction which is highly exothermic and so raises the temperature of the unreacted sample. The temperature accelerates the decomposition of the compound more rapidly and completely at a lower temperature as shown in the above diagram in dry O<sub>2</sub> then in N<sub>2</sub> atmosphere.

The third step in decomposition reaction is also reversible reaction.



This step should not be influenced by O<sub>2</sub> or N<sub>2</sub>. However there is a slight difference in curves for the two gases as shown in diagram. The small difference was due to the difference in the nature/composition of CaCO<sub>3</sub> formed in the two atmospheres. This is due to the particle size, surface area, lattice defects or due to the other physical characteristics of CaCO<sub>3</sub> formed.

#### d) *Sample holder*

The sample holders range from flat plates to deep crucible of various capacities. The shape of the TG curve will vary as the sample will not be heated in identical condition. Generally, it is preconditioning that the thermocouple is placed on near the sample as possible and is not dipped into the sample because it might be spoiled due to sticking of the sample to the thermocouple on heating. So actual sample temperature is not recorded, it is the temperature at some point in the furnace near the sample. Thus it leads to source of error due to the thermal lag and partly due to the finite time taken to cause detectable mass change. If the sensitivity of recording mechanism is not enough to record the mass change of the sample then this will also cause error in recording the weight change of the sample. If the composition of the sample contains is such that it reacts either with the sample, or product formed or the evolved gases then this will cause error in recording the mass change of the sample.

#### e) *Effect of sample mass*

The sample mass affects the TG curve in following

- i) The endothermic and exothermic reactions of the sample will cause sample temperature to deviate from a linear temperature change.

- ii) The degree of diffusion of evolved gases through the void space around the solid particles.
- iii) The existence of large thermal gradients throughout the sample particularly, if it has a low thermal conductivity.

Thus, it is preferable to use as small a sample as possible depending on the sensitivity of the balance.

f) *Effect of sample particle size*

The particle size will cause a change in the diffusion of the evolved gases which will alter the reaction rate and hence the curve shape. The smaller the particle size, greater the extent of decomposition at any given temperature. The use of large crystal may result in apparent very rapid mass loss during heating. This may be due to the mechanical loss of part of the sample by forcible ejection from the sample container, when the accumulated evolved gases within the coarse grains are suddenly released.

g) *Effect of heat of reaction*

The heat of reaction will affect the extent to which sample temperature proceeds or succeeds the furnace temperature. This depends on whether the reaction is exothermic or endothermic and consequently the extent of decomposition will also be affected. The other sample characteristics such as sample packing, nature of the sample and its thermal conductivity will also affect the shape of TG curves. If the sample is packed loosely then the evolved gases may diffuse more easily than if the sample packed tightly.

If the sample reacts with the sample container on heating then it will not give the mass of the product formed so the sample will change. We can avoid this effect by a sensible choice of sample container.

#### **9.14 Applications of thermogravimetric analysis**

So far we have studied how TGA can be used to understand the chemistry of decomposition of a particular compound. Information regarding the temperature range over which a particular sample appears to be stable or unstable can also be studied by TGA. Beside these thermogravimetric analysis can be used for various other applications. Some of are listed below

- i) Purity and thermal stability
- ii) Solid state reactions.
- iii) Decomposition of inorganic and organic compounds.
- iv) Determining composition of the mixture
- v) Corrosion of metals in various atmospheres

- vi) Pyrolysis of coal, petroleum and wood.
- vii) Roasting and calcinations of minerals.
- viii) Reaction kinetics studies.
- ix) Evaluation of gravimetric precipitates.
- x) Oxidative and reductive stability.
- xi) Determining moisture, volatile and ash contents.
- xii) Desolvation, sublimation, vaporizations, sorption, desorption, chemisorptions.

It is not possible to discuss all these applications at this level; it is worth to describe some of the applications which are more common.

### 9.15 Analysis of inorganic and organic mixtures

The single and pure compound gives characteristic TG curves. Now, we will see how TG Curves can be used in predicting relative quantities of the components of a mixture.

#### 9.15.1 Binary mixtures

Consider a mixture of two compounds AB and CD having characteristic TG Curves which are different from each other as shown in Figure 9

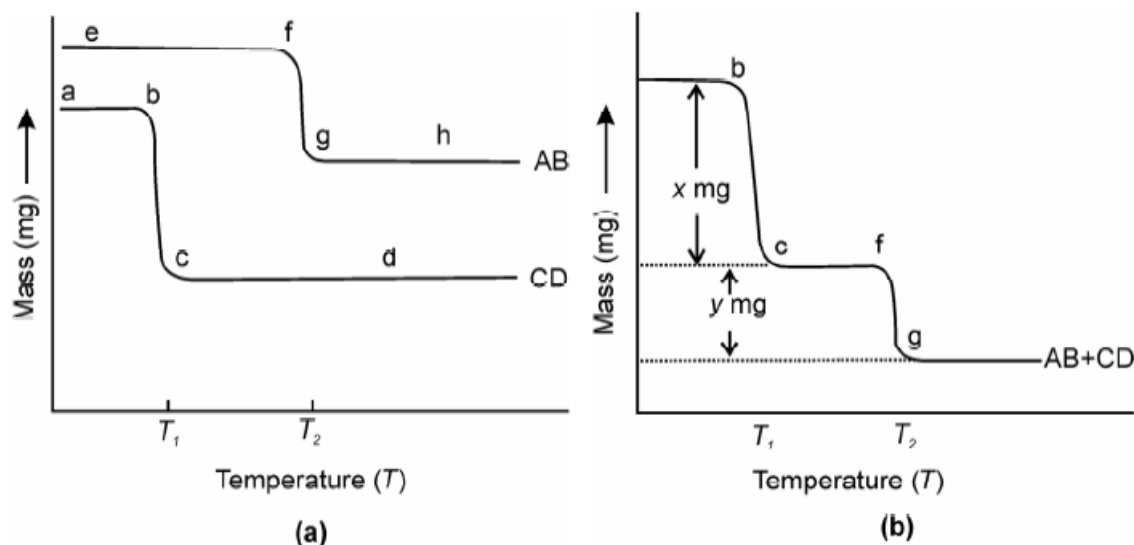


**Figure 9:** (a) Thermogravimetric curves of two compounds AB and CD and (b) their mixture

The decomposition of pure compound AB and CD occur at  $T_1$ , (labeled as bc) and temperature  $T_2$ , (labeled as fg) respectively, as illustrated in Figure 9(a). The TG curve of mixture of AB and CD together is shown in Figure 9(b). We can see from this figure, the plateaus (corresponding to the regions of constant mass) commence at about the same temperature as they do in the TG Curves for the pure compounds AB and CD. We can also notice that the mass loss overall up to  $T_1$  is  $x$  mg and from  $T_1$  to  $T_2$  it is an additional  $y$  mg. By

measuring these two quantities  $x$  and  $y$  from the TG curves we can determine the relative quantities of AB and CD in the original binary mixture.

For example; consider the mixtures of calcium and magnesium carbonates.

### 9.15.2 Analysis of a mixture of calcium and magnesium carbonates

A typical TG curve of a mixture of calcium and magnesium carbonates is shown in Figure 10. We can notice that a significant mass loss occurs before 210°C. This is due to the moisture present in the mixture. Another mass loss at about 480°C is due to the following reaction



Earlier we mentioned that  $\text{CaCO}_3$  decomposes at about 800°C. In Figure 9 mass loss between about 600°C and 900°C can be interpreted due to decomposition of  $\text{CaCO}_3$ .



Portion of the curve ab represents a mixture of MgO and  $\text{CaCO}_3$  and cd represents a residue of the mixture of MgO and CaO. Both these plateaus ab and cd represent weight  $m_1$  and  $m_2$ , respectively. In fact mass  $m_1$  is due to  $\text{CaCO}_3 + \text{MgO}$ .

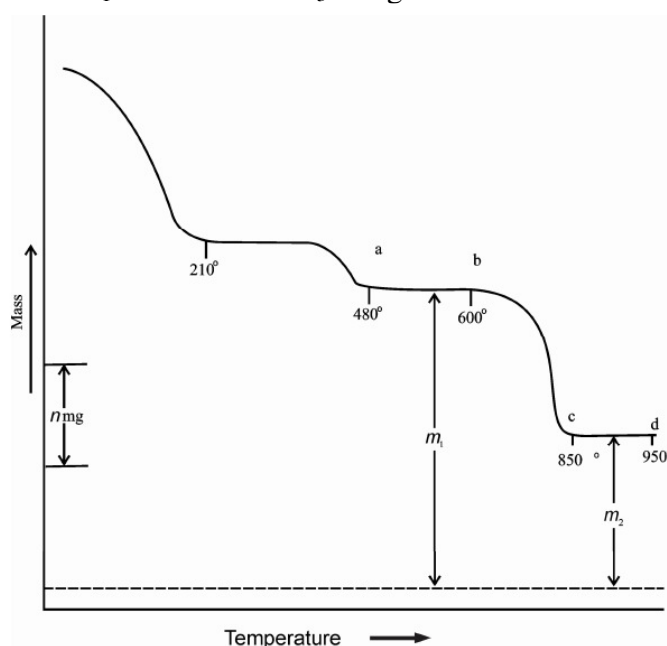


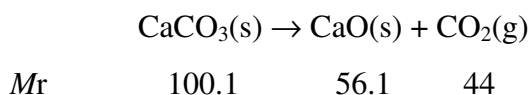
**Figure 10:** TG curve of mixture of calcium and magnesium carbonate

Thus,  $m_1 - m_2$  is the loss of  $\text{CO}_2$  between 500°C and 900°C due to the decomposition of  $\text{CaCO}_3$ . Using TGA curve we can relate the mass of different components formed during TGA experiment. The mass of CaO ( $m_3$ ) formed can be calculated using following Eq. (3)

$$m_3 = 1.27(m_1 - m_2) \dots (3)$$

This equation can be obtained as follows

The CaO is formed by the evolution of CO<sub>2</sub> on the decomposition of CaCO<sub>3</sub>,



From the above equation 1mole of CaCO<sub>3</sub> gives 1 mole of CO<sub>2</sub> and 1mole of CaO. Thus,

moles of CO<sub>2</sub> in the given examples =  $\frac{(m_1 - m_2)}{M_r(\text{CO}_2)}$  and this is equal to moles of CaO formed.

Thus the amount of CaO must be,  $m_3 = \frac{(m_1 - m_2)}{44} M_r(\text{CaO})$

where,  $M_r(\text{CaO})$  is the relative molar mass of CaO.

$$m_3 = \frac{(m_1 - m_2)}{44} \times 56 \text{ g}$$

$$m_3 = 1.27(m_1 - m_2) \text{ g}$$

We know the mass of residue left, i.e.,  $m_2$ , the mass of MgO ( $m_4$ ) can be calculated.

$$m_4 = m_2 - m_3$$

Here  $m_3$  is the mass of CaO formed, which is equal to  $1.27(m_1 - m_2)$ . Thus

$$m_4 = m_2 - 1.27(m_1 - m_2)$$

Mass of the Ca ( $m_{\text{Ca}}$ ) in the original sample can also be related to  $m_1$  and  $m_2$  by the following formula

$$m_{\text{Ca}} = 0.91(m_1 - m_2)$$

This can be obtained as follows:

We know, amount of Ca in CaCO<sub>3</sub> and CaO will be equal in moles, therefore amount of Ca in

$$m_{\text{Ca}} = m_3 \times \frac{A_r(\text{Ca})}{M_r(\text{CaO})} = 1.27(m_1 - m_2) \times \frac{A_r(\text{Ca})}{M_r(\text{CaO})}$$

where,  $A_r(\text{Ca})$  and  $M_r(\text{CaO})$  are the relative atomic mass and relative molar mass of Ca and CaO, respectively. Thus,

$$= 1.27(m_1 - m_2) \times 40/56 = 0.91(m_1 - m_2)$$

Similarly, mass of magnesium in the original sample can be related to  $m_1$  and  $m_2$

Thus, the mass of Mg in original sample ( $m_{\text{Mg}}$ )

$$= (\text{mass of residue} - \text{mass of CaO}) \times \frac{A_r(\text{Mg})}{M_r(\text{MgO})}$$

$$m_{\text{Mg}} = (m_2 - m_3) \times \frac{A_r(\text{Mg})}{M_r(\text{MgO})} = (m_2 - m_3) \times \frac{24.3}{40.3}$$

$$m_{\text{Mg}} = 0.60(m_2 - m_3)$$

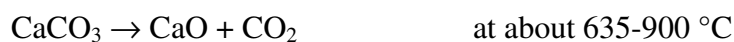
### 9.15.3 Mixture of calcium and magnesium oxalates

Calcium oxalate monohydrate is unsatisfactory weighing form for determining calcium as oxalate because its tendency to retain excess moisture even at 110°C, co-precipitated ammonium oxalate remain un-decomposed. The anhydrous calcium oxalate is hygroscopic but  $\text{CaCO}_3$  is excellent weighing form if heated to  $500 \pm 25$  °C as can be seen in TG curve of  $\text{CaC}_2\text{O}_4 \cdot \text{H}_2\text{O}$ . Above 635°C the decomposition of  $\text{CaCO}_3$  commences to become significant under usual laboratory conditions and completely converted to CaO at 900°C. Thus, calcium oxalate monohydrate decomposes in three steps,

First step is dehydration,

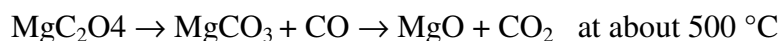
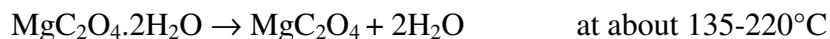
Second step involves removal of CO and formation of  $\text{CaCO}_3$

Third step includes  $\text{CaCO}_3$  decomposes to CaO. See Figure 11.



But magnesium oxalate dihydrate decomposes in two steps instead of three steps.

First, dehydration then removal of CO and  $\text{CO}_2$  simultaneously and forming MgO, there is no horizontal corresponding to  $\text{MgCO}_3$  as it is thermally unstable at this temperature.



The TG curve for the mixture of  $\text{CaC}_2\text{O}_4 \cdot \text{H}_2\text{O}$  and  $\text{MgC}_2\text{O}_4 \cdot 2\text{H}_2\text{O}$  shows two mass losses up to 500 °C, first at about 200°C due to loss of water and the second mass loss occurs in the 390-500°C range which is due to decomposition of both calcium and magnesium oxalates.

Thus, at 500°C, the composition of the mixture will be  $\text{CaCO}_3$  and MgO.

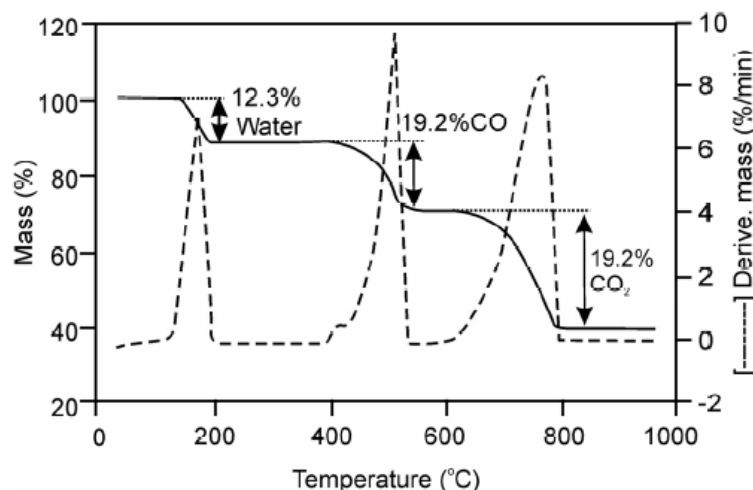


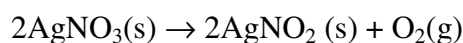
**Figure 11:** DTG/TG curve of calcium oxalate

Third mass loss after 500°C is due to only the decomposition of CaCO<sub>3</sub>. If  $m_1$  and  $m_2$  are the mass of the mixture at 500°C and 900°C then similar to the previous example we can calculate the amount of calcium and magnesium in the original sample.

#### 9.15.4 Analysis of a mixture of AgNO<sub>3</sub> and Cu(NO<sub>3</sub>)<sub>2</sub>

The TG curve of pure AgNO<sub>3</sub>, Cu(NO<sub>3</sub>)<sub>2</sub> and their mixture are given in Figure 12. Curve a is the curve of dry crystalline AgNO<sub>3</sub>. A horizontal extends to 340°C and is followed by descent as far as 473°C. At this temperature decomposition sets in abruptly and nitrous fumes are expelled up to 610°C. After that there is much slower mass loss from 610°C to 810°C.

Decomposition of AgNO<sub>2</sub>, which is not observed when CuO is present, no doubt the latter catalyses the decomposition. Above 810°C the weight is again constant due to the formation of pure Ag metal.



While the copper nitrate hexahydrate gives a quite different curve b. Water and nitrogen oxide are driven off up to 150°C to 200°C, then a horizontal indicates the existence of zone of a new compound, which has been analysed and it corresponds to a basic nitrate Cu(NO<sub>3</sub>)<sub>2</sub>·2Cu(OH)<sub>2</sub>. After that between 200°C and 610°C this compound decomposes vigorously from 250°C and subsequently more slowly. The residue is CuO which only become constant at 940°C.

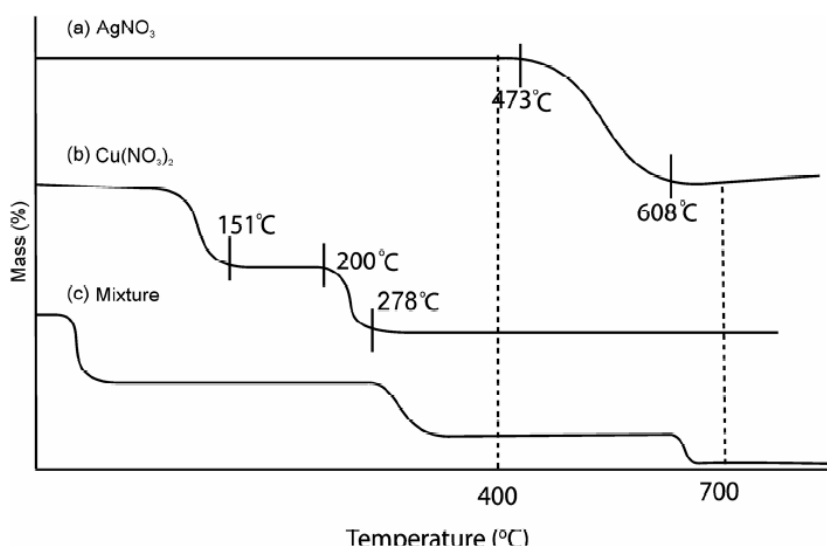
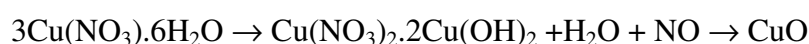


**Figure 12:** TG curve of nitrates: a: AgNO<sub>3</sub>, b: Cu(NO<sub>3</sub>)<sub>2</sub> and c: AgNO<sub>3</sub> + Cu(NO<sub>3</sub>)<sub>2</sub> mixture  
If a mixture of AgNO<sub>3</sub> and Cu(NO<sub>3</sub>)<sub>2</sub> is placed in thermobalance, the curve c is recorded. The horizontal related to the basic copper nitrate is, nevertheless, well marked. From 240°C

to 400°C there is a residue keeping constant mass ( $\text{AgNO}_3 + \text{CuO}$ ), while above 900°C a mixture of Ag + CuO is present.

If  $m_1$  and  $m_2$  are the mass of the sample at 400 °C and 700 °C, respectively, the amount of silver and copper in the sample can be calculated similar to previous example.

A binary alloy of Ag and Cu can be analyzed with  $\pm 3\%$  error by this method by dissolving the alloy in  $\text{HNO}_3$  and then running thermogram and recording successive weight at 400 °C and 700 °C by solving following simultaneous equations:

$$(170/108) x + (79/63) y = m_1$$

$$x + (79/63) y = m_2$$

where  $x$  and  $y$  are the masses of Ag and Cu in the alloy,  $m_1$  and  $m_2$  are the masses of the sample at 400 °C and 700 °C, respectively, 170 is the molar mass of  $\text{AgNO}_3$ , 1000 is the relative atomic mass of Ag, 79 is molar mass of  $\text{CuO}$  and 63 is the relative atomic mass of Cu.

### 9.15.5 Complex mixture

In this category we are considering the analysis of a mixture of calcium, strontium and barium oxalates. In the thermogram of a mixture of Ca, Sr and Ba oxalates it is noticed that in between 100 ° and 250 ° C the water of hydration is evolved from all metal oxalates, after the loss of the water of hydration, the curve exhibited a horizontal weight level from 250-360 °C, which corresponds to the composition for anhydrous metal oxalates. Then all the three oxalates decomposed simultaneously to the carbonates and the process completed at 500°C. Then from 500 °C to 620 °C the anhydrous carbonates were stable. On further heating, the  $\text{CaCO}_3$  decomposed in the temperature range 620°C- 860 °C to oxide followed by the decomposition of  $\text{SrCO}_3$  from 860 °C to 1100°C at which temperature  $\text{BaCO}_3$  began to decompose (see Figure 13 ). From weight loss curve, the following data are obtained.

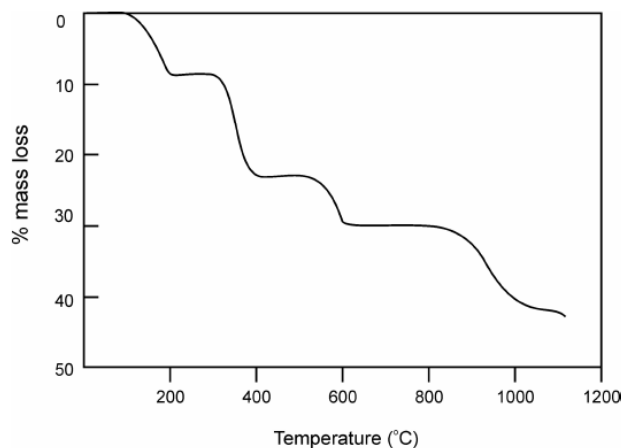


**Figure 13:** TGA Curve of the mixture of Calcium, Strontium and Barium oxalate



I- mass of hydrated oxalates at 100 °C(mass of the sample) =  $m_s$

II- mass of water of hydration =  $m_1$

III- mass of CO formed by the decomposition of metal oxalates =  $m_2$

IV- mass of CO<sub>2</sub> formed by the decomposition of CaCO<sub>3</sub> =  $m_3$

V- mass of CO<sub>2</sub> formed by the decomposition of SrCO<sub>3</sub> =  $m_4$

We can calculate the amount of Ca, Ba and Sr as follows

From the amount of CO<sub>2</sub> ( $m_4$ ) formed by the decomposition of SrCO<sub>3</sub>, we can calculate the mass of SrCO<sub>3</sub>. Simultaneously from the mass of CO<sub>2</sub> ( $m_3$ ) formed by the decomposition of CaCO<sub>3</sub>, we can calculate the amount of CaCO<sub>3</sub>.

From thermogram we know the total mass of all the carbonates, so by subtracting the amount of carbonates of Ca + Sr, we will get the mass of BaCO<sub>3</sub>.

From the mass of CaCO<sub>3</sub>, SrCO<sub>3</sub> and BaCO<sub>3</sub> we can calculate easily the amount of Ca, Sr and Ba present in the mixture. From the steps discussed above we can arrive on the following formula to calculate the amount of Ca =  $m_{Ca}$ , Sr =  $m_{Sr}$ , Ba =  $m_{Ba}$ .

Amount of Ca ( $m_{Ca}$ ) =  $0.91068 \times m_3$

Amount of Sr ( $m_{Sr}$ ) =  $1.9911 \times m_4$

Amount of Ba ( $m_{Ba}$ ) =  $0.58603 \times m_s - 1.9457 \times m_3 - 2.5788 \times m_4$

### 9.16 Summary

Thermal analysis comprises a group of techniques where the properties of material are studied as they change with temperature. To determine the thermo-physical properties several methods are commonly used: differential thermal analysis (DTA), differential scanning calorimetry (DSC), thermogravimetric analysis (TGA), dilatometry (DIL), evolved gas analysis (EGA), dynamic mechanical analysis (DMA), dielectric analysis (DEA) etc. In metallurgy, material science, pharmacy and food industry the main application of the DTA and DSC is used for studying phase transition under different atmospheric influences, temperatures and heating / cooling rates. Common laboratory equipment has a combination of two thermal analysis techniques. Most common is the simultaneous thermal analysis (STA) apparatus as the combination of thermogravimetric analysis (TGA) and differential thermal analysis (DSC).

### 9.17 Key words

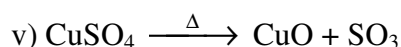
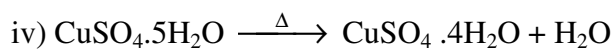
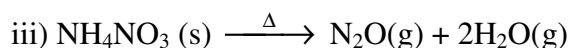
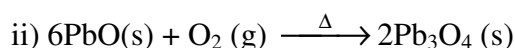
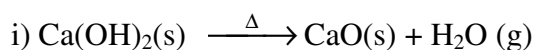
Thermogravimetric analysis (TGA); Types of TGA; Thermogravimetric curves; Plateau Isobaric mass change determination ; Evolved gas detection (EGD); Evolved gas analysis (EGA)

**9.18 References for further studies**

- 1) Principles and Applications of Thermal Analysis; Paul Gabbott; *John Wiley & Sons*, 2008.
- 2) Basic Concepts of Analytical Chemistry; S M Khopkar; *New Age International*, 1998.
- 3) Instrumental Methods of Chemical Analysis; Dr. B. K. Sharma; *Krishna Prakashan Media*, 2000.
- 4) Characterization and Analysis of Polymers; Arza Seidel; *John Wiley & Sons*, 2008.
- 5) Pharmaceutical Drug Analysis; Ashutosh Kar; *New Age International*, 2007.

**9.19 Questions for self understanding**

- 1) List the different components of a thermobalance.
- 2) What are common source of errors in thermogravimetric analysis?
- 3) Calculate the percentage mass change ( $m\%$ ) for the following reactions.



- 4) A thermogram of a magnesium compound shows a loss of 91.0 mg from a total of 175.0 mg used for analyte. Identify the compound either as MgO, MgCO<sub>3</sub>, or MgC<sub>2</sub>O<sub>4</sub>
- 5) What are the common instrumental factors affecting TG curves.
- 6) A mixture of CaO and CaCO<sub>3</sub> is analysed by TGA. The result indicates that mass of the sample decreases from 250.6 mg to 190.8 mg only between 600°C and 900°C. Calculate the percentage of calcium carbonate in the mixture.
- 7) Formulate the solid state reaction of sodium bicarbonate when heated. It decomposes between 100 and 225 °C with evolution of water and carbon dioxide. The combined loss of water and carbon dioxide totaled 36.6% by mass whereas the mass loss due to carbon dioxide alone was found to be 25.4 %.
- 8) Thermogravimetric studies of carbon black filled rubber sample is performed in inert atmosphere upto 950 °C and then quickly changing the atmosphere to air. The observed weight loss is ~ 66.41% upto 500 °C and the mass becomes constant and further the mass loss between 1300 °C to 2800 °C . Predict the composition of rubber.
- 9) The TGA and DTA data Manganese Phosphate Monohydrate are shown in Table

TGA	150 °C (- H <sub>2</sub> O)	360°C (- PH <sub>3</sub> )	800°C (- H <sub>2</sub> O)	Nil		Nil
DTA	160 °C (endo)	375 °C (exo)	850 °C (endo)	590 °C (exo)	900°C (exo)	1180 °C (exo)

Explain the probable transition of unidentified peaks in TGA.

- 10) What types of standard are required to calibrate the mass variation obtained with a TGA equipment?
- 11) What type of standards are required for temperature calibration of any TGA.
- 12) A mixture of CaCO<sub>3</sub> and CaO is analysed using TGA technique. TG curve of the sample indicates that there is a mass change from 145.3 mg to 115.4 mg between 500–900 °C. Calculate the percentage of CaCO<sub>3</sub> in the sample.
- 13) A 250 mg hydrated sample of Na<sub>2</sub>HPO<sub>4</sub> decreases to a mass of 145.7 mg after heating to 15 °C. What is the number of water hydration in Na<sub>2</sub>HPO<sub>4</sub>.
- 14) Draw a labeled diagram of the TG curve obtained by heating a mixture of 80 mg of CaC<sub>2</sub>O<sub>4</sub>.H<sub>2</sub>O and 80 mg of BaC<sub>2</sub>O<sub>4</sub>.H<sub>2</sub>O to 1200 °C. Calculate the amount of all mass losses.

---

**UNIT-10****Structure**

10.0 Objectives of the unit

10.1 Introduction

10.2 Theory

10.2.1 Static Thermogravimetric Analysis

10.2.2 Dynamic Thermogravimetric Analysis

10.3 Principle

10.4 Characteristics of DTA Curves

10.4 Instrumentation

10.5 Methodology

10.6 Applications

10.7 Differential Scanning Calorimetry DSC

10.8 The difference between a heat flow and a heat flux DSC

10.9 Instrumentation

10.10 Theory of DSC

10.11 Information is obtainable from a DSC curve

10.12 Applications in the area of polymers

10.12.1 Energy (Ordinate) Calibration

10.12.2 Transformation temperatures of a shape memory alloy

10.12.3 Epoxy Mixtures

10.13 Summary of the unit

10.14 Key words

10.15 References for further study

10.16 Questions for self understanding

---

## 10.0 Objectives of the unit

After studying this unit you are able to

- Explain the principle of DTA, DSC and thermometric titration,
- Describe the experimental setup of DTA, DSC and thermometric titration,
- Interpret the analytical information from DTA and DSC curves and enthalpogram,
- Describe the applications of DTA, DSC and thermometric titration,

## 10.1 Introduction

Differential thermal analysis (DTA) is a thermal analysis using a reference. The sample and the reference material (sample) are heated in one furnace. The difference of the sample temperature and the reference material temperature is recorded during programmed heating and cooling cycles.

Differential Scanning Calorimetry (DSC) measures the change of the difference in the heat flow rate to the material (sample) and to a reference material while they are subjected to a controlled temperature program.

Like differential thermal analysis (DTA), differential scanning (DSC) is also an alternative technique for determining the temperatures of the phase transitions like melting point, solidification onset, re-crystallization onset, evaporation temperature etc. With differential thermal analysis DTA, which is an older technique than differential scanning calorimetry, the result is a DTA curve (Figure 1b). DTA curve is a curve of temperature difference between the sample material and the reference material versus temperature or time. The result of DSC is a curve of heat flux versus time or temperature and is therefore used also for determination of the enthalpy, specific heat ( $C_p$ ) etc.

Broadly speaking the thermoanalytical methods are normally classified into the following three categories, namely

- i) Thermogravimetric Analysis (TGA),
- ii) Differential Thermal Analysis (DTA), and
- iii) Thermometric Titrations

## 10.2 Theory

A large number of chemical substances invariably decompose upon heating, and this idea of heating a sample to observe weight changes is the underlying principle of thermogravimetric analysis (TGA).

However, TGA may be sub-divided into two heads, namely

- a) Static (or Isothermal) Thermogravimetric Analysis, and

---

b) Dynamic Thermogravimetric Analysis.

### **10.2.1 Static Thermogravimetric Analysis**

In this particular instance the sample under analysis is maintained at a constant temperature for a period of time during which any changes in weight are observed carefully.

### **10.2.2 Dynamic Thermogravimetric Analysis**

In dynamic thermogravimetric analysis a sample is subjected to conditions of predetermined, carefully controlled continuous increase in temperature that is invariably found to be linear with time.

Differential thermal analysis is the most widely used and is probably a very suitable method for the identification and estimation purposes especially in the case of soils (clays) and minerals. The chemical or physical changes which are not accompanied by the change in mass on heating are not indicated in thermogravimetric but there is a possibility that such changes may be indicated in DTA.

## **10.3 Principle**

Differential thermal analysis is a technique in which the temperature of the substance under investigation is compared with the temperature of a thermally inert material such as  $\alpha$ -alumina and is recorded with furnace temperature as the substance is heated or cooled at a predetermined uniform rate. The range of temperature measurable in the course of DTA is much larger than TG determination. Thus, during TG, pure fusion reactions, crystalline transition, glass transition and crystallization and solid state reactions with no volatile product would not be indicated because they provide no change in mass of the specimen. However, these changes are indicated during DTA by endothermic or exothermic departure from the base line. Since DTA is a dynamic method, it is essential that all aspects of the technique be standardized in order to obtain reproducible results. These include pretreatment of specimen, particle size and packing specimen, dilution of the specimen and nature of the inert diluent. The principle of method consists in measuring the change in temperature associated with physical or chemical changes during the gradual heating of the substance. Thermal changes due to fusion, crystalline structure inversions, boiling, dissociation or decomposition reactions, oxidation and reduction reactions, destruction of crystalline lattice structure and other chemical reactions are generally accompanied by an appreciable rise or fall in temperature. Hence, all these are accounted in DTA. Generally speaking, phase transitions, dehydration, reduction and some decomposition reactions produce endothermic effects whereas crystallization, oxidation and some decomposition reactions produce exothermic

effects. In DTA a sample of material under investigation (specimen) is placed by the side of thermally inert material (the reference sample) usually calcite or  $\alpha$ - alumina in suitable sample holder or block. The temperature difference between the two is continuously recorded as they are heated. The block is heated in an electric furnace i.e. both are heated under identical conditions.

#### 10.4 Characteristics of DTA Curves

An idealized representation of the two major processes observable in DTA is illustrated in Figure 1, where  $\Delta T$  is plotted on y-axis and T on x-axis. Endotherms are plotted downwards and exotherms upwards. Similarly, the temperature of the sample is greater for an exothermic reaction, than that of the reference, for endotherms the sample temperature lags behind that of the reference

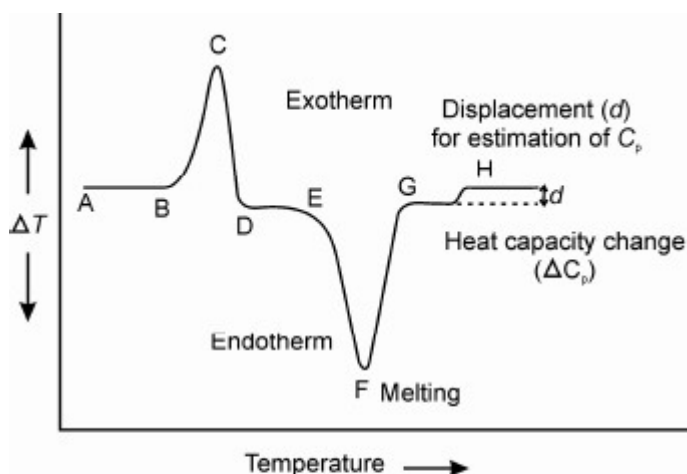


**Figure 1:** A representation of the DTA curve showing exotherm, endotherm and base line changes

When no reaction occurs in the sample material, the temperature of the sample remains similar to that of reference substance. This is because both are being heated exactly under identical condition i.e. temperature difference  $\Delta T(T_s - T_r)$  will be zero for no reaction. But as soon as reaction starts, the sample becomes either hot or cool depending upon whether the reaction is exothermic or endothermic. A peak develops on the curve for the temperature difference  $\Delta T$  against temperature of furnace or time. Let us consider the DTA curve in Figure 1 again, where  $\Delta T$  along the line AB is zero indicating no reaction but at B where the curve begins to deviate from the base line corresponds to the onset temperature at which the exothermic reaction starts and give rise to a peak BCD with a maximum at point C. Where rate of heat evolution by the reaction is equal to the difference between the rate of evolution of heat and inert reference material. The peak temperature C corresponds to the maximum rate of heat of evolution. It does not represent the maximum rate of reaction nor the

completion of the exothermic process. Thus, the position of C does not have much significance in DTA experiments. At some determinant point the heat of evaluation process is completed and after this point heat evaluation goes on decreasing up to D. The usefulness of the method arises from the fact that peak temperature is normally characteristic of the material in the sample. Area of the peak BCD is proportional to the amount of reacting material. For endothermic reaction the peak EFG will be obtained as shown in the idealised curve. This peak shows that the  $\Delta T$ , i.e.  $(T_s - T_r)$  will be negative because heat is absorbed and consequently  $T_s$  will be smaller than  $T_r$ . Note the levels of base lines of exotherm curve, AB and DE. Both are at different levels above x-axis. This is due to the fact that heat capacity of the sample has changed as a result of the exothermic process. Similar explanation can be given for the difference in levels of base lines of endotherm curve i.e. DE and GH. DTA curves are not only help in the identification of materials but their peak areas provide quantitative information regarding mass of sample ( $m$ ), heat of reactions (enthalpy change,  $\Delta H$ ).

#### 10.4 Instrumentation

A differential thermal analyzer is composed of five basic components, namely

- i) Sample holder with built-in thermocouple assembly,
- ii) Flow-control system,
- iii) Furnace assembly,
- iv) Preamplifier and Recorder, and
- v) Furnace Power Programmer and Controller.

A typical commercial differential thermal analyzer is schematically illustrated in Figure 2.

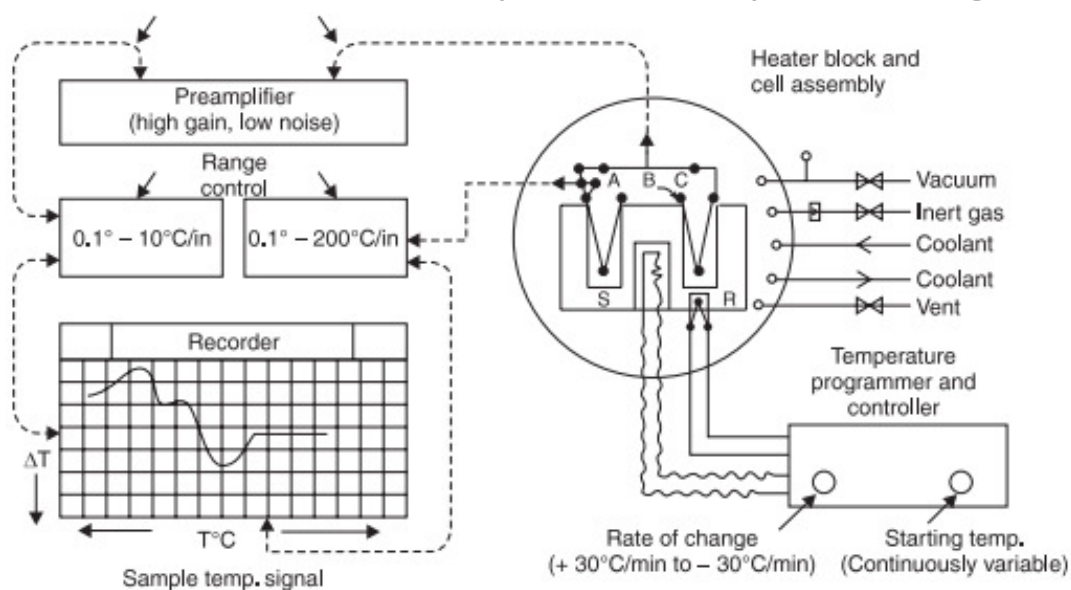


**Figure 2:** Schematic representation of thermal analyzer



- 
- a) Thermocouples employed are normally unsheathed Platinum Vs Platinum and Sodium Vs 10% Rhodium. The said two thermocouples help in measuring the difference in temperature between a sample S and an absolutely inert reference substance R, as both are subjected to heating in a ceramic or metal block inside a furnace being operated by a temperature programmer and controller.
- b) The output of the differential thermocouple is amplified adequately through a high gain, low-noise preamplifier and subsequently hooked to the recorder, one axis of which is driven by the block temperature signal and is measured by a third thermocouple.
- c) Heating/Cooling Device, a sufficient versatility is achieved by the aid of a pressure-vacuum, high-temperature electric furnace. An almost constant heating rate is usually achieved by using a motor-driven variable auto transformer. Both heating rates and cooling rates may be conveniently adjusted continuously:
- i) From 0°-30°C/minute by some instruments, and
- ii) From a choice of several commonly employed heating rates viz., 2°, 4°, 8° and 16°C/minute. Usual workable sample temperatures are upto : 500°C. Exceptional maximum temperatures are upto : 1000°C.
- d) Relatively small sample volumes help in two ways: first, they make evacuation easy ; and secondly, they minimize thermal gradients.

### 10.5 Methodology

- i) Insert a very thin thermocouple into a disposable sample tube 2 mm in diameter and containing 0.1-10 mg of sample,
- ii) Another identical tube is either kept empty or filled with a reference substance, such as quartz, sand, alumina or alundum powder,
- iii) The two tubes are simultaneously inserted into the sample block and subsequently heated (or cooled) at a uniform predetermined programmed rate, and
- iv) DTA—being a dynamic process, it is extremely important that all aspects of the technique must be thoroughly standardised so as to obtain reproducible results.

A few of these aspects vital aspects are

- Pretreatment of the specimen,
- Particle size and packing of the specimen,
- Dilution of the specimen,
- Nature of the inert diluent,
- Crystalline substances must be powdered, and sieved through 100-mesh sieve,

- For colloidal particles (e.g., clays), micelle-size is very critical, and
- Either to suppress an unwanted reaction (e.g., oxidation), or to explore the study of a reaction

(e.g., gaseous reaction product)—the atmosphere should be controlled adequately. Figure 3, depicts the differential thermal analysis investigation of calcium acetate monohydrate at a uniform programmed heating rate of 12°C/minute.

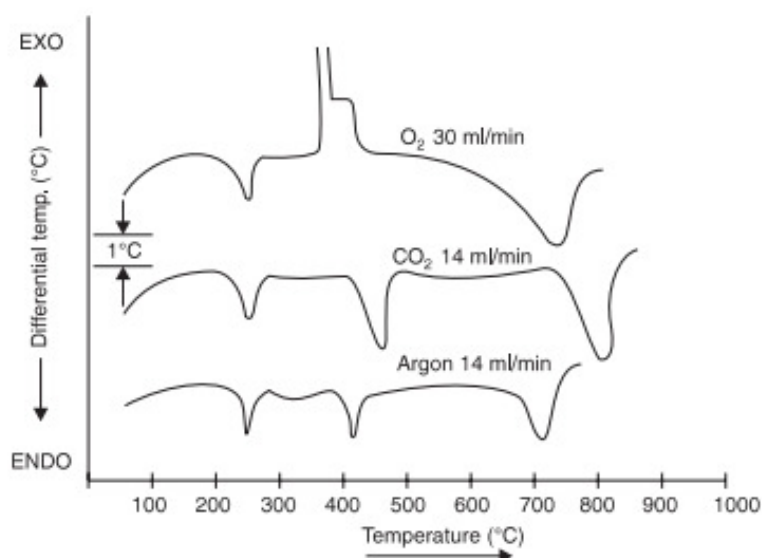
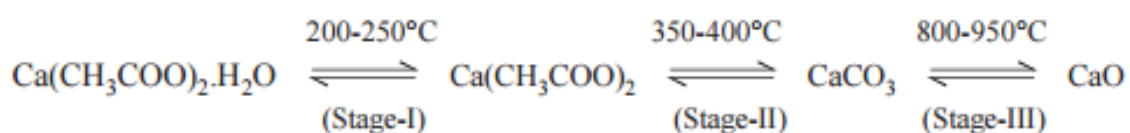


**Figure 3:** DTA-Investigation of Calcium Acetate Monohydrate, 12°C. min<sup>-1</sup>

The chemical reactions involved in the differentiated thermal analysis of calcium acetate monohydrate may be expressed as follows



*Stage I:* The endothermal dehydration of calcium acetate monohydrate occurs giving rise to the anhydrous salt. It is easily noticed by an endothermal band on DTA curve between 200°C and 250°C.

*Stage II:* The anhydrous salt undergoes endothermal decomposition reaction at 350-400°C resulting into the formation of CaCO<sub>3</sub>. It has been observed that this decomposition reaction seems to be almost alike in the presence of either CO<sub>2</sub> or Ar.

*Stage III:* The decomposition of calcium carbonate to calcium oxide, which is a function of the partial pressure of the CO<sub>2</sub> in contact with the sample. The endothermal band for the

---

carbonate decomposition is sharply peaked spread over a relatively narrower temperature range in an atmosphere of CO<sub>2</sub>.

### 10.6 Applications

The various important applications of DTA are

- i) Rapid identification of the compositions of mixed clay
- ii) Studying the thermal stabilities of inorganic compounds
- iii) Critically examining in a specific reaction whether a new compound is actually formed or the product is nothing but an unreacted original substance, and
- iv) DTA offers a wide spectrum of useful investigations related to reaction kinetics, polymerization, solvent retention, phase-transformations, solid-phase reactions and curing or drying properties of a product.

### 10.7 Differential Scanning Calorimetry DSC

Differential Scanning Calorimetry (DSC) is a thermal analysis technique that looks at how a material's heat capacity (C<sub>p</sub>) is changed by temperature. A sample of known mass is heated or cooled and the changes in its heat capacity are tracked as changes in the heat flow. This allows the detection of transitions such as melts, glass transitions, phase changes, and curing. The biggest advantage of DSC is the ease and speed with which it can be used to see transitions in materials. For these reasons, DSC is the most common thermal analysis technique and is found in many analytical, process control, quality assurance, and R&D laboratories.

### 10.8 The difference between a heat flow and a heat flux DSC

The term differential scanning calorimetry refers to both the technique of measuring calorimetric data while scanning, as well as a specific instrument design. The technique can be carried out with other types of instruments

The DSC can be used to obtain the thermal critical points like melting point, enthalpy specific heat or glass transition temperature of substances. The schematic principle of the DSC is described in Figure 4. The sample and an empty reference crucible is heated at constant heat flow. A difference of the temperature of both crucibles is caused by the thermal critical points of the sample and can be detected.

### 10.9 Instrumentation

In DSC the instrument used is a differential scanning calorimeter. There are two types, heat-of instruments are in use, they are

- i) flux DSC and

ii) Power compensation DSC, depending on the method of measurement used.

In a heat-flux DSC instrument, the temperature difference between sample and reference is recorded, after suitable calorimetric calibration, as a direct measure of the difference in heat flow rate or the difference in power.

In a power compensation DSC instrument the difference in power supplied to the sample and to the reference, to keep their temperatures as nearly the same as possible, is measured directly.

The power difference in units of watts ( $\Delta P$ ) should be plotted as ordinate. Since endothermic reactions require a positive input of power into the sample, the DSC convention demands that endothermic peaks should be plotted upwards, and  $t$  or  $T$  increasing from left to right. However, the DTA convention (endotherms downwards) is quite often used, and it is recommended that the ordinate axis be labelled with the endothermic (or exothermic) direction.

### 10.10 Theory of DSC

Differential scanning calorimetry (DSC) monitors heat effects associated with phase transitions or chemical reactions as a function of temperature. In a DSC the difference in heat flow to the sample and a reference at the same temperature is recorded as a function of temperature. The reference is an inert material such as alumina, or just an empty aluminum pan. The temperature of both the sample and reference are increased at a constant rate. Since the DSC is at constant pressure, heat flow is equivalent to enthalpy changes

$$\left(\frac{dq}{dp}\right)_p = \frac{dH}{dt} \text{-----} (1)$$

Here  $dH/dt$  is the heat flow measured in  $\text{mcal sec}^{-1}$ . The heat flow difference between the sample and the reference is

$$\Delta\left(\frac{dH}{dt}\right) = \left(\frac{dH}{dt}\right)_{\text{sample}} - \left(\frac{dH}{dt}\right)_{\text{reference}} \text{-----} (2)$$

and can be either positive or negative. In an endothermic process, such as most phase transitions, heat is absorbed and, therefore, heat flow to the sample is higher than that to the reference. Hence  $\Delta dH/dt$  is positive. Other endothermic processes include helix-coil transitions in DNA, protein denaturation, dehydrations, reduction reactions, and some decomposition reactions. In an exothermic process, such as crystallization, some cross-linking processes, oxidation reactions, and some decomposition reactions, the opposite is true and  $\Delta dH/dt$  is negative.

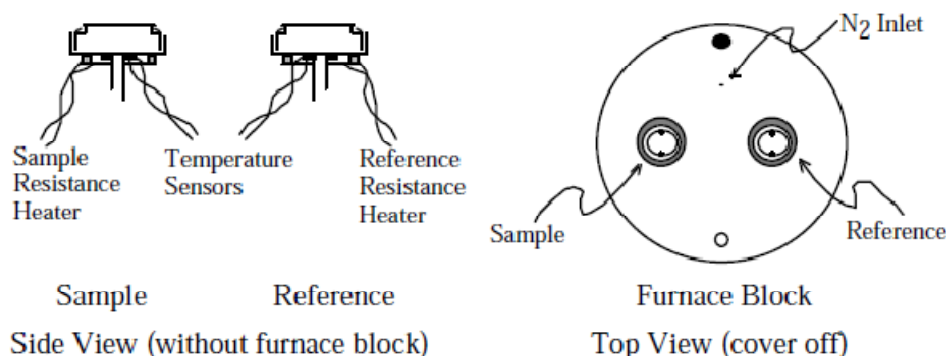


**Figure 5:** Differential scanning calorimeter sample and reference holder

The calorimeter consists of a sample holder and a reference holder as shown in Figure 5. Both are constructed of platinum to allow high temperature operation. Under each holder is a resistance heater and a temperature sensor. Currents are applied to the two heaters to increase the temperature at the selected rate. The difference in the power to the two holders, necessary to maintain the holders at the same temperature, is used to calculate  $\Delta H/dt$ . A schematic diagram of a DSC is shown in Figure 6. A flow of nitrogen gas is maintained over the samples to create a reproducible and dry atmosphere. The nitrogen atmosphere also eliminates air oxidation of the samples at high temperatures. The sample is sealed into a small aluminum pan. The reference is usually an empty pan and cover. The pans hold up to about 10 mg of material.

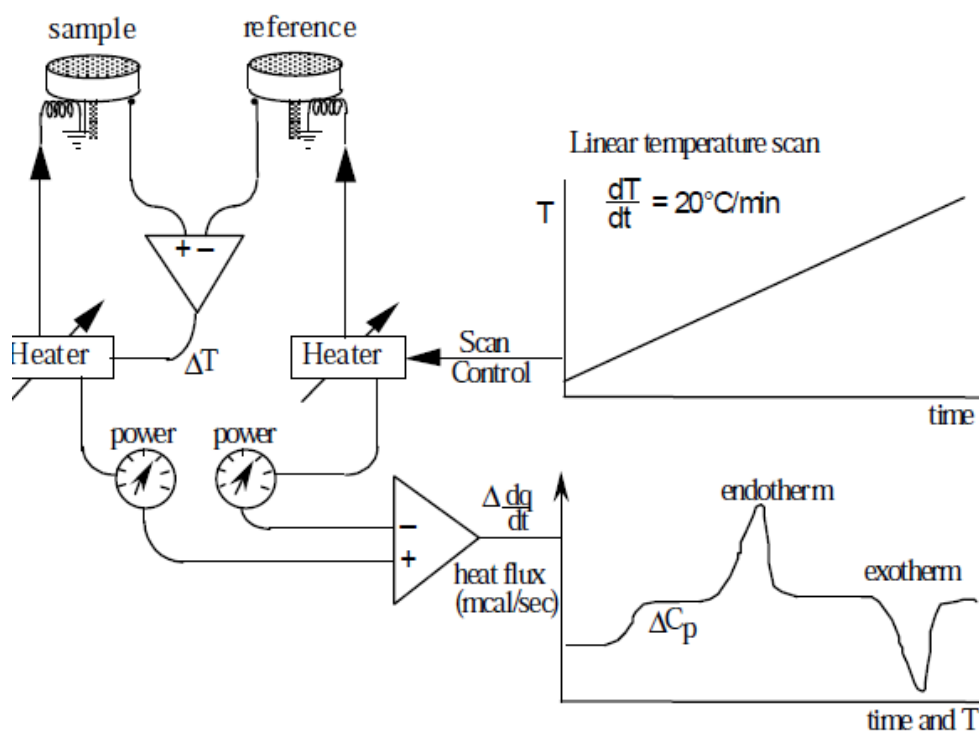


**Figure 2:** Schematic of a DSC

During the heating of a sample, for example, from room temperature to its decomposition temperature, peaks with positive and negative  $\Delta H/dt$  may be recorded; each peak corresponds to a heat effect associated with a specific process, such as crystallization or melting (Figure. 7).

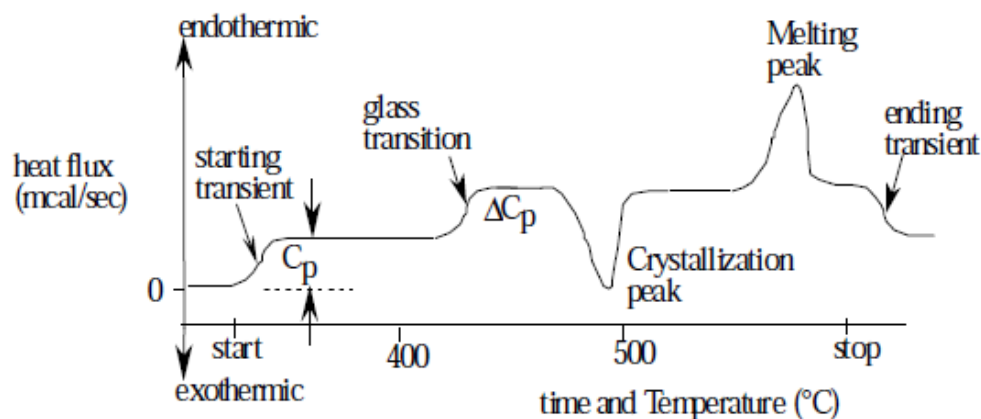


**Figure 7:** Typical DSC scan. The heat capacity of the sample is calculated from the shift in the baseline at the starting transient

### 10.11 Information is obtainable from a DSC curve

The first and most direct information is the temperature at which a certain process occurs, for example, the melting point of a polymer. The temperature at which a reaction, such as decomposition, starts is another important parameter. The decomposition peak temperature is associated with the temperature at which maximum reaction rate occurs. A special case in which the temperature of a phase transformation is of great importance in polymers is the glass transition temperature,  $T_g$ . The  $T_g$  is the temperature at which amorphous (noncrystalline) polymers are converted from a brittle, glasslike form to a rubbery, flexible form. The glass transition is not a first-order phase transition but one that involves a change in the local degrees of freedom through changes in the torsion angles along the polymer backbone. Above the glass transition temperature, segmental motions of the polymer are comparatively unhindered by the interaction with neighboring chains. Below the glass transition temperature, such motions are hindered greatly, and the relaxation times associated with such hindered motions are usually long compared to the duration of the experiment.

The operative definition of glass transition temperature is that at this temperature the specific heat, the coefficient of thermal expansion, the free volume, and the dielectric constant (in the case of a polar polymer) all change rapidly. The glass transition temperature is an important characteristic of every polymer, because the mechanical behavior of the polymer changes markedly.

In the DSC experiment,  $T_g$  is manifested by a sudden increase in the base line, indicating an increase in the heat capacity of the polymer (Figure 8). The glass transition is a second-order transition; no enthalpy is associated with the transition. As a result, the effect in the DSC thermogram is slight and is observable only if the instrument is sufficiently sensitive. The second direct information obtainable from a DSC thermogram is the enthalpy associated with processes.

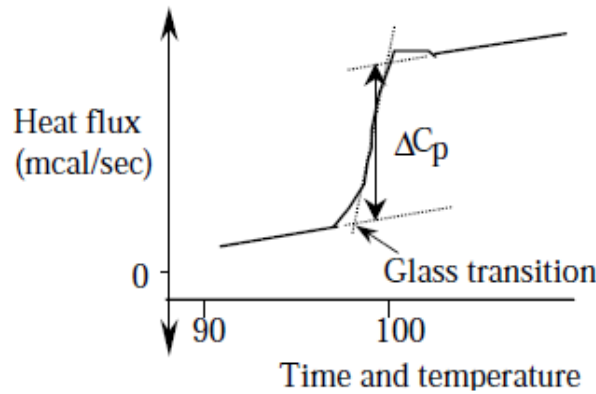


**Figure 8:** Glass transition

If there are sloping baselines before and after the glass transition, extropolate the baselines forwards and backwards (as shown by dotted lines) and take the baseline shift when the transition is about 63% complete (as shown by arrows).

The integral under the DSC peak, above the baseline, gives the total enthalpy change for the process,

$$\int \left( \frac{dH}{dt} \right)_{sample} dt = \Delta H_{sample} \text{ ----- (3)}$$

Assuming that the heat capacity of the reference is constant over the temperature range covered by the peak,  $\Delta H_{reference}$  cancels out because the integral above the baseline is taken. Therefore, equation 3 is also valid when the integral is taken from the DCS plot of  $\Delta dH/dt$ . Heat capacities and changes in heat capacity can be determined from the shift in the baseline of the thermogram. The heat capacity is defined as

$$C_p = \left( \frac{dq}{dT} \right)_p = \left( \frac{dH}{dT} \right)_p \text{ ----- (4)}$$

The temperature scan rate is

$$\text{Scan rate} = \frac{dT}{dt} \text{ ----- (5)}$$

Using the chain rule

$$C_p = \left( \frac{dH}{dT} \right)_p = \frac{dH}{dt} \frac{dt}{dT} \text{-----} (6)$$

where the last derivative is just the inverse of the scan rate. For differential measurements, we determine the difference in the heat capacity of the sample and the reference:

$$\Delta C_p = C_p(\text{sample}) - C_p(\text{reference}) \text{-----} (7)$$

$$\Delta C_p = \Delta \frac{dH}{dT} \frac{dt}{dT} \text{-----} (8)$$

where  $\Delta dH/dt$  is the shift in the baseline of the thermogram (Figure 3-4). The units of the heat flow are  $\text{mcal sec}^{-1}$  and the temperature scan rate is usually expressed as  $^{\circ}\text{C min}^{-1}$ . So to be consistent with units you must multiply by  $60 \text{ sec min}^{-1}$ .

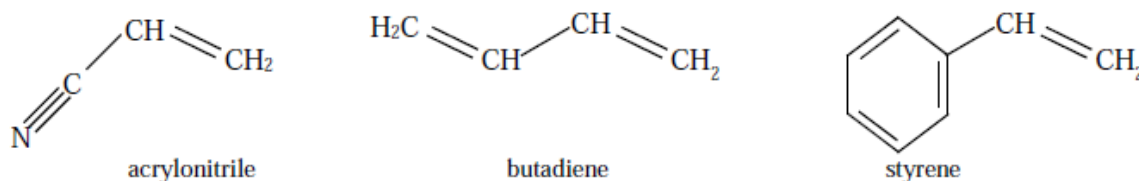
$$\Delta C_p = \left( \frac{\text{mcal}}{\text{sec}} \right) \left( \frac{\text{min}}{^{\circ}\text{C}} \right) \left( \frac{60 \text{ sec}}{\text{min}} \right) \text{-----} (9)$$

For determination of the bulk heat capacity of substances, greater accuracy is obtained by determining the baseline shift at several temperature scan rates. Rearranging Eq. 7 gives the difference in heat capacity between the sample and reference as the slope of the plot of baseline shift versus scan rate

$$\Delta \frac{dH}{dt} = \Delta C_p \frac{dT}{dt} \text{-----} (10)$$

### 10.12 Applications in the area of polymers

The study of polymers example, ABS, polystyrene, and polyethylene. Acrylonitrile butadiene styrene, ABS, is a co-polymer made from the monomers acrylonitrile, butadiene, and styrene, ABS is stronger than polystyrene. ABS is the plastic in Lego blocks and is commonly used in 3D-printing. Polystyrene is widely used in rigid packaging, including plastic petri dishes. Polystyrene is also used in foams, including polystyrene insulated beverage cups.



By themselves, styrene and acrylonitrile polymerize to give a random copolymer, Figure 9. ABS is a graft copolymer. ABS is produced by the polymerization of monomeric acrylonitrile and styrene in the presence of polybutadiene. The result is to “graft” polybutadiene sidechains on the acrylonitrile-styrene backbone.



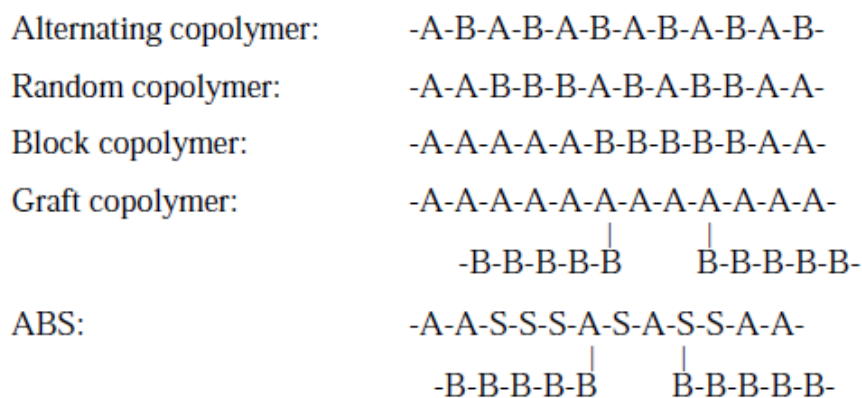


**Figure 9:** Copolymer types. ABS has a random copolymer backbone with grafted sidechains of polybutadiene.

ABS and polystyrene are amorphous polymers, which correspondingly have no distinct melting transition. The viscosity of ABS or polystyrene smoothly decreases with increasing temperature above  $T_g$ . 3D-printing with ABS is done at 230°C.

### 10.12.1 Energy (Ordinate) Calibration

In practice, the measurement of energy flow will necessarily involve an instrument calibration constant, the recorder chart speed, the sensitivity used, the units employed for area measurement, etc. The range switch on the instrument control panel gives nominal values for the rate of energy change, in millicalories per second, for a full scale displacement, to within +5%. There are two methods which may be used to calibrate the ordinate on the Model DSC-4. We will use "automatic" ordinate calibration, to yield an overall accuracy of  $\pm 1\%$  in our results. In this method, the instrument will electronically generate a 10 mCal/Sec calibration signal, which will be used to check the mV output at full scale. Set the Range setting on the DSC to 10 mcal/sec. Depress the black rocker switch. The output voltage for the 10 mCal/Sec calibration should give 10.0 mV. The Range setting gives the mCal/Sec value that corresponds to 10 mV output. The calibration constant, which should be close to 1.00, is then

$$\text{Calibration constant} = \frac{\text{expected output}}{\text{actual output}} = \frac{10 \text{ mV}}{\text{full scale deflection for 10 mcal/Sec}}$$

Other applications of Differential Scanning Calorimetry

- Metal alloy melting temperatures and heat of fusion.
- Metal magnetic or structure transition temperatures and heat of transformation.
- Intermetallic phase formation temperatures and exothermal energies.
- Oxidation temperature and oxidation energy.

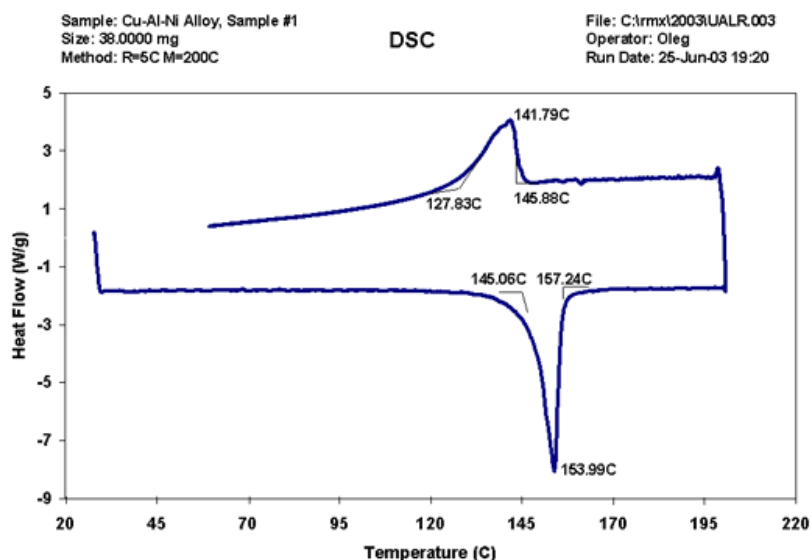
- 
- Exothermal energy of polymer cure (as in epoxy adhesives), allows determination of the degree and rate of cure.
  - Determine the melting behaviour of complex organic materials, both temperatures and enthalpies of melting can be used to determine purity of a material.
  - Measurement of plastic or glassy material glass transition temperatures or softening temperatures, which change dependent upon the temperature history of the polymer or the amount and type of fill material, among other effects.
  - Determines crystalline to amorphous transition temperatures in polymers and plastics and the energy associated with the transition.
  - Crystallization and melting temperatures and phase transition energies for inorganic compounds.
  - Oxidative induction period of an oil or fat.
  - May be used as one of multiple techniques to identify an unknown material or by itself to confirm that it is the expected material.
  - Determine the thermal stability of a material.
  - Determine the reaction kinetics of a material.

TMA can also be used to measure glass transition temperatures, melting temperatures, crystalline phase formation temperatures, and crystalline to amorphous transition temperatures. It is often more sensitive to detecting the transition, but cannot measure the energy of the transition as DSC does. It also may measure the temperature more accurately when sample thermal conductivity is low or its dimensions are large since DSC has to have a higher rate of temperature change commonly to detect the transitions.

#### *Illustrative Example 1*

##### **10.12.2 Transformation temperatures of a shape memory alloy**

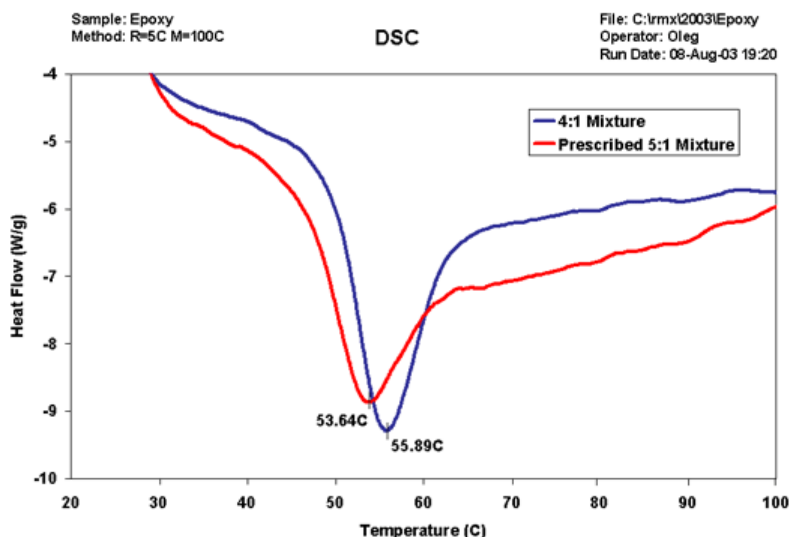
Cu-Al-Ni alloy shape memory material undergoes a martensite to austenite transformation upon heating. The lower curve of the DSC plot in the figure below shows the endotherm which results when the sample was heated at a rate of 5°C/min. from 30°C to 190°C in nitrogen gas flowing at a rate of 25ml/min. Upon cooling down, the austenite to martensite transformation yields an exotherm seen in the upper trace of the DSC plot. The temperatures of these transitions are a function of the alloy composition. There is a hysteresis in the transformation on heating and cooling which is notable. The on-set temperatures, 145.06°C on heating and 145.88°C on cooling are close, however.



Example 2

### 10.12.3 Epoxy Mixtures

The figure below shows DSC curves of a two-part room-temperature cured, low-shrinkage epoxy, with different resin to hardener ratios. The epoxies were held at room temperature for several weeks prior to the DSC measurements. The red curve shows the epoxy mixed in accordance with the manufacturer's instructions: 5 parts of epoxy resin with 1 part of epoxy hardener. The blue DSC curve shows the result for a 4 part epoxy resin to 1 part epoxy hardener ratio. The endothermic peak temperature of the prescribed mixture is 53.64°C and that of the 4:1 ratio mixture is higher at 55.89°C. The total endothermic energies are also different. Therefore, DSC can be used as a tool for quality control of epoxy mixture ratios



### 10.13 Summary of the unit

Differential Thermal Analysis (DTA) is a technique in which the difference in temperature between the sample and a reference sample ( $\Delta T_{sR}$ ) is monitored against time while the samples are exposed to a temperature programme.

---

The instrument is a differential thermal analyser and the record is the differential thermal or DTA curve. The temperature difference ( $\Delta T$ ) should be plotted on the ordinate with endothermic reactions downwards and  $t$  or  $T$  increasing from left to right.

The first recommendations clarified the terminology to be used, such as the sample, reference material, block and differential thermocouple. It is stated that "in DTA it must be remembered that, although the ordinate is conventionally labelled  $\Delta T$  the output from the thermocouple will in most instances vary with temperature and the measurement recorded is normally the e.m.f. output,  $E$ , i.e. the conversion factor,  $b$  in the equation

$$\Delta T = bE$$

is not constant since  $b = f(T)$ , and that a similar situation occurs with other sensor systems".

There should be clear distinction between different instrumental conditions and experimental regimes. The ICTAC recommendations specify that the nature, history and size of the sample, the geometry of the system, and sample holder, the temperature programme used, the gaseous atmosphere and flow rate, and the type, sensitivity and placement of the sensors, as well as the design of the sample holder should ideally be given. It has already been pointed out that the methods of data collection and processing also need to be described carefully.

Differential Scanning Calorimetry (DSC) is a technique in which the difference in heat flow rate (or power) to the sample and to the reference sample is monitored against time while the samples are exposed to a temperature programme.

The instrument is a differential scanning calorimeter and may be one of two types, heat-flux DSC or power compensation DSC, depending on the method of measurement used.

In a Heat-flux DSC instrument, the temperature difference between sample and reference is recorded, after suitable calorimetric calibration, as a direct measure of the difference in heat flow rate or the difference in power.

In a power compensation DSC instrument the difference in power supplied to the sample and to the reference, to keep their temperatures as nearly the same as possible, is measured directly.

The power difference in units of watts ( $\Delta P$ ) should be plotted as ordinate. Since endothermic reactions require a positive input of power into the sample, the DSC convention demands that endothermic peaks should be plotted upwards, and  $t$  or  $T$  increasing from left to right. However, the DTA convention (endotherms downwards) is quite often used, and it is recommended that the ordinate axis be labelled with the endothermic (or exothermic) direction.

---

### 10.14 Key words

Static Thermogravimetric Analysis; Dynamic Thermogravimetric Analysis; Characteristics of DTA Curves; Differential Scanning Calorimetry DSC; Theory of DSC; Energy (Ordinate) Calibration

### 10.15 References for further study

- 1) Introduction to Thermal Analysis: Techniques and applications; Michael Ewart Brown; *Springer Science & Business Media, 2012.*
- 2) Handbook of Thermal Analysis of Construction Materials; V.S. Ramachandran, Ralph M. Paroli, James J. Beaudoin, Ana H. Delgado; *William Andrew, 2002.*
- 3) Handbook of Thermal Analysis and Calorimetry: From Macromolecules to Man; Richard B. Kemp; *Elsevier, 1999.*
- 4) Principles of Thermal Analysis and Calorimetry; Peter J. Haines; *Royal Society of Chemistry, 2002.*
- 5) Thermal analysis of Micro, Nano- and Non-Crystalline Materials: Transformation, Crystallization, Kinetics and Thermodynamics; Jaroslav, Peter Simon; *Springer Science & Business Media, 2012.*

### 10.16 Questions for self understanding

- 1) Discuss the theory of DTA
- 2) Explain the followings
  - a) Static Thermogravimetric Analysis
  - b) Dynamic Thermogravimetric Analysis
- 3) Explain the principle of DTA
- 4) Write a note on characteristics of DTA Curves
- 5) Discuss the followings
  - a) Instrumentation of DTA
  - b) Methodology involved in DTA analysis
- 6) Explain the applications of DTA
- 7) What is Differential Scanning Calorimetry (DSC)
- 8) Explain the difference between a heat flow and a heat flux DSC
- 9) Discuss the instrumentation of DSC
- 10) Explain the Theory of DSC
- 11) Discuss the Information is obtainable from a DSC curve
- 12) Explain the applications of DSC in the area of polymers

---

**UNIT-11****Structure**

- 11.0 Objectives of the unit
- 11.1 Introduction
- 11.2 Thermomechanical analysis
- 11.3 Instrumentation
  - 11.3.1 TMA probe types
- 11.4 TMA temperature calibration
- 11.5 Thermal expansion measurement
- 11.6 Glass transition temperature by TMA
- 11.7 Dynamic Mechanical Analysis (DMA)
- 11.8 Basic principles
- 11.9 Theory
- 11.10 Equipment
- 11.11 Free Vibration
- 11.12 Forced Vibration (Non-resonant)
- 11.13 Procedure
- 11.15 Evaluation
- 11.16 Summary of the unit
- 11.17 Key words
- 11.18 References for further studies
- 11.19 Questions for self understanding

---

## 11.0 Objectives of the unit

After studying this unit you are able to

- Explain the thermomechanical analysis
- Explain the procedure of determining glass transition temperature by TMA
- Define the Dynamic Mechanical Analysis (DMA)
- Explain the basic principles of DMA

### 11.1 Introduction

The dimensional and mechanical stability of materials is of paramount importance to their use in the everyday world where they may encounter a wide variation in temperature through design or by accident. Many polymers are processed at elevated temperatures so as to enable them to flow and be more amenable to fabrication. Food items are cooked, pasteurised or otherwise heated or frozen. Ceramics are fired so as to consolidate their final structure. The relationship between a material's dimensional and mechanical properties and its temperature is studied by the techniques described in this unit and, due to common concepts, the effect of heat on the electrical properties of materials is also considered.

### 11.2 Thermomechanical analysis

*Thermomechanical analysis (TMA) determines dimensional changes of solids, liquids or pasty materials as a function of temperature and/or time under a defined mechanical force.*

Or

*Thermomechanical Analysis (TMA) is defined as the measurement of a specimen's dimensions (length or volume) as a function of temperature whilst it is subjected to a constant mechanical stress.*

It is closely related to dilatometry, which determines the length change of samples under negligible load. In this way thermal expansion coefficients can be determined and changes in this property with temperature (and/or time) is monitored. Many materials will deform under the applied stress at a particular temperature which is often connected with the material melting or undergoing a glass-rubber transition.

Stress ( $\sigma$ ) is defined as the ratio of the mechanical force applied (F) divided by the area over which it acts (A).

The stress is usually applied in compression or tension, but may also be applied in shear, torsion, or some other bending mode as shown in Figure 1. The units of stress are  $\text{Nm}^{-2}$  or Pa. If the applied stress is negligible then the technique becomes that of thermodilatometry. This

technique is used to determine the coefficient of thermal expansion of the specimen from the relationship.

### 11.3 Instrumentation

A schematic diagram of a typical instrument is shown in Figure 1. The sample is placed in a temperature controlled environment with a thermocouple or other temperature sensing device, such as a platinum resistance thermometer, placed in close proximity. The facility to circulate a cryogenic coolant such as cold nitrogen gas from a Dewar vessel of liquid nitrogen is useful for subambient measurements. The atmosphere around the sample is usually controlled by purging the oven with air or nitrogen from a cylinder. Because of the much larger thermal mass of the sample and oven compared to a differential scanning calorimeter or a thermobalance, the heating and cooling rates employed are usually much slower for TMA.

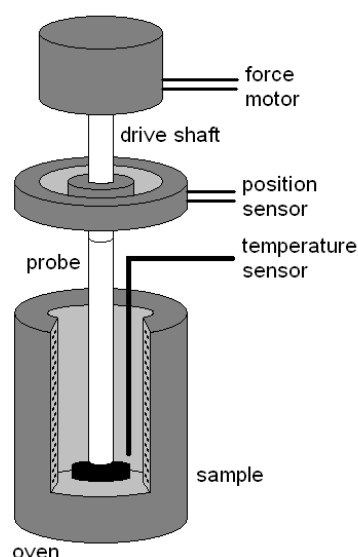


**Figure 1:** A schematic diagram of a typical TMA instrument

For compression measurements a flat-ended probe is rested on the top surface of the sample and a static force is applied by means of a weight or an electromagnetic motor similar in principle to the coil of a loudspeaker. Some form of proximity sensor measures the movement of the probe. This is usually achieved by using a linear variable differential transformer (LVDT) which consists of two coils of wire which form an electrical transformer when fed by an AC current. The core of the transformer is attached to the probe assembly and the coupling between the windings of the transformer is dependent upon the displacement of the probe.



### 11.3.1 TMA probe types

Following probe types are commonly employed in TMA (Figure 2). The compression, penetration, tension, volumetric

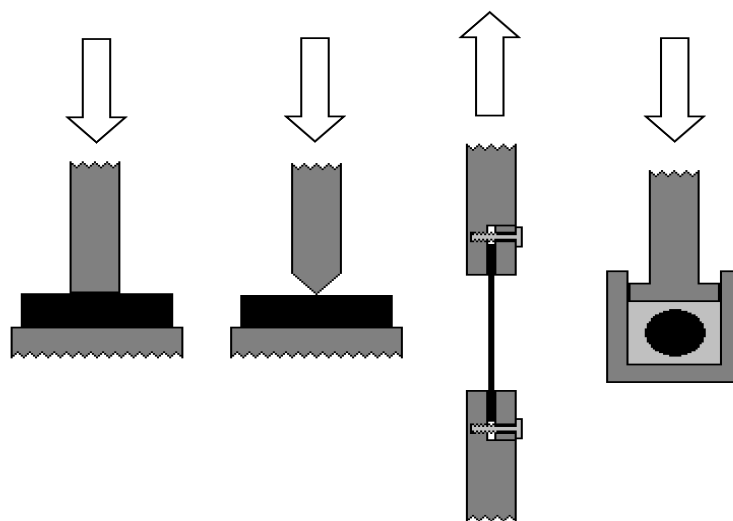


**Figure 2:** Different probe types commonly employed in TMA

- ✓ Compression probe used for applying low load over a wide area of sample for thermal expansion measurements (thermodilatometry)
- ✓ Penetration probe applies a high load over a small area for the purpose of measuring softening temperatures.
- ✓ Tension probe used for measuring non-self supporting specimens - such as thin films and fibres under tension.
- ✓ Volumetric probe used for measuring the thermal volumetric expansion of irregularly shaped specimens surrounded by an inert packing material (alumina powder or silicone oil).

### 11.4 TMA temperature calibration

TMA temperature calibration is usually done by using indium (156.6°C), tin (232.0°C) and bismuth (271.4°C). Heating rate: 5°C min<sup>-1</sup>, force 1 N, static air atmosphere. A multi-layered sandwich of specimens is prepared separated by alumina spacers. When the metal standard melts, the stack collapses slightly. The onset of the length change is taken as the melting point of the metal.

### 11.5 Thermal expansion measurement

Measurements of thermal expansion coefficients are useful in assessing the compatibility of different materials for fabrication into components. Mismatches in behaviour can cause stresses to build up when temperature changes occur resulting in eventual weakening and

failure of the structure. Many crystalline materials can exist in a number of polymorphic forms which are stable at different temperatures. The transition between crystal structures is usually accompanied by a change in density and thermal expansion coefficient which can be detected by TMA.

### 11.6 Glass transition temperature by TMA

Supporting information from differential scanning calorimetry is often useful in interpreting information from TMA, particularly when softening point determinations are made – since loss of mechanical integrity can occur due to melting, which gives an endothermic peak in DSC or a glass-rubber transition, which causes a step change in heat capacity.

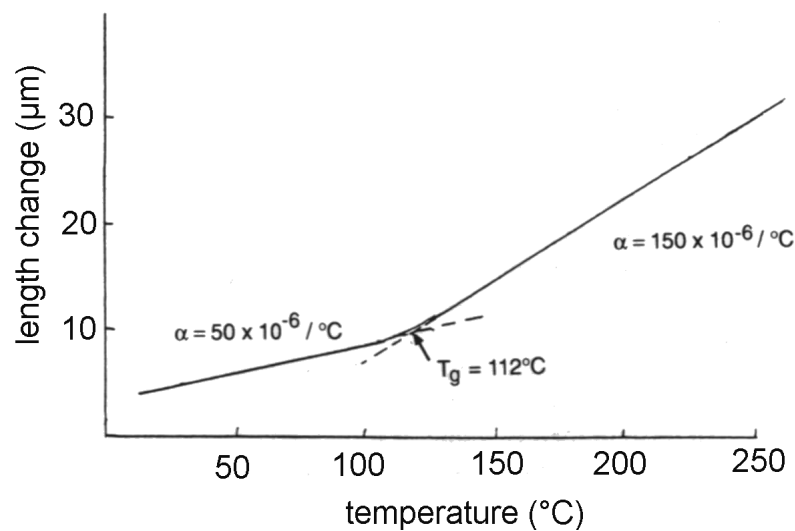


**Figure 3:** Change in length of a silicone gum rubber

Plots of the change in length of a sample of a silicone gum rubber are shown in Figure 3. Three experiments were carried out on the material with different applied forces. At zero force a change in slope of the curve can be seen around  $-60^\circ\text{C}$  due to the sample undergoing a change from glassy to rubbery behaviour. At this temperature the polymer chains acquire additional degrees of mobility which is seen as an increase in thermal expansion coefficient. The glass transition temperature ( $T_g$ ) can be defined by finding the intercept of tangents to the linear portions of the length versus temperature plot above and below this region. When a force is applied to the specimen the probe deforms the material in inverse proportion to its stiffness. Below  $T_g$  the polymer is rigid and is able to resist the applied force therefore its deformation is negligible. Above  $T_g$  the polymer becomes soft and the probe penetrates into the specimen. The temperature at which this occurs is called the materials' softening temperature and is highly dependent on the force applied to the sample.

---

### 11.7 Dynamic Mechanical Analysis (DMA)

Dynamic mechanical analysis is concerned with the measurement of the mechanical properties (mechanical modulus or stiffness and damping) of a specimen as a function of temperature.

DMA is also called forced oscillatory measurements, dynamic mechanical, thermal analysis (DMTA), dynamic thermomechanical analysis, and even dynamic rheology [Rheology is the study of the deformation and flow of materials]. DMRT is the preferred name because this mode of thermal analysis is rooted in the science of rheology.

Dynamic mechanical properties refer to the response of a material as it is subjected to a periodic force. These properties may be expressed in terms of a dynamic modulus, a dynamic loss modulus, and a mechanical damping term. Typical values of dynamic moduli for polymers range from  $10^6$  -  $10^{12}$  dyne/cm<sup>2</sup> depending upon the type of polymer, temperature, and frequency

DMA is a sensitive probe of molecular mobility within materials and is most commonly used to measure the glass transition temperature and other transitions in macromolecules, or to follow changes in mechanical properties brought about by chemical reactions. For this type of measurement the specimen is subjected to an oscillating stress, usually following a sinusoidal waveform. Thus dynamic mechanical analysis yields information about the mechanical properties of a specimen placed in minor, usually sinusoidal, oscillation as a function of time and temperature by subjecting it to a small, usually sinusoidal, oscillating force.

### 11.8 Basic principles

DMA can be simply described as applying an oscillating force to a sample and analyzing the material's response to that force. From this, one can calculate properties like the tendency to flow (called viscosity) from the phase lag and the stiffness (modulus) from the sample recovery. These properties are often described as the ability to lose energy as heat (damping) and the ability to recover from deformation (elasticity). One way to describe what we are studying is the relaxation of the polymer chains.

The applied force is called stress and is denoted by the Greek letter,  $\sigma$ . When subjected to a stress, a material will exhibit a deformation or strain,  $\gamma$ . The stress-strain curves of most materials are look like as shown in Figure 4.

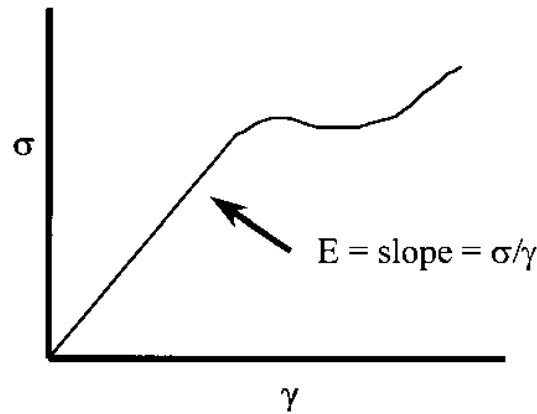


**Figure 4:** Stress–strain curves relate force to deformation

### 11.9 Theory

In DMA a sinusoidal oscillating stress is applied to a specimen, a corresponding oscillating strain will be produced. Unless the material is perfectly elastic, the measured strain will lag behind the applied stress by a phase difference ( $\delta$ ) shown in Figure 5. The ratio of peak stress to peak strain gives the complex modulus ( $E^*$ ) which comprises an in-phase component or storage modulus ( $E'$ ) and a  $90^\circ$  out-of-phase (quadrature) component or loss modulus ( $E''$ ).

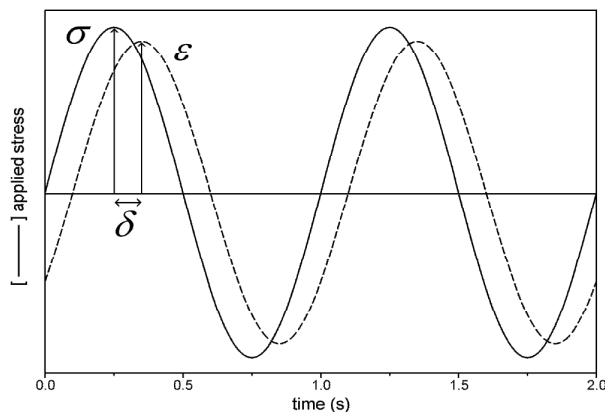


**Figure 5:** the measured strain lag behind the applied stress by a phase difference ( $\delta$ )

The storage modulus, being in-phase with the applied stress, represents the elastic component of the material's behaviour, whereas the loss modulus, deriving from the condition at which  $d\epsilon/dt$  is a maximum, corresponds to the viscous nature of the material. The ratio between the loss and storage moduli ( $E''/E'$ ) gives the useful quantity known as the mechanical damping factor ( $\tan \delta$ ) which is a measure of the amount of deformational energy that is dissipated as heat during each cycle. The relationship between these quantities can be illustrated by means of an Argand diagram, commonly used to visualise complex numbers, which shows that the complex modulus is a vector quantity characterised by magnitude ( $E^*$ ) and angle ( $\delta$ ) as shown in Figure 6.  $E'$  and  $E''$  represent the real and imaginary components of this vector thus:

$$E^* = E' + iE'' = \sqrt{(E')^2 + (E'')^2}$$

So that:

$$E' = E^* \cos \delta$$

and

$$E'' = E^* \sin \delta$$

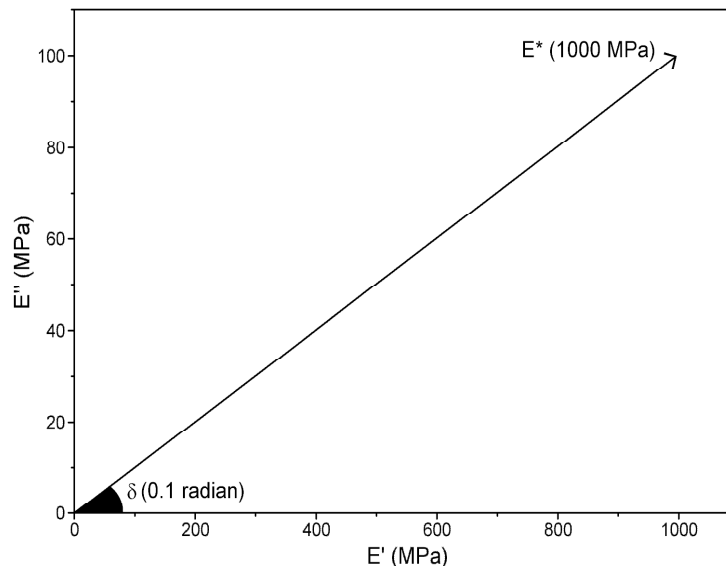


**Figure 6:** a vector quantity characterised by magnitude ( $E^*$ ) and angle ( $\delta$ )

Thus in DMA instruments apply an oscillating force (stress) and record an oscillating sample response. Modulus is calculated from the elastic response; e.g. sample response “in phase” with applied oscillatory stress. Damping is calculated from the viscous response; e.g. sample response “out of phase” with applied oscillatory stress.

### 11.10 Equipment

There are basically two types of DMA measurement. Deformation-controlled tests apply a sinusoidal deformation to the specimen and measure the stress. Force-controlled tests apply a dynamic sinusoidal stress and measure the deformation. Dynamic load may essentially be achieved in free vibration or in forced vibration. There are two designs of apparatus,

- i) Torsion type,
- ii) Bending, tension, compression, shear type.

### 11.11 Free Vibration

In free torsional vibration, one end of the specimen is clamped firmly while a torsion vibration disc at the other end is made to oscillate freely. The resultant frequency and amplitude of the oscillations, along with the specimen’s dimensions, are used to calculate the torsion modulus. Measurements are conducted at various temperatures to establish how the

torsion modulus varies with temperature. The term torsion modulus is intended to convey the idea that the stress is not necessarily purely shear and that the observation is not necessarily a shear modulus (except in the case of cylinders). On being twisted, the flat, clamped specimen is placed in torsional stress and, to an extent depending on the way it is clamped and on its shape, its two free edges are placed in tension and its center is placed in compression. Another free-vibration method is flexural vibration. In this, the specimen is firmly clamped between two parallel oscillation arms. One arm keeps the specimen oscillating so that the system attains a resonance frequency of almost constant amplitude. The modulus is calculated from the resonance frequency, the resultant amplitude, and the dimensions of the specimen.

Free-vibration apparatus (resonant) is highly sensitive and is eminently suitable for studying weak effects. The disadvantage is a drop in frequency combined with falling modulus due to elevated temperatures. Frequency-dependent measurements are difficult to perform and require the use of different test-piece geometries. They thus entail considerable experimental outlay

#### 11.12 Forced Vibration (Non-resonant)

Variable frequency apparatus applies constant amplitude (stress or deformation amplitude). The frequency may be varied during the measurement. Figure 7 shows the design of a torsion apparatus.

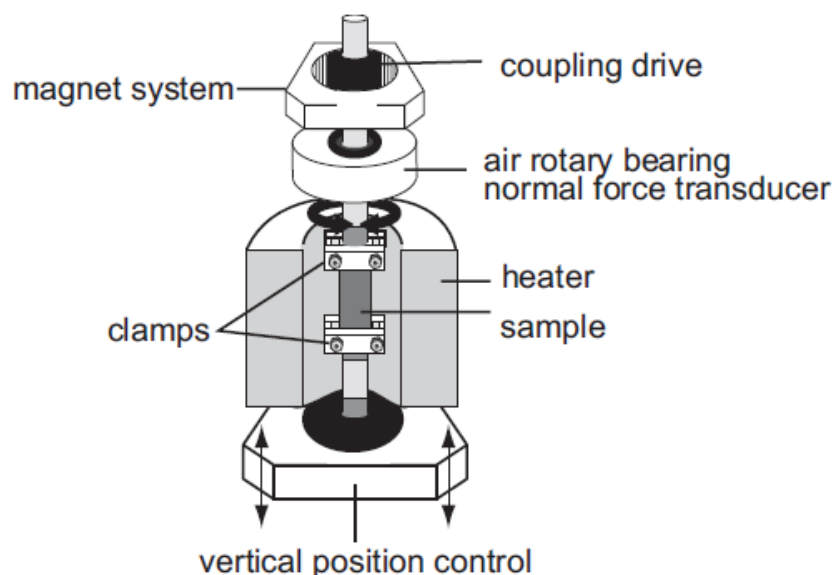


**Figure 7:** Schematic design of a torsion vibration apparatus with variable frequency

Firmly clamped at both ends, the specimen is electromagnetically excited into sinusoidal oscillation of defined amplitude and frequency. Because of the damping properties of the

material or specimen, the torque lags behind the deformation by a value equal to the phase angle  $\delta$ . The observed values for torque, phase angle, and geometry constant of the specimen may be substituted into the formulae to calculate the complex modulus  $E^*$ , the storage modulus  $E'$ , the loss modulus  $E''$ , and the loss factor  $\tan \delta$ .

The specimen should be dimensionally stable and of rectangular or cylindrical cross section. Suitable specimens have modulus values ranging from very high (fiber composites) down to low (elastomers). If appropriate plane-parallel plates are attached to the drive shafts, it is also possible to measure soft, gelatinous substances and viscous liquids. Most types of apparatus utilize vertical loading, which allows measurements under bending, tension, compression, and shear. Usually, the same apparatus is employed, with interchangeable clamping mechanisms applying the various types of load.

**11.Procedure**

A sample is held in place between two grips or confining elements. Next, an oscillatory (dynamic) force is applied to the sample. This is applied using an electric motor moving rotationally (typically back and forth) and linearly (typically up and down), and contains a frequency (speed of oscillation), and a force (energy input into sample). Resulting strain (displacement) is measured using LVDT measurement or by a force transducer. Plots Storage Modulus and Tan Delta (damping) vs. Temperature (Figure 8) calculates  $T_g$  (the “glass transition”, melting of amorphous phase) and Beta transitions (low temperature declines in Modulus).

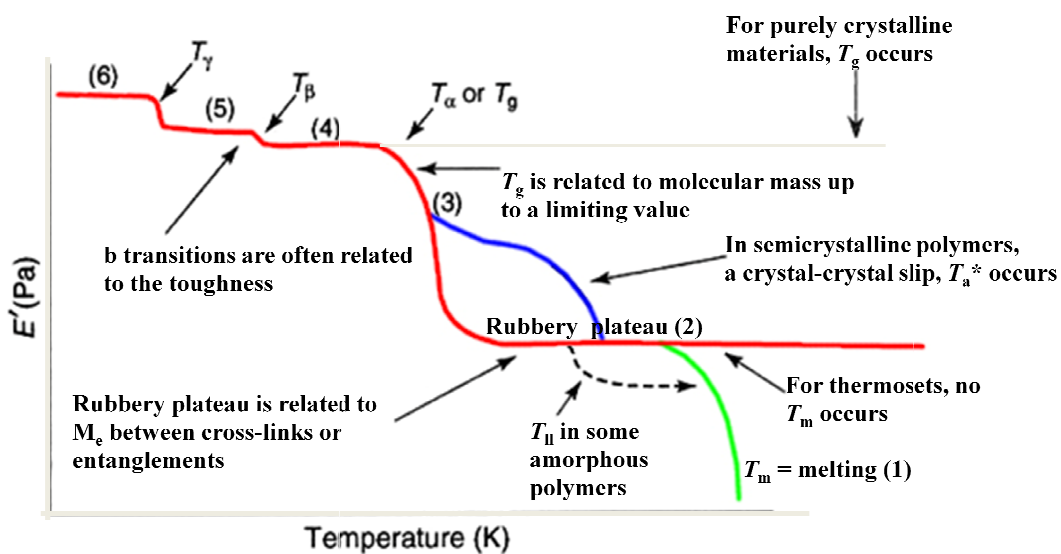


**Figure 8:** plots Storage Modulus and Tan Delta (damping) vs. Temperature

The following different methods of analysis can be done in DMA instrument

*Temperature scan:* Modulus and damping is recorded as the sample is heated

*Frequency scan:* Modulus and damping is recorded as the sample is vibrated at increasing speeds

*Stress scan:* Modulus and damping is recorded as the sample stress is increased

*Strain scan:* Modulus and damping is recorded as the sample strain is increased

*Transient testing (not oscillatory):* Creep-Relaxation and Stress-Recovery

*Multiplexed scan:* Combinations of above methods

### Evaluation

Because DMA is sensitive to variations in the stiffness of a material, it may be used to determine not only modulus and damping values directly, but also glass transition temperatures. It is particularly suitable for determining glass transitions because the change in modulus is much more pronounced in DMA than, for example, the cp change in a DSC measurement. Owing to discrepancies between the proposals made in various standards and the information provided by apparatus manufacturers, confusion has arisen about how to determine and state glass transition temperatures in practice. Although the modulus step that occurs during the glass transition can be evaluated much in the manner of a DSC curve, it is difficult to do so in practice.

For example,

The DMA curve of polycaprolactone measured at a mechanical vibration frequency of 1 Hz is shown in Figure 9.

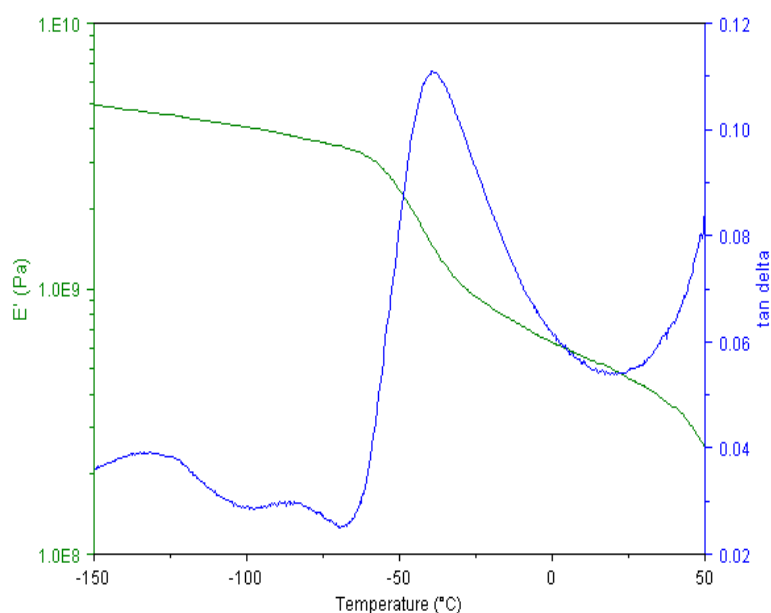


**Figure 9:** The DMA curve of polycaprolactone



---

The drop in storage modulus ( $E'$ ) and peak in damping factor ( $\tan \delta$ ) between  $-60$  and  $-30^\circ\text{C}$  is due to the glass transition ( $T_g$ ) of the amorphous polymer in this semi-crystalline material. Above  $50^\circ\text{C}$  the sample begins to melt and flow, thus losing all mechanical integrity. Below the  $T_g$  small peaks are evident in the  $\tan \delta$  curve at  $-80$  and  $-130^\circ\text{C}$ . These are the beta and gamma transitions in this polymer (the glass transition is known also as the alpha transition) and are caused by local motion of the polymer chains as opposed to large scale co-operative motion that accompanies the  $T_g$ . These small transitions are very difficult to observe by DSC but are often very important in determining the impact resistance of the polymer.

### Summary of the unit

In the 50's, the term "thermal analysis" meant simply heating a sample in a capillary melting point tube to measure the melting point, or incinerating it to measure its ash content. And that was about all there was to thermal analysis. Now the term is applied to a host of tests, including DSC (differential scanning calorimetry), TGA (Thermogravimetric analysis), and DMA (dynamic mechanical analysis). DMA is a shortened form of Dynamic Mechanical Thermal Analysis (DMTA), which is another name for Dynamic Mechanical Rheological Testing (DMRT). Many materials undergo changes of their thermomechanical properties during heating or cooling. For example, phase changes, sintering steps or softening can occur in addition to thermal expansion. TMA analyses can hereby provide valuable insight into the composition, structure, production conditions or application possibilities for various materials. The application range of instruments for thermomechanical analysis extends from quality control to research and development. Typical domains include plastics and elastomers, paints and dyes, composite materials, adhesives, films and fibers, ceramics, glass and metals.

Dynamic mechanical analysis (DMA) is a technique used to study and characterize materials. It is most useful for studying the viscoelastic behavior of polymers. A sinusoidal stress is applied and the strain in the material is measured, allowing one to determine the modulus. The temperature of the sample or the frequency of the stress is often varied, leading to variations in the modulus. This approach can be used to locate the glass transition temperature of the material.

DMA measures stiffness and damping, these are reported as modulus and  $\tan \delta$ . Because sinusoidal stress is applied, modulus can be expressed as

In-phase component, the storage modulus ( $E'$ ) and

---

Out of phase component, the loss modulus ( $E''$ )

Storage modulus ( $E'$ ) is a measure of elastic response of a material. It measures the stored energy. Loss modulus ( $E''$ ) is a measure of viscous response of a material. It measures the energy dissipated as heat.

Tan delta is the ratio of loss to the storage and is called damping. It is a measure of the energy dissipation of a material. It tells us how good a material will be at absorbing energy.

Basically tan delta can be used to characterize the modulus of the material. Delta should range between  $0^\circ$  and  $90^\circ$  and as delta approaches  $0^\circ$  it also approaches a purely elastic behaviour. As delta approaches  $90^\circ$  the material approaches a purely viscous behaviour.

The tan of delta is defined below

$$\tan(\delta) = E''/E'$$

$E''$  = storage modulus

$E'$  = loss modulus

Increasing Tan delta indicates that your material has more energy dissipation potential so the greater the Tan delta, the more dissipative your material is.

Decreasing Tan delta means that your material acts more elastic now and by applying a load, it has more potential to store the load rather than dissipating it!

For example, in case of nano-composites (and filled polymers), increasing the nano-particle content diminishes the value of Tan delta as nano-particles impose restrictions against molecular motion of polymer chains (due to the adsorption of polymer chain on the surface of the particles) resulting in more elastic response of the material.

### **Key words**

Thermomechanical analysis; TMA probe types; TMA temperature calibration; Thermal expansion measurement; Glass transition temperature by TMA ; Dynamic Mechanical Analysis (DMA)

### **References for further studies**

- 1) Dynamic Mechanical Analysis: A Practical Introduction; Kevin P. Menard; *CRC Press*, **2008**.
- 2) Principles and Applications of Thermal Analysis; Paul Gabbott; *John Wiley & Sons*, **2008**.
- 3) Introduction to Thermal Analysis: Techniques and applications; Michael Ewart Brown; *Springer Science & Business Media*, **2012**.

- 
- 4) Principles of Thermal Analysis and Calorimetry; Peter J. Haines; *Royal Society of Chemistry*, **2002**.
  - 5) Thermal analysis of Micro, Nano- and Non-Crystalline Materials: Transformation, Crystallization, Kinetics and Thermodynamics; Jaroslav, Peter Simon; *Springer Science & Business Media*, **2012**.
  - 6) Thermal Analysis of Polymers: Fundamentals and Applications; Joseph D. Menczel, R. Bruce Prime; *John Wiley & Sons*, **2014**.

**Questions for self understanding**

- 1) What is thermomechanical analysis?
- 2) Explain the instrumentation of thermomechanical analysis
- 3) Discuss the TMA probe types
- 4) How TMA temperature calibration can be done?
- 5) Explain the thermal expansion measurement in thermomechanical analysis
- 6) Discuss the measurement of glass transition temperature by TMA
- 7) What is Dynamic Mechanical Analysis (DMA)?
- 8) Explain the basic principles of DMA
- 9) Explain the theory of DMA
- 10) Discuss the equipment used in DMA

---

**UNIT-12****Structure**

- 12.0 Objectives of the unit
- 12.1 Introduction
- 12.2 Theory
- 12.3 Instrumentation
- 12.4 Procedure
- 12.5 Methodology
- 12.6 Precautions
- 12.7 Applications
- 12.8 Estimation of Benzene in Cyclohexane
- 12.9 Summary of the unit
- 12.10 Key words
- 12.11 References for further studies
- 12.12 Questions for self understanding

---

## 12.0 Objectives of the unit

After studying this unit you are able to

- Explain the theory of thermometric analysis
- Discuss the instrumentation of thermometric analysis
- Explain the procedure of thermometric analysis
- Discuss the methodology followed in thermometric analysis
- Explain the precautions need to take in thermometric analysis
- Discuss the applications of thermometric analysis
- Explain the estimation of Benzene in Cyclohexane using thermometric analysis

## 12.1 Introduction

Thermometry is the science and practice of temperature measurement. Any measurable change in a thermometric probe (e.g. the dilatation of a liquid in a capillary tube, variation of electrical resistance of a conductor, of refractive index of a transparent material, and so on) can be used to mark temperature levels, that should later be calibrated against an internationally agreed unit if the measure is to be related to other thermodynamic variables (if the measure is only needed to establish an ordering in thermal levels, no calibration is required). Thermometry is sometimes split in metrological studies in two subfields: contact thermometry and noncontact thermometry. As there can never be complete thermal uniformity at large, thermometry is always associated to a heat transfer problem with some space-time coordinates of measurement, given rise to time-series plots and temperature maps (profiles, if one-dimensional).

## 12.2 Theory

The thermometric titrations (TT) make use of 'heats of reaction' to obtain titration curves. In usual practice, the temperature of solution is plotted against the volume of titrant. TT is performed by allowing the titrant to flow from a thermostated-burette directly into a solution contained in a thermally-insulated vessel, and subsequently the observed change in temperature of the solution is recorded precisely either during continuous addition of titrant or after every successive incremental addition. The end-point is aptly indicated by a sharp break in the curve. As the dielectric constant of a solvent exerts little effect on the thermometric titrations, the latter may be employed effectively in most non-aqueous media. Hence, in a broader-sense TT may be utilized in a number of reactions with greater efficacy, for instance : complexation, precipitation, redox, neutralization. Further, TT can be used to

titrate gases against other gases devoid of a liquid-phase ; and to titrate liquid solutions with gaseous reagents.

### 12.3 Instrumentation

A standard thermometric titration assembly essentially consists of the following four vital components, namely

- i) Motor-driven Burette,
- ii) Adiabatic Titration Chamber
- iii) Thermister Bridge Assembly, and
- iv) Recorder.

Figure 1, represents the schematic thermometric titration assembly complete with a bridge-circuit. To minimise heat transfer losses from the solution by its immediate surroundings, the thermometric titrations are usually carried out in an isolated-beaker tightly closed with a stopper having provision for a burette-tip, a motorized-glass stirrer, and a temperature-monitoring arrangement.

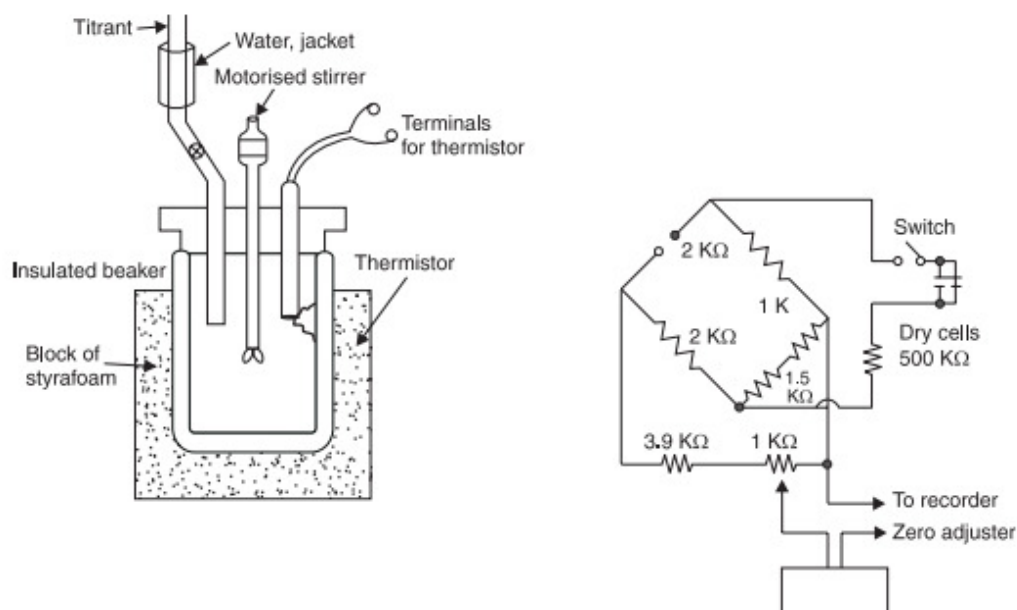


**Figure 1:** Schematic Thermometric Titration Assembly Complete with a Bridge-Circuit

### 12.4 Procedure

- a) Introduce the titrant from a burette that is duly mounted in a thermostated-water-jacket to maintain the temperature of the titrant within  $\pm 0.05^\circ\text{C}$ ,
- b) Experimental parameters are predetermined in such a fashion such that the volume of titrant needed for each titration must lie between 1-3 ml,

- c) Automated device delivering reagent at a steady and constant rate of 600  $\mu\text{l}$  per minute usually permits recording,
- d) Constant-speed motorized stirrer at 600 rpm is employed to effect uniform mixing of solution,
- e) Variations in temperature are measured with the help of a sensitive thermister-sensing-element with fast response, that is sealed completely in glass and immersed in solution,
- f) In the course of a thermometric titration, the thermister attached to the insulated-beaker is connected to one arm of the Wheatstone Bridge as displayed in Figure 11.5. The values of the circuit component listed are for a thermister having an approximate resistance of  $2\text{ K}\Omega$  and a sensitivity of  $-0.04\ \Omega/\Omega/^\circ\text{C}$  in the  $25^\circ\text{C}$  temperature range. Hence, an observed change of  $1^\circ\text{C} \equiv$  an unbalanced potential of  $15.7\text{ mV}$ , and
- g) The heat of reaction is either absorbed or generated upon addition of the titrant to the beaker, thereby unbalancing the Wheatstone Bridge caused by simultaneous variations in the resistance (temperature) in the insulated-beaker thermister. Thus, the bridge unbalance potential is promptly plotted by the recorder.

Note: i) To minimise the temperature variations between the titrant and the solution and also to obviate volume corrections, the concentration of the titrant is invariably maintained 10–100 times higher than that of the reactant, and

ii) To obtain optimum results, temperatures of the titrant and the solution must be always within  $0.2^\circ\text{C}$  of each other before a titration is commenced.

### 12.5 Methodology

Thermometric titration curves usually represent both the entropy and the free energy involved. The titrant is added to the solution at a constant rate in order that the voltage output of the thermister-temperaturetransducer changes linearly with time upto the equivalence point. TT-method affords exact end-point due to

- a) Coloured solutions, and  
b) Poisoning of Electrodes.

In usual practice it has been observed that thermometric titrations are mostly feasible with such systems that provide rates of temperature change more than  $0.01^\circ\text{C}/\text{second}$ . A few typical examples are cited below

S.No.	Titrant (M)	Solution (M)	Temp. Change ( $^\circ\text{C}$ )
1.	NaOH (1 M ; 1 ml)	HCl (0.33 M ; 30 ml)	+ 0.4 $^\circ\text{C}$
2.	Na <sub>2</sub> -EDTA (1 M)	MgCl <sub>2</sub> (0.033 M)	- 0.08 $^\circ\text{C}$

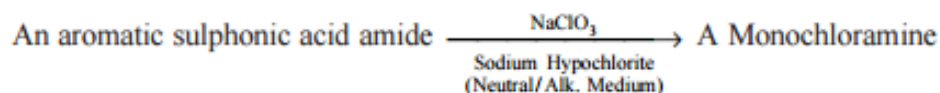
## 12.6 Precautions

- i) Lower limit of concentrations which can be titrated effectively is 0.002 M, ii) No transfer of heat between the titration vessel and its immediate surroundings is allowed, and
- iii) During titration temperature fluctuation must not exceed 0.001°C.

## 12.7 Applications

Various important applications of thermometric titrations are enumerated below

- i) Precipitation Reactions: e.g., Chloride ions ( $\text{Cl}^-$ ) with  $\text{Ag}^+$  ions. Besides, phase relations have been studied extensively in precipitation reactions.
- ii) Ion-combination Reactions: e.g., divalent cations like  $\text{Ca}^{2+}$ ,  $\text{Mg}^{2+}$  with EDTA (complexometric estimation),
- iii) Conversion of Amides to Amines : e.g.,



- iv) Estimation of  $\text{H}_2\text{O}$  and  $(\text{CH}_3\text{CO})_2\text{O}$  concentrations in a mixture : The concentration of either of these reactions in the presence of the other may be determined successfully by measuring the rise in temperature taking place during the exothermic reactions of water and acetic anhydride in glacial acid solution along with a trace of perchloric acid ( $\text{HClO}_4$ ) acting as a catalyst, and
- v) Benzene in Cyclohexane : Benzene may be estimated rapidly with fairly good accuracy in cyclohexane by measuring the heat of nitration, whereby a previously prepared standard nitrating acid mixture (benzene and cyclohexane) and the subsequent temperature rise is noted which is a direct function of the quantity of benzene present. Details involving various experimental parameters for the above estimation are enumerated below

## 12.8 Estimation of Benzene in Cyclohexane

### *Materials Required*

Thermometric titration assembly as per Figure 11.5, minus the burette; a stopwatch or timer ; standard nitrating acid mixture [mix 2 volumes of 70%  $\text{HNO}_3$  ( $d = 1.41$ ) with 1 volume of 95%  $\text{H}_2\text{SO}_4$  ( $d = 1.82$ )] ; Bakelite screw-cap bottle (4 oz. capacity) 2:

### *Procedure*

- 1) Weigh 50 g of sample in a Bakelite screw-cap bottle and in a similar bottle put the standard nitrating mixture. Place these two bottles in a thermostat maintained at 20°C until the contents have attained an equilibrium temperature,



- 2) Transfer 50 ml of the standard nitrating-acid to the insulated vessel and insert the motorised stirrer. Just wait for about 3-5 minutes and then start the motorized stirrer. After exactly 1 minute record the initial temperature,
- 3) Stop the motor. Insert the sample into the reaction vessel and start the stirrer. Now, start taking readings of the rise in temperature after each interval 1, 2, 3 and 5 minutes respectively, and
- 4) Plot a 'calibration curve' between the observed temperature-rise in a 3 minute interval Vs percent benzene present in cyclohexane. Run pure cyclohexane and standards containing 0.5-5.0 percent benzene by weight.

### 12.9 Summary of the unit

The titration is a basis quantitative analytical method. It allows a simple analysis to determine the amount of product in the sample following a chemical reaction without need do a comparison with a standard. The potentiometric titration following the potential of a solution also it is a differential method between a reference and a measurement electrodes. This potential can be interpret as a pH or a potential redox par example. Thermometry is the science and practice of temperature measurement. Any measurable change in a thermometric probe (e.g. the dilatation of a liquid in a capillary tube, variation of electrical resistance of a conductor, of refractive index of a transparent material, and so on) can be used to mark temperature levels, that should later be calibrated against an internationally agreed unit if the measure is to be related to other thermodynamic variables (if the measure is only needed to establish an ordering in thermal levels, no calibration is required).

### 12.10 Key words

Thermometric analysis; Instrumentation; Procedure of thermometric analysis; Methodology followed in thermometric analysis

### 12.11 References for further studies

- 1) A Practical Guide to Instrumental Analysis; Erno Pungor, G. Horvai; *CRC Press*, **1994**.
- 2) Thermometric Titrimetry: International Series of Monographs in Analytical Chemistry; L. S. Bark, S. M. Bark; *Elsevier*, **2013**.
- 3) Instrumental Methods of Chemical Analysis; Dr. B. K. Sharma; *Krishna Prakashan Media*, **2000**.
- 4) Undergraduate Instrumental Analysis, 7<sup>th</sup> Ed. James W. Robinson, Eileen Skelly Frame, George M. Frame II; *CRC Press*, **2014**.
- 5) Pharmaceutical Drug Analysis; Ashutosh Kar; *New Age International*, **2007**.

**12.12 Questions for self understanding**

- 1) Explain the theory of thermometric analysis
- 2) Discuss the instrumentation of thermometric analysis
- 3) Explain the procedure of thermometric analysis
- 4) Discuss the methodology followed in thermometric analysis
- 5) Explain the precautions need to take in thermometric analysis
- 6) Discuss the applications of thermometric analysis
- 7) Explain the estimation of Benzene in cyclohexane using thermometric analysis

**UNIT-13****Structure**

- 13.0 objectives of the unit
- 13.1 Introduction
- 13.2 Principle (Mode of action of catalysts)
- 13.3 Activity
- 13. 4 Industrial requirements of catalysis
- 13.5 Industrial processes using heterogeneous catalysis.
- 13.6 Thermodynamics and Kinetics aspects
  - 13.6.1 Thermodynamics Studies
- 13.7 Activation energy( $\Delta G_a$ )
- 13.8 Classification of Catalytic system
- 13.9 Summary of the unit
- 13.10 Key words
- 13.11 References for further studies
- 13.12 Questions for self understanding

### 13.0 objectives of the unit

After studying this unit you are able to

- Explain the mode of action of catalysts
- Discuss the activity of catalyst
- Explain the Industrial requirements of catalysis
- Discuss the industrial processes using heterogeneous catalysis.
- Explain the thermodynamics and kinetics aspects of catalytic action
- Calculate the Activation energy ( $\Delta G_a$ ) of a reaction with and without catalyst
- Write the classification of catalytic system

### 13.1 Introduction

Catalysis is the key to chemical transformations. Most industrial syntheses and nearly all biological reactions require catalysts. Furthermore, catalysis is the most important technology in environmental protection, i.e., the prevention of emissions. A well-known example is the catalytic converter for automobiles. Catalytic reactions were already used in antiquity, although the underlying principle of catalysis was not recognized at the time. For example, the fermentation of sugar to ethanol and the conversion of ethanol to acetic acid are catalyzed by enzymes (biocatalysts). However, the systematic scientific development of catalysis only began about 200 years ago, and its importance has grown up to the present day.

The term “catalysis” was introduced as early as 1836 by Berzelius in order to explain various decomposition and transformation reactions. He assumed that catalysts possess special powers that can influence the affinity of chemical substances. A definition that is still valid today is due to Ostwald (1895): “a catalyst accelerates a chemical reaction without affecting the position of the equilibrium.” Ostwald recognized catalysis as a ubiquitous phenomenon that was to be explained in terms of the laws of physical chemistry. While it was formerly assumed that the catalyst remained unchanged in the course of the reaction, it is now known that the catalyst is involved in chemical bonding with the reactants during the catalytic process. Thus catalysis is a cyclic process: the reactants are bound to one form of the catalyst, and the products are released from another, regenerating the initial state.

### 13.2 Principle (Mode of action of catalysts)

The suitability of a catalyst for an industrial process depends mainly on the following three properties:

- *Activity*
- *Selectivity*
- *Stability (deactivation behavior)*

The question which of these functions is the most important is generally difficult to answer because the demands made on the catalyst are different for each process. First, let us define the above terms.

### 13.3 Activity

Activity is a measure of how fast one or more reactions proceed in the presence of the catalyst. Activity can be defined in terms of kinetics or from a more practically oriented viewpoint. In a formal kinetic treatment, it is appropriate to measure reaction rates in the temperature and concentration ranges that will be present in the reactor.

- Reaction rate
- Rate constant  $k$
- Activation energy  $E_a$

Empirical rate equations are obtained by measuring reaction rates at various concentrations and temperatures. If, however, different catalysts are to be compared for a given reaction, the use of constant concentration and temperature conditions is often difficult because each catalyst requires its own optimal conditions. In this case it is appropriate to use the initial reaction rates obtained by extrapolation to the start of the reaction.

The number of active centers per unit mass or volume of catalyst can be determined indirectly by means of chemisorption experiments, but such measurements require great care, and the results are often not applicable to process conditions.

For optimization of catalyst production conditions, and deactivation studies, the following activity measures can be used:

- Conversion under constant reaction conditions
- Space velocity for a given, constant conversion
- Space–time yield
- Temperature required for a given conversion

Catalysts are often investigated in continuously operated test reactors, in which the conversions attained at constant space velocity are compared.

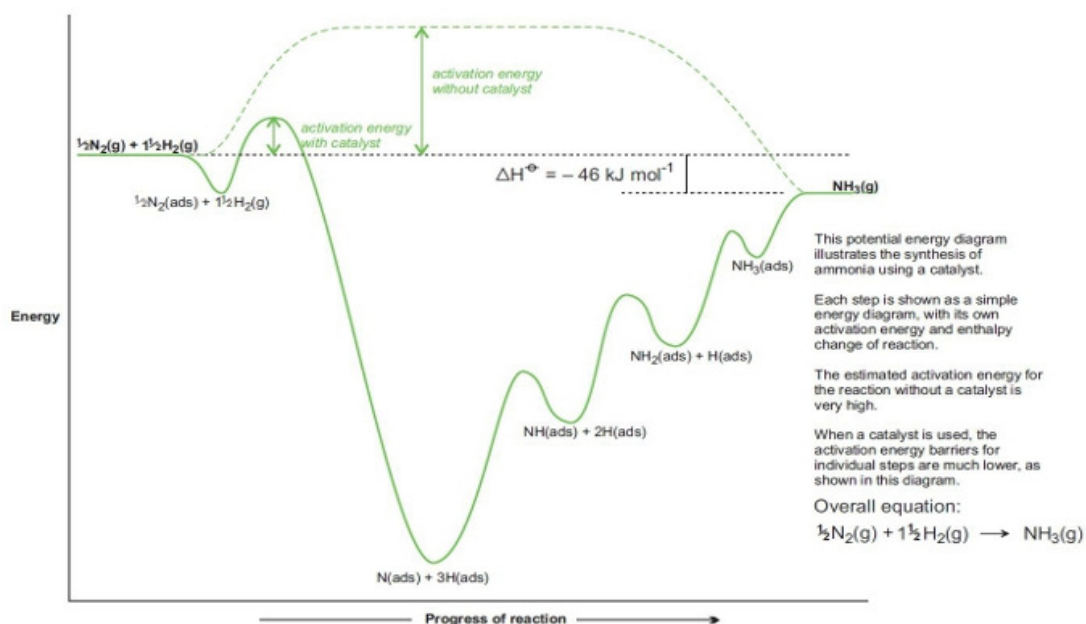
### 13.4 Industrial requirements of catalysis

Catalysts are substances that speed up reactions by providing an alternative pathway for the breaking and making of bonds. Key to this alternative pathway is a lower activation energy than that required for the uncatalysed reaction.

Catalysts are often specific for one particular reaction and this is particularly so for enzymes which catalyse biological reactions, for example in the fermentation of carbohydrates to produce biofuels.

Much fundamental and applied research is done by industrial companies and university research laboratories to find out how catalysts work and to improve their effectiveness. If catalytic activity can be improved, it may be possible to lower the temperature and/or the pressure at which the process operates and thus save fuel which is one of the major costs in a large-scale chemical process. Further, it may be possible to reduce the amount of reactants that are wasted forming unwanted by-products.

If the catalyst is in the same phase as the reactants, it is referred to as a **homogeneous** catalyst. A **heterogeneous** catalyst on the other hand is in a different phase to the reactants and products, and is often favoured in industry, being easily separated from the products, although it is often less specific and allows side reactions to occur.



The most common examples of catalysis in industry involve the reactions of gases being passed over the surface of a solid, often a metal, a metal oxide or a zeolite.

Process	Catalyst	Equation
Making ammonia	Iron	$\text{N}_2(\text{g}) + 3\text{H}_2(\text{g}) \rightleftharpoons 2\text{NH}_3(\text{g})$
Making synthesis gas (carbon monoxide and hydrogen)	Nickel	$\text{CH}_4(\text{g}) + \text{H}_2\text{O}(\text{g}) \rightleftharpoons \text{CO}(\text{g}) + 3\text{H}_2(\text{g})$
Catalytic cracking of gas oil	Zeolite	Produces: a gas (e.g. ethene, propene) a liquid (e.g. petrol) a residue (e.g. fuel oil)
Reforming of naphtha	Platinum and rhenium on alumina	$\text{CH}_3\text{CH}_2\text{CH}_2\text{CH}_2\text{CH}_2\text{CH}_3(\text{g}) \rightarrow \text{C}_6\text{H}_{12}(\text{g}) + \text{H}_2(\text{g})$
Making epoxyethane	Silver on alumina	$\text{C}_2\text{H}_4(\text{g}) + \frac{1}{2}\text{O}_2(\text{g}) \rightarrow \text{H}_2\text{C} \begin{array}{c} \diagup \text{O} \diagdown \\ \text{---} \end{array} \text{CH}_2(\text{g})$
Making sulfuric acid	Vanadium(V) oxide on silica	$\text{SO}_2(\text{g}) + \frac{1}{2}\text{O}_2(\text{g}) \rightarrow \text{SO}_3(\text{g})$
Making nitric acid	Platinum and rhodium	$4\text{NH}_3(\text{g}) + 5\text{O}_2(\text{g}) \rightarrow 4\text{NO}(\text{g}) + 6\text{H}_2\text{O}(\text{g})$

### 13.5 Industrial processes using heterogeneous catalysis.

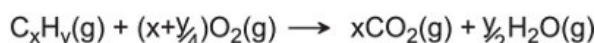
The gas molecules interact with atoms or ions on the surface of the solid. The first process usually involves the formation of very weak intermolecular bonds, a process known as physisorption, followed by chemical bonds being formed, a process known as chemisorption.

Physisorption can be likened to a physical process such as liquefaction. Indeed the enthalpy changes that occur in physisorption are cal-20 to -50 kJ mol<sup>-1</sup>, similar to those of enthalpy changes when a gas condenses to form a liquid. The enthalpies of chemisorptions are similar to the values found for enthalpies of reaction. They have a very wide range, just like the range for non-catalytic chemical reactions.

An example of the stepwise processes that occur in heterogeneous catalysis is the oxidation of carbon monoxide to carbon dioxide over palladium. This is a very important process in everyday life. Motor vehicles are fitted with catalytic converters. These consist of a metal casing in which there are two metals, palladium and rhodium, dispersed very finely on the surface of a ceramic

support that resembles a honeycomb of holes. The converter is placed between the engine and the outlet of the exhaust pipe.

The exhaust gases contain carbon monoxide and unburned hydrocarbons that react with the excess oxygen to form carbon dioxide and water vapour, the reaction being catalysed principally by the palladium



The exhaust gases also contain nitrogen(II) oxide (nitric oxide, NO), and this is removed by reactions catalysed principally by the rhodium



The accepted mechanism for the oxidation of carbon monoxide to carbon dioxide involves the chemisorption of both carbon monoxide molecules and oxygen molecules on the surface of the metals. The adsorbed oxygen molecules dissociate into separate atoms of oxygen. Each of these oxygen atoms can combine with a chemisorbed carbon monoxide molecule to form a carbon dioxide molecule. The carbon dioxide molecules are then desorbed from the surface of the catalyst. A representation of these steps is shown in Figure 1.

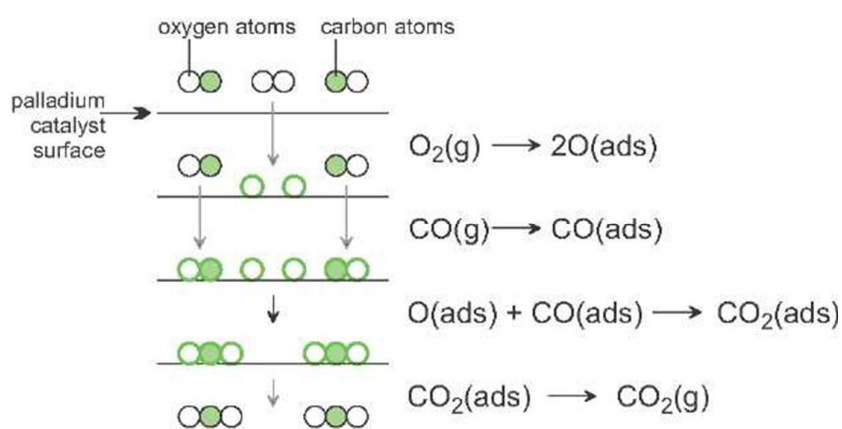


**Figure 1:** A mechanism for the oxidation of carbon monoxide

### 13.6 Thermodynamics and Kinetics aspects

#### *Kinetics aspects*

The rate constant,  $k$ , measures how fast a chemical reaction reaches equilibrium assuming the reactants were supplied with enough activation energy to enable the reaction to proceed in the forward direction—reactants to products. This requirement for input of energy symbolizes the fact that the reactants are unreactive under certain conditions. The reaction must have some sort



of energy input before it can proceed; otherwise, the reactants cannot cross the activation energy threshold and convert to products. The reaction is activated by energy supplied to the reactants by different energy sources. The rate of reaction, the rate constant, and the kinetic energy required for activation of reaction indicate how fast the reaction reaches equilibrium.

The transition state represents a threshold the reactants must pass before the reaction can proceed in the forward direction. The activation energy is the energy required to reach the transition state. Once this threshold is reached, the reaction proceeds in the favorable "downhill" direction. It is important to remember that each reaction has a different transition state threshold, with different activation energies, and determined by the reactants and the conditions in which the reaction is taking place. The value of  $k$  is affected by these two factors, and can be increased in the presence of a catalyst (such as an enzyme), which increases reaction rate. In chemical reactions, specifically, the catalyst can both provide more energy to the reactants and lower the transition state energy. The provider of activation energy can also be a spark, heat, or anything else that gives off energy. Regardless of what provides the activation energy, a kinetic or nonspontaneous reaction is one in which the most stable state is that of the reactants. The change in energy between the reactants and products, also known as  $\Delta G$ , relates to thermodynamics and will be discussed shortly.

A process concerned for Kinetics could be a chemical reaction (change between different molecules or materials), or a transformation between two material structures (or phases), for which only the crystalline structure (atomic arrangement) changes, while the chemical compositions (concerned elements, ionic valence state, etc) remain the same. Indeed, such "phase transformation" will be one of the major topic throughout this Kinetics course. Typical examples of "phase transformation" include freezing of water, eutectoid transformation of steel between austenite ( $\gamma$ -Fe) and pearlite ( $\alpha$ -Fe + Fe<sub>3</sub>C), transition between graphite and diamond (but takes forever), etc.

In all processes of materials transformation, atomic (ionic) rearrangement takes place. When an atom (ion) moves in an environment surrounded by other atoms or ions, bonds are broken, new bonds are formed and the surrounding atoms are displaced (during the transition) from their equilibrium positions. This leads to a momentary increase in local energy, forming an intermediate (non-equilibrium) state, so-called transition (or activated) state. Thus, two

equilibrium states which are characterized by local minima in free energy ( $G$ , stands for Gibbs free energy) are separated by a maximum represented by the activated state, as shown below:

The local minima are state function, and intrinsic to the molecular (materials) structure, where inter-atomic interaction plays important role in determining the system energy. The energy-minimized state can usually be calculated by theoretical and computational methods. However, this is not true for the maximum (activated state), for which the structure is not in equilibrium and hard to predict.

For a process to occur, it must overcome the energy maximum. The larger the barrier ( $\Delta G_a$ ), the difference between the maximum and the initial minimum, the harder the process to occur, the slower the rate.

For a process or a reaction to occur, the thermodynamics must be favorable (i.e.,  $\Delta G < 0$ ), and the kinetics must be fast enough (small  $\Delta G_a$ ).

In general: Rate  $\propto$  (Kinetic factor)  $\times$  (Thermodynamic factor)

Kinetic factor refers to  $\Delta G_a$ , **activation energy**; while the thermodynamic factor refers to  $\Delta G = G_2 - G_1$ , the **driving force**.

Understanding of  $\Delta G = G_2 - G_1$ , the **driving force**

Kinetic theory: the rate of reaction is proportional to the probability to reach activated state, thus, rate  $\propto e^{-\Delta G_a / RT}$

### 13.6.1 Thermodynamics Studies

Thermodynamics can be considered in terms of the energy stored within a reaction, a reactant, or a product. Most often, thermodynamics is thought of as the different forms of energy that are converted every time a reaction emits energy or is initiated by energy. With respect to Gibbs free energy ( $\Delta G$ ), thermodynamics refers to either the energy released during a reaction, in which case  $\Delta G$  will be negative and the reaction exergonic or spontaneous. the energy consumed during a reaction, in which case  $\Delta G$  will be positive and the reaction endergonic or nonspontaneous. A thermodynamic reaction favors the products, resulting in a spontaneous reaction that occurs without the need to constantly supply energy. This indicates that the reactions' most stable state is that of the products.

Thus, going back to Diagram 2, thermodynamics is what describes the free energy between the reactants and the products. Because thermodynamic values apply only after the reactants have turned into products, they are said to describe the equilibrium state. The relationship between

free energy (aka, Gibbs free energy) and other thermodynamic quantities is expressed mathematically in the following equation:

$$G = U + pV - TS$$

Because "U" is the variable representing the internal energy of a system, it is closely correlated with the free energy. Changes in internal energy change the value of the free energy, in turn affecting chemical reactions in several ways: the rate of reaction, whether the reaction is spontaneous or non-spontaneous, and even whether or not activation energy will be needed to initiate the reaction

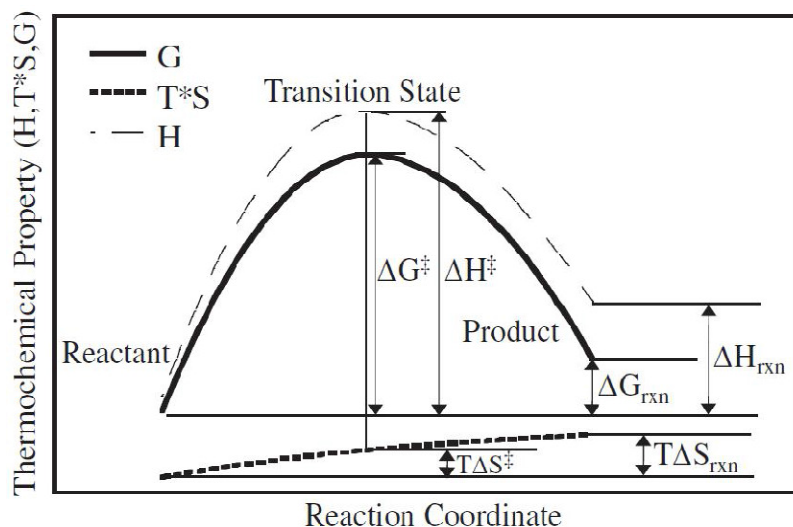


**Figure 2:** Thermodynamic graph

A thermodynamically favorable reaction or process means  $\Delta G < 0$ , that's to say, highly driven. The products are at a lower free energy, or more stable, than the reactants. Because of this, the reactants "want" to be converted into the products.

### 13.7 Activation energy ( $\Delta G_a$ )

It is the maximum in energy separating the two equilibrium states; overcoming this barrier represents the bottle-neck for the reaction to finish, thus a rate determining step. The rate can be given in terms of the transition state (often called activated complex) by considering the activation energy,  $\Delta G_a$ . The high hump of activation energy also indicates the high energy of the transition state, or activated complex that is at the top of the hump is so unstable.

It is often gets confused between thermodynamic quantities like *free energy* with kinetic ones like *activation energy*. Probably for this reason, "thermodynamics" and "kinetics" are often taught in separate courses as in our department.

The free energies are average energies over a large number of atoms. As a result of random thermal motion of the atoms (*depending on temperature*), the energy of any particular atom will vary with time and occasionally it may be sufficient for the atom to reach the *activated state*, which is called “thermal activation”.

### 13.8 Classification of Catalytic system

The numerous catalysts known today can be classified according to various criteria: structure, composition, area of application, or state of aggregation. Here we shall classify the catalysts according to the state of aggregation in which they act. There are two large groups: heterogeneous catalysts (solid-state catalysts) and homogeneous catalysts. There are also intermediate forms such as homogeneous catalysts attached to solids (supported catalysts), also known as immobilized catalysts.

In supported catalysts the catalytically active substance is applied to a support material that has a large surface area and is usually porous. By far the most important catalysts are the heterogeneous catalysts. The market share of homogeneous catalysts is estimated to be only ca. 10–15 %. In the following, we shall briefly discuss the individual groups of catalysts.

- ✓ Heterogeneous catalysts
- ✓ Bulk catalysts
- ✓ Homogeneous catalysts
- ✓ Acid/base catalysts
- ✓ Supported catalysts
- ✓ Transition metal compounds Catalysts
- ✓ Heterogenized Biocatalysts (enzymes)

Catalytic processes that take place in a uniform gas or liquid phase are classified as homogeneous catalysis. Homogeneous catalysts are generally well-defined chemical compounds or coordination complexes, which, together with the reactants, are molecularly dispersed in the reaction medium. Examples of homogeneous catalysts include mineral acids and transition metal compounds (e. g., rhodium carbonyl complexes in oxo synthesis).

Heterogeneous catalysis takes place between several phases. Generally the catalyst is a solid, and the reactants are gases or liquids. Examples of heterogeneous catalysts are Pt/Rh nets for the oxidation of ammonia to nitrous gases (Ostwald process), supported catalysts such as nickel on

kieselguhr for fat hardening, and amorphous or crystalline aluminosilicates for cracking petroleum fractions.

Of increasing importance are the so-called biocatalysts (enzymes). Enzymes are protein molecules of colloidal size [e. g., poly(amino acids)]. Some of them act in dissolved form in cells, while others are chemically bound to cell membranes or on surfaces. Enzymes can be classified somewhere between molecular homogeneous catalysts and macroscopic heterogeneous catalysts.

Enzymes are the driving force for biological reactions. They exhibit remarkable activities and selectivities. For example, the enzyme catalase decomposes hydrogen peroxide 10<sup>9</sup> times faster than inorganic catalysts. The enzymes are organic molecules that almost always have a metal as the active center. Often the only difference to the industrial homogeneous catalysts is that the metal center is ligated by one or more proteins, resulting in a relatively high molecular mass.

Apart from high selectivity, the major advantage of enzymes is that they function under mild conditions, generally at room temperature in aqueous solution at pH values near 7. Their disadvantage is that they are sensitive, unstable molecules which are destroyed by extreme reaction conditions. They generally function well only at physiological pH values in very dilute solutions of the substrate.

Enzymes are expensive and difficult to obtain in pure form. Only recently have enzymes, often in immobilized form, been increasingly used for reactions of nonbiological substances. With the increasing importance of biotechnological processes, enzymes will also grow in importance.

It would seem reasonable to treat homogeneous catalysis, heterogeneous catalysis, and enzymatic catalysis as separate disciplines.

### **13.9 Summary of the unit**

Catalysts are compounds that accelerate the rate of a reaction. Catalysts accelerate reactions by reducing the energy of the rate-limiting transition state. Catalysts do not affect the equilibrium state of a reaction. Transition state is an intermediate state in a chemical reaction that has a higher free energy than both the reactants and the products. Reactions can be sped up by the addition of a catalyst, including reversible reactions involving a final equilibrium state. Recall that for a reversible reaction, the equilibrium state is one in which the forward and reverse reaction rates are equal. In the presence of a catalyst, both the forward and reverse reaction rates will speed up equally, thereby allowing the system to reach equilibrium faster. However, it is very important to

keep in mind that the addition of a catalyst has no effect whatsoever on the final equilibrium position of the reaction. It simply gets it there faster.

Catalysts are compounds that accelerate the progress of a reaction without being consumed. Common examples of catalysts include acid catalysts and enzymes. Catalysts allow reactions to proceed faster through a lower-energy transition state. By lowering the energy of the transition state, which is the rate-limiting step, catalysts reduce the required energy of activation to allow a reaction to proceed and, in the case of a reversible reaction, reach equilibrium more rapidly.

### 13.10 Key words

Mode of action of catalysts; Activity; Industrial requirements of catalysis; Heterogeneous catalysis.; Thermodynamics and Kinetics aspects; Thermodynamics Studies; Activation energy( $\Delta G_a$ ) ; Classification of Catalytic system

### 13.11 References for further studies

- 1) Homogeneous Catalysis: Mechanisms and Industrial Applications; Sumit Bhaduri, Doble Mukesh; *John Wiley & Sons*, **2014**.
- 2) Homogeneous Catalysis with Metal Complexes: Fundamentals and Applications; Gheorghe Duca; *Springer Science & Business Media*, **2012**.
- 3) Industrial Catalysis: A Practical Approach; Jens Hagen; *John Wiley & Sons*, **2015**.
- 4) Handbook of Asymmetric Heterogeneous Catalysis; Kuiling Ding, Yasuhiro Uozumi; *John Wiley & Sons*, **2008**.
- 5) Principles and Practice of Heterogeneous Catalysis; John Meurig Thomas, J. M. Thomas, W. John Thomas; *John Wiley & Sons*, **2015**.
- 6) Organometallic Chemistry and Catalysis; Didier Astruc; *Springer Science & Business Media*, **2007**.

### 13.12 Questions for self understanding

- 1) Discuss the mode of action of catalysts.
- 2) Explain briefly activity of catalyst.
- 3) Discuss the industrial requirements of catalysis;
- 4) With example explain the industrial processes using heterogeneous catalysis
- 5) Explain the catalytic action in terms of thermodynamics and kinetics aspects.
- 6) What is activation energy ( $\Delta G_a$ )? Explain its significance.
- 7) Discuss the classification of catalytic system.

**UNIT-14****Structure**

- 14.0 Objectives of the unit
- 14.1 Introduction
- 14.2 Acid–base catalysis
- 14.3 Catalysis involving transition metal salts and metal complexes
- 14.4 Condition to be satisfied by a Metal to act as a catalyst
- 14.5 Hydrogenation of olefins
- 14.6 Importance of Wilkinson’s catalyst
- 14.7 Role of Rhodium Metal in the catalytic process
- 14.8 Mechanism of hydrogenation of olefins using Wilkinson’s catalyst
- 14.9 Advantages
- 14.10 Disadvantages
- 14.11 Modification over the original Catalyst
- 14.12 Asymmetric hydrogenation
  - 14.12.1 Industrial Catalytic asymmetric hydrogenation
- 14.13 The mechanism of Asymmetric Hydrogenation using a Chiral catalyst
- 14.14 Asymmetric Hydrogenation of Ketones and Isomerisation
- 14.15 Hydrosilylation
- 14.16 Hydrocyanation
- 14.17 Hydrocyanation of Alkenes
- 14.18 Summary of the unit
- 14.19 Key words
- 14.20 References for further studies
- 14.21 Questions for self understanding

## 14.0 Objectives of the unit

After studying this unit you are able to

- Explain the Acid–base catalysis process
- Write the mechanism of hydrogenation of olefins
- Explain the importance of Wilkinson’s catalyst
- Discuss the catalyst used for Asymmetric hydrogenation
- Explain the industrial catalytic asymmetric hydrogenation
- Explain the Hydrosilylation reaction
- Explain the Hydrocyanation reaction
- Explain the Hydrocyanation reaction of Alkenes

## 14.1 Introduction

Until the 1950, organometallic chemistry was an unexplored area of chemistry. Tremendous interest in this field originated predominantly from the two discoveries of i) synthesis of ferrocene in 1952 and ii) the low pressure catalytic polymerization of ethylene, discovered by Ziegler in 1952.

No area of chemistry has produced more suppresses and challenges during the past few decade as organometallic chemistry. This field continues to be one of great excitement and research activity. Elegant and skilful synthetic programmers are being supplemented by an unusual number of chance discoveries.

Synthetic chemists take an intellectual approach. Structural chemists are able to press their various techniques in elucidating the structure of various products formed. Industrial chemists exploit and extent the result by developing numerous catalytic processes of great importance.

Some organometallic compounds of transition metals with both saturated and unsaturated organic systems are of great utility as catalysts in organic chemistry and also in some industrial process. For example,  $[\text{RhCl}(\text{PPh}_3)_3]$ , Wilkinson’s catalyst in the hydrogenation of olefins,  $\text{HCo}(\text{CO})_4$  in the hydroformylation of olefins,  $\text{TiCl}_3\text{-Al}(\text{C}_2\text{H}_5)_3$  in polymerization of olefins,  $[\text{Ni}(\text{acac})_2]$  in cyclooligomerization of acetylenes etc....

## 14.2 Acid–base catalysis

Acceleration of a chemical reaction by the addition of an acid or a base, the acid or base itself not being consumed in the reaction. The catalytic reaction may be acid-specific (acid catalysis), as in the case of decomposition of the sugar sucrose into glucose and fructose in sulfuric acid; or base-

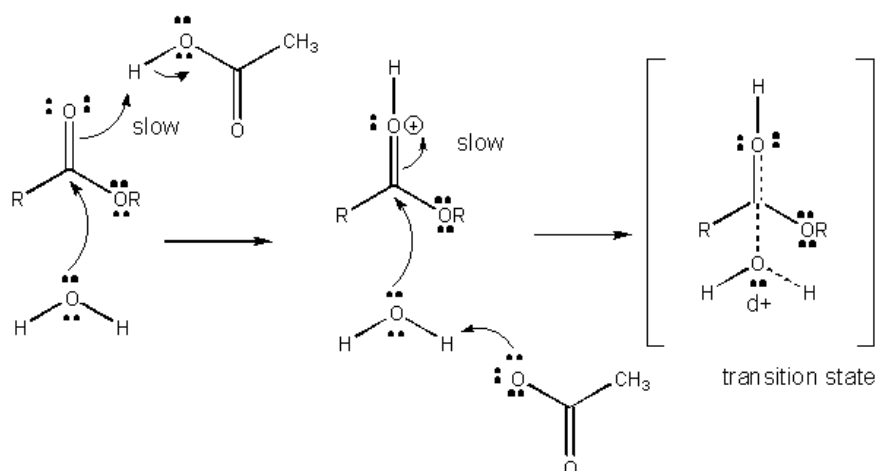


specific (base catalysis), as in the addition of hydrogen cyanide to aldehydes and ketones in the presence of sodium hydroxide. Many reactions are catalyzed by both acids and bases.

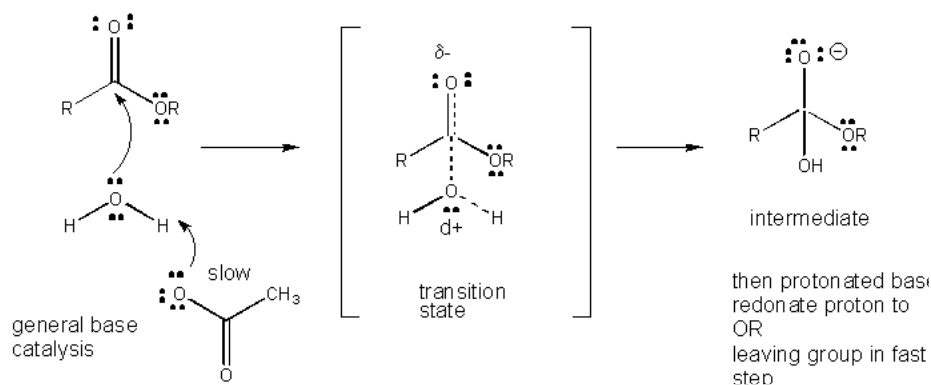
The mechanism of acid- and base-catalyzed reactions is explained in terms of the Brønsted–Lowry concept of acids and bases as one in which there is an initial transfer of protons from an acidic catalyst to the reactant or from the reactant to a basic catalyst. In terms of the Lewis theory of acids and bases, the reaction entails sharing of an electron pair donated by a base catalyst or accepted by an acid catalyst.

Acid catalysis is employed in a large number of industrial reactions, among them the conversion of petroleum hydrocarbons to gasoline and related products. Such reactions include decomposition of high-molecular-weight hydrocarbons (cracking) using alumina–silica catalysts (Brønsted–Lowry acids), polymerization of unsaturated hydrocarbons using sulfuric acid or hydrogen fluoride (Brønsted–Lowry acids), and isomerization of aliphatic hydrocarbons using aluminum chloride (a Lewis acid). The general acid base catalysis mechanism can be represented as

as



Mechanism of general acid catalysis



Mechanism of general base catalysis

### 14.3 Catalysis involving transition metal salts and metal complexes

The d orbitals are what give transition metals their distinguished properties. The transition metal ions the outermost d orbitals are incompletely filled with electrons so they can easily give and take electrons. This makes transition metals prime candidates for catalysis. The outermost s and p orbitals are usually empty and therefore less useful for electron transfer.

The principal reasons why transition metals contribute the essential ingredient in catalyst systems can be summarized as the following headings,

- a) Bonding ability
- b) Careful choice of ligands
- c) Ligand effects
- d) Variability of oxidation state
- e) Variability of co-ordination number

A d-block metal ion has nine valence shell orbitals to accommodate its valence electrons and to form hybrid molecular orbitals in bonding with other groups. The d orbitals are illustrated in the following figure. The special configuration enable the d metal to form both  $\sigma$ - and  $\pi$ - bonds which is one of the key factors in imparting catalytic properties to the transition metals and their complexes. The interactions between the catalyst and the substrate should be "just right"; that is, neither too strong nor too weak. If the interaction is too weak, the substrate will fail to bind to the catalyst and no reaction will take place. On the other hand, if the interaction is too strong, the catalyst gets blocked by substrate or product that fails to dissociate

### 14.4 Condition to be satisfied by a Metal to act as a catalyst

1. At least two moderately stable oxidation states for the metal separated by two units should exist.

Example,  $\text{Rh}^+$  and  $\text{Rh}^{3+}$  in Wilkinson's Catalyst.

2. It should be capable of forming complexes with a range of coordination numbers and of forming moderately stable co-ordinatively unsaturated species.

Example, coordination numbers 3, 4, 5 and 6 for rhodium in Wilkinson's catalyst.

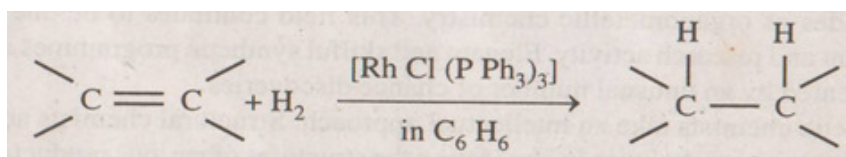
3. It must have the ability to match the substrate orbitals.

For example, if the substrate is an alkene, then this means that the metal must have an empty orbital capable of accepting  $\sigma$ - donating from the alkenes and a filled orbital of  $\pi$ - back donating to the alkene.

The metals Fe, Ru, Os, Co, Rh, Ir, Ni, Pd and Pt meet all of these requirements most effectively. As a consequence the most versatile catalyst comes from this group of metal.

### 14.5 Hydrogenation of olefins

Hydrogenation of olefins is a reaction of major industrial importance, being used in the petrochemical industries and in the pharmaceutical industries where the preparation of drugs often involves the hydrogenation of specific double bonds. It is for the hydrogenation of specific double bonds in compounds containing several double bonds that the search for new more efficient and above all more selective catalysts has been most vigorous. One very successful catalyst for this process is  $[\text{Rh}(\text{Cl})(\text{PPh}_3)_3]$ , chlorotris (triphenylphosphine) rhodium(I). This is an effective homogeneous catalyst in solution of aromatic hydrocarbon such as benzene and toluene. As it very often happens with important discoveries this particular catalyst was discovered independently by two groups and now almost universally referred to as catalyst. The net reaction is



### 14.6 Importance of Wilkinson's catalyst

An ideal hydrogenation catalyst should be capable of catalyzing hydrogenations at or near atmospheric pressure and room temperature. This is because it eliminates the need for expensive vessels capable of withstanding high pressure and high temperature. In this respect this catalyst is remarkably effective because the hydrogenation of isolated double or triple bonds takes place at atmospheric pressure and at room temperature. The applications of Wilkinson's catalyst are important in pharmaceutical industries for making specific drugs in spite of the high cost of the catalyst.

Preparation of the Catalyst  $[\text{RhCl}(\text{PPh}_3)_3]$

This red-violet colored compound is prepared by refluxing ethanolic  $\text{RhCl}_3 \cdot 3\text{H}_2\text{O}$  with an excess of  $\text{PPh}_3$ .

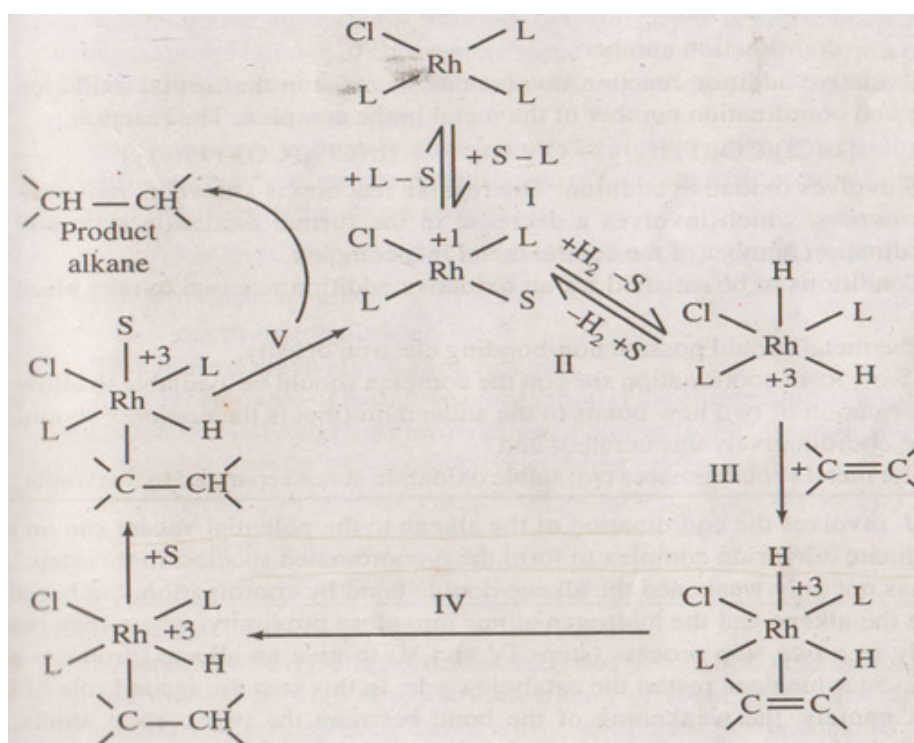
### 14.7 Role of Rhodium Metal in the catalytic process

The role of the metal in the catalytic process is three-stage. Firstly the metal provides a low energy path for cleaving the H-H bond in  $\text{H}_2$ . Secondly the metal coordinates with the alkene thereby weakening the bonding between the carbon atoms. Thirdly the metal provides a

mechanism for transferring the two hydrogen fragments to the alkene carbon atoms yielding an alkane.

### 14.8 Mechanism of hydrogenation of olefins using Wilkinson's catalyst

On passing hydrogen into a solution of the catalyst in benzene followed by the addition of olefin the alkane is formed. The precise mechanism of this process is complicated and has been the subjected of much speculation and controversy. But the following scheme is a simplified but a reasonable one. For the sake of simplicity  $\text{PPh}_3$  is represented as L in the catalytic cycle



*Step-I* Involves a reasonable loss of one  $\text{PPh}_3$ . This is indicated by two lines of evidence.

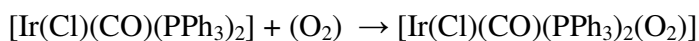
1. In less sterically hindered phosphine complexes, the catalytic effect disappears as small ligands do not readily dissociate which is essential for catalysis, they render the catalyst ineffective.

2. In the corresponding iridium complex in which the metal-phosphorous bond is stronger apparently no dissociation takes place and hence catalytic behavior disappears.

*Step- II* Is oxidative addition leading to the formation of a 5-coordinated species  $[\text{RhCl}(\text{H})_2\text{L}_2]$  in which the oxidation state of Rh is +3 this step is an oxidation reaction. The coordination number of the central metal ion is increased from 4 to 5 in this step. Hence this step is also an addition reaction. Since this step involves both oxidation and addition, it is referred to as an oxidative

addition reaction or *oxid* reaction. In this reaction which is reversible the first role of the catalyst i.e cleavage of the H-H bond is accompanied. This is identified by NMR peaks characteristics of Rh-H bond.

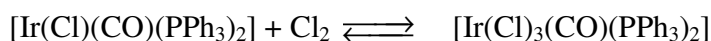
Note: The term oxidative addition was introduced by Vaska, who studied some addition reactions of the complex, *trans* -[Ir(Cl)(CO)(PPh<sub>3</sub>)<sub>2</sub>(O<sub>2</sub>)] which is called Vaska's compounds



Ir      Oxidation number +1                      →                      +3

          Co-ordination number 4                      →                      6

Oxidative addition reaction involves an increase in the formal oxidation state and co-ordination number of the metal in the complex. The reaction,



also involves oxidative addition. The reverse reaction is known as reductive elimination, which involves a decrease in the formal oxidation state and co-ordination number of the central metal in a complex.

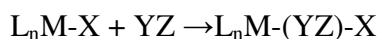
Conditions to be satisfied for an oxidative addition reaction to take place are,

1. The metal should possess non-bonding electrons density
2. Two vacant co-ordination sites on the complex should be available to allow formation of two new bonds to addendum (that is the complex should be coordinatively unsaturated) and
3. The metal should possess two stable oxidation state separated by two units.

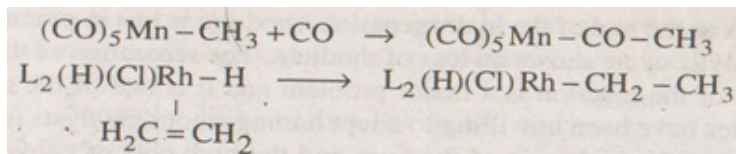
*Step-III* involves the coordination of the alkene to the potential vacant site on the 5-coordinate dihydrido complex to form the 6-coordinated species. In this step the metal has not only weakened the alkene double bond by coordination, but has also brought the alkene and the hydrogen atoms into close proximity where they react probably in a two-step process to give an alkane (product) and [RhClL<sub>2</sub>S] which can restart the catalytic cycle. In this step the second role of the catalytic namely the weakening of the bond between the two carbon atoms is accomplished.

*Step- IV* is an insertion reaction. It involves the insertion of olefins into metal-H bond to give metal-alkyl derivatives.

Note: The concept of insertion is of wide applicability in chemistry when defined as a reaction where an atom or a group of atom is inserted between two atoms initially bound together. For example,



Some representative examples are

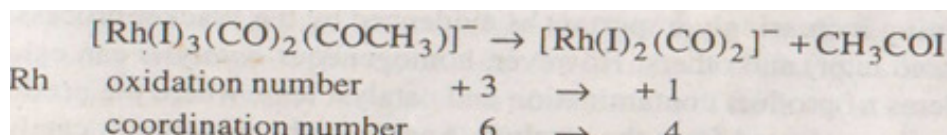


Carbonyl insertion into M-alkyl bond to give metal-acyl derivatives and olefin insertion into M-H bond to give metal alkyl derivatives are the partial steps in most of the catalytic cycles in industrial process. In addition insertion into M-N and M-O bonds are also known.

*Step V*- Is the reductive elimination step. The metal is reduced from +3 state to +1 state and coordination number of the central metal is reduced from 6 to 4. In this step the product alkane is formed. The third role of the catalyst namely the transfer of hydrogen fragments to the alkene yielding the product alkane is achieved in steps IV and V.

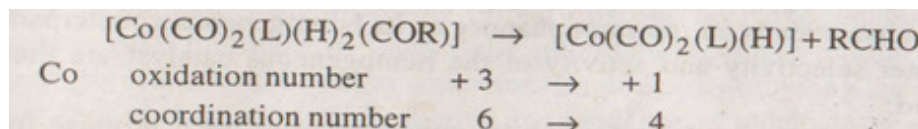
Note: In this reductive elimination reaction two substrates X and Y present in the catalyst system bonded to one or more centres combine to form a product XY, which then leaves the coordination sphere of the metal. This is essentially the reverse of *oxid* reaction.

An example of reductive elimination is the elimination of acetyl iodide in the Rh- catalysed carbonylation of methanol. One of the steps in the above reaction is



This is reductive elimination reaction.

Another example of reductive elimination is the elimination of an aldehyde in the cobalt catalysed hydroformylation of olefins one step in the process in which reductive elimination occurs is



### 14.9 Advantages

1. Compared with the older process which was likewise homogeneously catalyzed and marked by high reaction temperature of about 2500C and by pressure around 750 atmosphere this new process under considerably milder reaction condition.

2. It is possible selectively hydrogenate biologically active substrate such as steroids. The value of this catalyst is based upon the fact that the hydrogens are transferred specifically to cis position.
3. This catalyst is specific for the hydrogenation of terminal olefins due to steric reasons.

#### **14.10 Disadvantages**

1. Being a soluble catalyst it cannot be removed easily at the end of the reaction by simple filtration. Due to this imperfect separation of alkane and rhodium complex at the end of hydrogenation, rhodium is lost in practice although the catalytic cycle shows no loss of rhodium. The separation of the catalyst at the end of the reaction is a major problem and it is one of the reasons why industries have been unwilling to adopt homogeneous catalyst more widely.
2. Because of the high cost of rhodium and the higher cost of converting it into Wilkinson's catalyst this process is highly expensive.

#### **14.11 Modification over the original Catalyst**

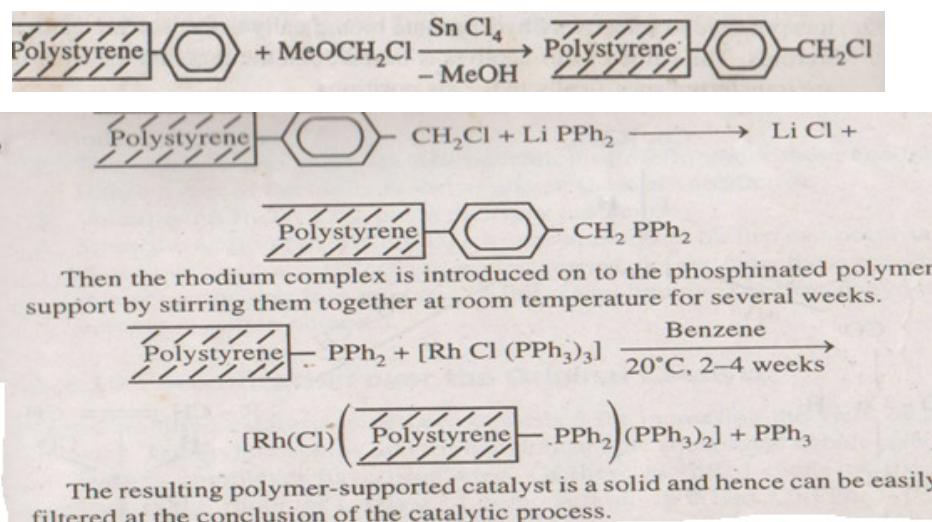
Removal of the catalyst at the end of the catalytic reaction is made easy by building the catalyst on an insoluble support. The types of support used are beds either of cross-linked polymers such as polystyrene or polyvinylchloride or of inorganic materials such as silica. The resulting polymer-supported catalyst is a solid and hence can be easily filtered off at the end of catalytic process. This process of converting a homogeneous catalyst into a heterogeneous catalyst into a heterogeneous one is called anchoring of catalyst. In the anchored catalyst all the rhodium atoms have identical coordination sites leading to high selectivity thus the selectivity are retained in this modified process.

Note: in recent years the discovery and utility of homogeneous hydrogenation, isomerisation, oligomerization, carbonylation reactions etc... have expanded enormously. Commercial processes based on homogeneously catalyzed routes are becoming increasingly important as evidenced by the Wacker process and others. However, homogeneous catalysis can exhibit the problems of product contamination and catalyst loss, where the products are not easily separated from the catalyst. Anchoring homogeneous catalysts to polymers or other supports effectively heterogenise them, allowing their use in fixed beds and simplifying catalyst recovery. Thus, the anchoring of homogeneous catalyst has become the objective of the several groups of the chemist.

When a homogeneous catalyst is heterogenised in such a way that it can react mechanistically in the same manner of its homogeneous counterpart, the greater selectivity and activity of the homogeneous catalyst are thus preserved.

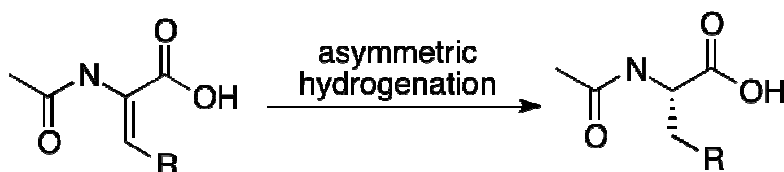
In general, polymer-bound catalyst appears to offer great promise for practical applications in specific and selective chemical transformations at comparatively mild conditions.

Polymer-supported Wilkinson's catalyst is prepared as follows. Phosphine groups are introduced on to the polymer support by the following series of reactions.



### 14.12 Asymmetric hydrogenation

Asymmetric hydrogenation is a chemical reaction that adds two atoms of hydrogen preferentially to one of two faces of an unsaturated substrate molecule, such as an alkene or ketone. The selectivity derives from the manner that the substrate binds to the chiral catalysts. In jargon, this binding transmits spatial information (what chemists refer to as chirality) from the catalyst to the target, favoring the product as a single enantiomer. This enzyme-like selectivity is particularly applied to bioactive products such as pharmaceutical agents and agrochemicals.

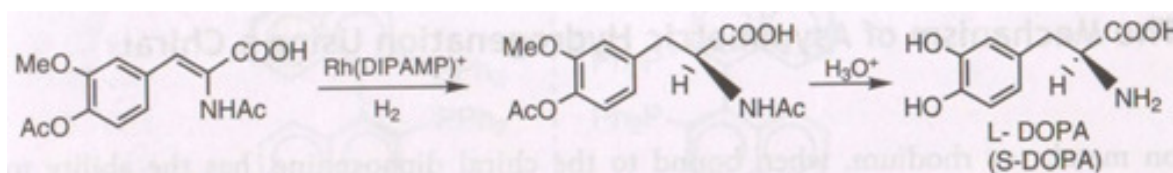


#### 14.12.1 Industrial Catalytic asymmetric hydrogenation

Knowles aim was to develop an industrial synthesis of the amino acid L-DOPA which has proved useful in the treatment of Parkinson's disease. By testing enantiomers of phosphines with



varied structures, Knowles and his colleagues quickly succeeded in producing usable catalysts that provided a high enantiomeric excess of the product L-DOPA.



The ligand used in Monsanto's industrial synthesis of L-DOPA was the diphosphine ligand DIPAMP. A cationic rhodium complex with this ligand afforded extraordinarily high levels of enantioselectivity in the hydrogenation of achiral enamides. This was the first demonstration that a chiral transition metal complex could effectively transfer chirality to a nonchiral substrate with selectivities that even rival those given by enzymes. The synthesis gave a mixture of the enantiomers of DOPA in 100% yield with 97.5% of L-DOPA. Thus Knowles has in a short time, succeeded in applying his own basic research and that of the others to come up with an industrial synthesis of an important drug. This was the first catalytic asymmetric synthesis. A variety of chiral diphosphines are nowadays used and many of them are found to give very good results in hydrogenation reactions. These phosphines can be broadly classified as follows.

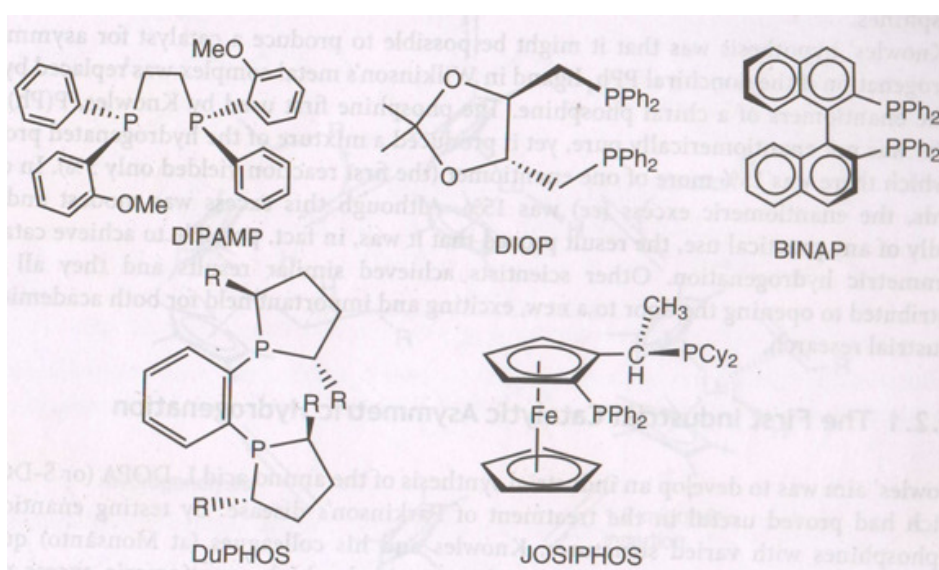
Diphosphines having chiral phosphorus atoms (DIPAMP).

Diphosphines having a chiral backbone (DIOP).

Ligands having atropisomerism (BINAP).

Those carrying chiral substituents on the phosphorus site.

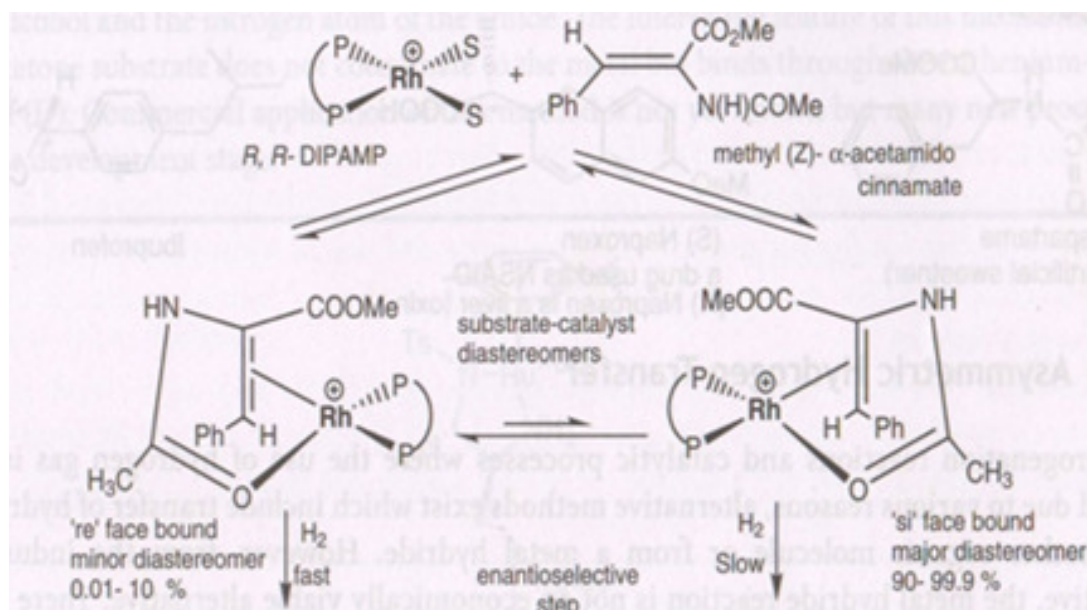
Ligands having a planar symmetry.

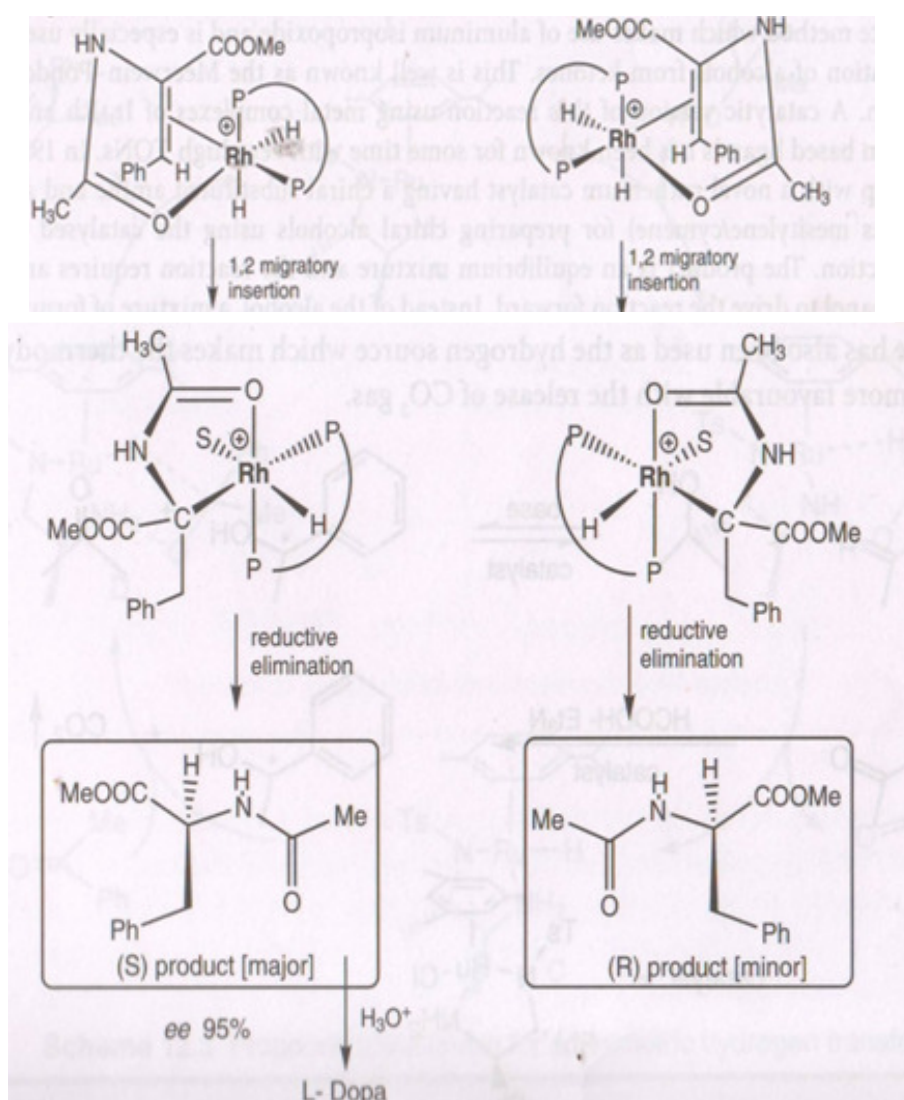


### 14.13 The mechanism of Asymmetric Hydrogenation using a Chiral catalyst

Transition metal say rhodium, when bound to the chiral diphosphine, has the ability to multaneously bind both  $H_2$  and substrate. The complex obtained then undergoes an migratory insertion and  $H_2$  is added to the double bond in the substrate. This is the vital stage ring hydrogenation when a new chiral complex is formed the chiral product is released from is complex. Thus using a substrate that is prochiral the chirality has been transferred from the ural catalyst to the product. This product contains more of one enantiomer than the other that the synthesis is asymmetric.

The reason for the enantiomeric excess lies in the hydrogenation stage as hydrogen can in two ways that give different enantiomers at different rates. These two pathways utilize different transition state complex which are diastereomers and therefore have different strategies. Hydrogenation takes place are rapidly via the complex with the lowest energy thus producing an excess of one of the enantiomers. To develop better asymmetrical hydrogenation catalyst it is important to increase the energy difference between the transition state complexes in order to obtain better enantiomeric excess. This is of vital intrest in industrial applications in which the aim is to achieve economy in the process as well as to use environmentally acceptable methods that is the process with as few waste products as possible. This development has been led by Noyori.

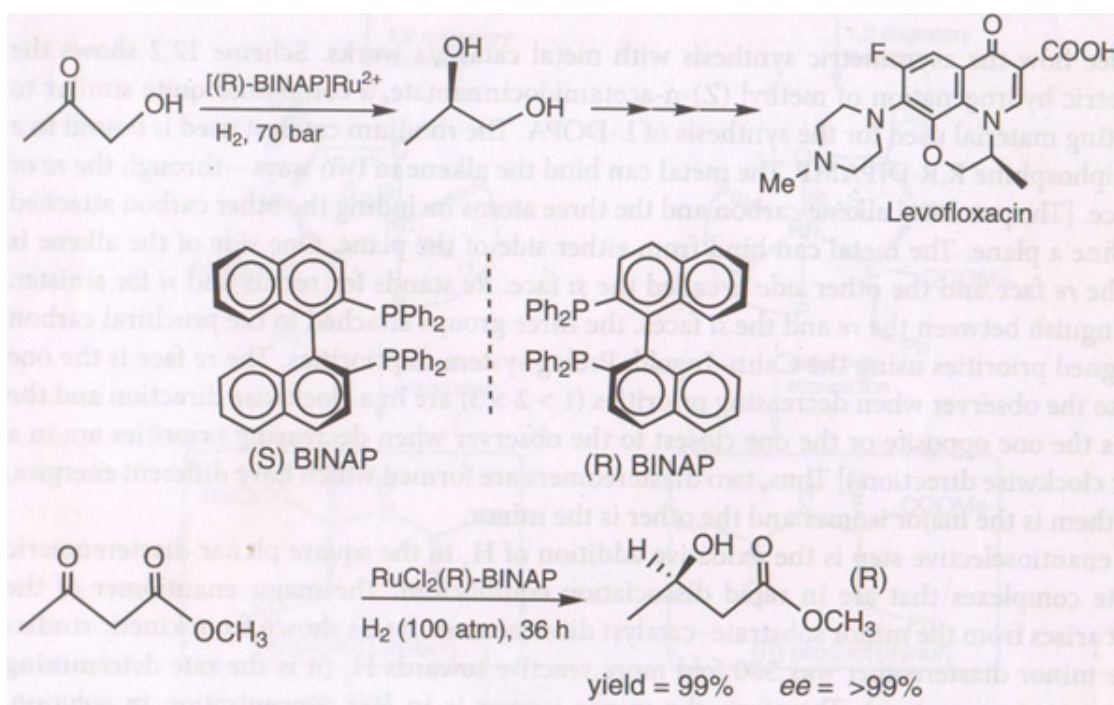




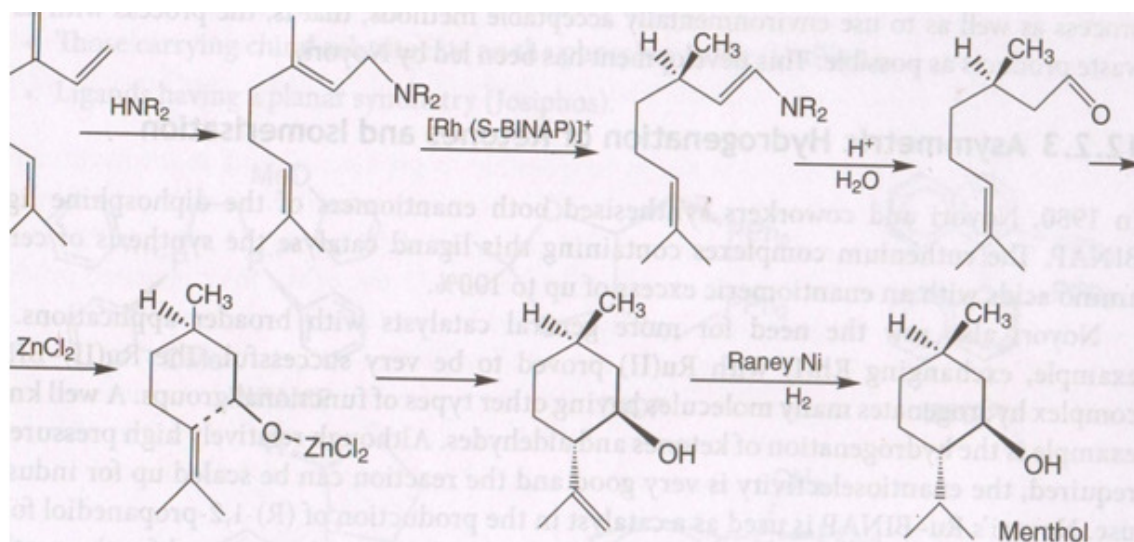
#### 14.14 Asymmetric Hydrogenation of Ketones and Isomerisation

In 1980 Noyori and coworkers synthesized both enantiomers of the diphosphine ligand BINAP. The ruthenium complexes containing this ligand catalyze the synthesis of certain amino acids with an enantiomeric excess of up to 100%.

Noyori also saw the need for more general catalysts with broader applications for example exchanging Rh(I) with Ru(II) proved to be very successful. The Ru(II)-BINAP complex hydrogenates many molecules having other types of functional groups. A well-known example is hydrogenation of ketones and aldehydes. Although relatively high pressures are required, the enantioselectivity is very good and the reaction can be scaled up for industrial use. Noyori's Ru-BINAP is used as a catalyst in the production of (R)-1,2-Propanediol for the industrial synthesis of an antibiotic, levofloxacin. Similar reactions are used for the synthesis of other antibiotics.



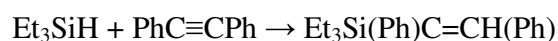
The Takasago International Company has been using BINAP in the industrial synthesis of a chiral aromatic compounds, menthol since the early 1980. The key reaction in this process is the enantioselective isomerisation of an allylamine to an asymmetric enamine. The enamine is then hydrolysed followed by a Lewis acid ( $\text{ZnCl}_2$ ) catalyzed ring closer reaction that gives the menthol skeleton. In the final step, the isopropenyl group is hydrogenated over Raney nickel to (-) menthol



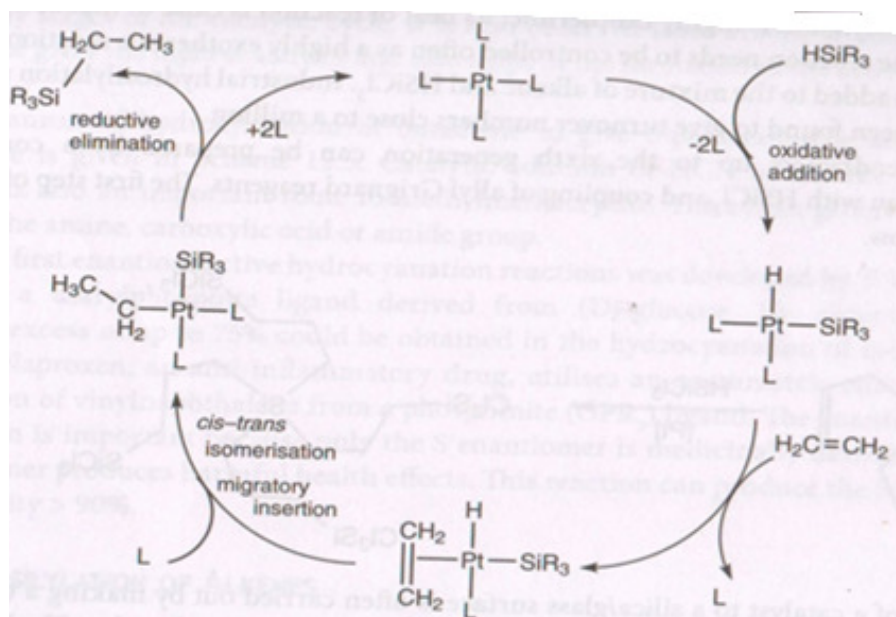
### 14.15 Hydrosilylation

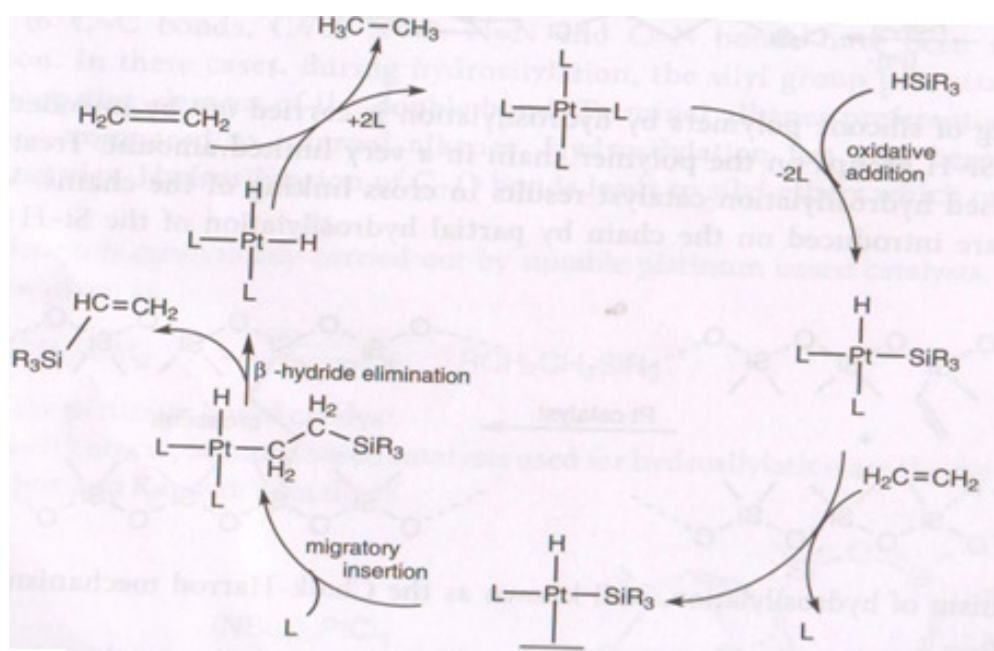
Hydrosilylation, also called catalytic hydrosilation, describes the addition of Si-H bonds across unsaturated bonds. Ordinarily the reaction is conducted catalytically and usually the substrates are unsaturated organic compounds. Alkenes and alkynes give alkyl and vinyl silanes; aldehydes and ketones give silyl ethers. The process was first reported in academic literature in 1947. Hydrosilylation has been called the "most important application of platinum in homogeneous catalysis."

The catalytic transformation represents an important method for preparing organosilicon compounds. An idealized transformation is illustrated by the addition of triethylsilane to diphenylacetylene



The reaction is related mechanistically to hydrogenation, and similar catalysts are sometimes employed for the two catalytic processes. Popular industrial catalysts are "Speier's catalyst,"  $\text{H}_2\text{PtCl}_6$ , and Karstedt's catalyst (an alkene-stabilized platinum(0) catalyst). One prevalent mechanism, called the Chalk-Harrod mechanism, assumes an intermediate metal complex that contains a hydride, a silyl ligand ( $\text{R}_3\text{Si}$ ), and the alkene substrate. The reaction usually produces anti-Markovnikov addition alkane, i.e., silicon on the terminal carbon.<sup>[1]</sup> Variations of the Chalk-Harrod mechanism. Some cases involve insertion of alkene into M-Si bond followed by reductive elimination. In certain cases, hydrosilylation results in vinyl or allylic silanes resulting from beta-hydride elimination.

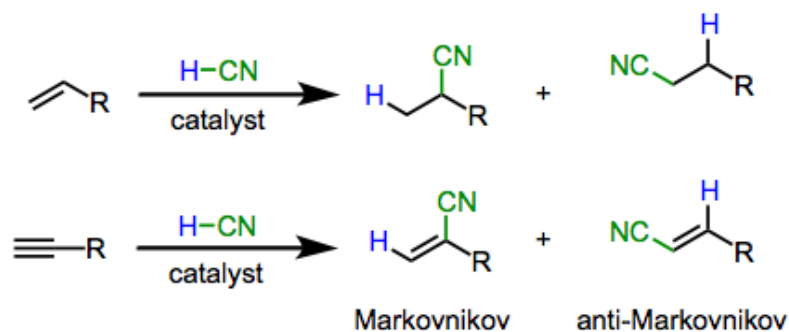




### 14.16 Hydrocyanation

Hydrocyanation of alkenes and alkynes refers to the transition-metal-mediated or -catalyzed addition of hydrogen cyanide across a carbon-carbon  $\pi$  bond. This reaction may be used to synthesize nitriles from alkenes or alkynes in a Markovnikov or anti-Markovnikov fashion.

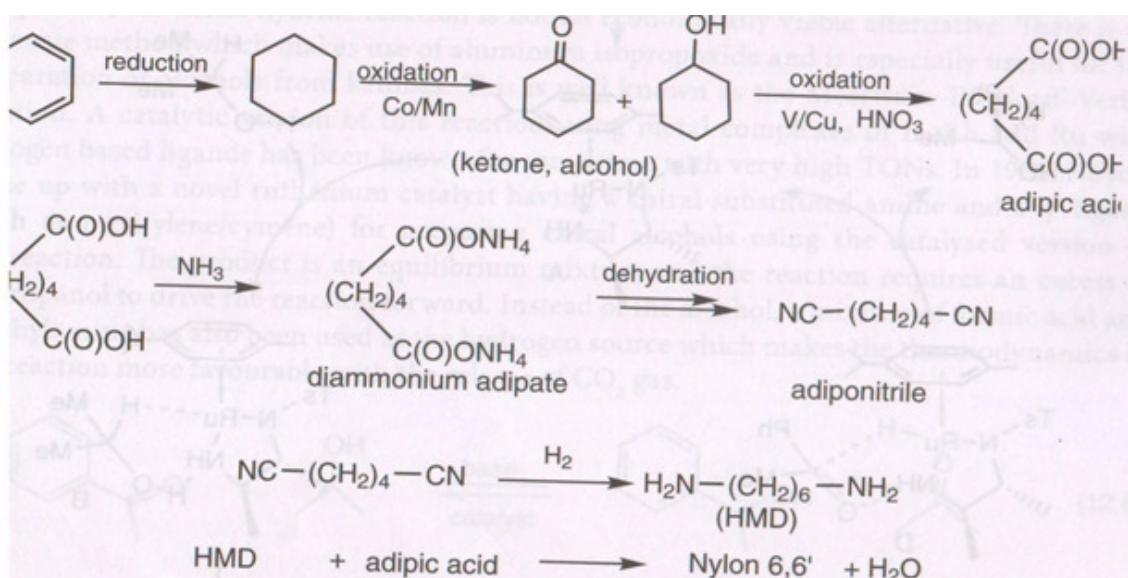
The addition of hydrogen cyanide across activated carbon-carbon  $\pi$  bonds, such as the C=C bond of  $\alpha,\beta$ -unsaturated carbonyl compounds, is a well-known, synthetically useful transformation. Because this process requires a sufficiently electrophilic substrate, unactivated alkenes will not undergo addition under conditions useful for activated substrates. However, the addition of hydrogen cyanide across a  $\pi$  bond is a thermodynamically favorable process, and the high activation barriers associated with addition to unactivated alkenes and alkynes may be surmounted using transition-metal catalysis. Transition-metal catalyzed addition of cyanide across  $\pi$  bonds may occur in a Markovnikov or anti-Markovnikov fashion to provide fully saturated nitriles or vinyl nitriles.



### 14.17 Hydrocyanation of Alkenes

Hydrocyanation is a process by which  $H^+$  and  $CN^-$  ions are added to a molecular substrate, usually substrate is an alkene and the product is a nitrile. Since cyanide is a good  $\sigma$  donor and acceptor ligand, its presence accelerates the rate of substitution of the ligand trans to it by the trans effect. A key step in hydrocyanation is the oxidative addition of hydrogen cyanide to low metal complexes. The most important industrial application of hydrocyanation is in the induction of Nylon-6,6.

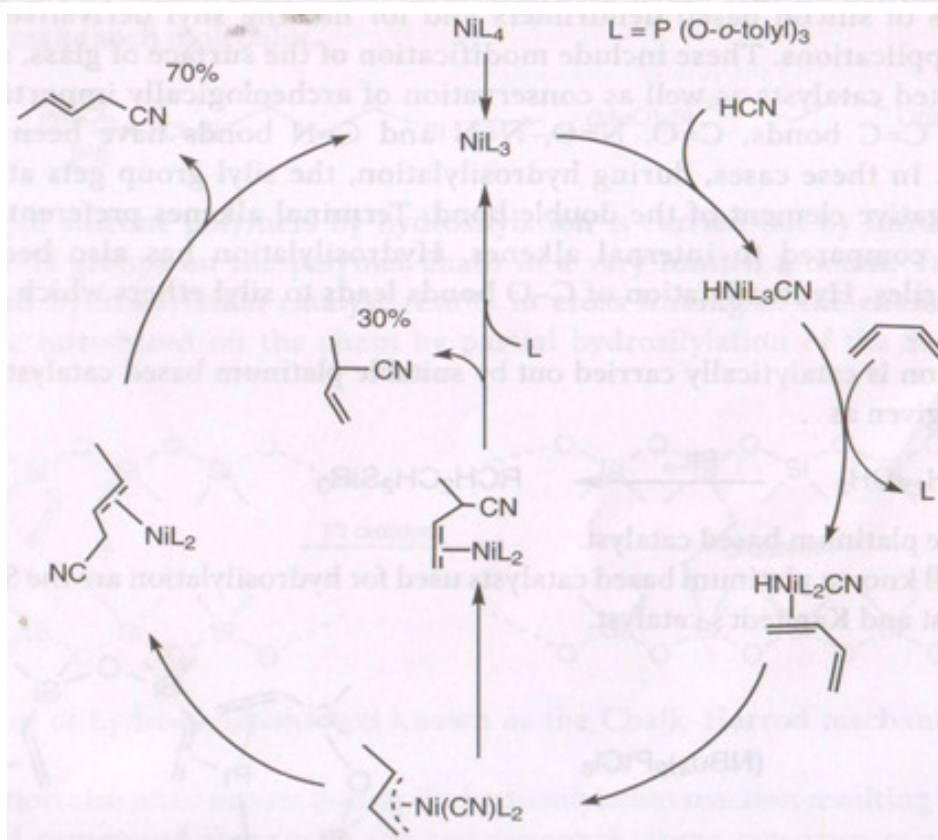
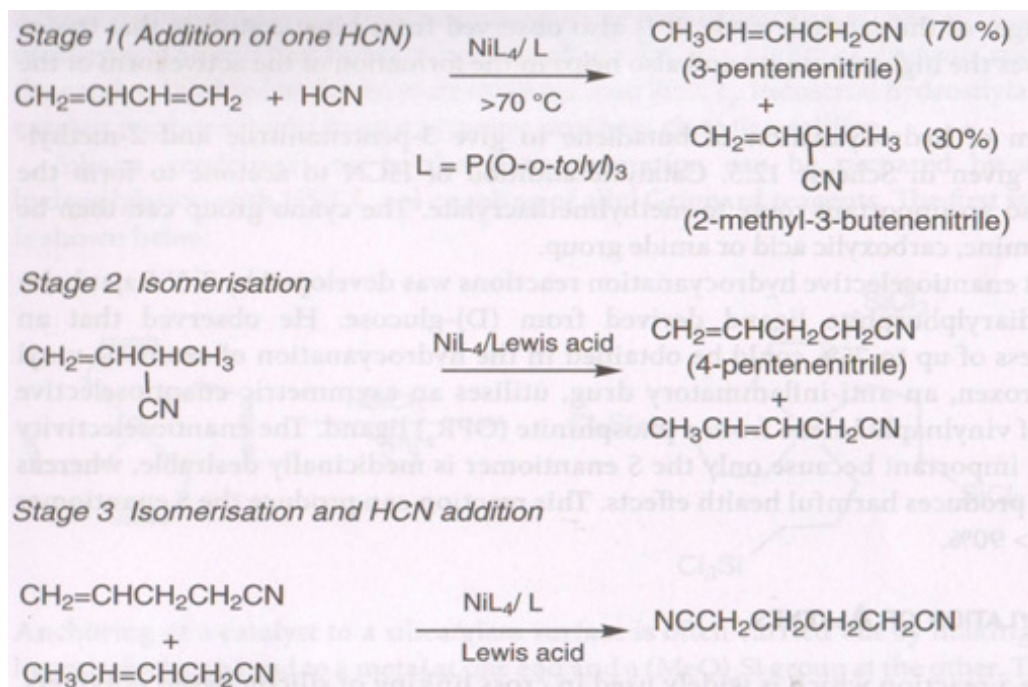
Condensation polymerization of hexamethylenediamine (HMD) and adipic acid is the common route to obtain Nylon-6,6. Traditionally this was prepared by using benzene as a starting material. This method of production involved a complex set of steps



Alternative procedures using homogeneous catalysis and 1,3-butadiene as precursor have developed. BASF demonstrated selective dicarbonylation of butadiene to give adipic acid. Dupont developed double anti-Markovnikov addition of HCN to butadiene using Nickelphosphite catalysts to make adiponitrile. The process for adiponitrile developed during 1960 and commercialized in 1971 operates in three stages. Today more than nine adiponitrile prepared annually is by catalytic hydrocyanation.

Nature of the phosphorus ligand is significant in these reactions and only phosphites catalysts of sustained activity. If instead of phosphate an alkyl phosphine is used catalysts of sustained activity. If instead of phosphate an alkyl or aryl or aryl phosphine is used in addition of Ni(0) to

Ni(II) will occur with the formation of complexes of the type  $L_2Ni(CN)_2$  lead to catalyst deactivation.





### 14.18 Summary of the unit

Many catalytic hydrogenations with molecular hydrogen actually involve atomic hydrogen dispersed in and over the catalyst. In many reductions with hydrogen donors, it may not be easy to decide just how hydrogen transferred. For example, formic acid may be regarded as providing a proton and a hydride or two hydrogen atoms. However, for suitable hydrogen donor properties, it seems clear that compounds containing hydrogen bonded to elements or groups with similar electronegativity to that of hydrogen itself provide the best hydrogen donors. In this respect formic acid, ammonium formate, triethylammonium formate, hydrazinium monoformate, phosphinic acid and phosphinates, phosphorus acid and phosphites, hydrazine, alcohols, amines, hydrocarbons, hydrides of boron, aluminium, silicon and tin are all hydrogen donors to catalytic transfer reductions. An added advantage gained when the products of the decomposing donors have large negative enthalpies of formation. Thus, CO<sub>2</sub> from formic acid provide added driving force to the reactivity of these substances as hydrogen donors.

Hydrocyanation is the process in which HCN is added across a double bond of an alkene to form a nitrile. In the last decades, more studies have therefore focused on the synthesis of nitriles, based on HCN addition to alkenes or to related systems in the presence of a transition metal catalyst, most commonly based on nickel. The most outstanding example for the application of hydrocyanation is the DuPont adiponitrile process. The synthesis of adiponitrile (AdN) based on a nickel-catalyzed double hydrocyanation of butadiene is a major industrial success for homogeneous catalysis. In the first step, hydrocyanation of butadiene leads to a mixture of mononitriles, the desired 3-pentenitrile (3PN) and the undesired 2-methyl-3-butenitrile (2M3BN). The branched isomer needs to be isomerized to the linear 3PN. The second hydrocyanation of 3PN produces AdN. This reaction only proceeds with the assistance of a Lewis acid co-catalyst.

### 14.19 Key words

Acid–base catalysis; transition metal salts and metal complexes; Metal to act as a catalyst; Hydrogenation of olefins; Wilkinson's catalyst; Asymmetric hydrogenation; Hydrosilylation Hydrocyanation; Hydrocyanation of Alkenes

### 14.20 References for further studies

- 1) Homogeneous Catalysis: Mechanisms and Industrial Applications; Sumit Bhaduri, Doble Mukesh; *John Wiley & Sons*, 2014.

- 2) Homogeneous Catalysis with Metal Complexes: Fundamentals and Applications; Gheorghe Duca; *Springer Science & Business Media*, **2012**.
- 3) Industrial Catalysis: A Practical Approach; Jens Hagen; *John Wiley & Sons*, **2015**.
- 4) Handbook of Asymmetric Heterogeneous Catalysis; Kuiling Ding, Yasuhiro Uozumi; John Wiley & Sons, **2008**.
- 5) Principles and Practice of Heterogeneous Catalysis; John Meurig Thomas, J. M. Thomas, W. John Thomas; *John Wiley & Sons*, **2015**.
- 6) Organometallic Chemistry and Catalysis; Didier Astruc; *Springer Science & Business Media*, **2007**.

#### **14.21 Questions for self understanding**

- 1) What are Acid–base catalysis? Explain their actions
- 2) Discuss the catalysis involving transition metal salts and metal complexes.
- 3) Explain the condition to be satisfied by a Metal to act as a catalyst.
- 4) Discuss the Hydrogenation of olefins.
- 5) Explain the importance of Wilkinson’s catalyst.
- 6) Explain the role of Rhodium metal in the catalytic process.
- 7) Discuss the mechanism of hydrogenation of olefins using Wilkinson’s catalyst.
- 8) Discuss the advantages and disadvantages Wilkinson’s catalyst.
- 9) Write a note on modification over the original Wilkinson’s Catalyst.
- 10) What is Asymmetric hydrogenation?
- 11) Discuss the industrial catalytic asymmetric hydrogenation.
- 12) Explain the the mechanism of Asymmetric Hydrogenation using a Chiral catalyst.
- 13) Discuss the Asymmetric Hydrogenation of Ketones and Isomerisation.
- 14) Explain the catalytic Hydrosilylation process.
- 15) Discuss the catalytic Hydrocyanation reaction.
- 16) Explain the Hydrocyanation reaction of Alkenes.

**UNIT-15****Structure**

- 15.0 Objectives of the unit
- 15.1 Introduction
- 15.2 Fischer–Tropsch process
- 15.3 Fisher-Tropsch synthesis
- 15.4 Mechanism of Fisher- Tropsch synthesis
- 15.5 Ziegler–Natta catalyst
- 15.6 Importance of Ziegler-Natta catalyst
- 15.7 Mechanism of Ziegular-Natta catalysis
- 15.8 Summary of the unit
- 15.9 Key Words
- 15.10 References for further studies
- 15.11 Questions for self understanding

### 15.0 Objectives of the unit

After studying this unit you are able to

- Explain the Fischer–Tropsch process
- Write the scheme of Fisher-Tropsch synthesis
- Write the mechanism of Fisher- Tropsch synthesis
- Draw the structure of Ziegler–Natta catalyst
- Explain the importance of Ziegler-Natta catalyst
- Write the mechanism of Ziegular-Natta catalysis

### 15.1 Introduction

The Fischer-Tropsch (FT) process, originally developed by Franz Fischer and Hans Tropsch in early 1920s, is a series of chemical reactions that involve the conversion of hydrogen and carbon monoxide into liquid hydrocarbons by using a catalyst.

This process is a key component of gas to liquid technology. It produces synthetic lubrication oil and synthetic fuel including natural gas, biomass or coal. Generally, these products are of higher quality than those derived through conventional means, having no sulphur or aromatics.

In the FT process, typical cobalt catalysts are produced using Oxford Catalysts' patented technology with superior stability, selectivity and activity to conventional catalysts, and without any loss of performance.

The FT process has gained importance as a source of low-sulfur diesel fuel and in addressing the cost and supply of petroleum-derived hydrocarbons.

Although several catalysts can be used for Fischer-Tropsch synthesis, the transition metals of ruthenium, nickel, cobalt and iron are some of the most common catalysts. Selection of FT process catalysts is based on the diesel fuels production and high molecular weight linear alkanes. Nickel can be also be used as the catalyst, but it tends to promote methane formation. Cobalt is more active and usually preferred over ruthenium owing to the high cost of ruthenium.

On the other hand, iron is relatively inexpensive and has high water-gas-shift activity, so it is more suitable for obtaining synthetic gas with low hydrogen/carbon monoxide ratio like those derived through coal gasification. In addition to the active metal, the catalysts include various promoters such as copper, potassium and high surface area binders such as alumina or silica. The presence of sulfur compounds in the synthetic gas can poison the FT catalysts. The cobalt-based catalysts have higher sensitivity to sulfur than its iron counterparts, which in turn contributes to

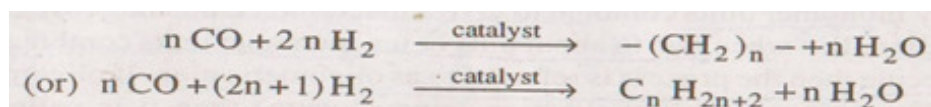
higher catalyst replacement costs for Co. Therefore, cobalt catalysts are preferred for FT synthesis of synthetic gas derived from natural gas, where the synthetic gas has relatively low sulphur content and high hydrogen to carbon monoxide ratio. Iron catalysts are preferred deriving synthetic gas from low quality feed stocks such as coal.

### 15.2 Fischer–Tropsch process

The Fischer–Tropsch process is a collection of chemical reactions that converts a mixture of carbon monoxide and hydrogen into liquid hydrocarbons. It was first developed by Franz Fischer and Hans Tropsch at the "Kaiser-Wilhelm-Institut für Kohlenforschung" in Mülheim an der Ruhr, Germany, in 1925. The process, a key component of gas to liquid technology, produces a synthetic lubrication oil and synthetic fuel, typically from coal, natural gas, or biomass. The Fischer–Tropsch process has received intermittent attention as a source of low-sulfur diesel fuel and to address the supply or cost of petroleum-derived hydrocarbons. A Fischer–Tropsch-type process has also been suggested to have produced a few of the building blocks of DNA and RNA within asteroids.

### 15.3 Fisher-Tropsch synthesis

The Fisher-Tropsch synthesis was discovered in Germany in the year 1920 and was used during the Second World War to produce liquid hydrocarbon fuel from coal. The mixture of CO and H<sub>2</sub> is pressed over certain transition metal surface. The basic reaction is given by the equations



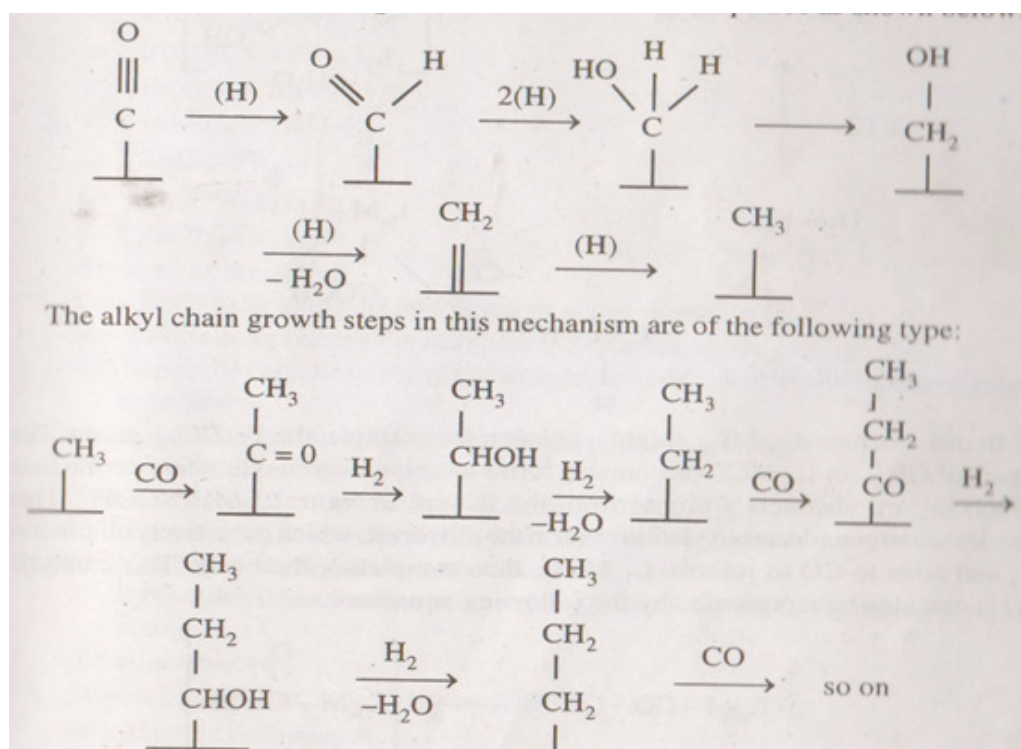
This equation is an oversimplification because oxygen containing products such as alcohols, acids, and esters are also formed apart from the hydrocarbons. The original process is used CO and H<sub>2</sub> with 100 atmosphere pressure and temperature of about 400 °C over an alkaline-doped iron heterogeneous catalyst. The process from then on has undergone considerable refinement and is currently being used in South Africa. The mechanism of Fisher-Tropsch synthesis is complicated. Work has been carried out on heterogeneous and homogeneous system, using mono and polynuclear metal complexes.

The rapid and at time drastic increase in the price of crude oil which has occurred over the last few decades coupled with the realization that crude oil supplies whether limited by technical or political factors, are likely to fall short of potential demand has rekindled interest in coal both as a source of energy and as a feed-stock for the petrochemical industries. At the current rate of

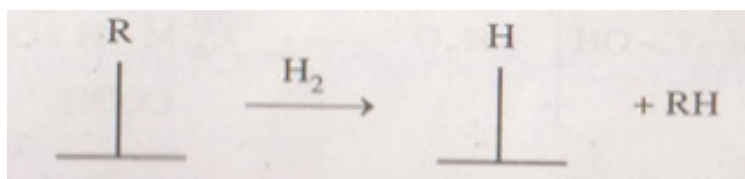
energy consumption, the known coal reserves are sufficient for more than 250 years. The most direct method of using coal as a primary energy source is combustion, However if coal is to replace crude oil in the production of fuels and organic chemicals, it is necessary to develop efficient methods of converting coal into gas, liquid hydrocarbons and some organic chemicals. One method of at least partially accomplishing these goals is the Fischer-Tropsch synthesis, where synthesis gas namely a mixture of CO and H<sub>2</sub> obtained by burning coal in the presence of oxygen and steam is converted into a number of hydrocarbon product.

#### 15.4 Mechanism of Fischer-Tropsch synthesis

The widely accepted mechanism for this process involves the generation of a methyl group on the surface of the catalyst followed by a series of steps in which methylene groups are successively inserted between the metal and the alkyl group thus building up a linear alkyl group. Then the linear alkyl group is served from the metal in a hydrogenation step. Thus a product hydrocarbon molecules is released. The methyl group is assumed to be formed by the reaction of adsorbed hydrogen atoms formed by surface dissociation of H<sub>2</sub> with adsorbed CO in a sequence as shown below



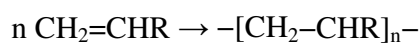
Finally the production of hydrocarbon takes place in a hydrogenation step as shown below, where R is a long hydrocarbon chain and RH is the product hydrocarbon.



### 15.5 Ziegler–Natta catalyst

A Ziegler–Natta catalyst, named after Karl Ziegler and Giulio Natta, is a catalyst used in the synthesis of polymers of 1-alkenes (alpha-olefins). Two broad classes of Ziegler–Natta catalysts are employed, distinguished by their solubility:

- Heterogeneous supported catalysts based on titanium compounds are used in polymerization reactions in combination with cocatalysts, organoaluminum compounds such as triethylaluminum,  $\text{Al}(\text{C}_2\text{H}_5)_3$ . This class of catalyst dominates the industry.
- Homogeneous catalysts usually based on complexes of Ti, Zr or Hf. They are usually used in combination with a different organoaluminum cocatalyst, methylaluminoxane (or methylalumoxane, MAO). These catalysts traditionally include metallocenes but also feature multidentate oxygen- and nitrogen-based ligands. Ziegler–Natta catalysts are used to polymerize terminal 1-alkenes (ethylene and alkenes with the vinyl double bond):



The transfer of hydrogen atoms to form C-C bonds. These reactions are catalysed by transition metal complexes. While investigating the multiple insertion of ethane into an Al-alkyl bond to give long chain Al-alkyls. K.Ziegler and his co-workers discovered that small amounts of Ni inhibit this polymerization reaction. This stimulated an extensive study of the effect of the transition metals on the Al-alkyl polymerization system. In the early 1950s these studies led to the discovery that certain transition metal complexes in the presence of Al-alkyl compounds will catalyse the polymerization of ethane under mild reaction condition to give a material of molecular weight in excess of 50,000. This discovery was of tremendous technical importance because previously ethene had been considered a very difficult molecule to polymerise needing pressure of over 1000 atmosphere and temperature of the order of  $200^\circ\text{C}$ .

G. Natta extended Ziegler's work to the polymerization of propene and higher  $\alpha$ -olefins using Ziegler-type catalysts based on Ti. After these discoveries many metal combinations have been found to be capable of catalyzing alkene polymerisation and the definition extended to include any combination of alkyl hydride or halide of Groups I-III with a transition metal salt or complex of Groups IV-VIII of the periodic table.

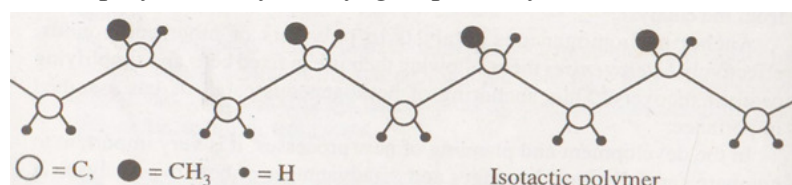
The most familiar example is the original Ziegler catalyst formed from  $\text{TiCl}_4$  and  $\text{AlR}_3$ . In the inert hydrocarbon solvent used an insoluble mixed halide-alkyl complex of Al and Ti is formed. This material is the active catalyst for the polymerization of ethylene, presumably acting as a heterogeneous catalyst.

Note: In recent years, the utility of homogeneous hydrogenation, isomerization, oligomerization, carbonylation reactions etc.... have expanded enormously. commercial process based on homogeneously-catalyzed routes are becoming increasingly important as evidenced by the Wacker's process and others. However homogeneous catalyst can exhibit the problems of product contamination and catalyst loss, where the products are not readily separated from the catalyst. Anchoring homogeneous catalyst to polymers or other compounds effectively heterogenises them, allowing their use in fixed beds and simplifying catalyst recovery. Thus anchoring of homogeneous catalyst has assumed importance.

### 15.6 Importance of Ziegler-Natta catalyst

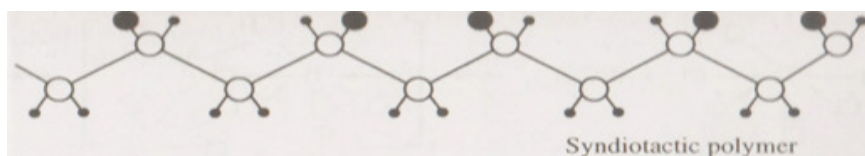
The Ziegler-Natta catalysis of alkene polymerization which operates at modest temperatures and pressure leads to the formation of stereoregular polymers. this is in direct contrast to the high temperature and pressure polymerization of alkenes. Stereoregularity often introduces some very desirable properties into yield long linear head-to-tail chains consisting of sequences of monomeric units having the same steric arrangement. These polymers are called isotactic polymers. The advantages of stereoregularity are that it conveys greater mechanical strength to the polymer enabling it to be used in making string and rope as well as more rigid articles such as industrial buckets. They possess higher melting and are stronger than nylon.

One of the features of organometallic polymerization catalyst is that they produce stereoregular polymers. For example, propylene forms two stereoregular polymers namely isotactic and syndiotactic polymers and one non-regular polymer namely atactic polymer. in isotactic polymer. In isotactic polymer, they methyl groups always lie on the same side of the chain.

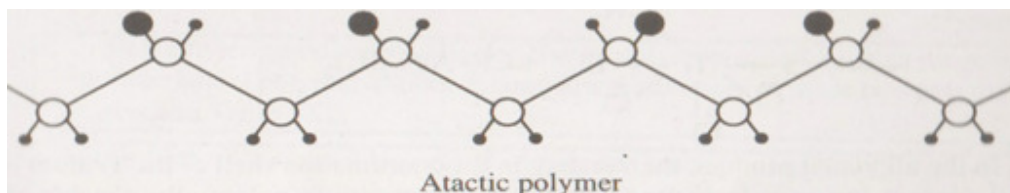


In syndiotactic polymers methyl groups alternate along the chain





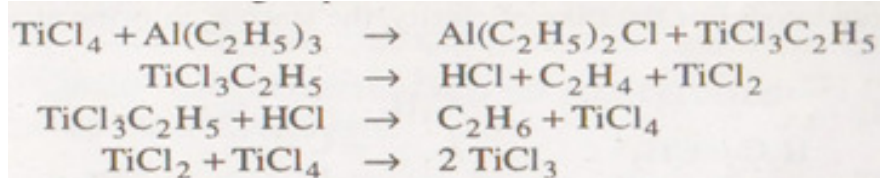
In atactic polymer, the methyl groups have no regularity along the chain.



When the double bond of the propylene attaches itself to Ti, the methyl group must always point away from the surface of the crystal simply because the reaction occurs on the surface. Thus when the molecule migrates and is increased into the Ti-C bond, it always has the same orientation. This is called cis-insertion of the alkene and explains why the polymers produced are stereoregular.

### 15.7 Mechanism of Ziegler-Natta catalysis

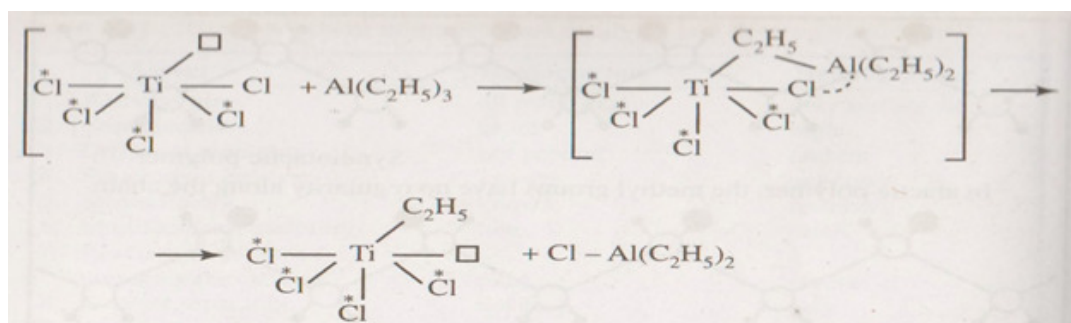
The most familiar example of Ziegler-Natta catalyst is the one formed from  $\text{TiCl}_4$  and  $\text{Al}(\text{C}_2\text{H}_5)_3$ . These components react in a way that is not completely understood but may involve the following steps.



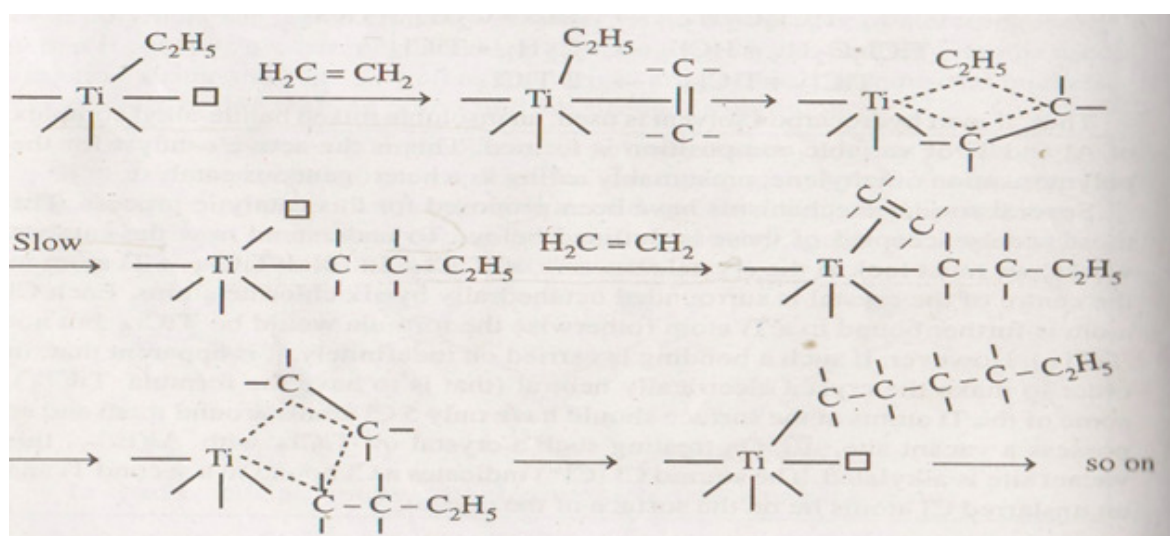
Thus, if inert hydrocarbon solvent is used, an insoluble mixed halide-alkyl complex of Al and Ti of variable composition is formed. This is the active catalyst for the polymerization of ethylene, presumably acting as a heterogeneous catalyst.

Several similar mechanisms have been proposed for this catalytic process. The most widely accepted of these is outlined below. To understand how the catalyst works, we must look at the crystal structure of  $\text{TiCl}_3$ . In solid  $\text{TiCl}_3$ , a Ti atom in the centre of the crystal is surrounded octahedrally by six chlorine atoms. Each Cl atom is further bound to a Ti atom (otherwise the formula would be  $\text{TiCl}_6$  but not  $\text{TiCl}_3$ ). However if such bonding is carried on indefinitely, it is apparent that in order to make the crystal electrically neutral (i.e., to have the formula  $\text{TiCl}_3$ ), some of the Ti atoms at the surface should have only 5 Cl atoms around them and so possess a vacant site. On treating such crystal of  $\text{TiCl}_3$  with  $\text{Al}(\text{C}_2\text{H}_5)_3$ , this vacant site is alkylated. The

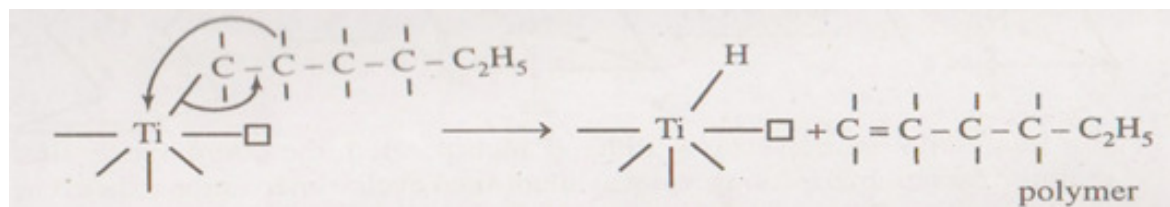
starred Cl (Cl\*) indicates a Cl bound to a second Ti and an unsaturated Cl atoms lie on the surface of the crystal.



In the alkylated product, the vacancy in the coordination shell of the Ti atom is still present but in a fresh position. This vacant site is potentially capable of coordinating an alkene such as  $\text{C}_2\text{H}_4$ . The alkene coordinates to the Ti atom as a  $\pi$ -donor in its vacant coordination site. The electropositive nature of the Ti atom allows the electrons in the Ti- $\text{C}_2\text{H}_4$  bond to flow towards the  $\text{C}_2\text{H}_5$  group. This weakens the bond which is labile and is cis to the newly arrived alkene  $\pi$ -bond. When an alkene and an alkyl group are bound to adjacent sites on a metal atom, they react to give what is known as an insertion product through a concerted four centre rearrangement. This step is assumed to be the rate determining step. The alkyl group shifts to one carbon of the alkene double bond, while the other carbon develops a sigma bond to the Ti atom. When the arrangement of the alkyl on to the alkene carbon is complete, a new coordination site is opened up on the Ti atom cis to the new longer alkyl group. This regeneration of the vacant site enables the process to be repeated. For the sake of clarity, the starred chlorine atoms have been omitted.



The presence of vacant site enables the chain to continue growing by switching back and forth between the two sites.



Termination would occur by a reverse insertion reaction in which a hydride ion shifts to the metal.

Polyethylene produced by Ziegler-Natta catalysis is superior to that produced by free radical polymerization. A comparative account of these two polymers is given in below table.

Polyethylene produced by Ziegler-Natta catalysis		Polyethylene produce by free radical polymerization
1	Produced under milder reaction conditions	Produced under severe conditions of about 190 - 210 °C and 1500 atm pressture
2	Has high density, 0.95-0.97 g/cc	Has lower density, 0.91-0.94 g/cc
3	Has higher melting point, 135 °C	Has lower melting point 115 °C
4	Contains straight chains with very little branch	Consist of branched chains
5	Relatively hard and stiff	Relatively softer
6	Has higher molecular weight 20,000-30,000	Has relatively lower molecular weight

### 15.8 Summary of the unit

The Fischer-Tropsch (F-T) reaction converts a mixture of hydrogen and carbon monoxide derived from coal, methane or biomass—to liquid fuels. The F-T process was discovered by German scientists and used to make fuels during World War II. There has been continued interest of varying intensity in F-T technology ever since. Both iron-based and cobalt-based catalysts have been examined.

In Ziegler-Natta polymerisation, monomers are treated with a catalyst, such as a mixture of titanium chloride (or related compounds, like oxovanadium chloride) with triethylaluminum (or trimethylaluminum). Other components are often added, such as magnesium chloride, to modify the catalyst and improve performance. Ziegler-Natta polymerization is a method of vinyl

polymerization. It's important because it allows one to make polymers of specific tacticity. It was discovered by two scientists, and I think we can all figure out what their names were. Ziegler-Natta is especially useful, because it can make polymers that can't be made any other way, such as linear unbranched polyethylene and isotactic polypropylene. Free radical vinyl polymerization can only give branched polyethylene, and propylene won't polymerize at all by free radical polymerization. So this is a pretty important polymerization reaction, this Ziegler-Natta stuff.

### 15.9 Key Words

Fischer–Tropsch process; Fisher-Tropsch synthesis; Mechanism of Fisher- Tropsch synthesis; Ziegler–Natta catalyst; Importance of Ziegler-Natta catalyst; Mechanism of Ziegular-Natta catalysis

### 15.10 References for further studies

- 1) Homogeneous Catalysis: Mechanisms and Industrial Applications; Sumit Bhaduri, Doble Mukesh; *John Wiley & Sons*, **2014**.
- 2) Homogeneous Catalysis with Metal Complexes: Fundamentals and Applications; Gheorghe Duca; *Springer Science & Business Media*, **2012**.
- 3) Industrial Catalysis: A Practical Approach; Jens Hagen; *John Wiley & Sons*, **2015**.
- 4) Handbook of Asymmetric Heterogeneous Catalysis; Kuiling Ding, Yasuhiro Uozumi; *John Wiley & Sons*, **2008**.
- 5) Principles and Practice of Heterogeneous Catalysis; John Meurig Thomas, J. M. Thomas, W. John Thomas; *John Wiley & Sons*, **2015**.
- 6) Organometallic Chemistry and Catalysis; Didier Astruc; *Springer Science & Business Media*, **2007**.

### 15.11 Questions for self understanding

- 1) What is Fischer–Tropsch process?
- 2) Explain the Fisher-Tropsch synthesis.
- 3) Discuss the Mechanism of Fisher- Tropsch synthesis
- 4) What is Ziegler–Natta catalyst?
- 5) Discuss the importance of Ziegler-Natta catalyst.
- 6) Explain the mechanism of Ziegular-Natta catalysis

**UNIT-16****Structure**

- 16.0 Objectives of the unit
- 16.1 Introduction
- 16.2 Zeolites as shape selective catalysts
- 16.3 Zeolites
- 16.4 Clays used as catalysts.
- 16.5 Pillared Clays
- 16.6 Advantages
- 16.7 Decomposition of isopropanol using oxide catalyst
- 16.8 Catalytic converter
- 16.9 Summary of the unit
- 16.10 Key words
- 16.11 References for further studies
- 16.12 Questions for self understanding

## 16.0 Objectives of the unit

After studying this unit you are able to

- Explains the structure and preparation procedure of zeolites
- Explain the use of zeolites as shape selective catalysts
- Explain the use of clays as catalysts.
- Discuss the advantages of pillared plays
- Explains the procedure of decomposition of isopropanol using oxide catalyst
- Explain the catalytic converter

## 16.1 Introduction

The industrial uses of clay minerals as catalysts date from the early 'thirties. The application of catalysis to the thermal cracking of oil started in about 1931; pre-heated oil was passed downwards through fixed beds of granular catalyst, often attapulgite, under pressure (80 lb. per sq. in.) and at about 900~ as in the Houdry and Hydroforming systems. The catalyst had to be periodically burned off to regenerate it, and was reintroduced at the top of the reaction column. An improvement on this static process came when the granulated catalyst was kept moving counter current to the pre-heated oil. This led about 1939 to the fluid-flow method of catalysis in which powdered catalysts are used in a fluid, free-flowing condition, circulated by the air-lift method well-known in the movement of liquids. The motive power for the circulation of the fluid is obtained from the static head of gas-solid columns and by the introduction under pressure of oil vapours to the oil-cracking reactor, and of air to the catalyst reactivator. An up-flow system has recently given way to a down-flow technique, which gives greater efficiency and accuracy of control. Clay minerals have played an important part in these petroleum techniques, and it is with this astonishingly rapid development of new catalytic techniques in our minds that we may review this morning the part which clay minerals have played and may play in catalysis.

## 16.2 Zeolites as shape selective catalysts

Shape selective catalysis differentiates between reactants, products, or reaction intermediates according to their shape and size. If almost all of the catalytic sites are confined within the pore structure of a zeolite and if the pores are small, the fate of reactant molecules and the probability of forming product molecules are determined by molecular dimensions and configurations as well as by the types of catalytically active sites present. Only molecules whose dimensions are

less than a critical size can enter the pores, have access to internal catalytic sites, and react there. Furthermore, only molecules that can leave appear in the final product.

Shape selective catalysis can be used to increase yields of preferred products or to hinder undesirable reactions. It has been 25 years since Weisz and Frillette first described the concept of shape selectivity. The significance of this phenomenon was recognized immediately. Scientific experimentation went hand-in-hand with the exploration of commercial possibilities. Desktop laboratory experiments were soon followed by development work, and pilot plant demonstrations soon led to the construction and start—up of commercial units.

### 16.3 Zeolites

Most shape selective catalysts today are molecular sieve zeolites. Zeolites are porous crystalline aluminosilicates possessing intracrystalline channels with reproducible morphology. They are built up from  $\text{SiO}_4$  and  $\text{AlO}_4$  tetrahedral elements, cross—linked to each other through the oxygens. In natural zeolites, aluminum or silicon occupy all the tetrahedra but in some synthetic zeolites gallium, germanium, boron, and phosphorus have been also incorporated into the framework. Natural zeolites are frequently found in rocks of volcanic origin (e.g., glassy tuffs near alkaline lakes).

Synthetic zeolites are made by precipitation from supersaturated alkaline solutions of various inorganic or organic bases. The organic cations (often various tetraalkylammonium hydroxyls) serve as templates to direct crystallization toward the desired structure.

Zeolites have four properties which make them interesting and valuable for heterogeneous catalysis:

- 1) They have exchangeable cations, allowing the introduction of different cations with various catalytic properties;
  - 2) If these cationic sites are exchanged to H, they can have a very high number of very strong acid sites;
  - 3) They have pore diameters with one or more discrete sizes; and
  - 4) They have pore diameters that are in the order of molecular dimensions, i.e., less than 1 nm.
- Properties 1 and 2 account for catalytic activity and properties 3 and 4 are responsible for the molecular sieving action.

### 16.4 Clays used as catalysts.

Although the clay mineralogist is bringing some order out of chaos in the classification of clays we are faced with rather a large number of trade names when we come to study the literature of clay catalysts. I shall name some of the better known ones, beginning with the kaolinitic group, The clays of this group have not been much used in catalysis and are not cursed with strange nomenclature. Dickite, nacrite, and halloysite are not worked commercially, so we are left with the familiar china clays and ball clays of commerce. These are clays with a 7 Angstrom unit basal spacing of the lattice.

The 10 Angstrom unit clays or illite group includes attapulgite, which is the clay mineral of Florida fuller's earth, Floridin, Florex, and Florigel, the products of Florida and Georgia in the United States. (I should add that Florite is a bauxite catalyst made by the same company). These clays in granulated and powder form are the most important clay catalysts in the world. They are not known to exist in Britain in commercial quantities; some Russian clays seem to be similar. The montmorillonite group tend to lose activity on heating above 500~ ; certainly they lose their adsorptive power. There may be catalytic reactions in which the kilned material is more active. But for low temperature catalytic reactions where regeneration of the catalyst does not involve the use of high temperatures, drying of the montmorillonite to the optimal moisture content is an obvious suggestion. This precaution is necessary in the essential oil reactions to be described later.

### 16.5 Pillared Clays

Pillared clays (PILCs) are one of the promising porous materials which can be utilized as catalysts in a number of reactions. More than thirty years have passed since the first announcement of pillared interlayered clay. The preparative techniques have progressed remarkably with a wide variety of pillared solids being made. Recent advances in the synthesis of PILCs have expanded considerably the scope of their potential catalytic applications. PILCs are formed by intercalation of polymeric metal hydroxides or oligomerichydroxycations into the interlamellar space of the cationic clays, followed by thermal treatment, allows pillaring of the clays, with a modification of the interlayer distance and typically also an increase of the thermal stability.

The catalytic behaviour of PILCs is usually associated to the modification of the acidity (by substituting tetrahedral and octahedral sites), by active sites introduced during the pillaring



process and by intercalation with organometallic complexes. The method of pillaring could largely affect the final characteristics and performances. Also anionic clays could be pillared. These materials, particularly those having isopoly- and heteropoly-anions intercalated between the layers, show a quite interesting catalytic behavior. Moreover, the transition metal oxide pillars can be modified by oxidation/reduction to become catalytically active and the pillars of the clay create specific and stable active sites. In these contexts first row transition metals like iron, titanium, vanadium and chromium-pillared materials are mostly studied. So there is enough scope of developing new catalytic materials for different applications by varying the transition metal oxide pillars only.

This area of research is still growing and need further exploration as potential catalyst which is very limited in the literature. Generally, it is also claimed that the pillaring procedure significantly improves the performances with respect to the starting clays. As a result there is now a renewed interest in the pillared material as polyfunctional catalysts and catalyst supports. Several research groups have investigated the characteristics of PILCs and their use as catalysts or catalytic materials. The general conclusion which may be derived from these studies that pillared clays are very interesting and promising catalysts in a broad range of applications, for example in acid-catalyzed reaction catalytic hydrotreating of heavy vacuum gas oil alkylation of aromatics, the synthesis of bulk and fine chemicals (a broad range of reactions such as dehydrogenation, hydroxylation, disproportionation, esterification, epoxidation, alkylation, isomerization, Fischer-Tropsch, methane reforming, hydrogenation, aromatization, etc.), upgrading of lubricant oils and for the reduction of pollutants (selective catalytic reduction of NO<sub>x</sub> and catalytic removal of organic volatile compounds).

The best clay base for pillaring is a high-swelling Na-montmorillonite. It is mineral clay that can hold guest molecules between its layers. Many different cations, including hydroxy-aluminium, hydroxy-chromium, hydroxy-titanium and hydroxy-zirconium polycations have been used for the preparation of pillared montmorillonite characterised by surface area of 200-400 m<sup>2</sup>/g, pore volume of 0.15-0.30 cm<sup>3</sup>/g and interlayer spacing of 1-2 nm. Vaughan and Lussier demonstrated that montmorillonite interlayered with hydroxy-aluminium pillars will promote catalytic

### 16.6 Advantages

The main groups of uses for clay catalysis are in the essential oil, glyceride oil and petroleum oil fields, as well as in general organic synthesis or pyrolysis, not covered by these fields. A very

great number of reactions have been studied not only to throw light on the nature of the reactions themselves and of the role of the catalyst, but as part of the huge research programme which has revolutionised the oil industry converting it from a fuel-producing to a chemical-producing industry.

- **Glyceride oils.** Clay catalysts have been used, experimentally at any rate, for dehydrating castor and fish oils to produce drying oils to eke out limited supplies of linseed and tung oils; and contrariwise, in China, where petroleum products were unobtainable, tung oil and other glyceride oils were cracked with a clay catalyst to yield hydrocarbon products.
- **Petroleum oil.** The original aim of using clay and other catalysts in the petroleum industry was to reduce the temperatures required for cracking crude residual oil to increase the yield of motor spirit and light gas oil. The emphasis later passed to the production of high octane fractions by catalytic isomerisation or "reforming," as well as to desulphurisation. And more recently catalytic processes have been developed so highly that a considerable range of pure chemicals can be produced. Most of this development has been carried out, of course, in the United States by all the larger companies, but in Britain big developments are on the way, notably the Shell Chemicals processes and the Catarole process of Petrochemicals Ltd.
- **General organic synthesis.** This leads us imperceptibly towards the wide field of general organic synthesis. A few reactions will be mentioned.
- **Dehydrations.** --Resin alcohols produced from colophony or abietic acid by hydrogenation can be dehydrated by Tonsil activated clay to produce unsaturated hydrocarbons utilisable in the textile industry. Simple reactions have been studied with the production of unsaturated hydrocarbons and ethers from primary aliphatic alcohols over Japanese acid clay. Cyclohexanol can be converted to cyclohexene. Under severer conditions, that is to say, at higher temperatures, the reactions are called pyrolytic, and are akin to the cracking of petroleum crudes in heterogeneous catalysis. Many single chemicals have been pyrolysed over clays.
- **Condensations.** An enormous number of condensation reactions have been catalysed by clays. Aldehydes and ketones passed over kaolin with ammonia yield pyridine bases. Nitriles are formed over clays with ammonia acting on acetic acid, adipic acid, fatty acids, and so on. Alcohols and amines from paratoluidine and other compounds. Members of the anthraquinone series condense with phthalic anhydride over clay catalysts.

- **Dechlorinations.** A chloride atom is removed in other condensations, as when benzylchloride and benzene form diphenylmethane over clay. Chlorobenzol, chlortoluol and chlorinated paraffins have been dechlorinated with clays. Some examples of chlorination are mentioned. Isomeri-ation and cyclisation.--Aldehydes may be converted to ketoncs over clay catalysts, and cyclisation is by no means confined to the hydrocarbons already mentioned. Thus unsaturated aliphatic acids yield cyclopentenones. Some elegant examples have been given of such reactions among the essential oils.
- **OxMations and reductions.** Natural gas has been oxidised to alcohols, mainly, over silicates. Silica gel helps to form phenols from benzol and water, but I have no record of clays being used in this reaction.

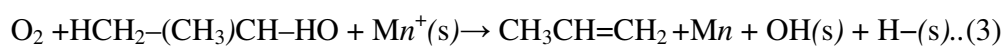
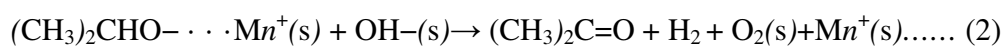
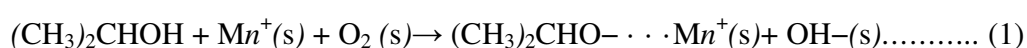
### 16.7 Decomposition of isopropanol using oxide catalyst

The adsorption and reaction of alcohols on metaloxide catalysts has been used as a chemical probe reaction for many years. Alcohol reactions have been studied extensively using temperature programmed decomposition (TPD), steady-state kinetic studies, in situ spectroscopy, microcalorimetry and many ultra-high vacuum surface science studies as cited by Rekoske and Barteau. Isopropanol decomposition has long been considered as a chemical probe reaction for surface acid-base properties. Isopropanol undergoes dehydration to give propylene on acidic surface sites and dehydrogenation via a concerted mechanism on adjacent acidic and basic surface sites to give acetone.

Ai and Suzuki were the first to correlate various acidic and basic properties of metal oxide catalysts with their rates of dehydration and dehydrogenation of isopropanol. Isopropanol adsorption has also been employed as a method of measuring the surface titania content in mixed titania-silica catalysts. Zaki and coworkers have done in situ IR spectroscopy studies of isopropanol adsorption on  $\text{Al}_2\text{O}_3$ ,  $\text{CeO}_2$ ,  $\text{TiO}_2$ ,  $\text{ZrO}_2$  and  $\text{HfO}_2$ . Other metal oxides that have been extensively studied are  $\text{ZnO}$  and  $\text{MoO}_3$ .

All these investigations adsorbed isopropanol at room temperature and found that isopropanol adsorbs both dissociatively as a surface isopropoxide intermediate and as physisorbed isopropanol at room temperature. In some cases, also intact isopropanol was chemisorbed via coordinative bonding to the metal oxide surface. This coordinatively bonded isopropanol was also found on  $\text{Y}_2\text{O}_3$  at up to 250 °C. Upon evacuation most of the physisorbed isopropanol desorbed leaving only the surface isopropoxide species and the coordinatively bonded

isopropanol. Dehydroxylated surfaces dissociated isopropanol to give isopropoxide species and surface hydroxyls. The hydroxyl species desorbed as water upon heating to sufficiently high temperatures. The surface isopropoxide species underwent further C–H bond scission at higher temperatures to give acetone. Two kinds of surface isopropoxide species were observed on metal oxide catalysts. One of the surface alkoxides is terminally bonded to a single cation and the other is bridge bonded to two cations. Hussein and Gates propose that the bridge bonded species yield propylene and the terminal species give acetone. The surface reactions to the acetone and propylene are shown below:

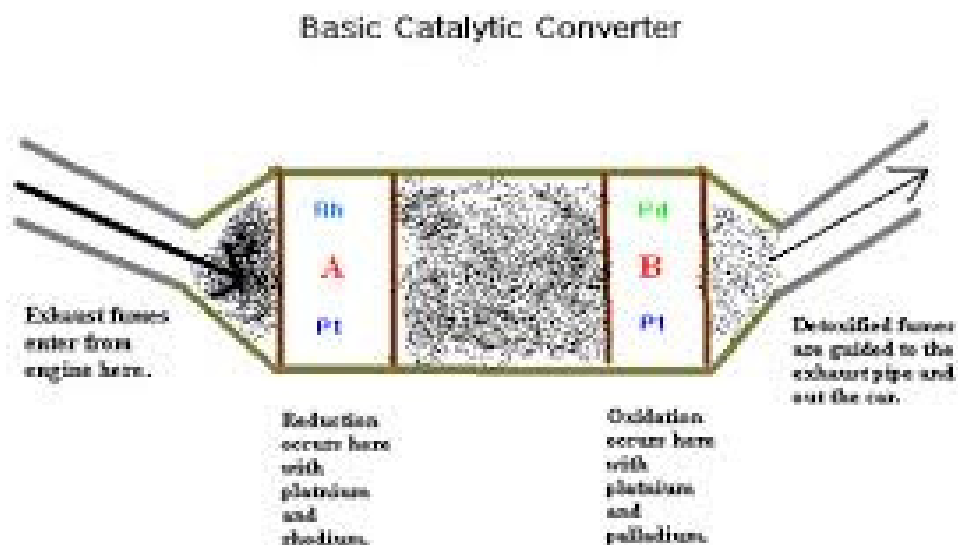


where  $\text{Mn}^+$  is the positive metal cation to which the surface isopropoxide species are bonded. One of the objectives of the present investigation is to determine the number of active surface sites per  $\text{m}^2$  ( $N_s$ ) and also the isopropanol oxidation turnover frequencies on the various metal oxide catalysts. Isopropanol can distinguish between acidic and redox surface sites.

### 16.8 Catalytic converter

A catalytic converter is a vehicle emissions control device that converts toxic pollutants in exhaust gas to less toxic pollutants by catalyzing a redox reaction (oxidation or reduction). Catalytic converters are used with internal combustion engines fueled by either petrol (gasoline) or diesel—including lean-burn engines.

The first widespread introduction of catalytic converters was in the United States automobile market. To comply with the U.S. Environmental Protection Agency's stricter regulation of exhaust emissions, gasoline-powered vehicles starting with the 1975 model year must be equipped with catalytic converters. These "two-way" converters combined oxygen with carbon monoxide (CO) and unburned hydrocarbons (HC) to produce carbon dioxide (CO<sub>2</sub>) and water (H<sub>2</sub>O). In 1981, two-way catalytic converters were rendered obsolete by "three-way" converters that also reduce oxides of nitrogen (NO<sub>x</sub>); however, two-way converters are still used for lean-burn engines.



Although catalytic converters are most commonly applied to exhaust systems in automobiles, they are also used on electrical generators, forklifts, mining equipment, trucks, buses, locomotives and motorcycles. They are also used on some wood stoves to control emissions. This is usually in response to government regulation, either through direct environmental regulation or through health and safety regulations.

The catalytic converter's construction is as follows:

1. The catalyst support or substrate. For automotive catalytic converters, the core is usually a ceramic monolith with a honeycomb structure. Metallic foil monoliths made of Kanthal (FeCrAl) are used in applications where particularly high heat resistance is required. Either material is designed to provide a large surface area. The cordierite ceramic substrate used in most catalytic converters was invented by Rodney Bagley, Irwin Lachman and Ronald Lewis at Corning Glass, for which they were inducted into the National Inventors Hall of Fame in 2002.
2. The washcoat. A washcoat is a carrier for the catalytic materials and is used to disperse the materials over a large surface area. Aluminum oxide, titanium dioxide, silicon dioxide, or a mixture of silica and alumina can be used. The catalytic materials are suspended in the washcoat prior to applying to the core. Washcoat materials are selected to form a rough, irregular surface, which greatly increases the surface area compared to the smooth surface of the bare substrate. This in turn maximizes the catalytically active surface available to react

with the engine exhaust. The coat must retain its surface area and prevent sintering of the catalytic metal particles even at high temperatures (1000 °C).

3. The catalyst itself is most often a mix of precious metals. Platinum is the most active catalyst and is widely used, but is not suitable for all applications because of unwanted additional reactions and high cost. Palladium and rhodium are two other precious metals used. Rhodium is used as a reduction catalyst, palladium is used as an oxidation catalyst, and platinum is used both for reduction and oxidation. Cerium, iron, manganese and nickel are also used, although each has limitations. Nickel is not legal for use in the European Union because of its reaction with carbon monoxide into toxic nickel tetracarbonyl. Copper can be used everywhere except North America, where its use is illegal because of the formation of dibenzodioxins.

Upon failure, a catalytic converter can be recycled into scrap. The precious metals inside the converter, including platinum, palladium and rhodium, are extracted. Prices paid for converters vary depending on the type and market prices.

Environmental impact Catalytic converters have proven to be reliable and effective in reducing noxious tailpipe emissions. However, they also have some shortcomings in use, and also adverse environmental impacts in production:

- An engine equipped with a three-way catalyst must run at the stoichiometric point, which means more fuel is consumed than in a lean-burn engine. This means approximately 10% more CO<sub>2</sub> emissions from the vehicle.
- Catalytic converter production requires palladium or platinum; part of the world supply of these precious metals is produced near Norilsk, Russia, where the industry (among others) has caused Norilsk to be added to Time magazine's list of most-polluted places.<sup>[32]</sup>

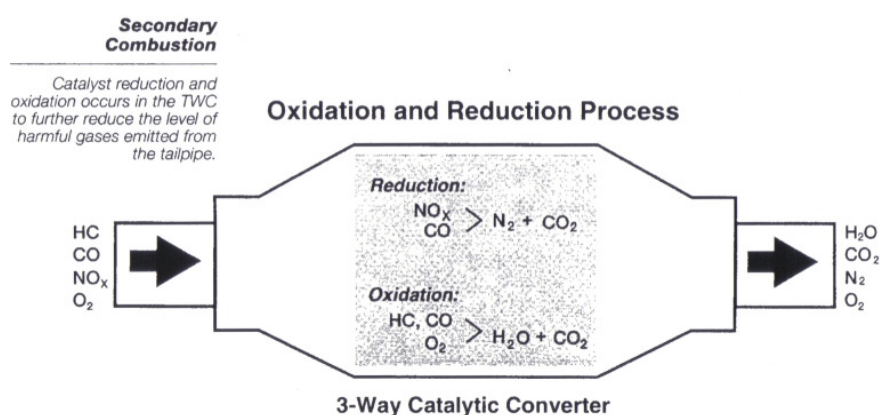
A **two-way** (or "oxidation") catalytic converter has two simultaneous tasks:

1. Oxidation of carbon monoxide to carbon dioxide:  $2\text{CO} + \text{O}_2 \rightarrow 2\text{CO}_2$
2. Oxidation of hydrocarbons (unburned and partially burned fuel) to carbon dioxide and water:  $\text{C}_x\text{H}_{2x+2} + [(3x+1)/2] \text{O}_2 \rightarrow x\text{CO}_2 + (x+1) \text{H}_2\text{O}$  (a combustion reaction)

This type of catalytic converter is widely used on diesel engines to reduce hydrocarbon and carbon monoxide emissions. They were also used on gasoline engines in American- and Canadian-market automobiles until 1981. Because of their inability to control oxides of nitrogen, they were superseded by three-way converters.

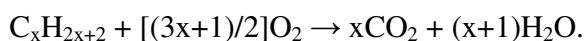
### Three-way

Three-way catalytic converters (TWC) have the additional advantage of controlling the emission of nitrogen oxides ( $\text{NO}_x$ ), particularly nitrous oxide, a greenhouse gas over three hundred times more potent than carbon dioxide, a precursor to acid rain and currently the most ozone-depleting substance.<sup>1</sup> Technological improvements including three-way catalytic converters have led to motor vehicle nitrous oxide emissions in the US falling to 8.2% of anthropogenic nitrous oxide emissions in 2008, from a high of 17.77% in 1998.



Since 1981, "three-way" (oxidation-reduction) catalytic converters have been used in vehicle emission control systems in the United States and Canada; many other countries have also adopted stringent vehicle emission regulations that in effect require three-way converters on gasoline-powered vehicles. The reduction and oxidation catalysts are typically contained in a common housing; however, in some instances, they may be housed separately. A three-way catalytic converter has three simultaneous tasks:

1. Reduction of nitrogen oxides to nitrogen and oxygen:  $2\text{NO}_x \rightarrow x\text{O}_2 + \text{N}_2$
2. Oxidation of carbon monoxide to carbon dioxide:  $2\text{CO} + \text{O}_2 \rightarrow 2\text{CO}_2$
3. Oxidation of unburnt hydrocarbons (HC) to carbon dioxide and water:



These three reactions occur most efficiently when the catalytic converter receives exhaust from an engine running slightly above the stoichiometric point. For gasoline combustion, this is between 14.6 and 14.8 parts air to one part fuel, by weight. The ratio for Autogas (or liquefied petroleum gas (LPG)), natural gas and ethanol fuels is each slightly different, requiring modified fuel system settings when using those fuels. In general, engines fitted with 3-way catalytic converters are equipped with a computerized closed-loop feedback fuel injection system using

one or more oxygen sensors, though early in the deployment of three-way converters, carburetors equipped for feedback mixture control were used.

Three-way converters are effective when the engine is operated within a narrow band of air-fuel ratios near the stoichiometric point, such that the exhaust gas composition oscillates between rich (excess fuel) and lean (excess oxygen). Conversion efficiency falls very rapidly when the engine is operated outside of this band. Under lean engine operation, the exhaust contains excess oxygen, and the reduction of  $\text{NO}_x$  is not favored. Under rich conditions, the excess fuel consumes all of the available oxygen prior to the catalyst, leaving only stored oxygen available for the oxidation function.

Closed-loop engine control systems are necessary for effective operation of three-way catalytic converters because of the continuous balancing required for effective  $\text{NO}_x$  reduction and HC oxidation. The control system must prevent the  $\text{NO}_x$  reduction catalyst from becoming fully oxidized, yet replenish the oxygen storage material so that its function as an oxidation catalyst is maintained.

Three-way catalytic converters can store oxygen from the exhaust gas stream, usually when the air-fuel ratio goes lean. When sufficient oxygen is not available from the exhaust stream, the stored oxygen is released and consumed (see cerium(IV) oxide). A lack of sufficient oxygen occurs either when oxygen derived from  $\text{NO}_x$  reduction is unavailable or when certain maneuvers such as hard acceleration enrich the mixture beyond the ability of the converter to supply oxygen.

### 16.9 Summary of the unit

Zeolites are hydrated aluminosilicates of the alkaline and alkaline-earth metals. About 40 natural zeolites have been identified during the past 200 years; the most common are analcime, chabazite, clinoptilolite, erionite, ferrierite, heulandite, laumontite, mordenite, and phillipsite. More than 150 zeolites have been synthesized; the most common are zeolites A, X, Y, and ZMS-5. Natural and synthetic zeolites are used commercially because of their unique adsorption, ion-exchange, molecular sieve, and catalytic properties.

### 16.10 Key words

Zeolites as shape selective catalysts; Zeolites; Clays used as catalysts. ; Pillared Clays ; Decomposition of isopropanol using oxide catalyst; Catalytic converter



**16.11 References for further studies**

- 1) Homogeneous Catalysis: Mechanisms and Industrial Applications; Sumit Bhaduri, Doble Mukesh; *John Wiley & Sons*, **2014**.
- 2) Homogeneous Catalysis with Metal Complexes: Fundamentals and Applications; Gheorghe Duca; *Springer Science & Business Media*, **2012**.
- 3) Industrial Catalysis: A Practical Approach; Jens Hagen; *John Wiley & Sons*, **2015**.
- 4) Handbook of Asymmetric Heterogeneous Catalysis; Kuiling Ding, Yasuhiro Uozumi; *John Wiley & Sons*, **2008**.
- 5) Principles and Practice of Heterogeneous Catalysis; John Meurig Thomas, J. M. Thomas, W. John Thomas; *John Wiley & Sons*, **2015**.
- 6) Organometallic Chemistry and Catalysis; Didier Astruc; *Springer Science & Business Media*, **2007**.

**16.12 Questions for self understanding**

- 1) What are zeolites?
- 2) Write a note on zeolites as shape selective catalysts
- 3) Discuss about use of clays as catalysts.
- 4) What are pillared clays? Explain their uses.
- 5) Discuss the advantages of pillared clays
- 6) Explain the process decomposition of isopropanol using oxide catalyst
- 7) Write a note on catalytic converter